THE UNIVERSITY
of LIVERPOOL

THE NATURE AND CONSE.QUENCES OF MOLECULAR INTERACTIONS OF THE METASTASIS-INDUCING PROTEIN, S100A4

A THESIS

Submitted for the Degree of Doctor of Philosophy

In the University of Liverpool

December 2002

By

Guozheng Wang

Molecular Medicine Group

School of Biological Sciences

University of Liverpool, Liverpool L69 7ZB

ACKNOWLEDGEMENTS

First of all, I wish to express my wholehearted thanks to Dr. Barraclough and Professor Rudland for allowing me to do my PhD part timely while I am working in their laboratory.

All stages of the work presented were discussed with my supervisor Dr. Barraclough who has contributed enormously to the strategy of this work and writing. To whom I wish to express my deep gratitude for his support and encouragement.

I also wish to express my thanks to Professor Rudland for the discussion and correction of my thesis while I am writing.

It is also my pleasure to extended my sincere thanks to the following people:

Dr. Fernig, School of Biological Sciences, University of Liverpool, for his guidance and help while I am using his optical biosensor and calculating all the kinetics of bindings.

Dr. Green and Dr. Smith, School of Biological Sciences, University of Liverpool, for their valuable discussions during this study and also for their hard work as my assessors

Dr. Hongmei Zhang, Laboratory of Protein Science, Qinghua University, Bejing, for help in providing valuable images of S100P monomer and dimer.

Dr. Hailan Chen, School of Biological Science, University of Liverpool, for providing non-myosin A expression construct. Dr. Shu Zhang, School of Biological Sciences, University of Liverpool, for providing some recombinant rat S100A4 protein.

Dr. Mike White and Dr. David Spiller for allowing me to use their confocal microscopes and also for their technical helps.

The work was supported by Welcome Trust, North West Cancer Research Fund, and

Cancer and Polio Research Fund.

Contents

Abbreviations

Abbreviations	Full name
Amp	Ampicillin
AMV-RT	avian myeloblastosis virus reverse transcriptase
ATP	adenosine triphosphate
bp	base pairs
BSA	bovine serum albumin
C-FABP	fatty acid-binding protein
dATP	2'-deoxyadenosine triphosphate
dCTP	2'-deoxycytidine triphosphate
ddH_2O	double-distilled water
dsRED	a red fluorescent protein
DEAE	diethylaminoethyl
DEPC	diethyl pyrocarbonate
dGTP	2'-deoxyguanosine triphosphate
DIP	deionised formamide
DMEM	Dulbecco's modified Eagle's medium
DMS	dimethyl sulphate
DMSO	dimethyl sulphoxide
DNA	deoxyribonucleic acid
dNTP	deoxyribonucleoside triphosphate
dTTP	2'-deoxythymidine triphosphate
ECL	enhanced chemiluminescence
ECM	extracellular matrix
EDTA	ethylene diaminetetraacetic acid
EGTA	ethyleneglycolbis(2-aminoethyl-ether)tetraacetic acid
ETS	a DNA binding domain
FCS	fetal calf serum
GST	Glutathione S-transferase
GFP	green fluorescent protein
HEPES	N-2-hydroxyethylpiperazine-N'-2-ethanesulphonicacid
HGF	hepatic growth factor

IPTG	isopropylthio-p-D-galactoside
kbp	kilo-base pairs
MCS	multiple cloning site
MetAP2	metastasis associated protein 2
MHC-IIA	non-muscle myosin heavy chain A
MHC-IIB	non-muscle myosin heavy chain B
MHC-IIAF21	Recombinant human non-muscle myosin heavy chain A *C*-terminal 21 kDa fragment
MHC-IIBF17	Recombinant human non-muscle myosin heavy chain B *C*-terminal 17 kDa fragment
MMP	Matrix metalloproteinase
MMTV	Mouse Mammary Tumour Virus promotor
MOPS	3-[N-morpholino]propane sulphonic acid
MRNA	messenger RNA
MT-MMP	membrane-type MMP
Ni-NTA	Nickel-nitriloacetic acid
NMR	nuclear magnetic resonance
NP-40	Nonidet P-40
OPN	osteopontin
PBS	phosphate-buffered saline
PBST	PBS + tween 20
PCR	polymerase chain reaction
PKC	protein kinase C
PMSF	phenylmethylsulphonylfluoride
RM	routine medium
RNA	ribonucleic acid
RT-PCR	reverse transcription PCR
SDS	sodium dodecyl sulphate
SDS-PAGE	SDS-PolyAcrylamide gel electrophoresis
SPR	surface plasmon resonance
SV40	simian virus 40
TCA	trichloroacetic acid
TEMED	N ,N,N' ,N' ,tetramethy lethylenediamine
Tris	tris(hydroxymethyl)methylamine
uPA	urokinase

uPAR	urokinase receptor
X-gal	5-bromo-4-chloro-3-indolyl-p-D-galactoside
VEGF	vascular endothelial growth factor
VEGFR	vascular endothelial growth factor receptor
YAPD	a yeast culture medium

Abstract

S100A4, an EF-hand type calcium binding protein, has been shown to promote tumour metastasis. In order to understand the mechanism of the metastasis-inducing properties of S100A4, the molecular interactions between S100A4 and some target proteins, as well as the consequences of these interactions have been investigated *in vitro* and *in vivo* in this project.

In mammalian cells, there exist two isoforms of non-muscle myosin heavy chain, named non-muscle myosin A and B (MHC-IIA and MHC-IIB), which have about 75% amino acid sequence identity. MHC-IIA was reported by Kriajevska and her colleagues to be a target protein of S100A4 and the effects of S100A4 on PKC phosphorylation and bundling of MHC-IIA had also been reported thereafter. However, no studies have been carried out to explore the possible interaction between S100A4 and MHC-IIB, the isoform of MHC-IIA. In this study, the interaction of S100A4 with MHC-IIB and its binding affinity were determined. The Kd from their kinetic parameters was 4 μM and the Kd from the extent of binding at equilibrium was 6.3μM determined using an optical biosensor. Their binding affinity is about 10 times lower than that of S100A4/MHC-IIA (Kd from their kinetic parameters was 250nM and Kd from the extent of binding at equilibrium was 660 nM). The effects of S100A4 on the PKC phosphorylation and self-assembly of MHC-IIB were studied and compared with that of MHC-IIA. The results showed that S100A4 inhibited the phosphorylation of MHC-IIB by PKC, but not as effectively as that on MHC-IIA. Although S100A4 inhibited the self-assembly of MHC-IIA in a Ca^{2+}-dependent manner, it showed no effect on MHC-IIB self-assembly. The effects of PKC phosphorylation of MHC-IIA and IIB on the binding of S100A4 were also investigated using gel overlay and an optical biosensor. The results showed that PKC phosphorylation of MHC-IIA reduced its binding to S100A4, but the PKC phosphorylation of MHC-IIB had no effect on its binding to S100A4. These results show that S100A4 preferentially interacts and affects MHC-IIA *in vitro*

The yeast two-hybrid system was used to investigate the interactions of S100A4 with its

targets proteins *in vivo*. The interactions of S100A4 with MHC-IIA, MHC-IIB and another *in vitro* target, p53, did not occur in the yeast two-hybrid system. However, S100A4 was found to interact with S100A1 from a yeast two-hybrid library, constructed with mRNA extracted from a human breast cancer specimen. The interaction of S100A4 and S100A1 was confirmed by experiments *in vitro*. Point mutations of S100A4 and S100A1 suggest that the interaction of S100A1 and S100A4 is similar to that of S100A4 homodimerisation so it is probably heterodimerisation. The affinity of the S100A4/S100A1 interaction was also analysed using the biosensor. The data supported the monomer (S100A1)-monomer (S100A4) interaction model. The Kd of S100A4/S100A1 from kinetic parameters was 300nM and the Kd from the extent of binding at equilibrium was 500nM. The Kd of S100A4/S100A4 from kinetic parameters was 670nM and Kd from the extent of binding at equilibrium was 1,000nM. In the yeast two-hybrid system, S100A4 was shown to associate preferentially with S100A1 than with itself. It is possible that the S100A4/S100A1 heterodimers could be formed substantially if the two proteins co-exist in a cell. Further experiments showed that S100A4 and S100A1 proteins were co-expressed and co-localised in some cell lines, such as MDA-MB-231, a malignant breast cancer cell line, suggesting that the interaction may have biological significance.

To test *in vitro* for biological significance, S100A4 was pre-incubated with S100A1 and the mixture was added to the PKC phosphorylation and sedimentation reactions of MHC-IIA. The results showed that S100A1 itself had no obvious effects on the phosphorylation and sedimentation of MCH-IIA. However, S100A1 reversed partially the inhibitory effects of S100A4 on PKC phosphorylation and self-assembly of MHC-IIA.

To investigate if there is any biological effect of the interaction *in vivo*, S100A1 was up-regulated by transfection of its cDNA into cell lines Rama 37, a rat benign mammary cell line, and KP1-Rama 37, a transfected Rama 37 cell line expressing S100A4. Two new cell lines, RT4-Rama 37 and KT6-KP1-Rama 37, with S100A1 up-regulated were isolated. The cell motility and clone-forming ability in soft agar of the parental cell lines and the

resultant transfected cell lines along with the cell lines transfected with control vector were compared. The results showed that S100A1 had no effect on Rama 37 cells in term of cell motility and cloning efficiency, but had significant inhibitory effect on the increase of cell motility and clone forming ability induced by S100A4 in KP1-Rama 37 cells. The results suggest that S100A1 has an antagonistic effect on S100A4 and its presence in cells could affect S100A4-induced tumour metastasis.

Chapter One

Introduction

1.1 The multiple steps of tumour metastatic process

The metastatic spread of cancer is a major obstacle to its successful treatment (John & Tuszynski 2001). Even after the primary cancer has been excised, the threat of death remains due to the metastases that may occur through the presence of tumour cells remaining at sites other than that of the primary cancer of the patient. Therefore metastasis has been an important target of cancer research for many years. However, cancer metastasis is a complex process and develops through multiple steps with many factors involved. The details of the mechanisms are still far from clear.

1.1.1 Adhesion and motility

When cells of a solid tumour invade adjacent tissues or enter blood or lymphatic vessels, the cells must detach from other tumour cells and be able to move away from the primary tumour. To detach from other tumour cells means that the cells have lost adhesion or cell-cell interaction. However, cell adhesion is also required for cell motility, which is believed to be essential for metastasis too. This process involves many different proteins and regulatory mechanisms. Some of these are described below.

There are various family members of cell adhesion receptors, such as those of the cadherin family, the immunoglobulin superfamily, the selectin family, the integrin family and CD 44. The maintenance of normal epithelial cell-cell interaction is the function of E-cadherin, a member of the cadherin family. E-cadherin is often reduced or lost in tumours of epithelial origin (Shiozaki *et al.*, 1991). Loss or reduced expression of α-catenin, a binding partner of E-cadherin, could also interrupt cell-cell interaction and has been linked to metastasis (Rimm *et al.*, 1995).

CD44 is a major cell surface receptor for the glycosaminoglycan, hyaluronan (HA). The major physiological role of CD44 is to maintain organ and tissue structure via cell-cell and cell-matrix adhesion (Goodison *et al.,* 1999). CD44 is subject to a wide array of post-translational carbohydrate modifications, including N-linked, O-linked and glycosaminoglycan side chain additions (Naot *et al.,* 1997). These modifications, which differ in different cell types and cell activation states, can have profound effects on HA binding function and are the main mechanism of regulating CD44 function. Some glycosaminoglycan modifications also affect ligand-binding specificity, allowing CD44 to interact with proteins of the extracellular matrix, such as fibronectin, collagen and immunoglobin superfamily adhesion molecules (Naot *et al.,* 1997). Changes in CD44 expression are associated with a wide variety of cancers and the degree to which they spread; however, in other cancers, the CD44 pattern remains unchanged. Increased expression of CD44 is associated with increased binding to HA and increased metastatic potential in some experimental tumour systems; however, in other systems, increased HA binding and metastatic potential are not correlated with one another (Lesley *et al.,* 1997). In addition to the post-translation modifications and level of CD44, its splice variants contribute a lot to the diversity of its functions. For example, some of the CD44 splice variants might be linked closely with gastric carcinoma tumourigenesis and differentiation (Ue, *et al.,* 1998). It was also reported that the magnitude of CD44 variant synthesis at the protein level correlates with lymph node metastasis (Naot *et al.,* 1997;Hsieh *et al.,* 1999).

Several different CD44 variants can bind to osteopontin (OPN) but the common form of CD44 does not. OPN binding to CD44 variants/beta1-containing integrins promotes cell spreading, motility, and chemotactic behaviour (Katagiri *et al.,* 1999). OPN is a calcium-binding phosphoprotein and is known to contribute importantly to cell adhesion interactions. The relationship of OPN and metastasis will be discussed later in Section 1.2. The integrins family is composed of 15α and 8β subunits that are contained in over twenty different $\alpha\beta$ heterodimeric combinations on cell surfaces. Integrins, generally, mediate adhesion between cells and the extracellular matrix (ECM), although some members are also involved in cell-cell interactions (Berman & Kozlova 2000). Once a cell is spread over

the ECM, contractile forces are transmitted through the integrin–cytoskeletal connection to provide the force needed to generate movement (Holly *et al.,* 2000). Besides their function of mediating specific binding of cells to components of the connective tissues, integrins also transduce signals from the extracellular space into the cells and regulate the expression of various genes (Dedhar 1999). Integrins also play an essential role with regard to tumour cell adhesion, migration, invasiveness and metastasis formation. The αvβ3 integrin was defined as an important adhesion molecule in metastasis of different types of tumours, such as epithelial ovarian carcinoma (Gillan *et al.,* 2002), melanoma (Felding-Habermann *et al.,* 2002;Voura *et al.,* 2001) and breast cancer (Felding-Habermann *et al.,* 2001). Matrix metalloproteinase-2 (MMP-2) binds directly to the αvβ3 and is thus localised, in proteolytically active form on the surface of cancer cells. This process is thought to facilitate cellular invasion processes (Brooks *et al.,* 1996). αvβ3 is also involved in critical events of blood vessel formation during tumour angiogenesis (Brooks *et al.,* 1994). The α6β4 integrin is normally a laminin receptor involved in maintaining proper epithelial architecture (Mercurio *et al.,* 2001), but upon cellular transformation, α6β4 signaling is required for chemotaxis and invasion of carcinomas (O'Connor *et al.,* 1998).

The selectins are a family of intercellular adhesion molecules that mediate the attachment of leukocytes to the endothelial lining of blood vessels. There is some evidence for the involvement of E-, P- and L-selectin in the metastasis of different tumour types (Krause & Turner 1999). For example, P-selectin facilitates human carcinoma metastasis in immunodeficient mice by mediating early interactions of platelets with blood-borne tumour cells via their cell surface mucins, and this process can be blocked by heparin (Borsig *et al.,* 2001). L-selectin expressed on endogenous leukocytes also facilitates metastasis in both syngeneic and xenogeneic (T and B lymphocyte deficient) systems (Borsig *et al.,* 2002). *In vivo*, pretreatment of nude mice by injecting intravenously C-raf anti-sense, which greatly reduced the hepatic E-selectin induction, singnificantly reduced the number of liver metastases of CX-1 cells, a highly metastatic human colorectal carcinoma cell line, relative to controls without the pretreatment (Khatib *et al.,* 2002). In a syngeneic mice model, an antibody to E-selectin was shown to cause a marked, specific

and Fc-independent inhibition of experimental liver metastasis of H-59 cells, a metastatic murine carcinoma cell line, reducing the median number of metastases by 97% relative to the control groups (Brodt *et al.*, 1997).

Immunoglobulin superfamily adhesion molecules, containing one or more immunoglobin-like domains, are involved in the interactions with variety of ligands and play a major part in regulating embryonic neural development, wound healing and inflammation (Brummendorf & Rathjen 1995). I-CAM1, a member of the immunoglobulin super family, has been characterised as a marker of progression in malignant melanomas. As I-CAM 1 can bind to the β2 integrins expressed on circulating leucocytes, a large heterotypic cell clump may be formed and mediate adherence of the tumour cell to the endothelium (Gahmberg *et al.*, 1997), suggesting some of the immunoglobulin superfamily adhesion molecules (I-CAMs) are also involved in tumour metastasis.

In general, motility or migration is a necessary ability of tumour cells to spread. This process is through dynamic contact with the ECM mediated by integrins (Holly *et al.*, 2000). The rate of cell migration is a consequence of variation in adhesiveness, too strong adhesion result in no movement, no adhesion means lack of traction and there is no movement too (Palecek *et al.*, 1997). Maximum migration can only be achieved in an optimal strength of adhesion. Besides the strength of adhesion, many factors, for example, hepatocyte growth factor (HGF), autocrine motility factor (AMF), can modulate cell motility (Weidner *et al.*, 1993;Nabi *et al.*, 1992).

1.1.2 Invasion and proteolysis

One family of enzymes that has been shown previously to play a role in tumour progression is the matrix metalloproteinase (MMP) family (Yana & Seiki 2002). The main function of MMPs, also known as matrixins, is to degrade extracellular matrix, including basement membrane in physiological functions, such as wound healing, bone resorption and mammary involution. MMPs, however, also contribute to pathological conditions

including rheumatoid arthritis and coronary artery disease (John & Tuszynski 2001). Tumour cells are believed to utilize the matrix-degrading capability of these enzymes to spread to distant sites (John & Tuszynski 2001). An important proteolytic event in the metastatic cascade appears to be degradation of basement membrane components. Some evidence indicates that MMPs and tissue inhibitors of MMPs are involved in the event and are essential for tumour cell invasion and angiogenesis (Ray & Stetler-Stevenson 1994).

Gelatinase A is reportedly associated with tumour spread when activated (Yu *et al.*, 1996). Some novel MMPs that localize on the cell surface and mediate the activation of progelatinase A have been identified and named membrane-type matrix metalloproteinase-1 and -2 (MT-MMP-1 and -2, respectively) (Takino *et al.*, 1995;Strongin *et al.*, 1995). MT-MMP-1 is overexpressed in malignant tumour tissues, including lung and stomach carcinomas that contain activated gelatinase A. The expression of MT-MMP-1 also induced binding of gelatinase A to the cell surface by functioning as a receptor. MT-MMP-1 and its family may play a central role in the cell surface localization and activation of progelatinase A. The tumour cells may use exogenous progelatinase A to mediate, in part, proteolysis associated with invasion and metastasis (Sato & Seiki 1996).

Cathepsin D is an acidic lysosomal protease present in all cells. Cathepsin D is overproduced both *in vitro* and *in vivo* in most breast cancer cells. In estrogen receptor positive and negative breast cancer cell lines, the mRNA coding for pro-cathepsin D is overexpressed (Garcia *et al.*, 1996). Transfection of an expression vector containing a human cathepsin D cDNA under the control of an SV40 promoter increases the clonigenic potential of rat tumourigenic cells when intravenously injected into nude mice (Garcia *et al.*, 1990;Rochefort *et al.*, 1990). Several retrospective clinical studies indicate a significant correlation between high cathepsin D concentrations in the cytosol of primary breast cancer and further development of clinical metastases (Saad *et al.*, 1998). The mechanism of cathepsin D action in facilitating metastasis is unknown and may involve proteolytic activity in an acidic compartment, and/or interaction with the Man 6P/IGFII receptor (Rochefort 1991).

The serine protease urinary plasminogen activator or urokinase (uPA) and urokinase receptor (uPAR), produced in abundance by many malignant cells, play a key role in cancer cell invasion and metastasis (Rabbani & Xing 1998). uPAR will be discussed in Section 1.2. uPA converts plasminogen to plasmin, which in turn activates procollagenases in cancer cells that can break down different components of the ECM and thereby promote cancer invasion and metastasis (Fisher *et al.*, 2000). Increased uPA levels were found in a variety of human cancers, in particular those of breast, prostate, and colon, and were shown to correlate with the invasive and metastatic potential of these malignancies (Fisher *et al.*, 2000;Rabbani & Xing 1998;Frandsen *et al.*, 2001). The levels of uPA have also proven to be a useful prognostic marker of tumour progression (Brunner *et al.*, 1994).

1.1.3 Dissemination of tumour cells and colonization at secondary sites

Cancer cells may spread via blood and/or lymphatic vessels in which they can move freely and reach local lymph nodes and distant organs. Some cellular interactions, such as the formation of aggregates with other cancer cells or with host cells, e.g. lymphocytes and platelets, may result in the formation of large cellular emboli, which are more readily trapped in the distant capillary bed (Kinjo 1978). The organ-specific metastasis may be the results of the combination of several factors, for example, the anatomical location of the primary cancer, the fertile environment of the organ, and the molecular heterogeneity on the surfaces of the vascular endothelium and tumour cells (Chambers *et al.*, 2000). To explain the selection by cancer cells of secondary sites for colonization, both physical and chemical processes were proposed. The physical process is based on the sizes of cancer cells, i.e. the cells are trapped in the first capillary bed encountered. However, it fails to explain the specific organ in which metastasis occurs. Thus, a chemical process has been proposed. It is suggested that the secondary sites provide chemoattractant chemokines acting as homing signals for cancer cells to attach, move into the underlying matrix and to colonise (Nicolson & Custead 1982;Muller *et al.*, 2001).

Once the tumour cells migrate to a secondary site, the cells have to survive and grow in

order to establish metastatic foci. The further growth of the cells is supported by angiogenesis and by local growth factor, which may or may not be specific to the host organ.

1.1.4 Haemostatic factors

There is considerable evidence that the haemostatic system is involved in the growth and spread of malignant disease. Coagulopathy and angiogenesis are among the most consistent host responses associated with cancer (Saaristo *et al.,* 2000). These two processes may in fact be functionally inseparable as blood coagulation and fibrinolysis, in their own right, influence tumour angiogenesis and thereby might contribute to malignant growth. Angiogenesis and the development of metastases are intrinsically connected (Saaristo *et al.,* 2000). Vascular endothelial growth factors (VEGF), and members of the angiopoietin family, which bind to the VEGF receptor (VEGFR) or the Tie-2 receptor, respectively, promote neovascularisation and the growth of cancer cells at a secondary site (Saaristo *et al.,* 2000). VEGF is a multifunctional cytokine that promotes endothelial cell proliferation and migration *in vitro* and angiogenesis in various models. There are at least two VEGF receptor tyrosine kinases, Flt-1 (VEGFR1) and KDR (VEGFR2) (Shibuya 2001). Both are expressed primarily on vascular endothelial cells. Although both receptors are essential for angiogenesis, KDR can mediate most VEGF activities. Elevated VEGF expression was detected in many tumours. VEGF level was also shown to have prognostic significance in breast, bladder, colon and stomach cancers (Gasparini 2000;Papamichael 2001;Arii *et al.,* 1999). Up-regulation of VEGF in MCF-7 cells, a human breast cancer cell line, resulted in faster growth of the tumours with many more blood vessels when the transfected cells were planted subcutaneously in nude mice (Zhang *et al.,* 1995).

In addition, tumour angiogenesis appears to be controlled through both standard and non-standard functions of such elements of the haemostatic system as tissue factor, thrombin, fibrin, plasminogen activators, plasminogen, and platelets. "Cryptic" domains can be released from these proteins through proteolytic cleavage, and act systemically as angiogenesis inhibitors (e.g., angiostatin, antiangiogenic antithrombin III). Various

components of the haemostatic system either promote or inhibit angiogenesis and likely act by changing the net angiogenic balance (O'Reilly *et al.*, 1996;Wojtukiewicz *et al.*, 2001;Rickles *et al.*, 2001). Removal of inhibiting anti-angiogenic factors led to the growth of dormant metastases (Kirsch *et al.*, 2000). For a number of cancers it has been shown that the dormant state of metastasis can be mediated through inhibition of angiogenesis. A number of endogenous inhibitors, such as angiostatin, endostatin, thrombospondin-1, have shown success in some experimental cancer therapeutic trials (Kirsch *et al.*, 2000;Scappaticci 2002).

Due to the complexity of metastasis, a large number of metastases-related genes and their products have been reported in the last decades. However, only a few products of the genes have been confirmed so far to possess metastasis-promoting properties using animal models. Some known metastasis-promoting genes will be discussed in next section.

1.2 Metastasis-promoting genes

1.2.1 Urokinase Receptor (uPAR)

Urokinase Receptor (uPAR), a glycosyl phosphatidylinositol (GPI)-linked protein, is a multifunctional surface receptor with signalling and adhesive capabilities (Roldan *et al.*, 1990). As outlined in Section 1.1.2, uPAR and its ligand, uPA, play an important role in tumour invasion. It was also found that uPAR interacts not only with its ligand, uPA, but also with members of integrin family (Wei *et al.*, 1996), with activation of several groups of intracellular kinases, and convergence on a specific mitogen-activated protein kinase (MAPK) pathway (Aguirre-Ghiso *et al.*, 2001). UPAR, as a 'facilitator' of the cell-surface-based plasminogen activation, generates a proteolytic cascade important for matrix degradation in cancer invasion and tissue remodeling. Like uPA, uPAR was overexpressed in many types of cancers. When uPAR was up-regulated in a rat breast cancer cell line using gene transfer techniques, the experimental cells showed a 4-to 5-fold higher invasive capacity through Matrigel compared with control cells in a Boyden chamber assay (Xing & Rabbani 1996). When the experimental cells were injected into the

mammary fat pads of syngeneic female Fischer rats, the animals developed large metastatic lesions in liver, spleen and lymph nodes, indicating uPAR has metastatic promoting properties at least in the system (Xing & Rabbani 1996).

1.2.2 E1AF

E1AF is a member of the ets oncogene family of transcription factors which contain a family-specific ETS-domain involved in the binding to DNA sites containing a central 5'-GGAA/T-3' motif (de Launoit *et al.*, 2000). Although the target genes of these transcription factors are multiple, up-regulation of E1AF, by transfection or by stimulating cells with HGF (Hanzawa *et al.*, 2000), is mainly accompanied by an increase of type IV collagenase (MMP-9) expression, which may lead to an increase of cell invasion (Hanzawa *et al.*, 2000;Habelhah *et al.*, 1999). Therefore, the most frequently studied role of E1AF concerns its involvement in the metastatic process.

In fact, E1AF is over-expressed in metastatic human breast cancer cells and mouse mammary metastatic cancer (de Launoit *et al.*, 2000). In human squamous cell carcinomas (SCC), E1AF was mostly detected in invasive SCCs, whereas the majority of SCCs not expressing E1AF showed an expansive growth pattern (Hida *et al.*, 1997). Another report showed that over half of the lung tumour specimens examined expressed E1AF mRNA while normal lung tissue and concomitant normal cells within tumours did not. When the E1AF gene was transfected into and expressed in non-small-cell lung cancer (NSCLC) cell lines lacking E1AF expression, cell motility and invasion were increased about 2-fold (Hiroumi *et al.*, 2001). Transfection of the non-invasive human breast cancer cell line MCF-7 with an E1AF expression plasmid resulted in induction of invasive and motile activities *in vitro*. It was also observed that tumours derived from the E1AF transfectants were highly invasive, suggesting that the E1AF might have metastasis-promoting properties (Kaya *et al.*, 1996). To test the possibility, E1AF was up-regulated in a non-metastatic fibrosarcoma cell line by transfection. The up-regulated E1AF was shown to contribute to an invasive phenotype including elevated MT1-MMP levels and enhanced cell migration *in vitro* (Habelhah *et al.*, 1999). After co-implantation with a gelatin sponge

in syngeneic mice, the transfected cell lines with high level of E1AF, exhibited enhanced tumourigenicity and pulmonary metastasis as compared with parental cells treated in the same way, indicating E1AF has metastasis-promoting potential (Habelhah *et al.*, 1999).

1.2.3 Human cutaneous fatty acid-binding protein

Human cutaneous fatty acid-binding protein (C-FABP) was shown to be at a 5-17 fold higher level in certain malignant prostate and breast carcinoma cell lines than in the benign cell lines from the same tissues (Jing *et al.*, 2000). Transfection of a *C*-FABP expression construct into the benign, nonmetastatic rat mammary epithelial cell line, Rama 37, and inoculation of the *C*-FABP expressing transfectants into syngeneic female Wistar-Furth rats produced a significant number of animals with metastases. These results have demonstrated that elevated expression of *C*-FABP can induce metastasis and suggest that *C*-FABP is a metastasis-inducing gene, and under suitable conditions, it may induce metastasis of some human cancers. Up-regulation of the *C*-FABP was shown to increase the level of VEGF in rat Rama 37 model system, suggesting VEGF may play a crucial role in the metastatic cascade in this particular system (Jing *et al.*, 2001).

1.2.4 Osteopontin

Osteopontin (OPN) is a calcium-binding phosphoprotein that is a prominent component of the mineralized extracellular matrices of bones and teeth (Denhardt & Noda 1998). OPN is characterized by the presence of a polyaspartic acid sequence and sites of Ser/Thr phosphorylation that mediate hydroxyapatite binding, and a highly conserved RGD motif that mediates cell attachment/signalling (Rodan 1995). The RGD motif in OPN lies between amino acid residues 125 and 168, interacting with αv/β3, αv/βv, αv/β1, α8/β1, and αv/β1, α4/β1 (Bayless *et al.*, 1998; Barry *et al.*, 2000; Bayless & Davis 2001). OPN is also found to be a substrate for two MMPs, MMP-3 (stromelysin-1) and MMP-7 (matrilysin) (Agnihotri *et al.*, 2001). OPN was also reported as a major transcriptional target of HGF, and OPN overexpression dramatically increases the motile and invasive responses to HGF (Medico *et al.*, 2001). Transcription factor, T-cell factor 4 (Tcf 4) was shown to inhibit the expression of OPN (El-Tanani *et al.*, 2001).

OPN is involved in diverse biological events, including developmental processes, wound healing, immunological responses, tumourigenesis, bone resorption, and calcification (Denhardt & Noda 1998). Recently, OPN has been found in many kinds of human cancers. For example, OPN was significantly overexpressed in hepatic cellular carcinoma (HCC) with capsular infiltration, compared with HCC without capsular infiltration. The OPN-positive cancer cells were often dispersed in the periphery of cancer nodules and were adjacent to stromal cells (Gotoh *et al.*, 2002). OPN was over-expressed in cancer cells of non-small cell lung carcinomas (NSCLC) (Zhang *et al.*, 2001). OPN was also found in about 70% of infiltrating ductal carcinomas of the breast, using immunohistochemical staining (Kim *et al.*, 1998; Rudland *et al.*, 2002). The expression of OPN in human breast cancer was also shown to correlate with a poor prognosis of breast cancer patients (Rudland *et al.*, 2002). Of the patients who have been classified as OPN-negative in cancer specimen, 94% were alive, but only 26% of those classified as OPN-positive were alive, after 19 years of follow-up, suggesting OPN could be a useful prognostic marker for breast cancer patients.

Increased levels of OPN have been detected in the blood of patients with metastatic carcinomas. The plasma OPN level was associated with the presence of metastases to bone and with other measures of tumour burden, and it was correlated independently and negatively with survival in several types of cancer (Hotte *et al.*, 2002). Up-regulation of OPN in rat mammary tumour-derived epithelial cell line, Rama 37 which yields benign, non-metastasizing adenomatous tumours in syngeneic Furth-Wistar rats, was shown to induce the metastatic properties in the Rama 37 cells in the syngeneic animal model (Oates *et al.*, 1996), indicating that OPN has metastasis-promoting propertities.

The molecular mechanism of OPN-induced metastasis is not clear. It was found that overexpression of OPN increased the cell motility and invasiveness of the non-invasive human mammary epithelial cell line, 21PT and also resulted in increased uPA mRNA expression (Tuck *et al.*, 1999). MMP-2 was also shown to play a direct role in

OPN-induced cell migration, invasion, and tumour growth. Both an MMP-2-specific antisense S-oligonucleotide and an MMP2-specific antibody were shown to reduce the tumour size of OPN-treated cells in nude mice. OPN-stimulated MMP-2 activation was shown to be through NF-kappaB-mediated induction of MT1-MMP (Philip *et al.*, 2001). OPN is also a ligand of the CD44 receptor, which mediates tumour cell adhesion, migration and metastasis formation (Weber *et al.*, 1996). OPN is a calcium binding protein (Denhardt *et al.*, 1995) so the overexpression of OPN may alter the calcium signaling.

1.3 Calcium ions and metastasis

Apart from OPN, many other calcium-binding proteins were also shown relating to tumour metastasis. Cell adhesion, as an important factor in tumour metastasis, requires Ca^{2+}. Two major adhesion receptor families, cadherins and selectins, are Ca^{2+}-dependent cell adhesion molecules as outlined above. Cell adhesion also triggers intracellular calcium signalling pathways (Dunican & Doherty 2000). Calcium signalling, as a universal signalling, is also involved in the regulation of cancer cell metastatic processes. For example, in many cases, binding of integrins to ECM triggers intracellular signalling pathways. The intracellular Ca^{2+} signalling participates in a positive feedback loop that enhances integrin-mediated cell adhesion (Sjaastad *et al.*, 1994), and transient changes in endothelial Ca^{2+} may govern multiple steps of tumour cell extravasation (Lewalle *et al.*, 1998). However, the regulatory roles of intracellular signalling mechanisms in these events are still poorly understood.

1.3.1 Calcium signalling

Calcium is a universal, intracellular secondary messenger that plays a regulatory role in processes or events, such as cell adhesion, motility, growth, secretion, apoptosis, necrosis, proliferation and differentiation, signal transduction, muscle contraction, the conduction and transmission of the nervous impulse (Kallenberg 2000; Berridge *et al.*, 1999; Berridge *et al.*, 2000b). Ca^{2+} operates throughout the life history of a typical cell: it triggers new life at fertilization, it controls many developmental processes. How can a simple ion such as Ca^{2+} control all these processes? The answer is that Ca^{2+} signals are enormously versatile,

thus Ca^{2+} can operate within small cellular compartments, or it can act more globally and pervade the entire cytoplasm of a cell and also penetrate organelles such as mitochondria and the nucleus. Ca^{2+} signals can also have durations lasting from microseconds to hours, and occur transiently or in a pulsed manner. The pulsed Ca^{2+} signal not only depends on amplitude but also on frequency. The oscillation of the Ca^{2+} signal is a very important aspect as it makes the signal more specific and meaningful (Dolmetsch *et al.*, 1998).

Intracellular Ca^{2+} is stored mainly in the endoplasmic reticulum (ER) or sarcoplasmic reticulum (SR) in muscle cells, where Ca^{2+} concentrations can be as high as 3mM (Ashby & Tepikin 2001). In some cells, the ER accounts for approximately 75% of the total intracellular Ca^{2+} reserve. Extending like a net over the entire cytoplasm, the ER determines, in great part, the generation of important Ca^{2+} signals that are involved in most vital functions of the cell. Mitochondria are the other important reserves of intracellular Ca^{2+}, accounting for the remaining 25% of the Ca^{2+} reserve in some cells such as endothelial cells.

Ca^{2+} signals result generally from the opening of Ca^{2+} channels or the activity of Ca^{2+} transporters. These are located either in the plasma membrane, or inside the cell on the ER or SR. The plasma membrane Ca^{2+} channels can be classified into different types, according to their activation mechanism: voltage-operated channels, receptor-operated channels, mechanically-activated channels and the so-called 'store-operated channels' that are opened following the depletion of internal Ca^{2+} stores (Berridge *et al.*, 2000a). Ca^{2+} release from the ER and SR occurs via three types of channel. Of these, inositol 1,4,5-trisphosphate (IP_3) receptors (Europe-Finner & Newell 1985) and ryanodine receptors (Bennett *et al.*, 1998) are the best characterised. A third type of channel, known as SCaMPER (sphingolipid Ca^{2+}-release-mediating protein of endoplasmic reticulum), seems to release Ca^{2+} in response to an increase in intracellular sphingolipid concentrations (Mao *et al.*, 1996). The differential expression of these Ca^{2+} entry or release channels allows cells to respond to a diverse range of stimuli and to produce Ca^{2+} signals that are tissue specific.

The release or entry of Ca^{2+} into the cytoplasm through the opening of different types of channels can result in local or global Ca^{2+} signalling. There are several advantages to using local Ca^{2+} signals, rather than global increases in Ca^{2+}, to control cell processes. For example, as the local Ca^{2+} signals have only a limited spatial range, and the Ca^{2+} concentration declines sharply with distance from the site of origin, regulation of cellular activities relies on close localization of the Ca^{2+} channels to their targets. This close proximity allows Ca^{2+} to have a highly specific effect (Berridge *et al.,* 1988). In addition, local Ca^{2+} signals can have a rapid effect at relatively low energy cost to the cells, in contrast to global Ca^{2+} changes. The limited number of Ca^{2+} ions used to generate local signals can be removed from the cytoplasm more rapidly than global Ca^{2+} signals, and without consuming as much ATP (Berridge 1990).

In addition to controlling the local functions of cells, local Ca^{2+} signals are responsible for the generation of global Ca^{2+} signals, such as waves and oscillations. Essentially, global Ca^{2+} signals arise via the co-ordinate recruitment of many elementary Ca^{2+} release and entry channels. The mechanisms to achieve a global Ca^{2+} signal, and the balance between Ca^{2+} influx and release, are cell-type specific. Thus different cell types use distinct Ca^{2+} signals, as appropriate to their physiology (Petersen 2000). The ability to use Ca^{2+} in different modes helps cells to achieve a multitude of signals varying in amplitude, frequency, kinetics and localization, and also to avoid the deleterious effects associated with extensive Ca^{2+} increases.

1.3.2 Calcium binding proteins

Ca^{2+} is probably the most evolutionary-ancient and energetically inexpensive second messenger. Cells have evolved many classes of intracellular Ca^{2+} binding proteins, which act to regulate the level of cytosolic Ca^{2+} and to transduce the intracellular Ca^{2+} signals. The diversity of Ca^{2+} binding proteins contributes a great deal to the versatility of Ca^{2+} signals. In order to understand the mechanism of the various responses evoked by calcium in the cell, the identification and characterization of a number of calcium receptors have

been undertaken in the past three decades. Advances in determining the amino acid sequence and three-dimensional structure of proteins have led to the description of two families of calcium-binding proteins, the annexin family (Barwise & Walker 1996a) and the EF-hand homologue family (Kretsinger 1973).

The annexins have a molecular weight of 35- or 67 kDa (Weinman 1991). The amino acid sequences of members of the annexin family show that each protein contains conserved internal repeats of about 70 amino acids. Mammalian annexins possess four or eight homologous internal repeats, which may be calcium and phospholipid-binding domains. The proteins are present in a wide range of tissues and cell types, with each cell type possessing all of, or a subset of, the proteins. The proteins are localized on the inner surface of the plasma membrane associated with the cytoskeleton and, in some cases also with intracellular structures and even nuclear (Barwise & Walker 1996b; Tzima *et al.,* 1999; Geisow *et al.,* 1990). Some members of the family are major substrates for tyrosine and/or serine kinases (Schmitz-Peiffer *et al.,* 1998). The precise functions of the proteins are largely unknown, but they are likely to play important roles in cellular regulation (Barwise & Walker 1996a). Previously suggested functions include inhibition of phospholipase A2 (Tzima *et al.,* 2000), membrane-cytoskeletal linkage and control of membrane fusion events in exocytosis (Gerke & Moss 2002). It has been also suggested that they may be involved in the regulation of cell surface receptors (Kim & Hajjar 2002; Brownstein *et al.,* 2001).

The other large group of Ca^{2+}-binding proteins is the EF-hand superfamily. The term EF-hand was first used by Kretsinger and Nockolds (Kretsinger 1973) nearly 30 years ago as a graphical description of the calcium-binding motif observed in parvalbumin. EF-hands have been identified in numerous calcium-binding proteins by the similarity of amino acid sequence and confirmed in some crystal structures. The EF-hand motif consists of two alpha helices, termed "E" and "F", joined by a calcium-binding loop (Kretsinger 1973). This structural motif has turned out to be widespread, and is found in a large number of protein families: some 66 subfamilies, more than 160 different Ca^{2+}-modulated proteins,

are known to date (Nakayama 2000).

Functional EF-hands occur usually in pairs. Most EF-hand motifs bind Ca^{2+}, occasionally some of them additionally bind Mg^{2+}, Zn^{2+} or Cu^{2+}(Groves & Palczewska 2001). EF-hand proteins undergo conformational changes upon binding of Ca^{2+} (Nelson & Chazin 1998). This event is a crucial step in many Ca^{2+}-dependent cellular processes. EF-hand proteins have a broad range of functions and they are important intracellular calcium sensors (Isobe & Okuyama 1988).

1.3.3 S100 protein family

One group of EF-hand-containing calcium-binding proteins is the S100 protein group, so-called because of their property of being soluble in 100% ammonium sulphate (Moore 1965). S100 proteins are mainly low molecular weight, acidic proteins (Zimmer *et al.*, 1995). In general, the S100 family members have molecular weights between 9 and 14 kDa (Donato 2001). However, three large proteins, profilaggrin, trichohyalin and repetin, have also been classified as S100 proteins because the S100 motif, the EF hand, is found within the sequence of each of these proteins (Markova *et al.*, 1993; Rothnagel & Rogers 1986; Krieg *et al.*, 1997). The low molecular weight S100 proteins have two distinct EF-hands with different affinities for calcium. Both EF-hands are flanked by hydrophobic regions and separated by a central flexible linker region.

1.3.3.1 Members of the S100 family

There are 21 members of the S100 family, 18 low molecular weight and 3 high molecular weight proteins, discovered so far. The alignment of the 18 low molecular weight S100 proteins is given in (Figure 1.1) to show the common arrangement of the structural features. The sequences in the 4 α –helices and *C*-terminal Ca^{2+} binding loop are highly conserved among all the members. However, the sequences in *N*-terminus, *C*-terminus, *N*-terminal Ca^{2+} binding loop and linker region between α-helix 2 and α-helix 3 are very diverse.

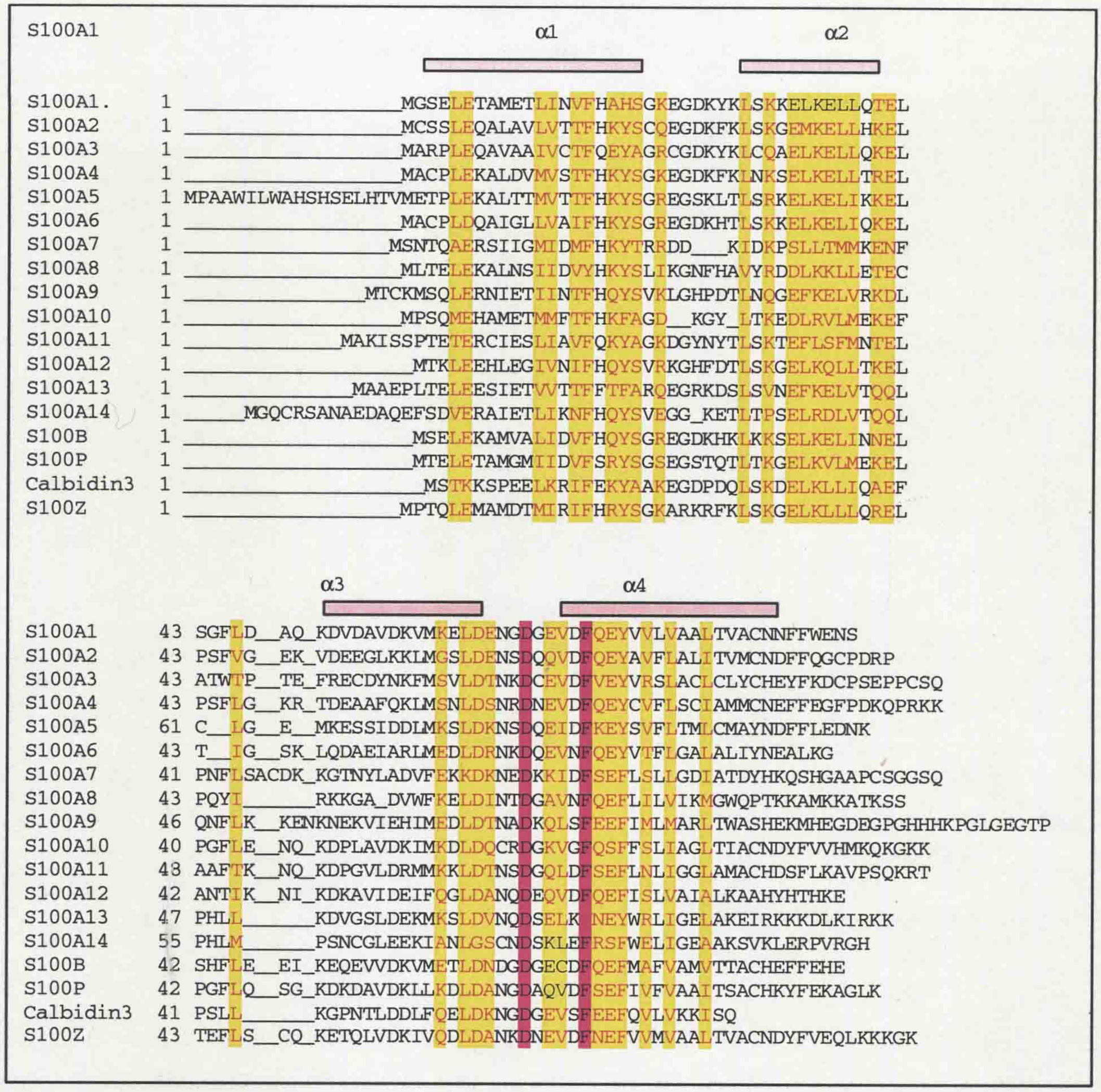

Figure 1.1. Sequence alignment of 18 members of the S100 family. The sequence alignment was generated by ESPript 2.0 program using human using human sequences obtained from Swiss-port database. Conserved residues are highlighted in yellow and red and fully conserved residues are highlighted in purple. Secondary structure (based on the apo-S100A1 NMR structure) is represented by pink filled rectangles for α-helices.

1.3.3.2 The structure and dimerisation of S100 proteins

A typical S100 protein consists of four α-helices and two β-sheets (Figure 1.2), which form

the backbone of the protein. Some residues in the backbone are highly conserved as shown in Figure 1.1. The Ca^{2+}-binding Loop 1 and Loop 2 are flanked by Helix 1 and 2, and Helix 3 and 4, respectively. In each loop, there is a β-sheet. The *N*-terminus and Linker region are the flexible regions and the residues in these regions are not highly conserved.

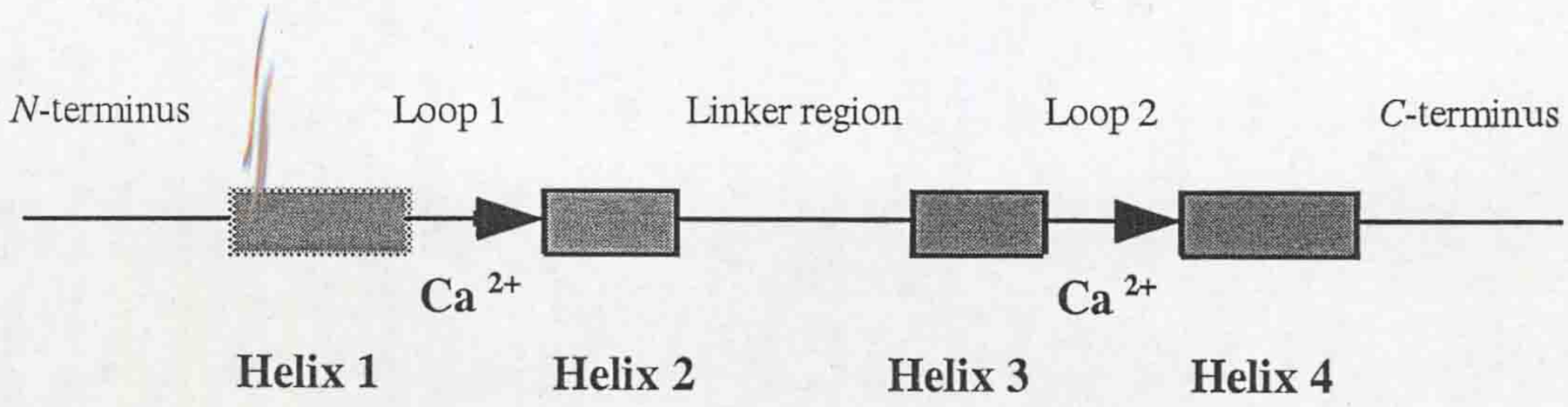

Figure 1.2. The diagram of the two-dimensional structure of S100 proteins ▭ α–helix ▶ β-sheet

The first typical 3D structure of S100 protein was for S100A6, characterised by Potts (Potts *et al.*, 1995a). Many other S100 protein structures have been published since. The basic structures of these S100 proteins are very similar. The recently determined crystal structure of S100P (Zhang *et al.*, 2003) is shown as an example (Figure 1.3) with main elements indicated. Two calcium-binding loops are closely located. On one side of the loops are helix 3 and helix 4 connected by linker region. On the other side of the loops are the helix 1 and helix 4, which are the main backbones of the structure.

Although the known structures of low molecular weight S100 proteins are very similar, there are also some differences between them. This is illustrated by the comparison between S100P and 6 other S100 proteins shown in Figure 1.4.

Most S100 proteins have the tendency to form dimers *in vitro* (Groves *et al.*, 1998). The first 3-dimensional structure of S100A6 homodimer characterised by Potts (Potts *et al.*, 1995b), revealing a symmetric homodimeric fold. The dimer interface is mediated primarily by hydrophobic interaction between side chains. Helix 4 and helix 4' form the

bulk of the dimer interface, from F70 to M82, packed antiparallel to each other. Residues in the *C*-terminus of helix 1, I13, F16, also contribute to the interface, making contacts with both helix 4 and helix 4'. The residues involved in the hydrophobic contacts are highly conserved, suggesting that many other S100 proteins could form dimers. The structure and dimer interface of S100P homodimer (Figure 1.5), which was crystallised by our collaborator (Zhang *et al.,* 2003), is very similar to that of S100A6. However, there are some exceptions. For example, Calbindin 3 is always monomer. S100B forms disulphide homodimers (Kilby *et al.,* 1996). There are also several reports to show that S100 proteins can form heterodimers, such as S100A8/S100A9 (Bhardwaj *et al.,* 1992), S100A1/S100B, S100B/S100A11, S100B/S100A6, and S100A1/S100A4. However, no 3D structure of S100 heterodimer has been resolved yet.

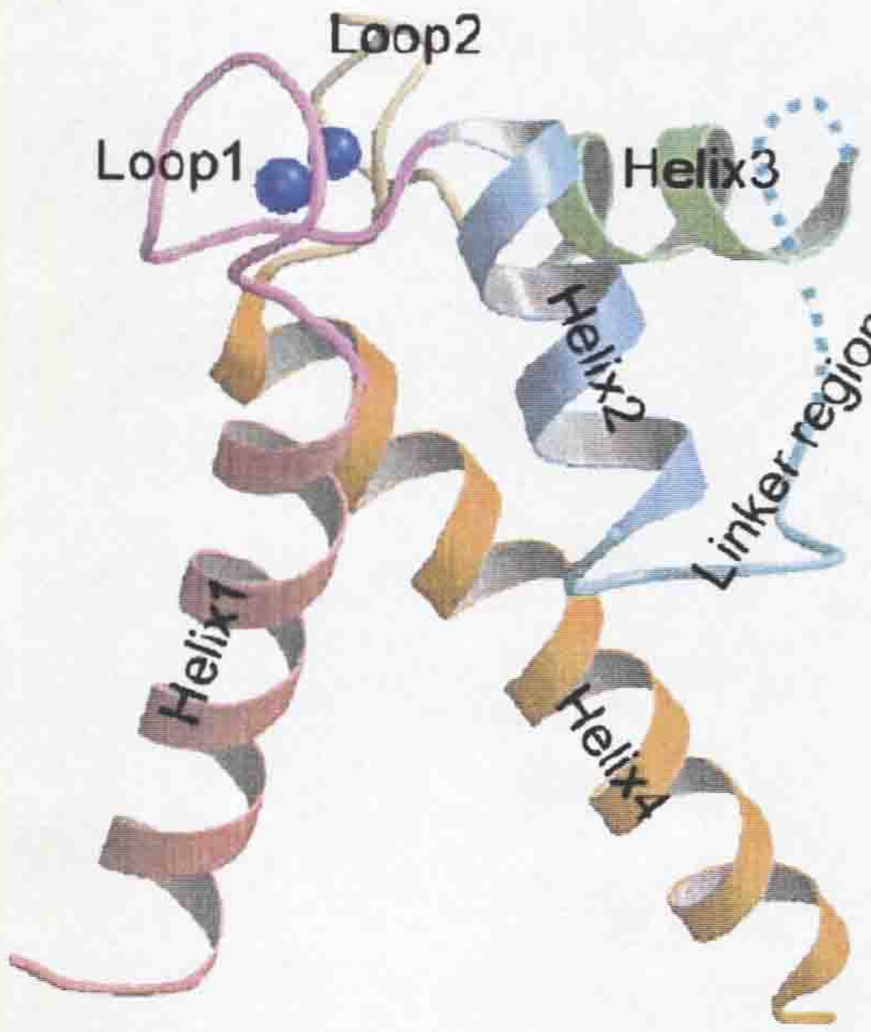

Figure 1.3. Ribbon representation of the S100P monomer. Calcium ions are in blue. Helices one, two, three and four are shown in flesh, lilac, pale-green and orange, respectively. Loops one and two are shown in pink and khaki. The linker region is in sky-blue, part of which is invisible in the crystal structure and thus marked with a broken line. The image was provided by Hongmei Zhang, Protein Science Laboratory, the University of Qinghua, as part of a collaborative study.

A

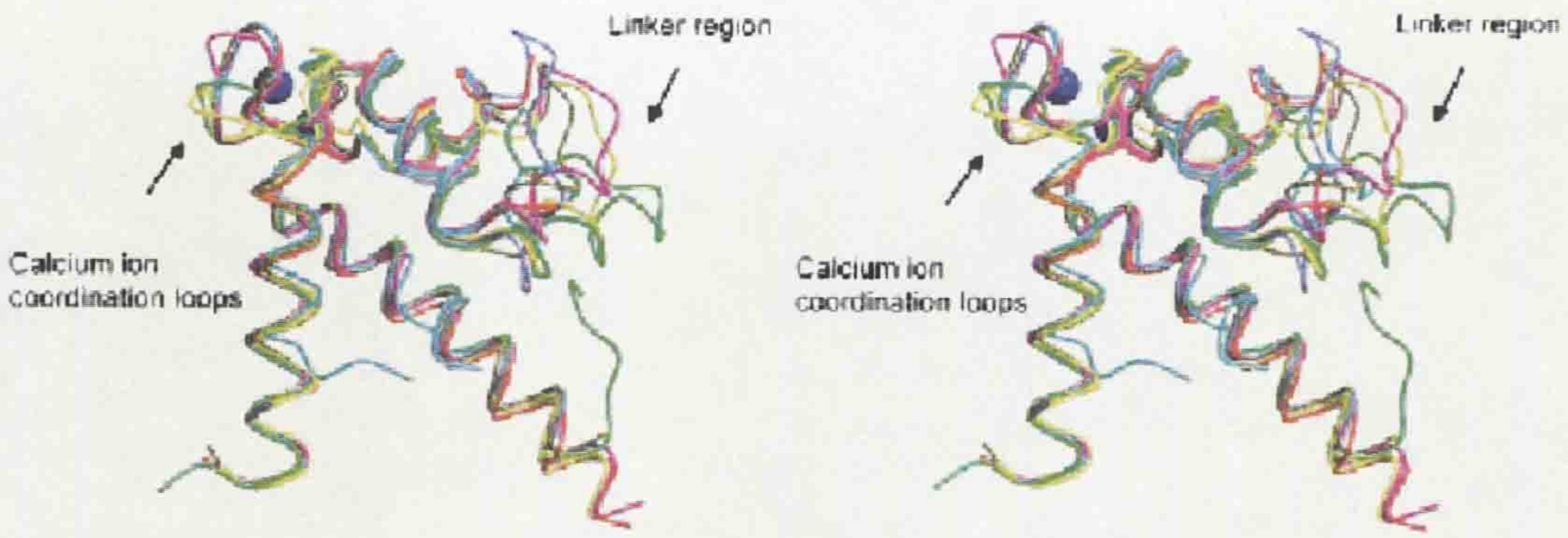

B

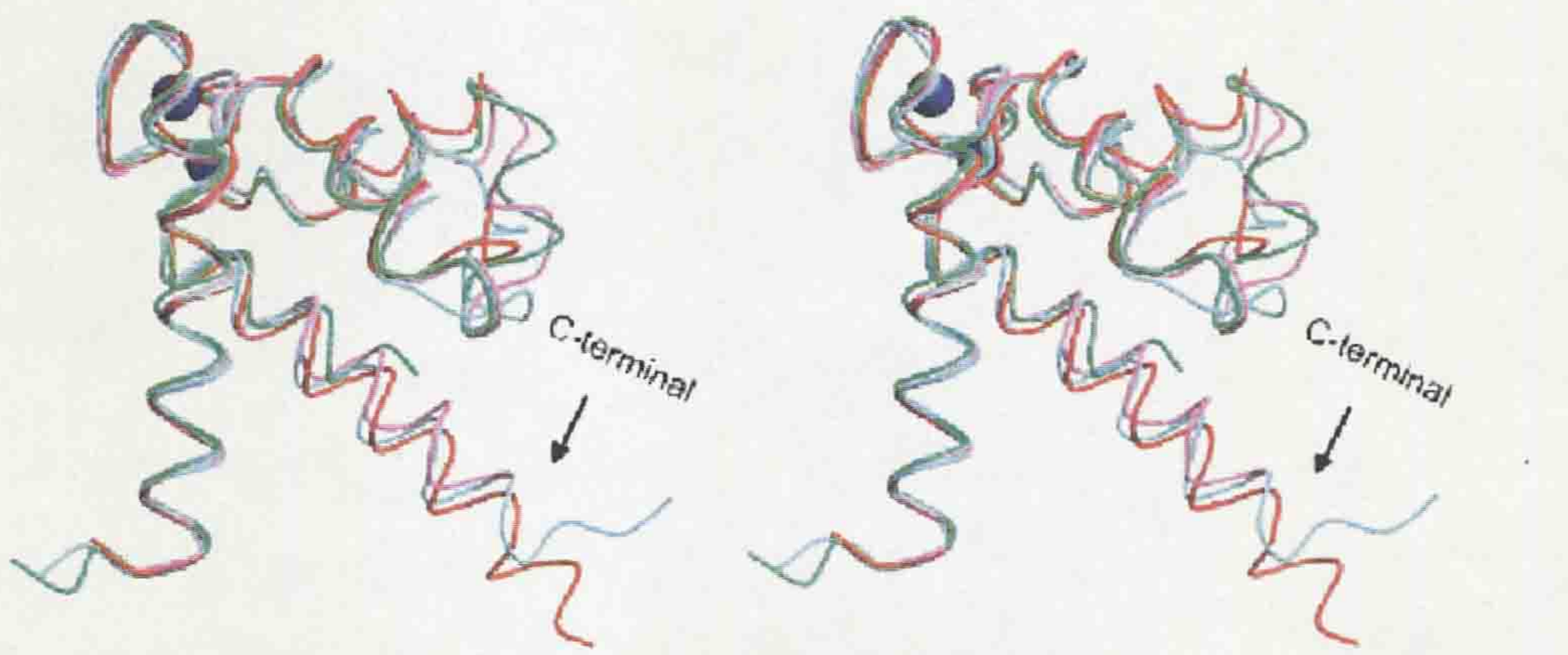

Figure 1.4. Comparison of 7 known three-dimensional structures of S100 proteins (Zhang *et al.*, unpublished data). Three-dimensional monomer backbone structures of S100 proteins were overlaid using CCP4 software. In (a), the structure of S100P (red), S100B (lilac), S100A7 (green), S100A11 (magenta), S100A10 (yellow), calcyclin (khaki) and calbindin (cyan) are compared and shows the overall similarity of these proteins with r.m.s.d values close to 1.0 Å, which mainly differ in the linker region. However, both S100A7 and Calbindin also have different *C*-terminal regions. (b) The structure of S100P (red) is compared with S100A8 (sky-blue), S100A9 (aquamarine) and S100A12 (pink) to show the similarity of the overall shape with r.m.s.d values above 1.1 Å, but with different structures of the *C*-terminal region and linker region. Calcium ions are shown in blue.

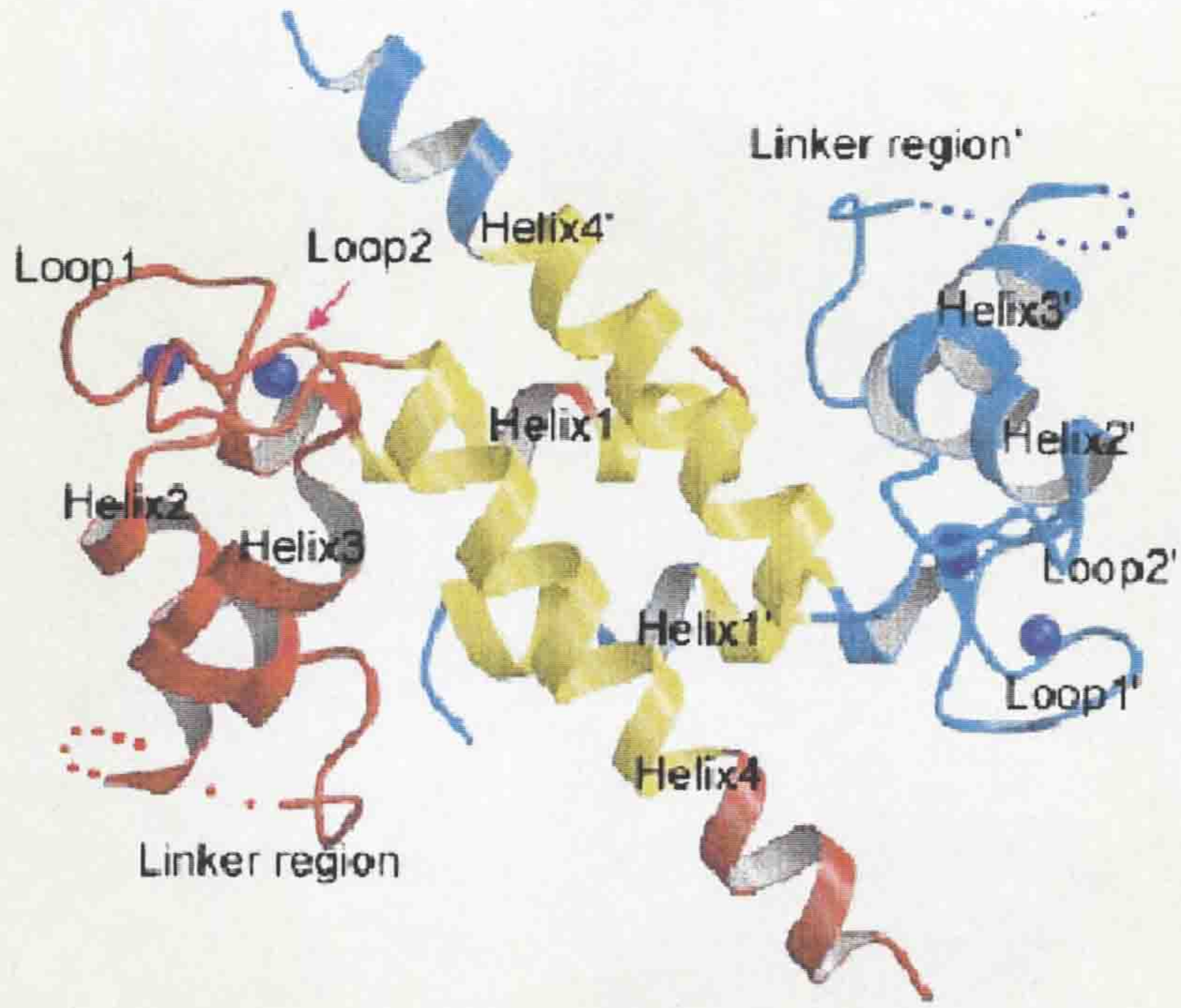

Figure 1.5. Ribbon model of the S100P dimer (Zhang *et al.*,., unpublished data). Two monomers are shown in red and royal blue respectively. Calcium ions are the blue spheres. Regions of contact between the subunits are marked in yellow.

1.3.3.3 Intracellular localisations and tissue distributions

Many of the S100 proteins are located in the cytoplasm of the cells, some are located in the nucleus, while others have been reported to occur in both the cytoplasm and the nucleus, and some are associated with cell membranes or with the cytoskeleton (Takenaga *et al.*, 1994b). For example, S100A1 and S100A4 are found predominantly in the cytosol of human smooth muscle cells (Takenaga *et al.*, 1994b). They are found strongly associated with the sarcoplasmic reticulum and with actin stress fibres in rat mammary cell lines (Davies *et al.*, 1993a; Gibbs *et al.*, 1995). S100A6 has been shown to be located in both the cell nucleus and the cytoplasm in human smooth muscle cell lines cells, where it associates with sarcoplasmic reticulum. When the intracellular Ca^{2+} concentration was increased by treatment of the cells with thapsigargin, S100A1, A4 and A6 became concentrated in the sarcoplasmic reticulum forming specific vesicular structures (Mandinova *et al.*, 1998). On the other hand, S100A2 is solely located in the nucleus (Shrestha *et al.*, 1998) under these conditions. The expression of S100 proteins can be cell type specific. For example, S100A1 and S100B occur mainly in neurons (Song & Zimmer 1996; McAdory *et al.*, 1998), however S100A1 is a major protein in muscle cells in mammals. S100A8 and S100A9 occur mainly in neutrophils and activated macrophages (Doussiere *et al.*, 2002). In order to clarify the biological roles of S100 proteins in cells, many studies have been carried out to try to identify their target proteins.

1.3.3.4 Interactions and possible target proteins

An increasing body of evidence indicates that many of the S100 proteins interact with cytoskeletal proteins and may serve as potential regulators of the dynamics of cytoskeleton (Selinfreund *et al.*, 1990). S100B and S100A1 have been reported to interact with tubulin and to block the self-assembly of microtubules as well as stimulating microtubule disassembly in brain extract (Hesketh & Baudier 1986). S100B and S100A1 also interact with type III intermediate filament subunits, GFAP and desmin, thereby inhibiting the self-assembly of the filaments (Bianchi *et al.*, 1994). S100A10 interacts with annexin II

(Thiel *et al.,* 1992) and promotes the annexin-dependent bundling of F-actin (Jones *et al.,* 1992; Kaczan-Bourgois *et al.,* 1996). S100A8, S100A9 and S100A12 translocate between the plasma membrane and vimentin intermediate filaments in monocytes and granulocytes upon changes in the concentration of cytosolic calcium ions (van den Bos *et al.,* 1996). All of the above observations suggest strongly that some S100 proteins respond to dynamic changes in the cytoskeleton and in cell morphology.

Some S100 proteins have been reported to interact with enzymes and to affect their activities. For example, S100A1 and S100B interact with fructose-1,6-bisphosphate aldolase (energy metabolism), phosphoglucomutase (energy metabolism), and membrane-bound guanylate cyclase (dark-adaptation of photoreceptors) and usually stimulate their activities, except that S100A1 inhibits the phosphoglucomutase (Landar *et al.,* 1996). S100A1 also inhibits glycogen phosphorylase (energy metabolism) (Zimmer and Dubuission 1993) and actomyosin ATPase (Zhao *et al.,* 2000). S100A8/S100A9 in myeloid cell inhibits casein kinases I and II, which are involved in cell maturation (Murao *et al.,* 1989).

It is well documented that S100 proteins have the ability to modulate phosphorylation of a number of cellular proteins (Baudier & Cole 1988; Baudier *et al.,* 1992; Lin *et al.,* 1994; Sheu *et al.,* 1994). For example, S100A1 activates *in vitro* the myosin-associated giant protein kinase, twitchin from *C. elegans*, in a calcium-dependent manner (Heierhorst *et al.,* 1996). The S100A1-binding site is a part of an autoregulatory sequence, which is responsible for intrasteric autoinhibition of twitchin kinase. In higher organisms, calcium-dependent interaction of S100A1 with MyoD (a member of the myogenic basic helix-loop-helix transcription factors) inhibits the phosphorylation of MyoD by PKC as well as the MyoD DNA binding activity (Baudier *et al.,* 1995). S100B was shown to be involved in microtubule-associated tau protein phosphorylation by calcium/calmodulin-dependent protein kinase II (Baudier & Cole 1988). Either the S100B or a mixture of S100A1 and S100B, both from a brain glial cell source, inhibited *in vitro* phosphorylation of purified F1/GAP43 by PKC in a dose-dependent manner (Sheu *et al.,*

1994a). S100B inhibition is thus substrate-selective and the effect of S100B on phosphorylation could not be explained by a direct inhibition of kinase activity (Sheu *et al.*, 1994a). From these observations mentioned above, the binding of S100 proteins to kinase substrates could be considered a general mechanism of S100 proteins in modulating protein phosphorylation.

S100 proteins have also been found to interact with another proteins. For example, S100B and S100A4 interact with p53, tumour suppressor protein and inhibit p53-dependent transcriptional activation (Delphin *et al.*, 1999;Grigorian *et al.*, 2001). S100A1, S100B, S100A10 and S100A11 interact with annexins (Garbuglia *et al.*, 2000;Rety *et al.*, 2000). S100A1 and S100B interacts with τ proteins that are associated with Alzheimer's disease. S100A1 binds to the ryanodine receptor and stimulates Ca^{2+}-induced Ca^{2+} release in skeletal muscle (Treves *et al.*, 1997).

Many S100 proteins also have potential extracellular roles. S100B, S100A1 and S100A4 have been reported to bind a receptor for advanced glycation end products RAGE (Schmidt & Stern 2001), and to stimulate neurite extension (Hofmann *et al.*, 1999;Huttunen *et al.*, 2000). S100B also stimulates astrocyte proliferation, neuronal apoptosis, IL-6 secretion by neurons, nitric oxide synthase secretion by astrocytes and microglia (Huttunen *et al.*, 2000;Donato 2001). S100A2 and S100A7 have been reported to act as a chemotactic agent for eosinophils and $CD4^+$ lymphocytes *in vitro*, respectively while S100A10 inhibits blood coagulation, (Komada *et al.*, 1996; Jinquan *et al.*, 1996). S100A12 is a chemotactic agent for neutrophils and macrophages *in vitro* (Miranda *et al.*, 2001).

In general, the interactions of S100 proteins with their target proteins are calcium-dependent. However, some interactions, such as S100A1 with aldolase A (Landar *et al.*, 1998) are calcium-independent, suggesting S100 proteins play roles not only in the calcium signal transduction pathways but also in other cellular processes.

1.3.3.5 S100 proteins and human diseases

S100 proteins are not only involved in physiological processes but are also associated with many human diseases. For example, high levels of S100B have been found in the brain tissues of patients suffering from Down's syndrome and Alzheimer's disease (Sheng *et al.*, 1994). Patients with Down syndrome characteristically have an extra copy of chromosome 21, the location of the human S100B gene (Allore *et al.*, 1988). This is consistent with the elevated level of S100B protein in this disease. S100A8 (MRP8) and S100A9 (MRP14) occur mainly in neutrophils, activated macrophages and endothelial cells in some inflammatory diseases and in the epidermis in psoriasis (Semprini *et al.*, 2002). The S100A8/S100A9 heterodimer has been suggested to regulate several steps of the inflammatory response (Kerkhoff *et al.*, 1998). The heterodimer is also found in body fluids in inflammatory conditions (Sorg 1992).

S100P and S100A9 are found to be overexpressed in both ulcerative colitis and Crohn's disease (Lawrance *et al.*, 2001). S100P is also found to be one of the overexpressed genes in the immortal MCF-10F, a human breast epithelial cell line, when compared with the mortal S130 cell line, the mortal counterpart of MCF-10F. In addition, S100P is highly expressed in chemically-transformed breast epithelial cell lines (BP1E and D3.1), breast cancer cell line T47D, as well as in three invasive ductal carcinomas, in comparion to their normal adjacent tissue (Guerreiro Da Silva *et al.*, 2000). The application of subtractive suppressive hybridization (SSH) techniques has identified S100P as being a differentially-expressed gene in three doxorubicin-resistant colon carcinoma cell lines (LoVo DxR, ARH D60 and KB-V1) in comparison with the drug-sensitive parental cell lines (Bertram *et al.*, 1998). Using a differential display method, S100P was found to be down-regulated in an androgen-responsive prostate cancer cell line after 30 hr of androgen deprivation. S100P is also dysregulated in other androgen-independent prostate cancer cell lines (Averboukh *et al.*, 1996). In tissue microarrays (TMA) analysis, one of the most highly overexpressed mRNAs in hormone-refractory CWR22R xenografts was the S100P mRNA, which was significantly associated with progression in clinical tumours ($P < 0.001$)

(Mousses *et al.*, 2002).

The levels of seven different S100 proteins (S100A1, S100A2, S100A3, S100A4, S100A5, S100A6, and S100B) have been determined immunohistochemically in the epithelial and connective tissues of a series of 35 specimens of colon carcinomas (Bronckart *et al.*, 2001). S100A2, S100A3, and S100B proteins were detected in normal colon tissues. The level of S100A6 increased in epithelial cells along with the increase in malignant characteristics (Maelandsmo *et al.*, 1997; Komatsu *et al.*, 2000a; Komatsu *et al.*, 2000b). The node-positive cancers failed to express S100A1; whilst half of the node-negative specimens did (Bronckart *et al.*, 2001), thus suggesting that S100A1 is not positively correlated with tumour metastasis. The levels of S100A5 were similar in epithelial tissues of different malignancy (Bronckart *et al.*, 2001). Another report showed that S100A1 and S100A2 could be detected in only a few normal tissues, whereas S100A4, S100A6, and S100B were expressed at higher levels in several kinds of cancer tissues (Ilg *et al.*, 1996). Since one S100 protein, S100A4 has been showed to have metastasis-promoting properties (Davies *et al.*, 1993a), great efforts have been made for over a decade in order to clarify its roles and the mechanisms in tumour progression.

1.4 S100A4

S100A4, also called p9Ka, Mts1, pEL98, 18A2, CAPL and 42A, is a typical S100 calcium-binding protein (Barraclough *et al.*, 1982). It was first discovered in derivative cells of rat mammary tumour-derived cell lines (Barraclough *et al.*, 1982; 1987, 1988). The S100A4 gene is located on chromosome 1q21 within the S100A gene cluster (Engelkamp *et al.*, 1993).

1.4.1 Intracellular localisation

The majority of immunoreactive staining for S100A4 is located in the cytoplasm of cells. In elongated myoepithelial-like cells, the pattern of immunofluorescent staining indicates its association with the cytoplasmic filamental structures. The identical pattern of staining for S100A4 and phalloidin staining in dual fluorescent labelling experiments suggested the

co-localisation of S100A4 and the actin-myosin filaments in the cells (Davies *et al.*, 1993b;Gibbs *et al.*, 1995). In human smooth muscle cells, S100A4 is relocated to the sarcoplasmic reticulum round the nucleus when the intracellular calcium is increased (Mandinova *et al.*, 1998).

1.4.2 Tissue distributions

S100A4 protein is expressed in the majority of rat tissues and in a diverse range of cell types, which include smooth muscle, brown adipose tissue, liver, some absorptive and keratinized epithelia, the acid-secreting parietal cells of the stomach, the neuronal cells within plexuses of the autonomic nervous system, and a proportion of cells of the immune system in spleen, lymph nodes, bone marrow, and blood (Gibbs *et al.*, 1995). S100A4 is found widely in both arteries and veins, particularly in the smooth muscle and in the endothelium of smaller vessels (Gibbs *et al.*, 1995). Mouse S100A4 (Mts1) immunoreactivity is also reported to be present only in white matter astrocytes in the intact spinal cord. Injury of sciatic nerve or dorsal root induced a marked and prolonged up-regulation of mouse S100A4-immunoreactivity in astrocytes in the region of the dorsal funiculus containing the central processes of the injured primary sensory neurons (Kozlova & Lukanidin, 1999). *In situ* hybridization of mouse embryos has shown the expression of Mts1 mRNA to be highest in trophoblast cells of an 8-day old embryo. In normal adult mouse tissues, immunocytochemistry reveals that Mts1 occurs in T cells in the thymus, spleen (Ford & Zain 1995) and appendix (Taylor *et al.*, 2002).

1.4.3 Interactions

It has been reported that S100A4 protein interacts *in vitro* with actin microfilaments, tropomyosin, and particularly non-muscle myosin heavy chains (Kriajevska *et al.*, 1994; Takenaga *et al.*, 1994c; Ford & Zain 1995). Although immunofluorescent staining shows that S100A4 colocalizes with stress fibres in fixed cells, no evidence for these interactions have been observed *in vivo*. In experiments *in vitro*, non-muscle myosin A has been reported to be a target for S100A4 (Kriajevska *et al.*, 1994). The mouse S100A4 (Mts1)-binding site is located within a 29-amino acid region at the *C*-terminal end of the

myosin heavy chain (within amino acids 1909-1937). Two-dimensional phosphopeptide analysis showed that Mts1 protein inhibits protein kinase C (PKC) phosphorylation of the platelet myosin heavy chain at Ser-1917 (Kriajevska *et al.,* 1998). High concentrations of S100A4 could disturb the formation of myosin filaments and inhibit the ATPase activity of myosin (Ford *et al.,* 1997). Moreover, the interaction of mouse S100A4 (Mts1) with the human platelet myosin or *C*-terminal fragment of the myosin heavy chain inhibits phosphorylation of the myosin heavy chain by casein kinase II *in vitro* (Kriajevska, *et al.,* 2000). Thus it has been suggested that Mts1 might also directly bind the beta subunit of casein kinase II, thereby modifying the enzyme's activity (Kriajevska *et al.,* 2000).

Studies have also shown that mouse S100A4 expression levels correlate with increased levels of detectable p53 in B16 murine melanoma (Parker *et al.,* 1994). Moreover, it has been reported recently that Mts1 binds to the extreme end of the *C*-terminal regulatory domain of p53 (Grigorian *et al.,* 2001) using several *in vitro* and *in vivo* approaches: co-immunoprecipitation, affinity chromatography, and Far Western blotting. The mouse S100A4 protein inhibits phosphorylation of the full-length p53 *in vitro* and its *C*-terminal peptide by protein kinase C, but not by casein kinase II. The Mts1 binding to p53 interferes with the DNA binding activity of p53 *in vitro* and reporter gene transactivation *in vivo*, and therefore this inhibition may have a potential regulatory function. Differential modulation of p53 target genes (p21/WAF, bax, thrombospondin-1, and mdm-2) transcription was observed upon Mouse S100A4 induction in tetracycline-inducible cell lines expressing wild type p53. Mouse S100A4 is also reported to cooperate with wild type p53 in the induction of apoptosis (Grigorian *et al.,* 2001).

A very recent report has shown that S100A4 interacts with the *N*-terminal half of MetAP2 (methionine aminopeptidase 2) a protein with peptidase activity, using yeast two-hybrid and other methods, such as pull-down assays and co-immunoprecipitations. The S100A4 binding site has been mapped to the region between amino acid residues 170 and 229 of MetAP2 (Endo *et al.,* 2002). The binding of S100A4 did not affect the methionine aminopeptidase activity of MetAP2 *in vitro*, but regulates MetAP2 intracellular

localization.

1.4.4 S100A4 and metastasis in model systems

The levels of S100A4 have been extensively investigated in different cell lines and tumour specimens. Higher levels of expression of S100A4 have been detected in specimens of breast cancer (Rudland *et al.*, 2000;Albertazzi *et al.*, 1998), in breast cancer cell lines (Lloyd *et al.*, 1996), human bile duct adenocarcinoma cell lines (Katayama *et al.*, 2000) and of colorectal adenocarcinoma (Takenaga *et al.*, 1997b), of pancreatic carcinomas (Rosty *et al.*, 2002), of esophageal squamous cell carcinoma (Ninomiya *et al.*, 2001), of gall bladder cancer (Nakamura *et al.*, 2002), of urinary bladder cancer (Davies *et al.*, 2002), of gastric adenocarcinoma (Yonemura *et al.*, 2000;El-Rifai *et al.*, 2001) , and of non-small cell lung cancer (Kimura *et al.*, 2000). The more important finding from these studies is that the levels of S100A4 are associated with metastasis in many of these cancers mentioned above. These observations have established a correlation of S100A4 with the level of malignancy in some tumours as well as with their metastases. However, it is hard to tell from these studies whether S100A4 is a causative factor in cancer metastasis or merely a passenger change. To establish a possible cause and effect relationship between S100A4 and metastasis, animal models have been employed as described below.

Syngeneic rat model. Rama 37, a benign rat mammary epithelial cell line (Dunnington *et al.*, 1983) was transfected with an expression plasmid, pSV2neo containing the rat S100A4 gene under the control of the SV40 large T Antigen promotor. These transfected cells produced tumours when injected at subcutaneous sites in the mammary glands with a shorter median latent period than the tumours produced by the parental untransfected Rama 37 cells in syngeneic rat hosts (Davies *et al.*, 1993a). The transfected cells yield a higher incidence of tumours than untransfected Rama 37 cells, many of which metastasize to lungs and/or lymph nodes in syngeneic rats (Davies *et al.*, 1993a; Barraclough *et al.*, 1998). The high level of S100A4 and the metastatic potential were maintained when the cells from a metastasis were re-injected into syngeneic rats (Davies *et al.*, 1993a). Transfection of a normal mammary-derived cell line, Rama 704, with the expression

vector for S100A4 induced neither tumours nor metastasis (Barraclough 1998). In a similar experiment, Rama 37 cells were transfected with the expression vector pSV2*neo* containing the human S100A4 gene (Lloyd *et al.,* 1998). The cells, which expressed a high level of human S100A4 mRNA, induced metastasis, whereas the cells transfected with the same vector but expressed an undetectable level of human S100A4, did not induce any detectable metastases when injected subcutaneously. In a bladder cancer system, overexpressing S100A4 in transfected MYU-3L cells produced primary tumours at similar frequencies and latencies to the parental cell line, but in addition induced a significant number of metastatic lesions primarily in the para-aortic lymph nodes or lungs (Levett *et al.,* 2002). Expression of S100A4 protein in the primary tumours was heterogeneous, but was stronger and more consistent in the metastases, suggesting that transfectants overexpressing S100A4 possess an enhanced ability to form the metastatic lesions in this rodent model of bladder cancer (Levett *et al.,* 2002).

Nude mouse model. Transfection of estrogen-responsive human breast cancer MCF-7 cells with the Mouse S100A4 gene under the control of a strong constitutive promoter conferred the ability for hormone-independent growth in nude mice (Grigorian *et al.,* 1996). Tumours derived from mouse S100A4 transfectants showed local invasion when the cells were transplanted into surrounding muscle and adipose tissues and metastasis to regional lymph nodes and lungs. These characteristics are rarely observed with the parental MCF-7 cells. Electron-microscopic analysis of MCF-7/mouse S100A4 cells showed structural changes in anchoring junctions, particularly in intermediate filament attachment sites (Grigorian *et al.,* 1996).

Transgenic mouse model. Rat S100A4 (p9Ka) acts synergistically with MMTV-*neu* in inducing malignant tumours in p9Ka and MMTV-*neu* bitransgenic mice. The mice expressing both rat S100A4 (p9Ka) and *neu* proteins had a slightly earlier incidence of palpable mammary tumours than the MMTV-*neu* offspring and specifically exhibited macroscopic metastatic lesions in the lungs. The rat S100A4 transgene is expressed in primary and secondary lesions of the bitransgenic offspring and its expression is

particularly associated with regions of invasion of primary lesions and metastases (Davies *et al.*, 1996). The parental MMTV-neu expressing animals produce primary tumours and no metastases whilst the p9Ka expressing parents produce no phenotype at all (Davies *et al.*, 1995). In another experiment, the mouse S100A4 gene, under the control of the MMTV promoter results in mouse S100A4 overexpression in the lactating mammary gland of transgenic mice. Animals bearing the transgene appear phenotypically normal. The Mouse S100A4 transgenic mice were then mated with the GRS/A strain, which is characterized by high incidence of mammary tumours and rarely metastasize. The mice bearing hybrid GRS/A-mouse S100A4 females were found to develop secondary tumours in the lungs (Ambartsumian *et al.*, 1996).

A further demonstration that S100A4 is able to induce metastasis is the use of antisense RNA to the S100A4 gene to suppress the expression of S100A4 in highly metastatic Lewis lung carcinoma cells. The antisense mRNA-transfected cells do show a reduced incidence of metastasis (Takenaga *et al.*, 1997a). Similarly transfecting a hammerhead ribozyme directed against S100A4 mRNA into S100A4 highly expressing osteosarcoma cells suppressed the ability to give rise to skeletal metastases upon intracardial injection into nude mice (Maelandsmo *et al.*, 1996). From the above experiments, it is clear that S100A4 can function as a tumour metastasis-promoting gene in animal models.

Further studies have evaluated the clinical significance of S100A4 in prognosis of patients with breast or other cancers. The association of S100A4 with patient survival was first investigated in primary tumours from a group of 349 patients treated between 1976 and 1982 for stage I and stage II breast cancer. After 19 years of follow-up, eighty percent of the S100A4-negative patients but only 11% of the S100A4-positive patients were alive. The former had a median survival of >228 months and the latter 47 months (Rudland *et al.*, 2000).

S100A4 has also been found to be associated with malignancy and metastasis in many other cancers. Overexpression of S100A4 has been detected in pancreatic carcinoma cell

lines (18/19, 95%) and tumour samples, 57 of 61 invasive pancreatic carcinoma (93%). In contrast, 3 of 18 high-grade pancreatic intraepithelial neoplasias (17%), and 0 of the 69 low-grade pancreatic intraepithelial neoplasias (0%) expressed S100A4 protein (Rosty *et al.*, 2002), whereas normal pancreatic tissue and tissue affected by chronic pancreatitis did not show any immunofluorescent staining. Expression of S100A4 was associated also with poor differentiation of the pancreatic adenocarcinomas (Rosty *et al.*, 2002). Significantly higher levels of S100A4 were also reported in esophageal tumour tissues than in the corresponding normal esophageal mucosa. Patients with S100A4-positive esophageal carcinoma had significantly poorer prognosis than those with S100A4-negative carcinoma (Ninomiya *et al.*, 2001). In a recent study, 25 of 60 gall bladder cancers were positively stained for S100A4. The 5-year survival rate of the group staining positively for S100A4 was significantly worse than that of the group staining negative for S100A4 (Nakamura *et al.*, 2002). In colon cancer, the level of S100A4 mRNA was significantly higher in carcinomas compared to normal specimens (Mann-Whitney U-test, P=0.05), and in liver metastases compared to carcinoma specimens (P=0.039) (Taylor *et al.*, 2002). The latter comparison included seven liver metastases and their matched primary carcinomas (P<0.001) from the same patient. Using *in situ* hybridization and immunocytochemistry techniques, S100A4 was shown to be present in both carcinoma cells and in T lymphocytes in the malignant specimens (Taylor *et al.*, 2002). Moderate or strong expression of immunoreactive S100A4 was found in 28% of 101 bladder tumours and moreover, staining for S100A4 was more frequently observed in invasive bladder tumours than in non-invasive tumours. In invasive tumours, staining for S100A4 was usually strongest in invasive regions and in single infiltrating cells. Statistically significant associations were found between immunocytochemical staining for S100A4 and metastasis and reduced patient survival (Davies *et al.*, 2002).

The combination of these experiments and observations, strongly suggests that S100A4 plays an important role in tumour metastasis, not only in animal models but also in many types of human cancers. Therefore, S100A4 becomes a very important molecule in the field of tumour metastasis. However, there is a little information on the roles and the

molecular mechanisms of S100A4 in cancer progression and metastasis.

1.5 Aim of this project

In order to understand the mechanisms of S100A4 in tumour metastasis, this project will focus on the interactions of S100A4 with known and unknown partners and the biological effects of those interactions.

Chapter Two

Material and Methods

2.1 Reagents

2.1.1 Reagents for molecular biology

Regents	Supplier
Agarose	Pharmacia
Ampicillin	Sigma
Bacto-agar	Difco
Bromophenol blue	Fisons
Caesium chloride	Sigma
Calcium chloride	Sigma
Chloramphenicol	Sigma.
Chloroform	Sigma
DEPC	Sigma
Dextran sulphate	Sigma
Deionised formamide	Sigma
Dimethylformamide.	Sigma
DNA polymerase I (Klenow fragment)	Roche
di-Sodium hydrogen orthophosphate	Sigma
dNTP	Pharmacia
DNase-free RNase	Sigma
DTT	Sigma
EDTA	Sigma
Ethanol	BDH
Ethidium bromide	Sigma
Ficoll	Sigma
Filter papers (3MM, DE81)	Whatman

Formaldehyde solution [40%(w/v)]	BDH
Glacial acetic acid	BDH
Glucose	Sigma.
Glycerol	Sigma.
Glycogen	Rocher
Guanidinium isothiocyanate	Fluka Biochemika
Hybond-N Nylon membrane	Amersham International plc.
Isoamyl alcohol	Fisons
Isopropanol	BDH
IPTG	Novabiochem
Lithium chloride	Sigma.
N-lauroylsarcosine (sodium salt)	Sigma
Lysozyme	Sigma.
Methanol	BDH
MOPS	Sigma.
Phenol	Sigma.
Salmon sperm DNA	Sigma
Sephadex G50	Pharmacia
Sodium acetate	Sigma
T4 DNA ligase and compatible buffer	New England Biolabs, Inc.
Taq DNA polymerase	Gibco
Tris-base	Sigma.
Tryptone	Difco
X-gal	Novabiochem
Xylene cyanol FF	BDH
Yeast extract	Beta Lab

2.1.2 Reagents for yeast two-hybrid

Reagents	Supplier
Supplements	Sigma
Adenine	Sigma
L-Arginine	Sigma
L-Aspartic acid	Sigma
L-Glutamic acid	Sigma
L-Histidine	Sigma
L-Isoleucine	Sigma
L-Leucine	Sigma
L-Lysine	Sigma
L-Methionine	Sigma
L-Phenylalanine	Sigma
L-Serine	Sigma
L-Threonine	Sigma
L-Tryptophan	Sigma
L-Tyrosine	Sigma
Uracil	Sigma
L-Valine	Sigma
DMF	Sigma
Lithium acetate	Sigma
ONPG	Sigma
PEG-3350	Sigma
Sorbitol	Sigma
X-Gal	Novabiochem
Yeast nitrogen base	Difco

2.1.3 Reagents for protein biochemistry

Reagents	Supplier
Acrylamide/Bis solution (37.5:1)	BDH
Ammonium persulphate	BDH
ATP	Life Tech
2–β-glycerol phosphate	Sigma
2–β-phosphorylserine	Sigma
BS3	Pierce
BSA	Sigma
Coomassie Brilliant Blue R250	Sigma
Diglycerol	Sigma
DEAE-sepharose	Sigma
Fast green	Sigma
Formaldehyde	BDH
Gelatin	Sigma
Glutaraldehyde	BDH
Histone 3	Sigma
Imidazole	Sigma
Immobilon PVDF-based membrane	Millipore
Dried milk	Marvel
2-mercaptoethanol	BDH
Nickel sulfate	Sigma
Detergent NP-40	BDH
Phenyl-Sepharose	Sigma
PMSF	Sigma
Protein assay kits	Bio-Red
Reduced glutathione	Sigma
Silver nitrate	BDH
Sodium acetate	Sigma
Sodium carbonate	Sigma
Sodium orthovanadate	Sigma
Sodium thiosulphate	Sigma
Spectra/por dialysis tubing	Spectrum

Standard molecular weight marker proteins	Sigma
Superdex 75	Pharmacia
TEMED	BDH
Triton X-100	BDH
Tween 20	Sigma

2.1.4 Reagents and consumables for tissue culture and cell biology

Reagents	Supplier
Boyden Chambers	Corning Costar
Cell culture dishes	Nunc
DiffQuik reagent	Dade Behring
DMEM	Gibco Bio-Cult
DMSO	Sigma
EGF	A gift from Dr. John Smith, University of Liverpool
FCS	Sigma
Freezing ampoules	Nunc
Fugene 6	Roche
35mm glass-bottomed microwell dishes	Matek Corporation
Hydromount	Mensura Tech Ltd
Hydrocortisone	Sigma
Insulin	Sigma
Isoton II cell counting fluid	Coulter Electronics
Lipofectamine	Gibco
Streptomycin (l0mg/ml) and Penicillin (10,000IU/ml) solution	Gibco
Paraformadehyde	Sigma
Trypsin	Gibco
Versene	Gibco
Zeocin	Invitrogen

2.1.5 Reagent for radioisotopes and autoradiography

Reagents	Supplier
[r^{32}P]ATP (3000Ci/mmol)	ICN
[α^{32}P]dCTP (3000Ci/mmol)	ICN
X-ray film	Fuji Photo Film Co
RX-Omat-AR5 film	Kodak
X-ray film developer and fixer	Kodak

2.1.6 Other materials

Reagents	Supplier
DNA Gel extraction kits	Qiagen
Plasmid miniprep kit	Life Tech
Plasmid midiprep kit	Life Tech
PCR purification kit	Life Tech
Random primed DNA labelling kit	Roche
Reverse transcription kit	Life Tech

2.1.7 Sources of antibodies

Reagents	Supplier
Rabbit anti-human S100A4	DAKO
Goat anti-human S100A1	Santa Cruze
Mouse anti-S100A1 monoclonal antibody	DAKO
Rabbit anti-MHC IIA *C*-terminus	Produced in the lab
Fluorescein isothiocyanate (FITC)-conjugated anti-mouse IgG	Sigma
Tetramethylrhodamine-isothiocyanate (TRITC)-conjugated anti rabbit IgG	Sigma
HRP conjugated anti-rabbit IgG	Sigma
HRP conjugated anti-Goat IgG	Sigma
HRP-conjugated anti-mouse IgG	Sigma

2.1.8 Source of plasmids

Reagents	Supplier
pET16(b+)	Novagen
pET11a	Novagen
pGEX-2T	Pharmacia
pDsRED2-N1	Clontech
pEGFP-C2	Clontech
pCDNA4	Invitrogen
pYESTrp2	Invitrogen
pHybLex/zeo	Invitrogen
pSH18-34	Invitrogen
PAD-GAL4	Stratagene
PBD-GAL4Cam	Stratagene

2.1.9 Cultured cell lines

Cell line	Description	Reference
Rama 37	Non-metastasizing benign cuboidal rat mammary epithelial cell line with low expression of p9Ka	Dunnington *et al.*, 1983
KP1-Rama 37	Rama 37 cell line transfected with multiple copies of the S100A4. This cell line has high metastatic ability and high expression of S100A4	Davies *et al.*, 1993a
MDA MB-231	Derived from a pleural effusion of a breast cancer patient	Fogh *et al.*, 1975
SKBr-3	Derived from a pleural effusion of a breast cancer patient	Fogh *et al.*, 1975
MCF-7A	Derived from a pleural effusion of a breast cancer patient	Soule *et al.*, 1973

2.2 Reagents and buffers

2.2.1 Reagents for agarose gel electrophoresis

Buffer	Preparation
TBE buffer (10 x)	0.89 M Tris-HCl, 0.89 M Boric acid, 25 mM EDTA, pH 8.3.
TAE buffer (50 x)	2 M Tris-acetate, 0.05 M EDTA, pH 8.0.
Agarose gel loading buffer	0.05% (w/v) bromophenol blue, 20% (v/v) glycerol.
Ethidium bromide	10 mg/ml in H_2O

2.2.2 Reagents for broths and agars

Buffer	Preparation
LB broth	1%(w/v) Tryptone, 0.5%(w/v) yeast extract, 1%(w/v) NaCl, pH 7.0.
LB agar	LB broth + 1.5% (w/v) agar
2xYT medium (1 litre)	1.6% (w/v) Tryptone, 1%(w/v) yeast extract, 0.5%(w/v) NaCl, pH 7.0
SOB medium	2%(w/v) Tryptone, 0.5%(w/v) yeast extract, 10mM NaCl, 2.5mm KCl, 10mM $MgCl_2$, pH 7.0
SOC medium	SOB medium plus 20mM glucose
Terrific broth	12%(w/v) Tryptone, 24%(w/v) yeast extract, 4% (v/v) glycerol with 10%(v/v) of a solution containing 0.17 M KH_2PO_4, 0.72M K_2HPO_4
Antibiotics stocks (-20°C)	Ampicillin 100mg/ml in H_2O Chloramphenicol 34mg/ml in 95% ethanol Kanamycin 50mg/ml in H_2O

2.2.3 Reagents for small- and large-scale isolation of plasmid DNA

Buffer	Preparation
Solution1: cell resuspension solution	10 mM EDTA, 50 mM Glucose, 25 mM Tris-HC1, pH 8.0
Solution 2: lysis solution	0.2 M NaOH, 1% (w/v) SDS prepared freshly.
Solution 3: neutralizing solution	5 M potassium acetate, 11.5%(v/v) glacial acetic acid
3M NaAc pH5.2	3M NaAc, 11.5%(v/v) glacial acetic acid
TE buffer	10 mM Tris-HCl, pH 7.5, 1 mM EDTA.

2.2.4 Buffers for the preparation of competent cells

Buffer	Preparation
RF1 buffer	100 mM KC1, 50 mM $MgCl_2$, 30 mM CH_3COOK, 10mM $CaCl_2$, 15%(w/v) glycerol, Final pH 5.8 with acetic acid, filted through a 0.2 μm Millipore filter.
RF2 buffer	10 mM MOPS, 75 mM $CaCl_2$, 10 mM KC1, 15%(w/v) glycerol, final pH 6.8 with NaOH, autoclaved.

2.2.5 Reagents for RNA extraction and Northern blotting

Buffer	Preparation
GuCNS reagent	4 M guanidine thiocyanate, 50 mM Tris-HCl, 25 mM EDTA, 0.05%(w/v) *N*-lauroylsarcosine, pH7.5, filter sterilize through a 0.2 μm Millipore filter. Prior to use, 2-mercaptoethanol added to 8%(v/v).
50 x Denhardt's solution	1% (w/v) BSA, 1% (w/v) Ficoll, 1% (w/v) polyvinylpyrrolidone.
20 x SSC	3 M NaCl, 0.3 M sodium citrate, pH 7.0
20 x SSPE	3 M NaCl, 0.2 M NaH_2PO_4, 20 mM EDTA, pH 7.7
Running buffer (1 x)	8 mM sodium acetate, 1 mM EDTA, 20 mM MOPS, pH 8.0
Formaldehyde gel	0.8%(w/v) agarose, 1 x formaldehyde gel running buffer, 2.2 M formaldehyde (pH>4.0)

Loading buffer	0.33 mg/ml ethidium bromide, 50% (v/v) glycerol, 1 mM EDTA, 0.17% (w/v) bromophenol blue, 0.17% (w/v) xylene cyanol FF, pH 8.0
Pre-hybridisation solution	50% (v/v) deionised formamide, 5 x SSPE, 2 x Denharde's solution, 0.1% (w/v) SDS, 40μg/ml salmon sperm DNA,
Hybridisation solution	50% (v/v) deionised formamide, 5 x SSPE, 2 x Denharde's solution, 0.1% (w/v) SDS, 80 μg/ml salmon sperm DNA, 5%(w/v) dextran sulphate, $2x10^6$cpm /ml [α-^{32}P]-labeled probe.

All components made up in DEPC-treated double distilled water.

2.2.6 Reagent for yeast culture

Buffer	**Preparation**
YAPD medium	1% (w/v) yeast extract, 2% (w/v) peptone, 2% (w/v) dextrose (D-glucose), 0.01% (w/v) adenine
YAPD agar plate	YAPD medium plus 2% (w/v) agar
SD selective medium (1 litre)	2.7 gram yeast nitrogen base, 5.0 gram NH_4Cl, 20 gram glucose, 100mg adenine, amino acids supplements added as required (L-histidine 40mg,L-leucine 200mg, L-tryptophan 40mg, uracil 40mg), H_2O to 900 ml, pH 5.8, autoclaved, cooled then add 100ml 10x drop solution.
SD selective plate	SD selective medium plus 18.22 % (w/v) sorbitol and 2% (w/v) agar

10x Drop Solution (1 litre)	L-isoleucine 300mg, L-valine 1500mg, adenine 200mg, L-arginine 200mg L-lysine 300mg, L-methionine 200mg, L-phenylalanine 500mg, L-tyrosine 300mg L-glutamic acid 1000mg, L-serine 400mg, L-threonine 2000mg, L-aspartic acid 1000mg

2.2.7 Reagents for yeast transformation

Buffer	Preparation
1xLiAc/1xTE	100mM lithium acetate (LiAc), 10mM Tris-HCl, 1mM EDTA, pH 7.5
1X LiAc/40%PEG-3350/1X TE	1xLiAc/1xTE plus 40% PEG-3350 pH 7.5

2.2.8 Reagents for lift assay and β-galactosidase assay

Buffer	Preparation
Z buffer	60 mM Na_2HPO_4, 40 mM NaH_2PO_4, 10 mM KCl, 1 mM $MgSO_4$-$7H_2O$, pH 7.0 autoclaved
X-Gal solution	X-Gal 50mg/ml in DMF
Z buffer with X-Gal (100ml)	98ml Z buffer, 0.27ml 2-mercaptoethanol, 1.67ml X-Gal stock solution
ONPG solution	ONPG 4 mg/ml in H_2O
Stop solution	1 M Na_2CO_3

2.2.9 Reagents for plasmid recovery from yeast

Buffer	Preparation
Yeast lysis buffer	2.5M LiCl, 50 mM Tris-HCl, pH 8.0, 4% (v/v) Triton X-100, 62.5 mM EDTA
Phenol-chloroform-isoamyl Alcohol (100ml)	50 ml neutralized phenol, 48 ml chloroform, 2 ml isoamyl alcohol

2.2.10 Reagents for His-tagged protein purification

Buffer	Preparation
8X Binding buffer	40 mM imidazole, 4 M NaCl, 160 mM Tris-HCl, pH 7.9
8X Charge buffer	400 mM $NiSO_4$
8X Wash buffer	480 mM imidazole, 4 M NaCl, 160 mM Tris-HCl, pH 7.9
4xElute buffer	4 M imidazole, 2 M NaCl, 80 mM Tris-HCl, pH 7.9
4X Strip buffer	400 mM EDTA, 2 M NaCl, 80 mM Tris-HCl, pH 7.9

2.2.11 Reagents for GST-tagged protein purification

Buffer	Preparation
10X GST binding buffer	43 mM Na_2HPO_4, 14.7 mM KH_2PO_4, 1.37 M NaCl, 27 mM KCl, pH 7.3
Normal elut buffer	10mM reduced glutathione, 50mM Tris-HCl, pH 8.0
Extreme elut buffer	20mM glutathione, 120mM NaCl, 100mM Tris HCl, pH 8.0
Regeneration buffer A	0.5M NaCl, M Tris-HCl pH 8.5
Regeneration buffer B	0.1M sodium acetate, 0.5M NaCl, PH 4.5

2.2.12 Reagents for S100 protein purification

Buffer	Preparation
Buffer A	20mM Tris-HCl pH 8.0
Buffer B	20mM Tris-HCl, 5mM DTT, pH8.0

2.2.13 Reagents for SDS –PAGE gel running

Buffer	Preparation
Stock acrylamide	30% (w/v) acrylamide, 0.8% (w/v) N-N'-methylene-bisacrylamide
Resolving gel buffer	3 M Tris-HCl, pH 8.8
Stacking gel buffer	0.5 M Tris-HCl, pH 6.8
Running buffer	50 mM Tris-HCl, 0.192M glycine, 0.1% SDS
Sample buffer (Laemmli buffer)	62.5 mM Tris-HCl pH 6.8, 2% SDS (w/v), 10% glycerol, 5% 2-mercaptoethanol, 0.001%(w/v) bromophenol blue

2.2.14 Reagents for Coomassie brilliant blue staining

Buffer	Preparation
Coomassie blue staining Buffer	0.25%(w/v) Coomassie brilliant blue R250, 50% (v/v) methanol, 10% (v/v) acetic acid
Destaining buffer	40%(v/v) ethanol, 10% (v/v) acetic acid

2.2.15 Reagents for Fast Green Staining

Buffer	Preparation
Fast green staining buffer	Fast green 1mg/ml, Isopropanol 50%(v/v), acetic acid 10% (v/v)
Destaining buffer	Iso-propanol-2 50%(v/v), acetic acid 10% (v/v)

2.2.16 Reagents for silver staining

Buffer	**Preparation**
Gel fixation buffer	Acetic acid 10% (v/v), Ethanol 40%(v/v)
Sensitizing buffer	Ethanol 30ml, glutaraldehyde (solution 25% w/v) 0.5ml, sodium thiosulphate.$5H_2O$ 2.0g, sodium acetate 6.8g, H_2O to 100ml
Silver nitrate buffer	Silver nitrate 0.25 g, formaldehyde (37%) 40µl, H_2O to 100ml
Developing buffer	Sodium carbonate 2.5g, formaldehyde (37%) 20µl, H_2O to 100ml
Stopping buffer	EDTA 1.46g, H_2O to 100ml
Gel preserving buffer	Glycerol (87% w/w) 4.5% (v/v), ethanol 30%

2.2.17 Reagents for Western blotting

Buffer	Preparation
Transfer buffer	50mM Tris-HCl, 0.192 M glycine, 20%(v/v) methanol
TBST buffer	50mM Tris-HCl, pH 7.2, 200mM NaCl, 0.03% (v/v) Tween 20
Blocking buffer	5% (w/v) Marvel dried milk in TBST buffer

Washing buffer	1% (w/v) Marvel dried milk in TBST
Antibody dilution buffer	5% (w/v) BSA in TBST

2.2.18 Reagents for Gel Overlay

Buffer	Preparation
Overlay buffer	0.5% (w/v) BSA, 0.25% (w/v) gelatin, 0.5% (v/v) NP40, 2 mM DTT, 100mM NaCl, 50 mM Tris-HCl, pH 7.5
Overlay wash buffer	50mM Tris-HCl pH 7.5, 100mM NaCl, 2mM DTT, 0. 5% (v/v) NP40
Overlay block buffer	3% (w/v) BSA, 100mM glycine in TBST

2.2.19 Reagent for GST-pull down assay

Buffer	Preparation
KTT buffer	140 mM KCl, 20 mM Tris-HCl (pH 7.4), 0.1% (w/v) Triton X-100, 5 mM dithiothreitol, with 1 mM $CaCl_2$, or 1 mM EGTA
GST elute buffer	20 mM Tris-HCl, pH 8.0, 150 mM NaCl, 5 mM dithiothreitol, 10 mM reduced glutathione, and 0.1% (w/v) Triton X-100

2.2.20 Reagents for protein phosphorylation by PKC

Buffer	Preparation
ADB buffer	20 mM MOPS, 25 mM beta-glycerol phosphate, 1 mM sodium orthovanadate, 1 mM dithiothreitol, 1 mM $CaCl_2$

PKC activation buffer 100µl	5 µl β-phosphorylserine (10mg/ml stock), 5 µl diglycerol (1mg/ml stock), 90 µl ADB buffer
[r-P^{32}]ATP mixture 100µl	1µl ATP (50 mM stock), 1 µl $MgCl_2$ (750 mM stock), 10 µl [r-P^{32}] ATP , 88 µl ADB buffer

2.2.21 Reagents for Biosensor

Buffer	Preparation
BS3 Solution	0.56 mg/ml in H_2O 100µl in each tube, stored at –80°C
Pi Buffer	10mM NaH_2PO_4, pH 7.7
PBST Buffer	137 mM NaCl, 2.7 mM KC1, 8 mM Na_2HPO_4, 1.5 mM KH_2PO_4, pH 7.4, 0.05% Tween 20, 0.02% NaN_3
20mM HCl	20 mM HCl in ddH_2O
3M Tris-HCl pH 8.0	3M Tris-base in H_2O, adjusted pH with HCl to 8.0

2.2.22 Reagents and Buffers for Cell Culture Procedures

Buffer	Preparation
PBS	137 mM NaCl, 2.7 mM KC1, 8 mM Na_2HPO_4, 1.5 mM KH_2PO_4, pH 7.4
Stock insulin	1mg/ml in 5mM HCl, filter sterilized and stored at –20°C
Insulin Solution (5µg/ml)	1 ml stock insulin was added to 0.18 ml concentrated HCl and 200 ml sterile saline, store at 4 °C
Hydrocortisone (5µg/ml)	Hydrocortisone 5µg/ml in 25%(v/v) ethanol and 75% (w/v) PBS
Trypsin/EDTA Solution	25 ml versene containing 0.5 ml 2.5%(w/v) trypsin

Basal medium (BM)	1 x DMEM, 0.375%(w/v) sodium bicarbonate, 20 mM L-glutamine, 100 lU/ml penicillin, 100 µg/ml streptomycin
Culture medium for Rama Cells (Routine Medium)	BM plus 5%(v/v) FCS, 50ng/ml insulin, and 50 ng/ml hydrocortisone.
Culture medium for MDA-MB-231	BM plus 10% (v/v) FCS, 1µg/ml insulin
Culture medium for MCF-7A	BM (0.5 x DMEM and 0.5 x RPMI) plus 5% (v/v) FCS, 1µg/ml insulin, and 1ng/ml EGF
Culture medium for SKBr-3	BM plus 20%(v/v) FCS
Freezing medium	DMEM supplemented with 20%(v/v) FCS, 7.5%(v/v) DMSO

2.2.23 Reagents for Cell Immunostaining

Buffer	Preparation
Fixation buffer	4% (w/v) paraformadehyde in PBS, incubate at 70°C and add NaOH to pH 7.0
Permeabilisation buffer (PBST)	1%(v/v) Triton X-100 in PBS
Blocking buffer	5%(w/v) BSA in PBST
Wash buffer	PBST
Antibody dilution buffer	5%(w/v) BSA in PBST

2.3 General Molecular Biology Methods

2.3.1 Small Scale Isolation of Plasmid DNA

Five ml of L-broth (Section 2.2.2) containing 100µg/ml ampicillin was incubated with a single colony of bacteria at 37°C overnight with vigorous shaking. Two x 1.5 ml aliquots of the culture were transferred to a microfuge tube. The bacterial cells were collected by centrifugation for 30 sec at 12,000 x g, and the supernatant was removed by aspiration. Plasmid DNA was isolated using a Plasmid Miniprep Kit (Gibco) or using the procedure of Birnboim and Doly (Birnboim & Doly 1979), as modified by Ish-Horowicz and Burke (Ish-Horowicz & Burke 1981) and described below. The bacterial pellet was resuspended by vortexing in 100 µl cell resuspension solution (Section 2.2.3) and left to stand at room temperature for 5 min. After adding 200 µl of NaOH/SDS solution (Section 2.2.3), the contents were mixed by inversion and left at room temperature for 5 min. 150 µl of potassium acetate solution (Section 2.2.3) was added and bacterial debris was removed by centrifugation at 12,000xg for 10 min. The supernatant was transferred to a fresh tube. DNA in the aqueous phase was precipitated by the addition of 1/10 volume of 3 M sodium acetate pH 5.6 (Section 2.2.3) and 2 volumes of ethanol at –70°C for 10 min. The precipitated DNA was collected by centrifugation at 12,000xg for 10 min at 4°C, and the resulting pellet washed with 70% (v/v) ethanol. The air-dried DNA pellet was dissolved in 20µl ddH_2O.

2.3.2 Medium Scale Extraction of Plasmid DNA

A 75 ml bacterial culture was grown overnight, and the DNA was extracted with a medium plasmid midi-kit (Life Tech) following a protocol provided by the manufacturer. The yield of DNA extracted was quantified spectrophotometrically based on the fact that at 260 nm, an optical density of 1.0 corresponds to 50 µg/ml of double-stranded DNA.

2.3.3 Purification of Plasmid DNA by Density Gradient Centrifugation

This procedure was adapted from the method of Radloff (Radloff *et al.*, 1967) and used to purify DNA for the purpose of DNA transfection into mammalian cells. 500ml of

overnight culture was harvested by centrifugation at 5,000 rpm at 4°C. The pellet was resuspended in 4 ml Solution 1 (Section 2.2.3), mixed, and 4ml Solution 2 (Section 2.2.3) was added and the mixture kept at room temperature for 10 min. Then 6ml of Solution 3 (Section 2.2.3) was added and mixed and the mixture kept at room temperature for 5min, then centrifuged at 15,000 rpm, 20 °C for 20min. The supernatant was transferred to a fresh 50ml tube and 10ml of isopropanol-2 was added, the mixture kept at room temperature for 10min, and centrifuged at 4°C, 10, 000 rpm for 10 min. The pellet was dissolved in 4ml of 1 x TE. 4.3 g of caesium chloride and 200µl of ethidium bromide (Section 2.2.1) were added to the mixture and dissolved. The contents were transferred to a 6 ml SORVALL ultracentrifuge tube and sealed. The CsCl density gradient was formed *in situ* by centrifugation at 40,000 rpm. for 20 h at 20°C in a TV1665 vertical rotor. The rotor was slowed without the use of the brake. The plasmid DNA was removed with a Pasteur pipette and the total volume was adjusted to 3 ml with ddH_2O. The ethidium bromide was removed by repeated extraction with isoamyl alcohol, and the band of plasmid DNA was precipitated by the addition of 1/10 volume of 3 M sodium acetate (Section 2.2.3) and 2.5 volumes of ethanol, followed by incubation at –70°C for 1 h. The plasmid DNA was collected by centrifugation at 12,000xg for 20 min at 4°C, and then dissolved in a suitable volume of sterile, ddH_2O. The yield of DNA was quantified as described in Section 2.3.2.

2.3.4 Restriction Endonuclease Digestions

Plasmid DNA was digested with restriction enzymes, which were used according to the manufacturers' recommendations. Restriction enzyme digests were monitored by agarose gel electrophoresis.

2.3.5 Treatment of DNA with Alkaline Phosphatase

The method for removal of the 5' phosphate group of DNA following digestion of DNA with restriction endonucleases was adapted from the method of Sambrook (Sambrook et al., 1989). Digests of plasmid DNA were adjusted to a total volume of 25 µl containing 1 mM $ZnCl_2$ and 1 unit of calf intestinal alkaline phosphatase, and the reaction incubated at 37 °C for 10 min. To inactivate the calf intestinal phosphatase, SDS and EDTA (pH 8.0)

were added to final concentrations of 0.5% (w/v) and 5 mM, respectively. Proteinase K was added to a final concentration of 100 μg/ml and the reactants incubated at 56°C for 30 min. The sample was extracted once with phenol/chloroform, followed by the addition of 0.1 volume 3 M sodium acetate (pH 5.6) and 2.5 volumes of ethanol to precipitate the DNA. The DNA was recovered by centrifugation at 12,000xg for 10 min at 4°C. The resultant pellet was washed with 70% (v/v) ethanol and then dissolved in sterile ddH_2O.

2.3.6 Agarose Gel Electrophoresis of DNA

Methods were adapted from those of Sambrook (Sambrook et al., 1989). Agarose gel electrophoresis was carried out in 1 x TBE buffer (Section 2.2.1). Gels were made 0.8%(w/v) in agarose for plasmid and genomic DNA, or 1.2%-2% (w/v) in agarose for PCR products. 1 kbp ladder was used as a DNA size marker. DNA was visualised on a UV transilluminator (302 nm) by inclusion of 500ng/ml ethidium bromide in the gel. For the isolation of fragments of digested DNA, or for purifying PCR products, a low-melting point agarose was used.

2.3.7 Gel extraction of DNA

Plasmid DNAs that had been digested with restriction enzymes, or PCR products were subjected to electrophoresis using 0.8%-2% (w/v) in agarose gels. The required fragment, visualised with ethidium bromide, was excised from the gel. The DNA fragment was extracted from the agarose using Gel extraction kit from Qiagen according to the protocol provided by the company.

2.3.8 Growth and storage of bacterial stocks

A single colony of *E. coli* was incubated in 3 ml L-broth (Section 2.2.2), containing 100μg/ml ampicillin if appropriate, and incubated in a 37°C shaking incubator overnight. Sterile glycerol was added to 15% (w/v) and the culture stored at –70°C in cryotubes. When required, the culture was thawed on ice, and a small amount streaked to produce single colonies onto a L-agar or L-amp agar plate (Section 2.2.2) and then incubated at 37°C overnight.

2.3.9 Preparation of frozen competent cells

The method presented here (Barraclough, personal communication) was used to prepare frozen competent cells. About 20 colonies of *E. coli* strain DH5α or XL1-Blue or BL21 DE3 from a freshly streaked L-broth plate were inoculated into 100 ml of SOB medium (Section 2.2.2). These cells were incubated at 37°C with shaking, until the optical density at 550 nm was 0.4. The cultures were chilled on ice for 10 min in universal tubes and recovered by centrifugation at 2,000 x g at 4°C for 10 min. After being drained, the cells were resuspended in 66 ml of ice-chilled RF1 buffer (Section 2.2.4), incubated on ice for 10 min and re-centrifuged as above. The resulting pellet of cells was resuspended in 16 ml of ice-cold RF2 buffer (Section 2.2.4). Following incubation on ice for 10 min, the cell suspension was aliquoted, snap frozen in liquid nitrogen and stored at –70°C.

2.3.10 Transformation of competent cells

The method was adapted from that of Hanahan (Hanahan 1985). Competent cells were removed from –70°C storage and thawed on ice. Ligation samples were mixed thoroughly with the cell suspension at 5 µl of ligation mixture per 100 µl of cells, and incubated on ice for 30 min. The samples were heat-shocked at 42°C for 50 sec, and incubated on ice for a further 2 min. After the addition of 800 µl SOC medium (Section 2.2.2), samples were incubated at 37°C with shaking for 45 min. The cells were collected by centrifugation for 10 sec at 12,000 x g, 750 µl of supernatant was removed, and the cells were resuspended in the remaining supernatant and plated on to SOB-amp plate (Section 2.2.2). In the case of the blue/white colony screening procedures, prior to plating, the cell suspension was mixed with 40 µl of 2%(w/v) X-gal (dissolved in dimethylformamide) and 40 µl of 200 mM IPTG. Control transformations containing no DNA were plated onto SOB agar and SOB-amp agar plates (Section 2.2.2), to assess viability and contamination, respectively.

2.3.11 Oligonucleotide synthesis and DNA sequencing

Oligonucleotides were purchased from MWG biotech or Invitrogen. DNA sequencing was carried out in the DNA sequencing laboratories in the School of Tropical Medicine or in the School of Biological Sciences at Liverpool University.

2.3.12 PCR

PCR reactions were carried out in a total volume of 50 µl, and each reaction contained 100 ng DNA, 10 pM of each primer, 1 x supplied PCR buffer (20 mM Tris-HCl, pH 8.0, 50 mM KC1), 0.2 mM of each dNTP, 1.5 mM $MgCl_2$ and 2.5 units of *Taq* DNA polymerase (Life Tech). A suitable annealing temperature for each pair of primers was calculated using the computer software "Oligo". The reactions were incubated on a T gradient thermal cycler (Biometra), for 1 cycle at 95°C for 5 min and for 30-35 cycles at: (1) 95°C for 45sec; (2) a suitable annealing temperature (depending on the primers used) for 50 sec and (3) 72°C for 90 sec. Negative controls, in which either DNA or enzyme was omitted, were also carried out.

2.3.13 Total RNA extraction from cultured cells

Cells were grown to approximately 80% confluence in 15 cm diameter tissue culture dishes. Prior to being harvested, cells were washed twice with ice-cold PBS. Cells were then frozen on a dry ice/ethanol mixture and scraped from the dish, while still frozen, into a sterile container using 3.5 ml GuCNS reagent (Section 2.2.5) per dish. The cells were scraped, transfered to a 14ml Falcon tube and homogenised at 16,000 rpm. for 1 min at room temperature using a Polytron PT 3,000 homogeniser to shear high-molecular-weight genomic DNA. The suspension was centrifuged at 8,000 rpm for 10 min at 4°C in Sorvall high-speed centrifuge to pellet any insoluble cellular debris. Aliquots of the supernatant, each of 3.5 ml, were carefully layered on 1 ml of a CsCl cushion (5.7 M CsCl, 100 mM EDTA pH 8.0) in a polycarbonate tube of a 6 x 5 ml centrifuge rotor (AH650). The samples were centrifuged for 20 h at 32,000 rpm. at 20°C in a Sorvall ultracentrifuge and slowed with the brake off. After centrifugation, the supernatant was removed carefully and the tube inverted and allowed to drain. The pellet was then resuspended in 360 µl of 0.1%(w/v) SDS per tube. The RNA was precipitated by adding l/10th volume of 3 M sodium acetate and 2.5 volumes of ethanol and was incubated overnight at –70°C. The RNA was recovered by centrifuging at 12,000 x g for 20 min at 4°C. The supernatant was removed, the pellet dried, then resuspended in 200 µl 0.1 % SDS (w/v) and the RNA concentration was determined by measuring the absorbance at 260 nm in a spectrophotometer. The yield of RNA

extracted was quantified on the basis that at 260 nm an optical density of 1 corresponds to 40 μg/ml RNA.

2.3.14 RT-PCR

For RT-PCR, 1 μg of total RNA or 0.5 μg of poly (A)-containing RNA was reverse transcribed using Superscript according to the supplier's protocol (Life Technologies Inc., Paisley, Scotland), and the resulting cDNA was amplified by 35 cycles of PCR using *Taq* polymerase (Life Technologies Inc.) with the following human S100A1-specific primers: 5'-primer, ACAGGTCTCCACACACAGCTCC; 3'-primer, AGGCTCGAGAGGAAGGGCGCTGC. PCR products were analysed by electrophoresis on 1.4% (w/v) agarose gels and stained with ethidium bromide. Control amplifications omitted the reverse transcriptase.

2.3.15 Random-primed labelling of DNA probes with [α^{32}P]dCTP

The procedure for labelling the DNA probes was a modified method of Feinberg and Vogelstein (Feinberg & Vogelstein 1984). The plasmid, which contained the specific DNA fragments to be used as probes, was digested with suitable restriction enzymes. DNA probe fragments isolated from an agarose gel with Gel Extraction kit (Qiagen) were labelled using a random-primed DNA labelling kit (Life Technologies Inc.). Fifty ng of DNA fragment in 11μl ddH_2O was denatured by heating for 10 min in a boiling water bath, followed by cooling on ice for 10 min. The following were added to the solution of DNA, 1 μl of dATP, 1 μl of dGTP and 1 μl of dTTP, 2 μl of reaction mixture, 30 μCi of [α^{32}P] dCTP (3,000 Ci/mmol aqueous solution from ICN) and 1μl (1 unit) of Klenow DNA polymerase. The reaction mixture was incubated for 30 min at 37°C. One μl of the reaction mixture was diluted in 100 μl of ddH_2O, and 2 μl samples were applied to each of six Whatman filter paper flags (approximately 8x8 mm^2). Three of the flags were washed as follows: 2 x 1 minute in a solution containing 5% (w/v) TCA, 1 x 1 min in 95%(v/v) ethanol and 1 x 1 min in diethyl ether. Three flags were left unwashed. The flags were then dried with compressed air. The radioactivity present on the washed and unwashed flag was determined by scintillation counting and the specific activity of the probe was calculated.

2.3.16 Denaturing agarose gel electrophoresis of RNA, Northern blotting and hybridisation

This method was adapted from that of Sambrook, *et al.,* (1989). Ten μg of total RNA was separated electrophoretically in 0.8%(w/v) formaldehyde-containing agarose gels (Section 2.2.5). RNA samples or size marker were resuspended in 20μl of 1 x formaldehyde gel running buffer, 50% (v/v) deionised formamide and 2.2 M formaldehyde (pH>4), incubated for 15 min at 65°C and then cooled on ice. Samples were loaded onto the gel after the addition of 2.5 μl of formaldehyde gel loading buffer (Section 2.2.5) and electrophoresis was performed at 3 to 4 V/cm of gel. The region of the gel containing the size markers was removed after electrophoresis. After electrophoresis, the gel was denatured with a solution containing 50 mM NaOH, 10 mM NaCl for 45 min, and then neutralized with 0.1 M Tris-HCl pH 7.5,10 mM NaCl for 45 min. The RNA was transferred onto Hybond-N Nylon membrane (Amersham International plc) via capillary transfer. After an overnight transfer using 20 x SSC (Section 2.2.5) as the blotting buffer, the membrane was air-dried. The RNA was fixed to the membrane by exposure to UV light (302 nm) for 3 min. The fixed membranes to be screened with hybridisation probes were incubated in 20 ml of pre-hybridisation buffer (Section 2.2.5) at 42°C for 4 h in a rotating hybridisation oven. Then the pre-hybridisation buffer was replaced with 10 ml of hybridisation solution containing radioactively-labelled DNA hybridisation probe (Section 2.2.5), and incubated at 42°C overnight. The hybridisation solution was then discarded, and the membrane rinsed at room temperature with a solution of 1 x SSC, 0.1 %(w/v) SDS for 30 min and, then with fresh 1 x SSC, 0.1%(w/v) SDS solution preheated at 65°C. Washing was continued for a further 60 min twice with shaking at 65°C. Finally, the membrane was rinsed once in 2 x SSC, excess liquid was removed, the filter was subject to autoradiography. To standardise loading levels between different RNA samples, the level of the constitutively-expressed non-muscle actin mRNA was determined by hybridising the transferred RNA with a radiolabelled actin cDNA probe.

2.4 General methods in Yeast two-hybrid system

2.4.1 Yeast two-hybrid systems

Yeast two-hybrid system takes advantage of the separable domains of some transcription factors (Chien *et al.*, 1991). The DNA binding domain (BD) and activating domain (AD) of a transcription factor are fused to bait and prey proteins, respectively. If the prey protein binds to the bait protein, the AD and BD have been brought together. This event can be made to trigger transcription of reporter genes. The binding strength can be estimated by the level of the expression of the reporter genes.

There are two basic yeast two-hybrid systems commercially available as follows.

1, **Gal4 system** (from Strategene or Clonetech). In this system, the DNA binding domain (BD) and transcription activating domain (AD) of Gal4, a yeast transcription factor, are fused with bait and prey proteins to produce Gal4 BD hybrid protein and Gal4 AD hybrid protein, respectively. GAL4 BD hybrid protein binds to the GAL4 UAS (upstream activating sequence), which is present upstream of a LacZ reporter gene, and is integrated into the yeast chromosome. The GAL4 AD hybrid protein binds transcription factors in the nucleus but does not bind to the GAL4 UAS. If the bait (X) and target (Y) protein interact, the AD and BD are brought close together and act with bound transcription factors to initiate the transcription of the reporter gene. The expression of the reporter gene, LacZ, can be detected by the lift assay (Staudinger *et al.*, 1993) or by directly measuring the activity of beta-glactosidase (Becker and Fikes, 1993)

The yeast strain in this system is YRG-2 with the genotype of Matα *ura3-52 his 3-200 ade 2-101 lys2-801 trp1-901 leu2-3 112gal4-542 gal80-538* LYS2::UAS_{GAL1}-HIS3 URA3::$UAS_{GAL417mer(x3)}$-$TATA_{cyc1}$-*lacZ*.

Vectors used for this system are pAD-GAL4-2.1 (Figure 2.1) and pBD-GAL4 Cam (Figure 2.2).

2, **LexA-B42 system** (Invitrogen). In this system, two separate hybrid proteins are

constructed, the LexA BD/protein X fusion known as the "bait" and the B42 AD/protein Y fusion known as the "prey". Protein Y can be replaced with a cDNA library in order to screen for unknown proteins that interact with the bait of interest. These two hybrids are on separate plasmids and are transformed into a yeast strain that contains two reporter genes (*lac*Z and an auxotrophic marker). The regulatory regions for these two reporters contain the LexA DNA binding sites (operator sequences) that act as upstream activating sequences (UAS) in yeast. If protein X interacts with protein Y in the nucleus, this will bring the activation domain together with the DNA-binding domain to reconstitute transcriptional activation and results in expression of the reporter genes. Positive interactions can be detected by selecting on plates lacking the auxotrophic marker (HIS3), followed by a second screen for β-galactosidase expression.

The yeast strain used for this system is L40 with the genotype of MATa *his3-200 trp1-901 leu2-3112 ade2* LYS2:: (4*lex*Aop-HIS3) URA3:: (8*lex*Aop-*lac*Z) GAL4.

The vectors used in this system are pHybLex/Zeo (Figure 2.3) and pYESTrp2 (Figure 2.4).

3, **Modification of LexA vector**. To avoid using Zeocin, a very expensive antibiotic, for routine selection, a modified LexA vector, pLexApAD vector, has been engineered. The selection marker for this vector is LEU2 instead of Zeocin. The map and MCS are shown in Figure 2.5.

Map

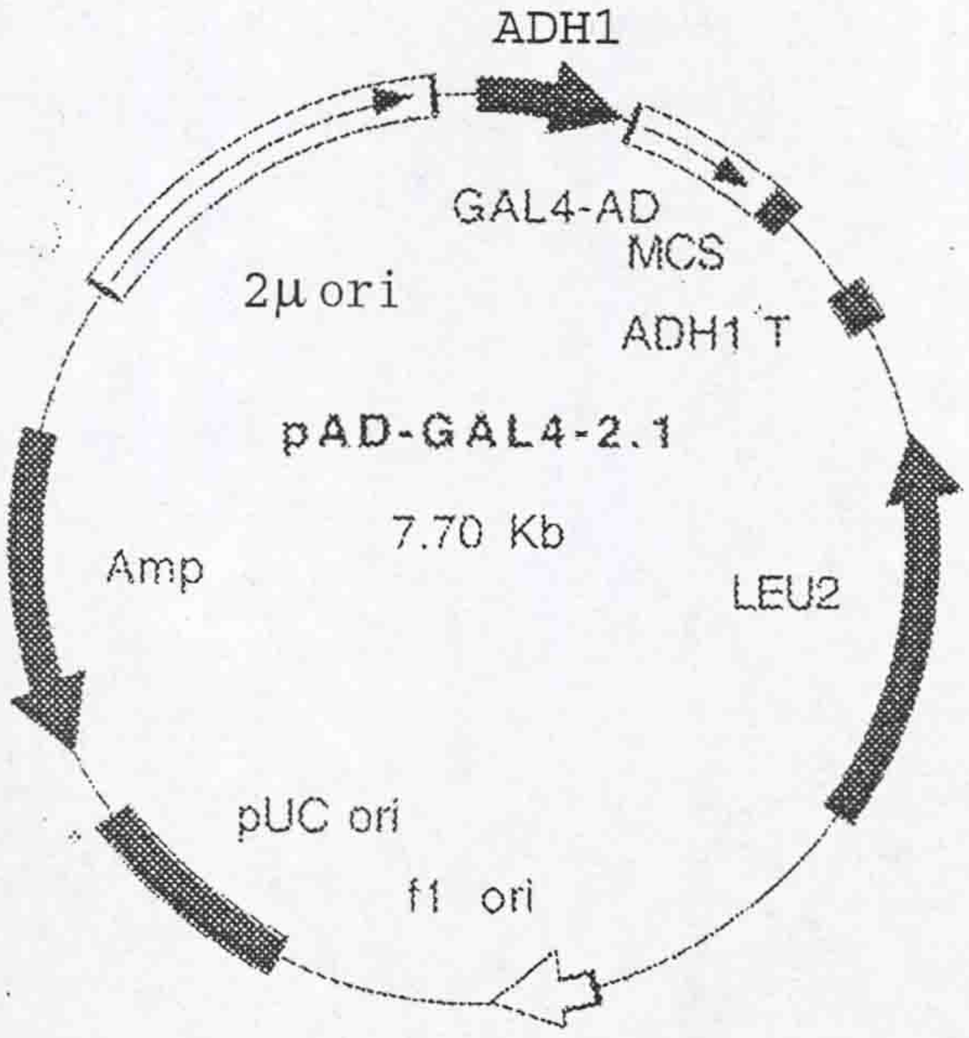

MCS

End of GAL4 activation domain — *Bam*HI

CCA AAC CCA AAA AAA GAG ATC GAA TTA GGA TCC TCT GCT

*Nhe*I — *Eco*RI — *Xho*I

AGC AGA GAA TTC AAT TCT CTA ATG CTT CTC GAG AGT ATT

*Sal*I — *Xba*I — *Pst*I

AGT CGA CTC TAG AGC CCT ATA GTG AGT CGT ATT ACT GCT

*Bgl*II — stop — stop — stop

GAG ATC TAT GAA TCG TAG ATA CTG AAA AAC

Figure 2.1 pAD-GAL4-2.1 vector. GAL4-AD:GAL4 activation domain (488-829); ADH1 p: yeast ADH1 promotor (4-408); ADH1 T: yeast ADH1 terminator (1168-1318); LEU2: yeast LEU2 selection marker (1615-2079). Amp: ampicillin resistance gene (5245-6102); 2μ ori: 2μ yeast origin; MCS: multiple cloning site region. This vector is for subcloning a bait gene downstream the GAL4 activation domain to express GAL4AD-bait fusion protein in yeast.

Map

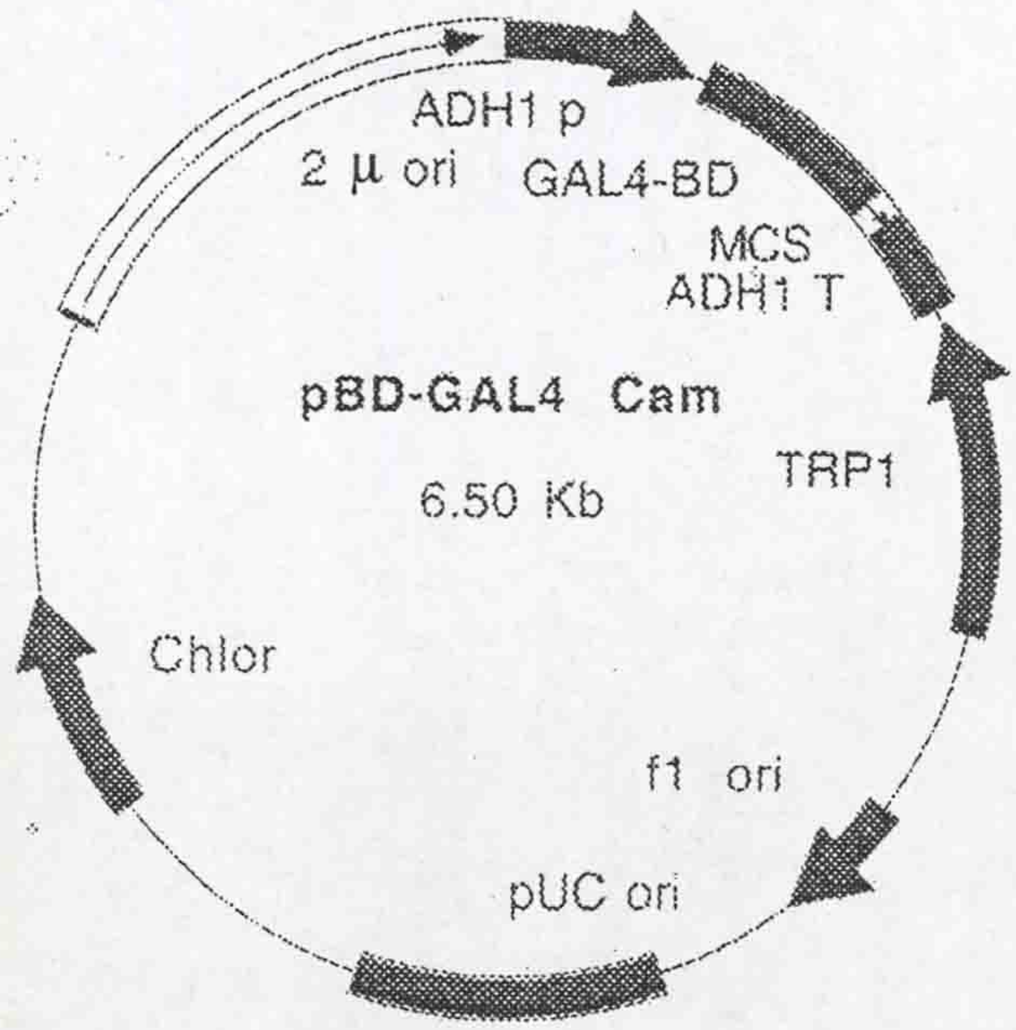

MCS

End of GAL4 binding domain — *Eco*RI — *Sma*I

```
5′ CAA AGA CAG TTG ACT GTA TCG CCG GAA TTC GCC CGG GCC
```

*Xho*I — *Sma*I — *Sal*I — *Xba*I

```
TCG AGC CCG GGT CGA CTC TAG AGC CCT ATA GTG AGT CGT ATT
```

*Pst*I — stop — stop

```
ACT GCA GCC AAG CTA ATT CCG GGC GAA TTT CTT ATG ATT TAT
```

stop

```
GAT TTT TAT TAT TAA A 3′
```

Figure 2.2 pBD-GAL4 Cam vector. GAL4 DNA binding domain (434-877); ADH1 p: yeast ADH1 promotor (4-408); ADH1 T: yeast ADH1 terminator (948-1154); TRP1: yeast TRP1 selection marker (1197-1871); Chlor: chloramphenicol resistance gene (4174-4275); 2 μ ori: 2μ yeast origin (5330-6489); MCS: multiple cloning site region. This vector is for subcloning prey gene downstream the GAL4 DNA binding domain to express GAL4-BD-prey fusion protein in yeast.

Map

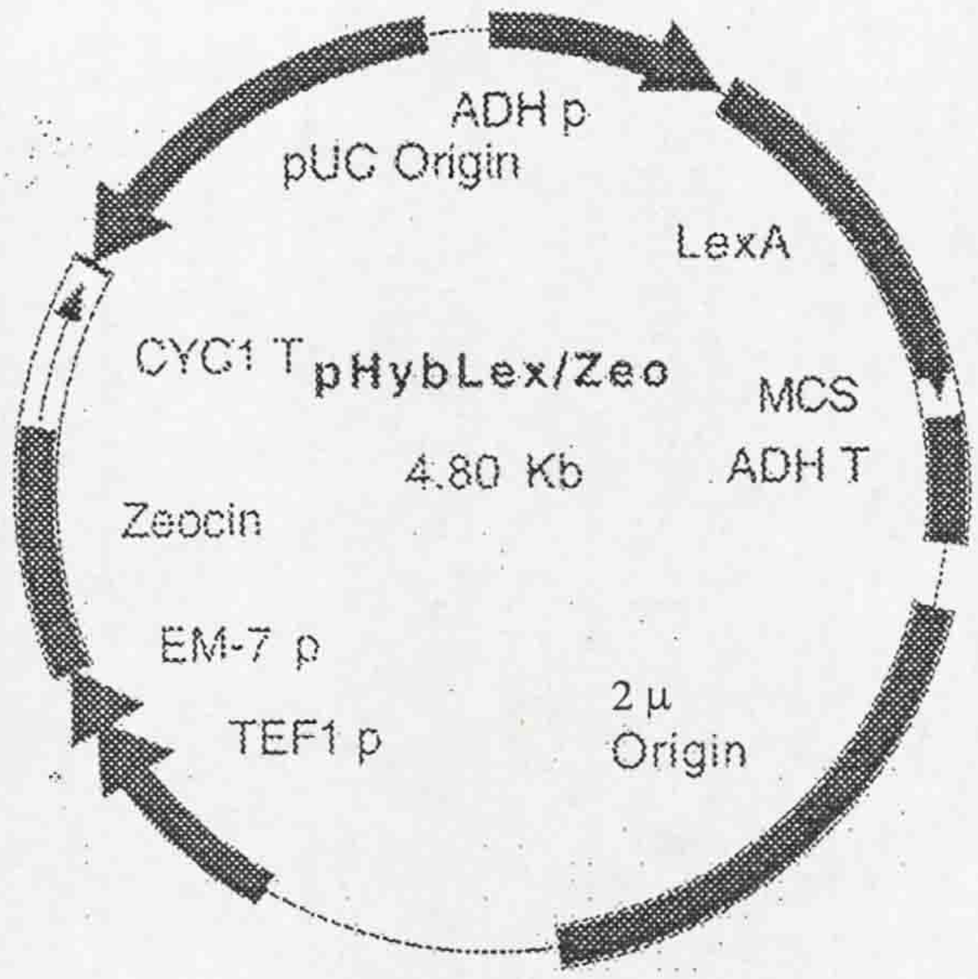

MCS

End of LexA *EcoR*I *Sac*I

AAC GGC GAC TGG CTG GAA TTC AAG CTT GAG CTC AGA TCT CAG

*Apa*I *Kpn*I *Not*I *Xho*I *Sal*I *Pst*I

CTG GGC CCG GTA CCG CGG CCG CTC GAG TCG ACC TGC AGC CAA

stop

GCT AAT TCC GGG CGA ATT TCT TAT GAT TTA TGA TTT TTA TTA

Figure 2.3 pHybLex/Zeo vector. ADH p: yeast ADH promotor(1-399); LexA: LexA open reading frame (420-1025); ADH T: yeast ADH terminator (1141-1298); 2 m Origin: 2 m yeast origin (1474-2308); TEF1 p: TEF1 promotor(2855-3263); EM-7 p: EM-7 promotor(3267-3334); Zeocin: Zeocin resistance gene (3335-3709); CYC1 T: CYC1 terminator (3710-4027); MCS: multiple cloning site region. This vector is for subcloning bait gene downstream the LexA gene to express LexA-bait fusion protein in yeast.

Map

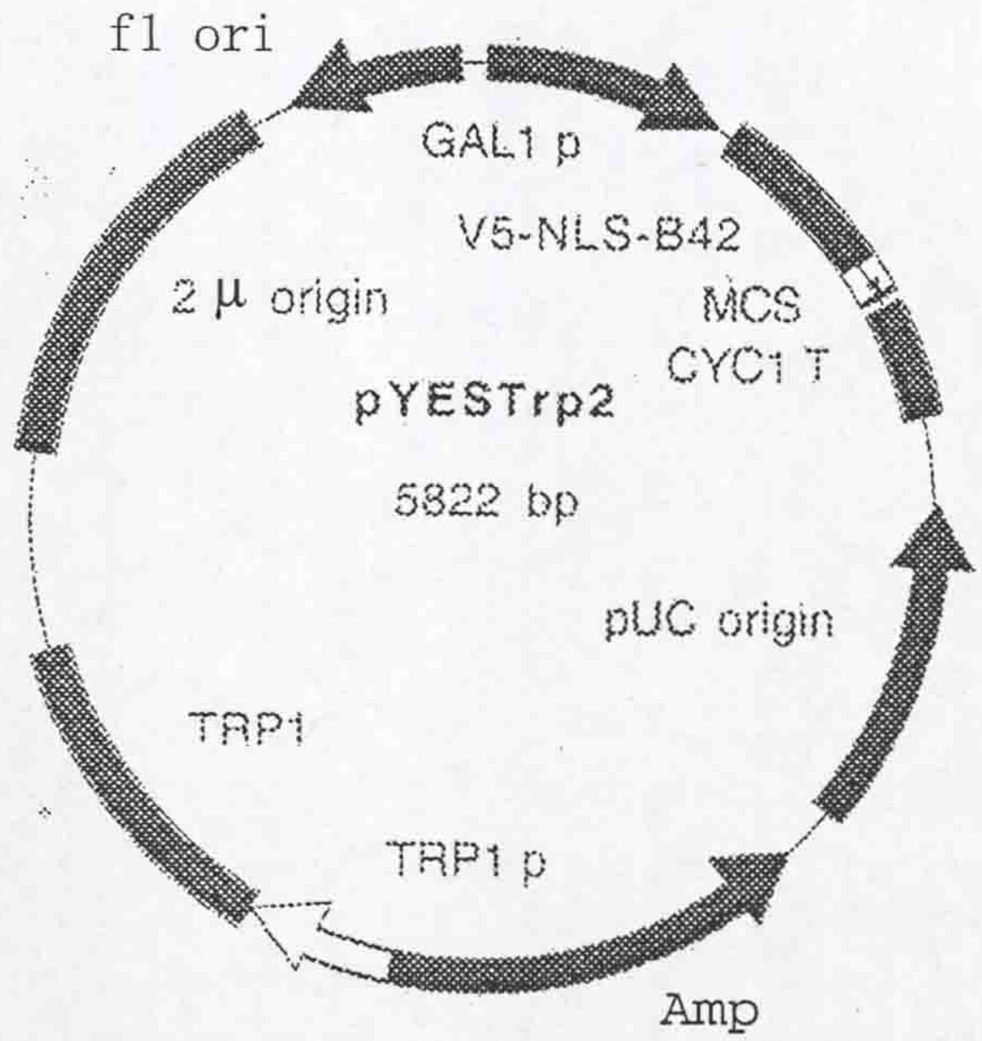

MCS

end of B42 *Hind*III *Kpn*I *Sac*I

```
CTC TTG CTG AGT GGA GAT GCC TCC AAG CTT GGT ACC GAG CTC
```

*Bam*HI *Eco*RI

```
GGA TCC ACT AGT AAC GGC CGC CAG TGT GCT GGA ATT CTG CAG
```

*Not*I *Xho*I *Sph*I

```
ATA TCC ATC ACA CTG GCG GCC GCT CGA GGC ATG CAT CTA GAG
```

stop

```
GGC CGC ATC ATG TAA
```

Figure 2.4 pYESTrp2 vector. GAL1 p: yeast GAL1 promotor (1-497); V5-NLS-B42: V5 epitope (559-600)-nuclear localisation signal (616-642)-B42 activation domain (646-883) fusion protein; CYC1 T: CYC1 terminator (997-1245); Amp: ampicillin resistance gene (2219-3105). TRP1: yeast TRP1 selection marker (3313-4089); f1 ori: fi origin (5396-5768); 2μ ori: 2μ yeast origin (4493-5327); MCS: multiplr cloning site region. This vector is for subcloning prey gene downstream the B42 activation domain to express B42-prey fusion protein in yeast.

Map

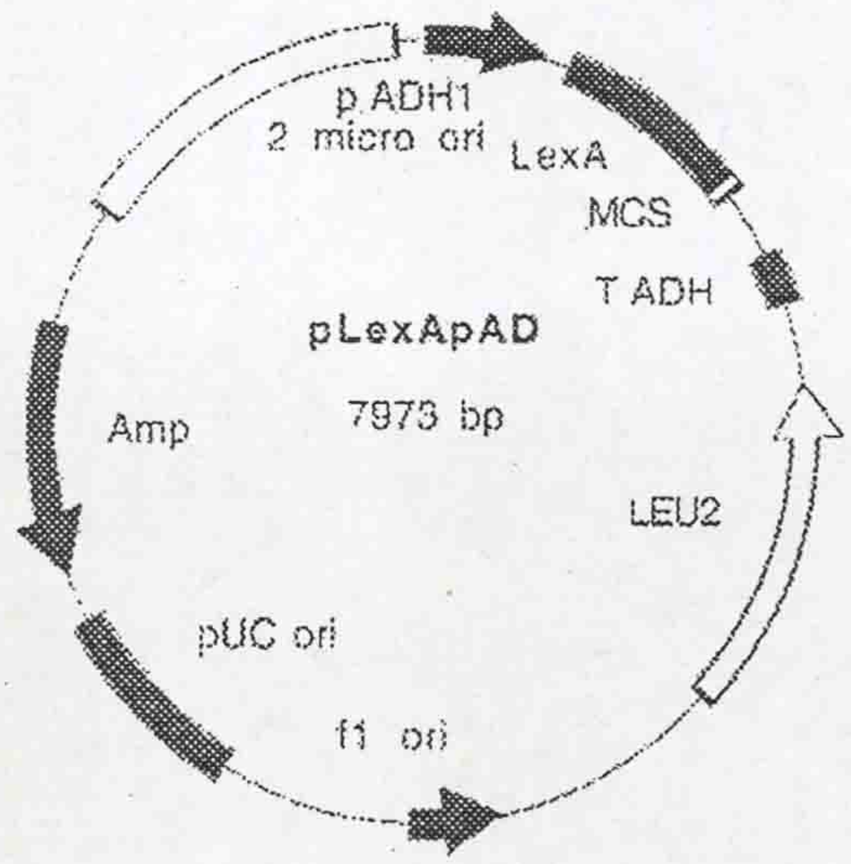

MCS

end of LexA *EcoR*I *Xho*I

5' -AAC GGC GAC TGG CTG GAA TTC AAT TCT CTA ATG CTT CTC GAG

Sal I *Xba* I *Pst* I

AGT ATT AGT CGA CTC TAG AGC CCT ATA GTG AGT CGT ATT ACT GCA

BgI II Stop Stop

GAG ATC TAT GAA TCG TAG ATA CTG AAA AAC-3'

Figure 2.5. pLexApAD vector. ADH p: yeast ADH promotor(4-408); LexA: LexA open reading frame (488-1193); ADH T: yeast ADH terminator (1432-1582); LEU2: yeast LEU2 selection marker (1897-2973). Amp: ampicillin resistance gene (5509-6366); 2 μ Origin: 2 μ yeast origin (6753-7917); MCS: multiple cloning site region. This vector is for subcloning bait gene downstream the LexA gene to express LexA-bait

2.4.2 Small scale yeast transformation

To prepare yeast competent cells 10ml of YPAD (Section 2.2.6) were incubated with a single clone of yeast strain, L40 or YRG-2, and shaken overnight at 30°C. After determining the OD_{600nm} of the overnight culture, it was diluted to an OD_{600nm} of 0.4 in 200 ml of YPAD and incubated for an additional 4 h. The cells were centrifuged at 4,000 rpm in a Sorvall Centrifuge and the pellet was washed once with 50ml ddH_2O. The cell pellet was then resuspended in 50 ml of 1xLiAc/1xTE (Section 2.2.7). After incubation at 30°C for 30 min, the cells were again collected by centrifugation and then resuspended in 0.8ml 1x LiAc/1xTE and 0.2ml denatured, sheared salmon sperm DNA (10mg/ml). After adding 9ml 1xLiAc/40% PEG-3350/1xTE buffer (Section 2.2.7) and mixing well, 300 µl of each of the yeast competent cells were aliquoted into 1.5ml microcentrifuge tubes. The competent cells can be used immediately for transformation or frozen at –80°C for use later. For transformation, 2 µg DNA was added to each tube of competent cells and incubated at 30°C for 30min. After two heat shocks at 42°C for 8 min each with an 8 min interval on ice between, the cells were centrifuged and the pellet was resuspended in 200 µl SD medium, the cells of each transformation were transferred to a 9cm SD selective agar plate. The plate was then incubated at 30°C for 4-7 days.

2.4.3 Lift assay

When the transformants grew to 1-2 mm in diameter, the lift assay (β-galactosidase filter assay) was performed. A dry Whatman filter circle was laid onto the yeast colonies that were on a selective plate. The filter paper was removed and put into nitrogen liquid for 30 s. At the same time, 2ml Z Buffer with X-Gal (Section 2.2.8) was placed in a lid of a 9cm petri dish. A Whatman filter circle was then carefully laid on the Z buffer-containing X-gal. The filter was removed from nitrogen liquid and placed colony side up on top of the wet filter in the petri dish lid, avoiding forming air bubbles between the two filter papers. Then the filter was covered with the bottom of the dish and the dish placed in 30°C incubator overnight. The development of blue colour was checked at 1 hour, 3 h, 6 h and 16 h.

2.4.4 Liquid beta-galactosidase assay

A single yeast transformant was cultured in 3ml SD selective medium overnight at 30°C with constant shaking. After recording the OD_{600nm} value, 1.0 ml of the culture was transferred to a clean glass test tube and centrifuged at 3,000rpm at room temperature for 5 min. The pellet was resuspended in 1.0 ml Z Buffer (Section 2.2.8) and 2 drops of 0.1%(w/v) SDS and 2 drops of chloroform were added. The mixture was vortexed vigorously for 1 min; 200 µl ONPG solution (4mg/ml) (Section 2.2.8) was added and mixed well. The glass tube was incubated at 30°C for 90min or stopped earlier when the colour became medium yellow. The reaction was stopped with 0.5 ml 1.0M Na_2CO_3. The cell debris was removed by centrifugation and the values of OD_{420nm} of the supernatant were recorded. Beta-galactosidase activity was calculated as follows: Miller units =1,000 x OD_{420nm} /(volume of cell was assayed in ml x time in min x OD_{600nm}).

2.4.5 Recovery of plasmid DNA from yeast

Five ml of YAPD with a single transformant was incubated overnight at 30°C with constant shaking. The cells were centrifuged at 2,500rpm for 5 min a bench top centrifuge and the cell pellet was resuspended in 0.3 ml of in Yeast Lysis Buffer (Section 2.2.9). Approximately 150 mg of glass beads (0.5µm) and 0.3 ml of phenol/chloroform were then added. After vortexing the mixture vigorously for 1 min, a drop of the solution was placed on a microscope slide to check the extent of lysis. Vortexing was continued until 80% of the cells were lysed. The lysate was centrifuged in a microcentrifuge at 1, 400 rpm for 1 min. The aqueous phase was transferred to a fresh 1.5ml tube and shaken twice with a phenol-chloroform-isoamyl alcohol mixture (Section 2.2.9). Plasmid DNA was precipitated from the upper aqueous phase with 0.1 volumes of 3M sodium acetate (Section 2.2.3) and 2.5 volumes of ethanol and resuspended in 25 μl of TE. The plasmid was amplified by growth in an *E.coli* strain, XL-1 blue and identified by DNA sequencing.

2.4.6 Yeast two-hybrid library screening

Large-scale library transformation. The yeast two-hybrid library (Invitrogene) was constructed from the mRNA extracted from a human breast cancer specimen. The yeast

strains transformed with bait plasmid were used to make competent cells. The procedures were similar to those described above except that a 500ml culture was used each time and the cells were resuspended in 1ml of denatured, sheared salmon sperm DNA, 500 μg library DNA, 70ml of 1x lithium acetate/40% PEG-3350/1xTE (Section 2.2.7) and 8.8ml of DMSO. After a second heat shock, the cells were immediately diluted with 400ml YPAD medium, collected by centrifugation and then washed once with YAPD (Section 2.2.6). The pellet was resuspended in 500 ml YAPD and incubated at 30°C for 1 hour with constant shaking. Cells were collected by centrifugation and washed with SD medium (Section 2.2.6) twice. Finally, the cells were resuspended in 10 ml SD medium and plated on 20 15 cm diameter SD agar selective (Section 2.2.6) plates.

Analysing the transformants. All the colonies growing on the selective plates were grided onto fresh SD selective agar plates. When the colonies grew to 1-2 mm in diameter, lift assays were carried out. The blue colonies identified within 16 h in the lift assay were cultured and the plasmids were recovered from them. All the recovered prey plasmids were co-transformed with bait plasmid in yeast L40. The plasmids that still gave blue coloured clones in lift assay and exhibited higher beta-galactosidase activities were subjected to DNA sequencing and further analysis.

2.5 Preparation of recombinant proteins

2.5.1 Expression of proteins in *E.coli* with the pET system

Two protein fragments were produced using pET16 b (+) vector (Novagen). Target genes are cloned in pET plasmids under the control of the strong bacteriophage T7 transcription and translation signals (Studier & Moffatt 1986).

For protein production, a recombinant plasmid was transferred to the host *E. coli* strain, BL21 DE3, containing a chromosomal copy of the gene for T7 RNA polymerase. These hosts are lysogens for bacteriophage DE3, a bacteriophage lambda derivative that has the immunity region of phage 21 and carries a DNA fragment containing the Lac I gene, the

LacUV5 promoter, and the gene for T7 RNA polymerase (Studier & Moffatt 1986). This fragment is inserted into the *int* gene, preventing DE3 from integrating into or excising from the chromosome without a helper phage. Once a DE3 lysogen is formed, the only promoter known to direct transcription of the T7 RNA polymerase gene is the lacUV5 promoter, which is inducible by isopropyl-ß-D-thiogalactopyranoside (IPTG). Addition of IPTG to a growing culture of the lysogen induces T7 RNA polymerase, which in turn transcribes the target DNA under the control of T7 promotor.

pET16b(+) Vector (Figure 2.6) for *N*-terminal his-tagged protein expression and pET11a vector (Figure 2.7) for non-tagged protein expression were used in this study.

Map

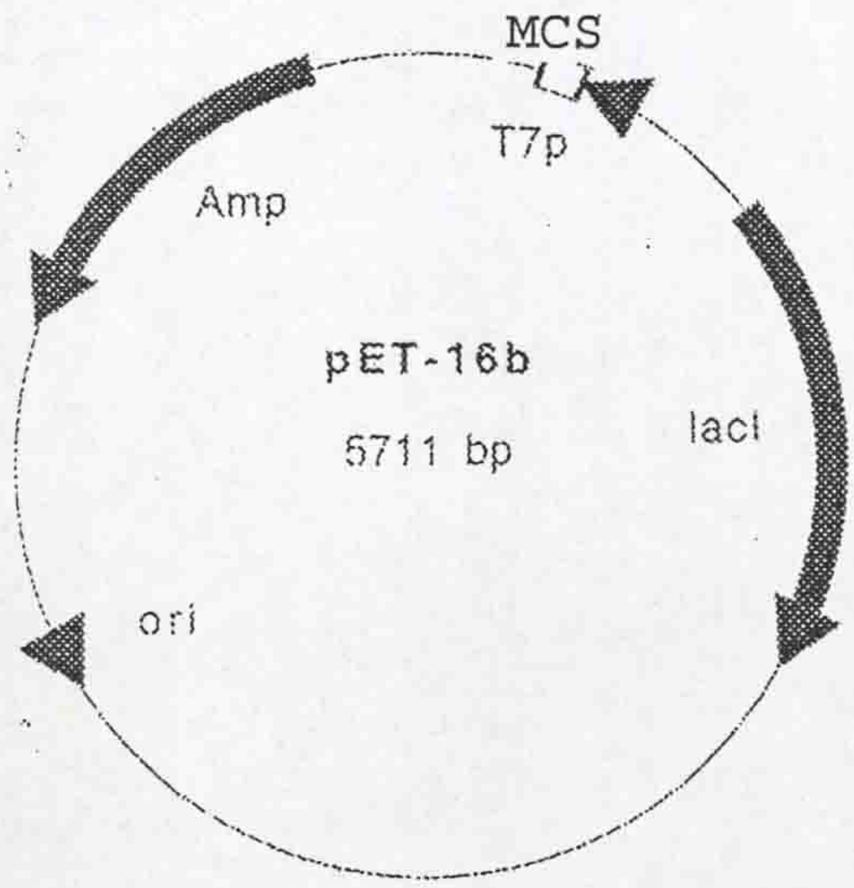

MCS

*Bgl*II — T7 promotor → — lac operator

AGATCTCGATCCCGCGAAATTAATACGACTCACTATAGGGGAATTGTGAGCG

lac operator — rbs

GATAACAATTCCCCTCTAGAAATAATTTTGTTTAACTTTAAGAAGGAGATATA

*Nco*I — His.Tag

CCATGGGCCATCATCATCATCATCATCATCATCACAGCAGCGGCCAT

MetGlyHisHisHisHisHisHisHisHisHisHis SerSerGlyHis

*Nde*I *Xho*I *Bam*HI

ATCGAAGGTCGTCATATGCTCGAGGATCCGGCTGCTAACAAAG

IleGluGlyArgHisMet

Factor Xa

Figure 2.6 pET-16b vector. T7 p: T7 promotor (466-482); Amp: ampicillin resistance gene (4646-5503); ori: pBR322 origin. *lacI*: *lacI* coding sequence (869-1948), MCS: multi-cloning sites (319-331); rbs: ribosome binding site. Factor Xa: Factor Xa enzyme cleavage site. Target gene can be inserted between *Nde*I nad *Bam*HI restriction sites for expressing His-tagged target protein in *E coli* strain, BL21.

Map

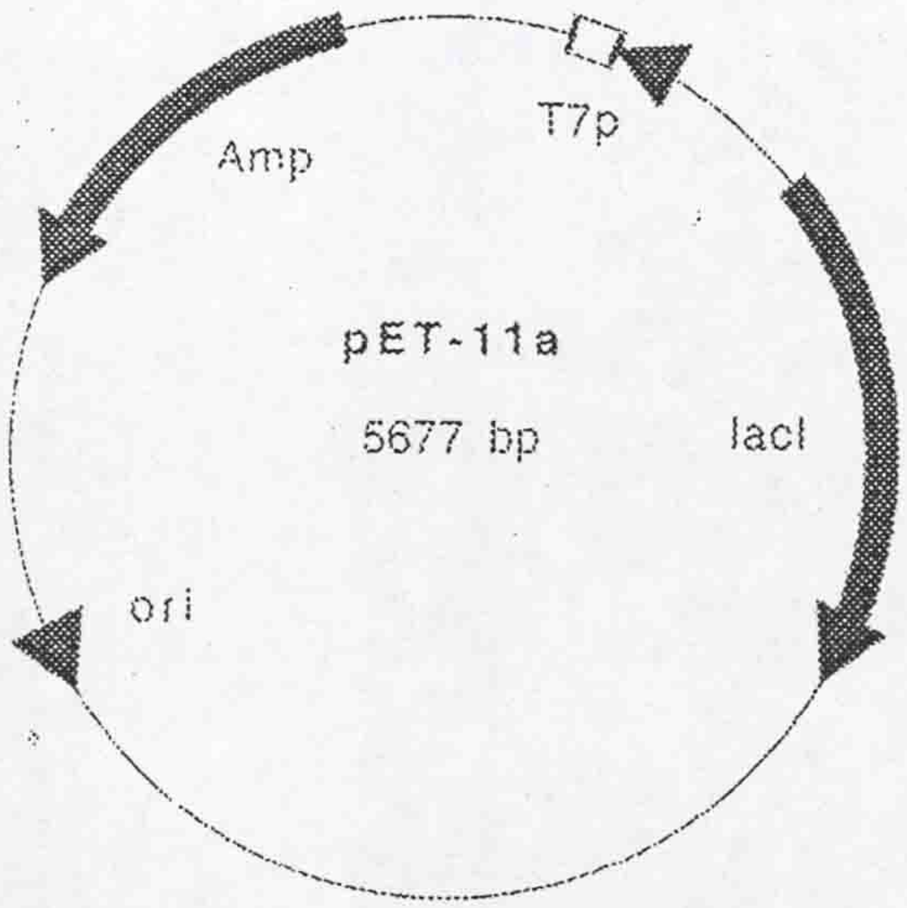

MCS

*Bgl*II T7 promotor lac operator
AGATCTCGATCCCGCGAAATTAATACGACTCACTATAGGGGAATTGTGAGCG

lac operator rbs
GATAACAATTCCCCTCTAGAAATAATTTTGTTTAACTTTAAGAAGGAGATATA

*Nde*I *Bam*HI
CATATGGCTAGCATGACTGGTGGACAGCAAATGGGTCGCGGATCCGGCTGC

stop
TAACAAAGCCC

Figure 2.7 pET-11a vector. T7 p: T7 promotor (432-448); Amp: ampicillin resistance gene (4612-5469); ori: pBR322 origin. *lacI*: *lacI* coding sequence, MCS: multi-cloning sites (319-359). Target gene can be inserted between *Nde*I nad *Bam*HI restriction sites for expressing non-tagged target protein in *E coli* strain, BL21.

2.5.2 Constructs for protein expression using pET expression system

The pET16-MHCIIB expression vector was constructed with 5'-3' primer CTGCTCGAG5587CGACACGCGGACCAG and 3'-5' primer CGAGGATCC 5931TTACTCTCTGACTGG. The coding sequence (coding 114 amino acids from R1863 to E1976) was amplified by PCR, digested with restriction enzymes *Xho*I and *Bam*HI and subcloned into pET16b(+) vector at *Xho*I and *Bam*HI sites.

The pET16-MHC-IIA expression vector was constructed by Dr. Hailan Chen. The coding sequence of MHC-IIA *C*-terminus (coding 149 amino acids from L1813 to E1961) was amplified by PCR with 5'-3 primer GGTTTTCCATGCTCGAGGCCAAGATTG and 3'-5' primer GGGGATCC GGGTGTCTGTCTGTC and subcloned into pET16(+) vector at restriction enzymes *Nde*I and *Bam*HI sites.

pET11a-S100A1 expression vector was constructed by ligating the S100A1 coding sequence into pET11a vector at *Nde*I and *Bam*HI sites. The S100A1 coding sequence was amplified by PCR with the 5' *Nde*I primer, CTGCGTTTGCAT**ATG** (translation start) GGCTCT GAGCTGG and 3'*Bam*HI primer. CGAGGATCC**TCA** (translation stop)ACTGTTCTCGGAGAAG.

pET11a-S100A2 expression vector was constructed by ligating the S100A2 coding sequence into pET11a vector at *Nde*I and *Bam*HI sites. The S100A2 coding sequence was amplified by PCR with the 5' *Nde*I primer CGAATCGTACAT**ATG**(translation start)TGCAGT TCTCTGGAG and 3'*Bam*HI primer GCAGGATCC**TCA**(translation stop)GGGTCGGTCTGGGCA G.

pET11a-S100A4 expression vector was constructed by ligating the S100A4 coding sequence into pET11a vector at *Nde*I and *Bam*HI sites. The S100A4 coding sequence was amplified by PCR with the 5' *Nde*I primer CGATGCACTCAT**ATG**(translation start)GCGTGC CCTCTGGAG and 3'*Bam*HI primer CATGGATCC**TCA** (translation stop)TTTCTTCCTGGGCTG.

pET11a-S100P expression vector was constructed by ligating the S100P coding sequence into pET11a vector at *Nde*I and *Bam*HI sites. The S100P coding sequence was amplified by PCR with the 5' *Nde*I primer GCATGCACTCAT**ATG**(translation start)ACGGAA CTAGAGACAGCCATG and 3'*Bam*HI primer CGTGGATCC**TCA** (translation stop)TTTGAGAGT ACTTGTGAC.

The coding sequences and junction sequences of the engineered expression vectors were checked by DNA sequencing.

2.5.3 Protein expression in *E.coli*

The expression construct was transformed into the BL21 DE3 strain of *E.coli,* which was grown on selective LB plates (Section 2.2.2) and incubated at 37°C overnight. Ten colonies from each of the transformations were cultured in 3ml of selective LB broth overnight at 37°C. One hundred µl of overnight culture from each colony was diluted into 3ml LB broth and incubated with constant shaking at 37°C. When the OD_{600nm} of the culture reached 0.6, 1mM IPTG was added and the culture continued to be incubated for 4-8 h, depending on the yield of target proteins. One ml of the overnight culture and 1ml of the IPTG-induced culture were collected in 1.5 microcentrifuge tubes by centrifugation in a microcentrifuge. The cell pellet was then resuspended in 200µl of 1x Laemmli Buffer (protein loading buffer) (Section 2.2.13) and incubated in boiling water both for 10min. The cell lysates were analysed SDS-PAGE. Expression of target proteins was identified by Coomassie blue staining of the gel and by Western blotting with specific antibodies. The colonies that produced a highest level of expression of the target protein were stored at –80°C for future use.

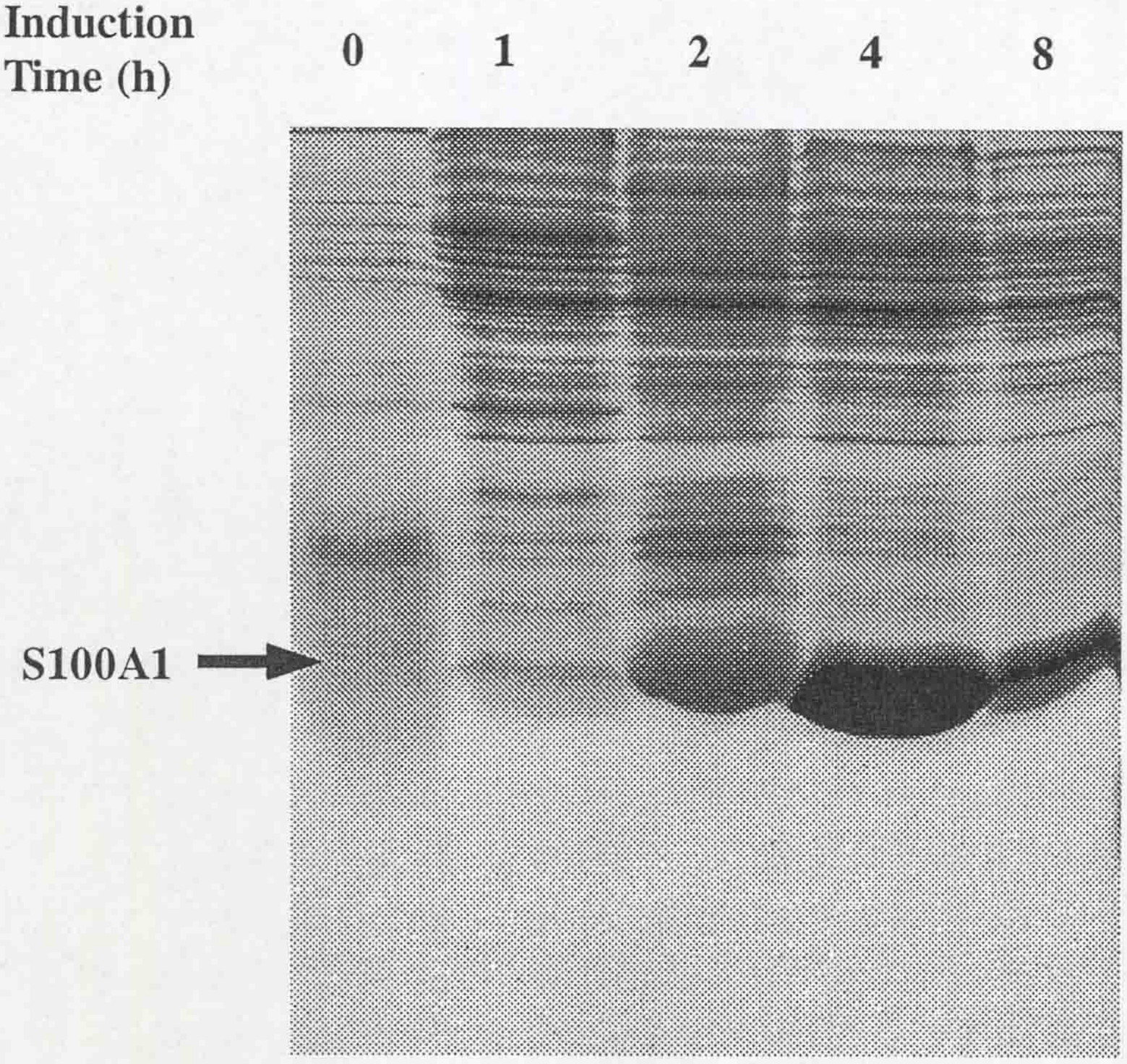

Figure 2.8 The induced expression of S100A1 in *E coli* BL21 DE3 with IPTG. The bacteria transformed with pET11a S100A1 were cultured in 50ml LB broth (Section 2.2.2) at 37°C with constant shaking until the OD_{600nm} reached 0.6. One ml sample was collected for control (*lane 1*), then 1 mM IPTG was added to the remaining culture to induce the expression of S100A1 protein. Samples were collected at different times after the induction, 1 h (*lane 2*), 2 h (*lane 3*), 4 h (*lane 4*), 8 h (*lane 5*). Samples were centrifuged and the resultant cell pellets were resuspended in 100 µl 1x Laemmli Buffer, boiled for 5 min and 20 µl of each sample was analysed on a SDS-PAGE (15%). The gel was stained with Coomassie brilliant blue. The arrow indicates the position of recombinant S100A1.

For large-scale production of soluble target proteins, the bacteria were cultured overnight in 50 ml selective LB broth. Next morning, the culture were diluted 200 times in 1-4 litre LB broth with suitable antibiotics and incubated at 37°C with constant shaking. When the OD_{600nm} reached 0.6, IPTG was added to a concentration of 1mM and the culture was

incubated further for a period of time determined by the results of pilot times course. The bacteria were collected by centrifugation and resuspended in an ice-cold buffer suitable for purification. The bacteria were normally sonicated to assist their lysis and shearing of the genomic DNA. After sonication, the cell lysate was centrifuged at 15,000 rpm for 30 min in a Sorvall centrifuge. The cleared lysate was stored at –80°C or directly used in purification procedures.

2.5.4 Purification of his-tagged proteins

Ni-NTA His•Bind Resin was used for rapid one-step purification of recombinant proteins containing a His•Tag® sequence by metal chelation chromatography (Hoffmann & Roeder 1991). The His•Tag sequence binds to Ni^{2+} cations, which are immobilized on the Ni-NTA His•Bind Resin. The unbound proteins can be washed away with low concentrations of imidazole buffer and the target protein is recovered by elution with higher concentrations of imidazole buffer. The Ni-NTA His•Bind Resins use nitriloacetic acid (NTA) as the chelator, which has four sites available for interaction with metal ions. NTA chemistry minimizes leaching of the metal during purification and is compatible with up to 20 mM 2-mercaptoethanol for reduction of disulphide bonds. Ni-NTA His•Bind Resin has a binding capacity of 5–10 mg protein per ml resin.

To prepare the column, 2.5ml of the NTA His•Bind slurry were transferred to a 10 ml column and allowed to settle by gravity. After washing with 30 ml ddH_2O, 10 ml of 1x $NiSO_4$ (Section 2.2.10) was applied to the column. The column was then washed with 30 ml of 1x binding buffer (Section 2.2.10) to remove the unbound Ni^{2+}. The column was loaded with cell lysate in 1x binding buffer and washed with 60 ml 1x washing buffer (Section 2.2.10). The his-tagged protein was eluted with 10 ml 1x elute buffer (Section 2.2.10).

2.5.5 Further purification of MHC-IIAF21 and MHC-IIBF17 protein

The MHC-IIAF21and MHC-IIBF17 proteins recovered from His-binding columns were first dialysed for 16 h against 20mM Tris-HCl (pH 7.5), 0.5M NaCl with the buffer

changed twice. The concentration of the proteins was determined by Bradford method (Section 2.6.1). For further purification, half volume of ddH_2O was added and the mixture was incubated at 4°C for 3 h. The MHC-IIAF21 and MHC-IIBF17 filaments were formed in the low salt buffer and the filaments were precipitated by centrifugation at 15,000 x g for 20 min in a Sorvall centrifuge. The resultant pellets were resuspended in 10mM Tris-HCl (pH 7.5), 0.5 M NaCl or Pi buffer (Section 2.2.21) with 0.2%(w/v) SDS for biosensor assays. The proteins were aliquoted and stored at –80 °C.

2.5.6 Purification of non-tagged S100 proteins

S100 proteins were purified on three columns: DEAE Sepharose (ion exchange), Phenyl Sepharose (hydrophobic), and Superdex75 (gel filtration). S100A1, S100A2, S100A4 and S100P were purified using the same methodology and so that for S100A1 purification will serve as an example.

2.5.6.1 Ion-exchange chromatography

The DEAE Sepharose column (25 cmx2.6 cm) was equilibrated overnight with buffer A (Section 2.2.12) at a flow rate of 2 ml/min. The bacterial extract was passed through the column and the unbound protein was washed away with buffer A until a flat Uvicord reading was obtained. The bound proteins were eluted with a 600 ml linear gradient of 0-600 mM NaCl in buffer A and then with 500 ml of buffer A/2M NaCl. Twenty ml fractions were collected at the beginning of the salt gradient (Figure 2.9 A). Twenty µl samples from each fraction were analysed on SDS-PAGE and fractions with right size of protein band were identified (Figure 2.9 B) and pooled for further purification.

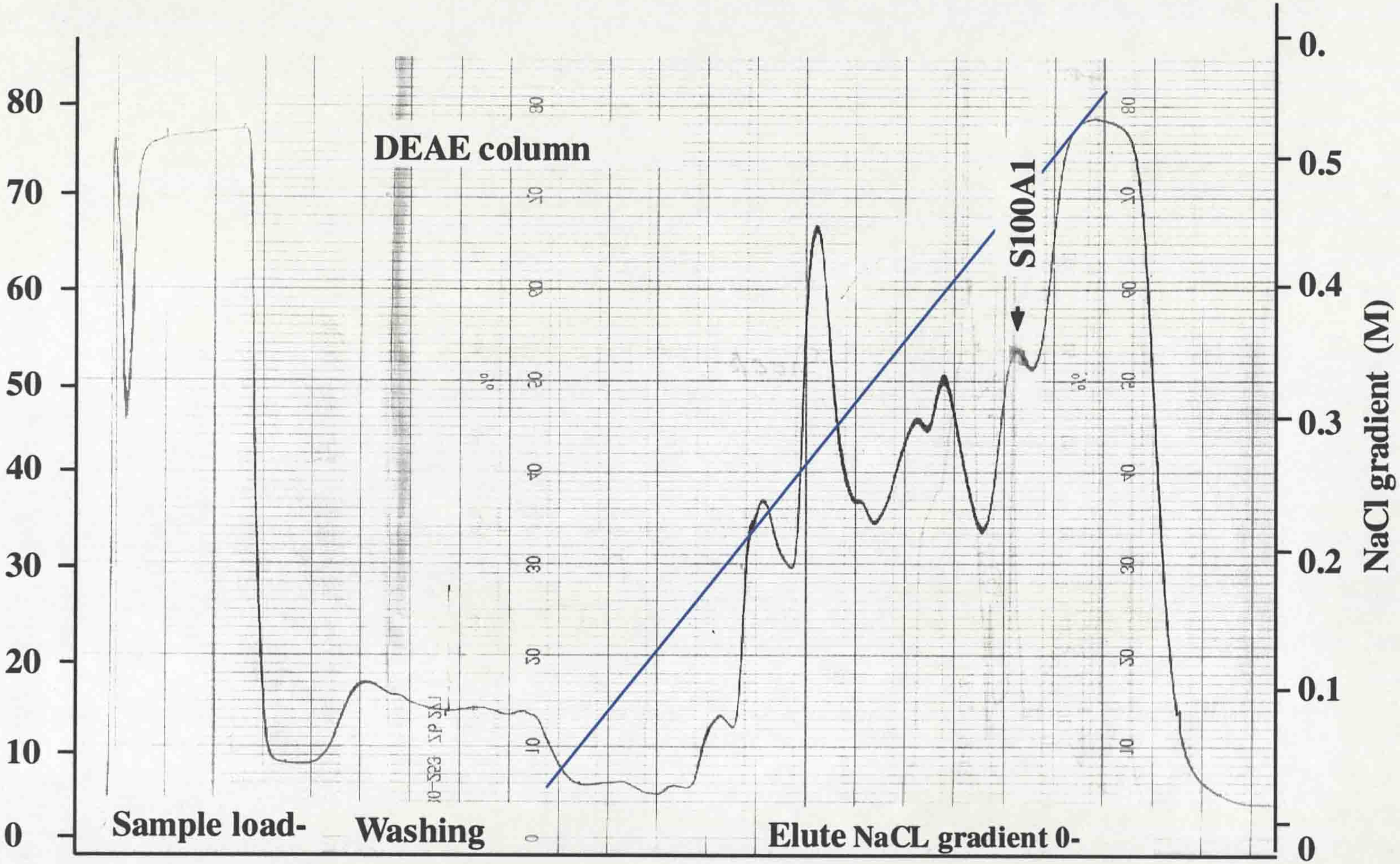

Figure 2.9A. Elution profile of S100A1 protein eluted from a DEAE column. The flow rate was 2ml/min. Collection: 20ml/fraction. Arrow indicates the fractions containing S100A1 protein.

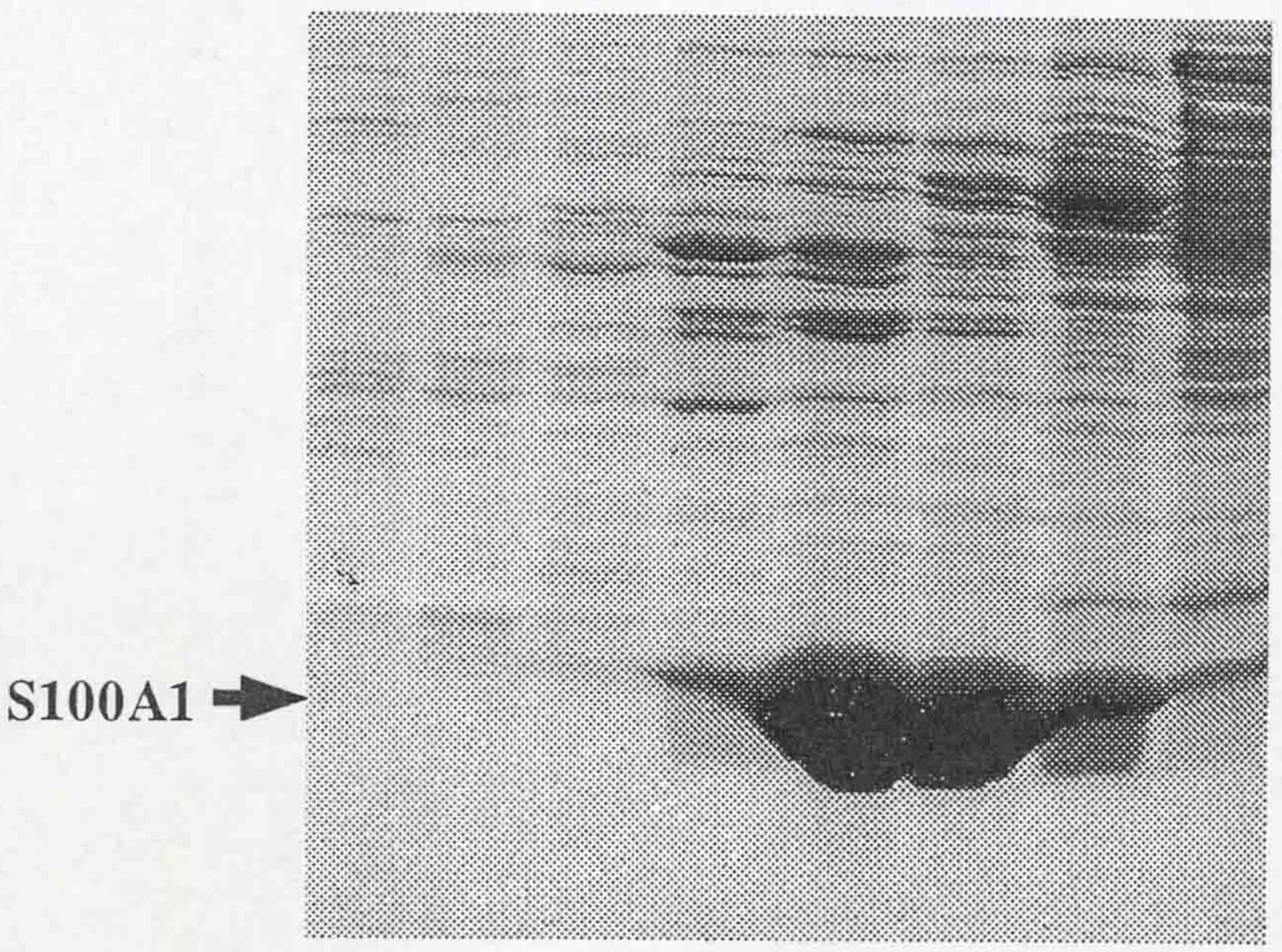

Figure 2.9. Partial purification of S100A1 by DEAE chromatography. **A** The cell lysate containing S100A1 protein was applied at the flow rate of 2 ml/min to a DEAE-Sepharose column equilibrated in a buffer A (Section 2.2.12). After unbound proteins had been washed through the column with buffer A (Section 2.2.12), a linear gradient of NaCl (0-600 mM) in buffer A was applied to the column as indicated in blue line. Proteins eluted from the column during the application of the gradient were collected as 20 ml fractions (total 30 fractions). **B**. The samples of the fractions were analysed on 15% SDS-PAGE. The gels were stained with Coomassie blue (Section 2.6.3). The S100A1 recombinant protein was eluted mainly in fractions 25 and 26.

2.5.6.2 Hydrophobic-interaction chromatography

The second chromatography step used a Phenyl Sepharose column (15 cm x 1.5 cm), which was equilibrated with buffer B containing 0.1mM $CaCl_2$ (Section2.2.12) at 2 ml/min for 2 h prior to use. The pooled sample was adjusted to a final concentration of 5mM Ca^{2+} with 1M $CaCl_2$ and applied to the column at 1 ml/min. The column was washed with 75 ml buffer B, followed by 75 ml buffer B containing 0.5M NaCl and then 75 ml buffer B. The bound S100 protein was eluted with buffer B containing 1mM EGTA. The peak fractions were collected (Figure 2.10A) and analysed using SDS-PAGE (Figure 2.10B).

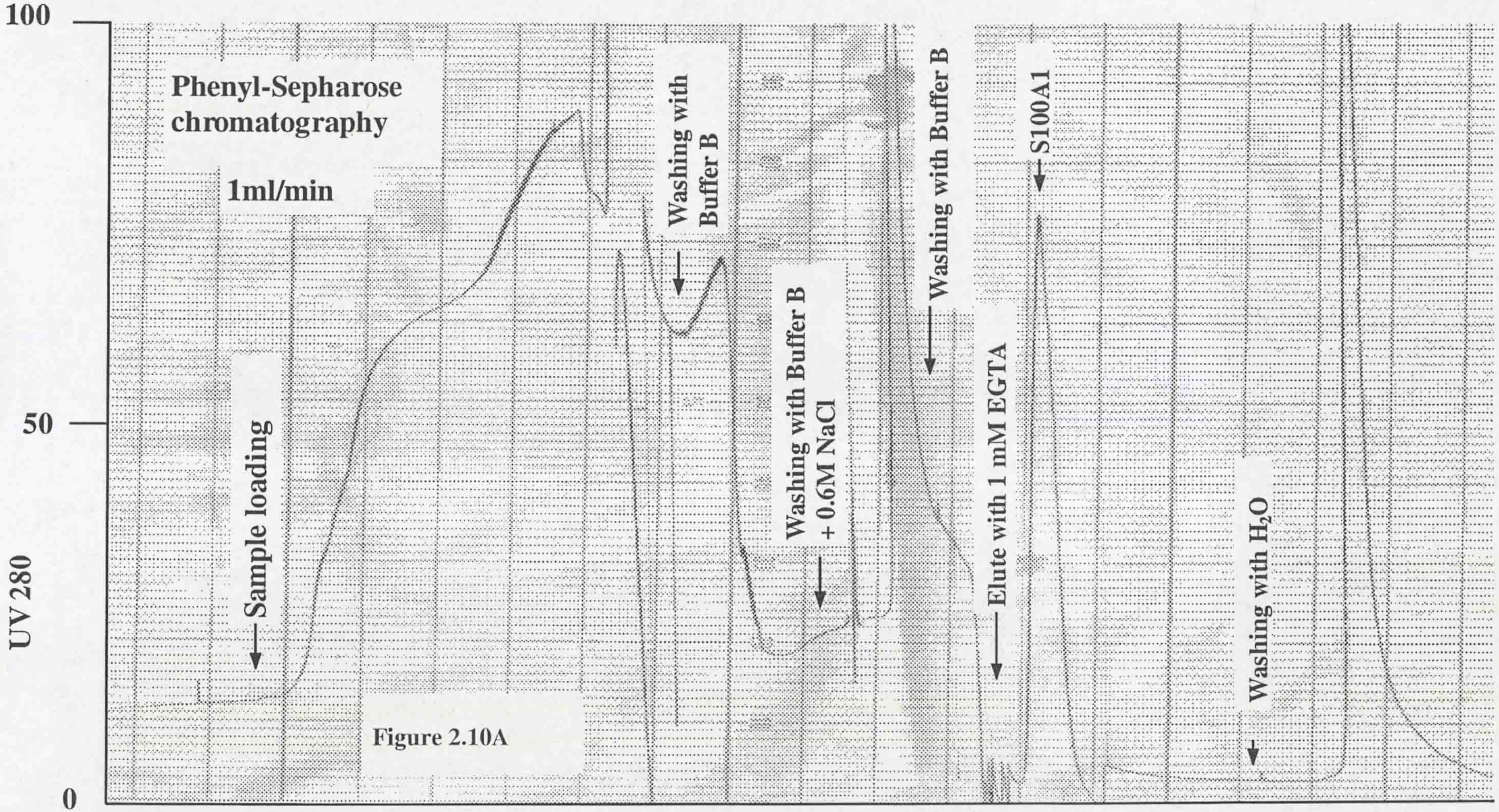
100
50
0
UV 280
Phenyl-Sepharose chromatography
1ml/min
Sample loading
Washing with Buffer B
Washing with Buffer B + 0.6M NaCl
Washing with Buffer B
S100A1
Elute with 1 mM EGTA
Washing with H_2O

Figure 2.10A

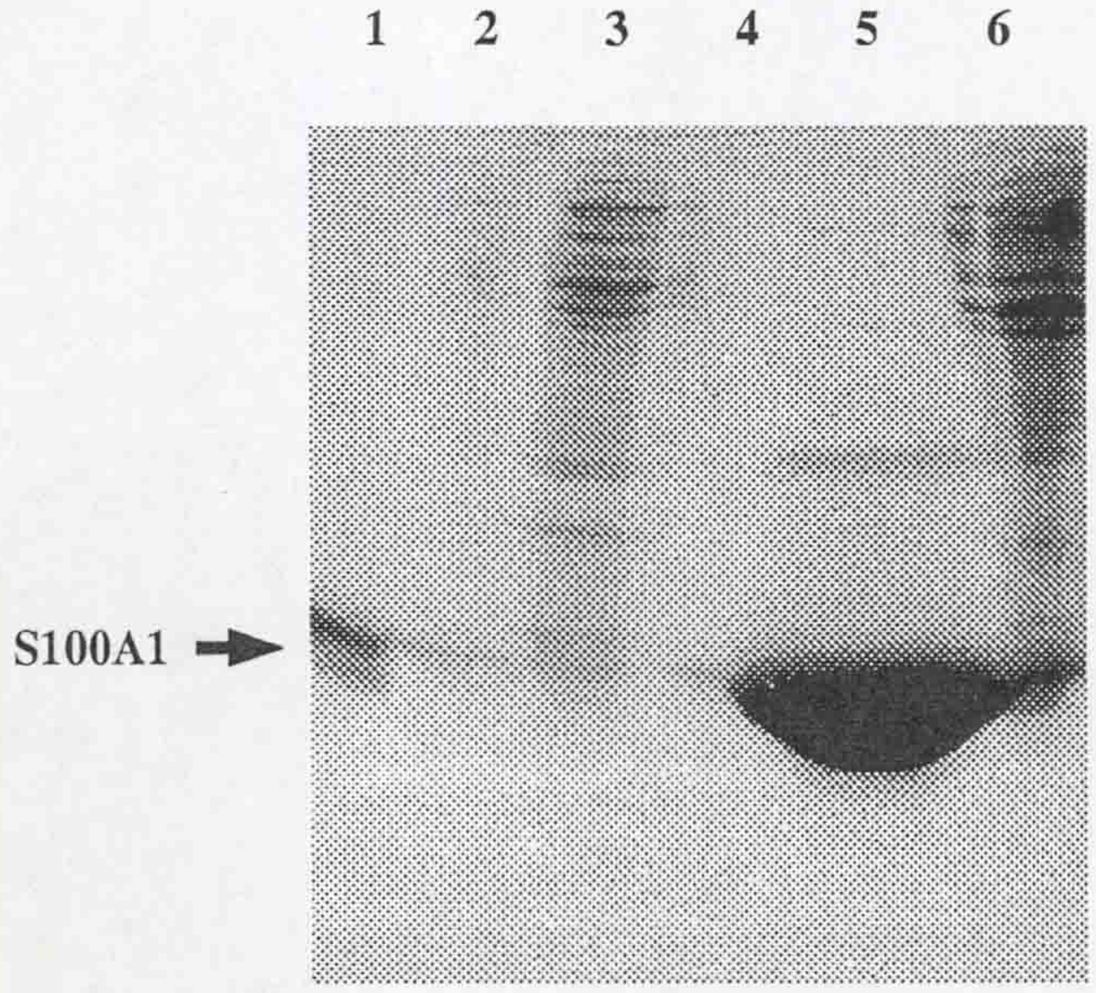

Figure 2.10. Purification of S100A1 by a phenyl-Sepharose chromatography. Flow rate: 1ml /min. **A.** .At the point indicated by A in the figure, the pooled samples collected from DEAE-Sepharose column were applied to the phenyl-Sepharose column. At the point indicated by B, C, D in the figure, the column was washed with buffer B (Section 2.2.12), buffer B containing 0.6 M NaCl, and buffer B, respectively. At point indicated by E in the figure, the column was eluted with buffer B containing 1mM EGTA. At the point indicated by F, the column was washed by H_2O. **B**. Fractions collected from phenyl-Sepharose column were analysed on 15% SDS-PAGE. Twenty µl from each fraction was loaded on each well. *Lane 1*, pooled sample from previous DEAE column, lane 2, pass through; lane 3 washings with buffer B + 0.6M NaCl; lane 4, washings with buffer B collected before elution; lane 5, elute with buffer B + 1 mM EGTA; lane 6, washing with H_2O. The gel was stained with Coomassie blue (Section 2.6.3).

2.5.6.3 Size exclusion chromatography (gel filtration)

Fractions with recombinant protein from the phenyl-Sepharose column were pooled and dialysed using a dialysing tubing (3,000 Dalton cut off, Spectrum) against Pi buffer (Section 2.2.21) + 0.2 M NaCl for 24 h with two buffer changes. The protein in Pi buffer + 0.2 M NaCl was concentrated to 6mg/ml with ULTRAFREE-15 Centrifugal Filter Device (Millipore, 3,000Da cut off) by centrifugation at 3,000g at 4°C. The Superdex 75 column (fractionation range 3 kDa to 70kDa) was packed in a C 16/70 column (Pharmacia), washed with PBST (Section 2.2.21) and equilibrated with Pi buffer + 0.2 M NaCl overnight. 3mg of the concentrated protein in 0.5ml was loaded each time on to the Superdex 75 column and run at 2ml/min with Pi buffer + 0.2 M NaCl. The elution profile was measured as OD at 280 nm and fractions were collected (Figure 2.11) and analysed on SDS-PAGE (data not shown). The two peaks indicated by B and C (Figure 2.11) contained the S100A1 protein. As the elution time for peak B (35min) is similar to that of lysozyme (35min, molecular weight 24 kDa) (data not shown), the size of S100A1 is close to that of a dimer. Therefore, the S100A1protein in peak C should be in monomer form. Very similar chromatographic patterns were observed for other S100 proteins purified. The late eluting S100 protein peaks containing small molecular weight (presumably monomers) were collected and their purities normally reached 99% and no SDS resistant multimers were observed when analysed on SDS-PAGE (Figure 2.12). Concentration of the pooled protein was determined as described in Section 2.6.1 and then aliquoted. The protein aliquots were immediately frozen at –80 °C and used only once after thawing.

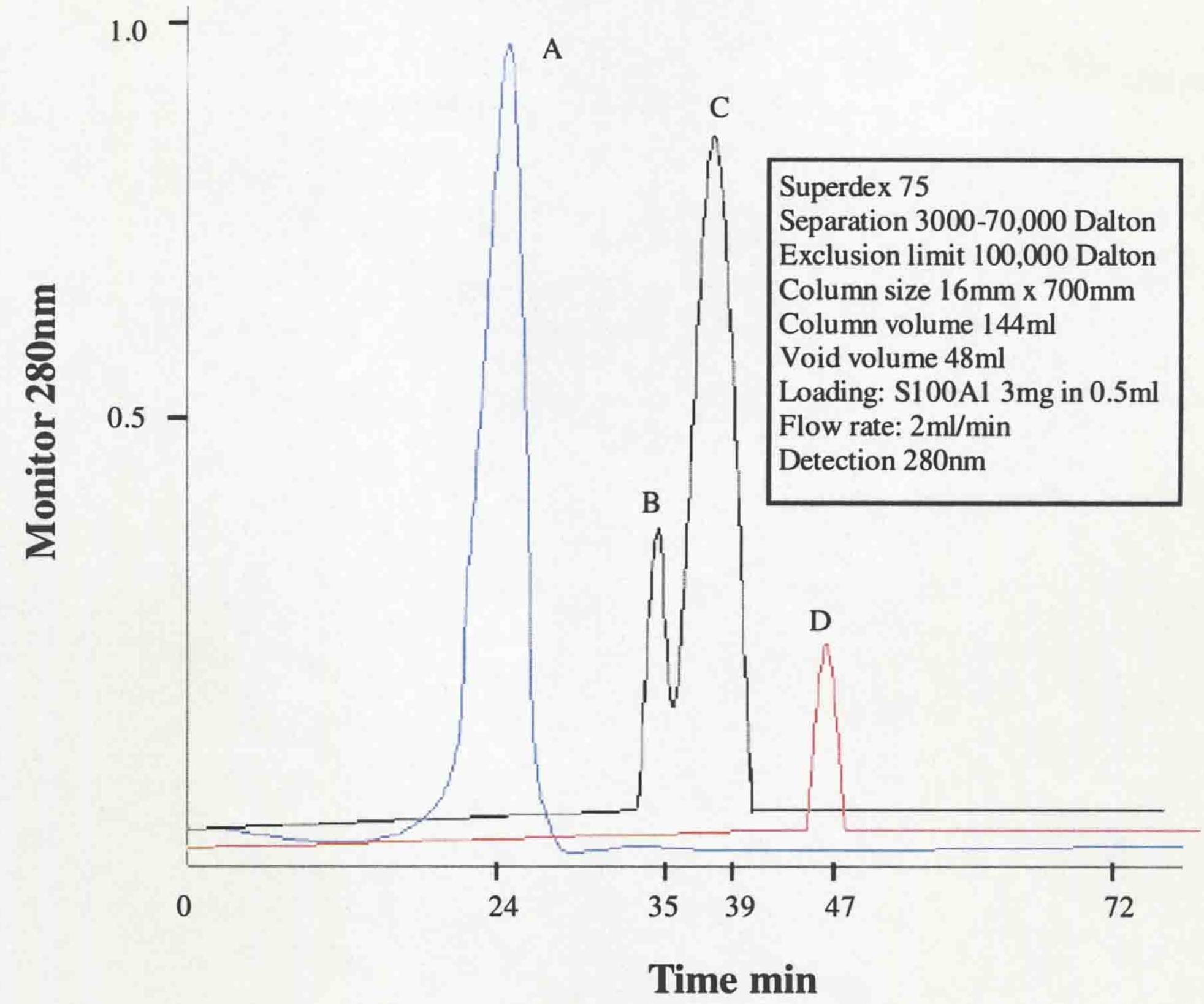

Figure 2.11 Purification of S100A1 by Gel filtration chromatography. The Superdex-75 column was self-packed and tested using 0.2ml 1% (w/v) bromophenol blue dye (indicated by D) and 0.1ml α-2-macroglobulin (0.5mg/ml, molecular weight, 170 kDa) (indicated by A) separately. The calculated void volume of the packed column was 48ml and the included volume was 50 ml. The S100A1 was eluted in two peaks indicated by B and C. Only peak C was collected, and immediately aliquoted for store at –80°C

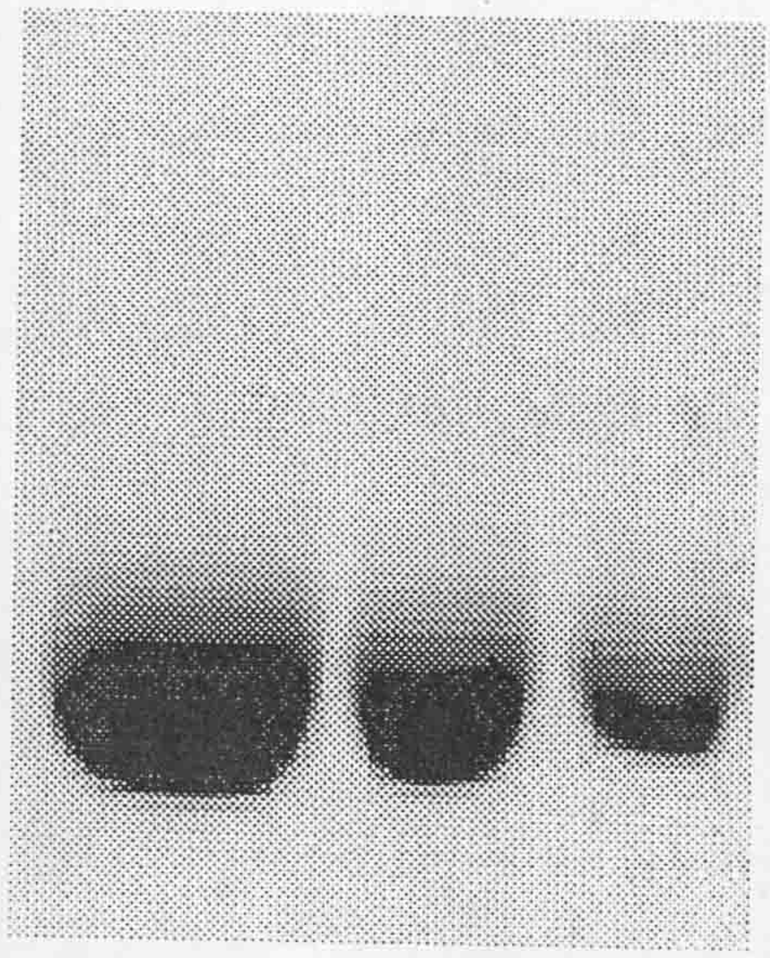

Figure 2.12. Purified S100 proteins. The S100 proteins were collected from the late peak following Superdex-75 chromatography and analysed on 15% SDS-PAGE. Twenty µl from each pooled (estimated 20µg, 12µg and 6µg proteins) collection was loaded on the gel. S100A1 was originally expressed using the pET11a-S100A1 vector, S100A2 was expressed using the pET11a-S100A2 vector and S100A4 was expressed using the pJLA602-S100A4 vector. The gel was stained with Coomassie blue (Section 2.6.3).

2.5.7 GST and GST-S100A1 fusion protein expression

The pGEX-2T expression vector for GST and GST-S100A1 proteins was purchased from Pharmacia (Figure 2.13).

Map

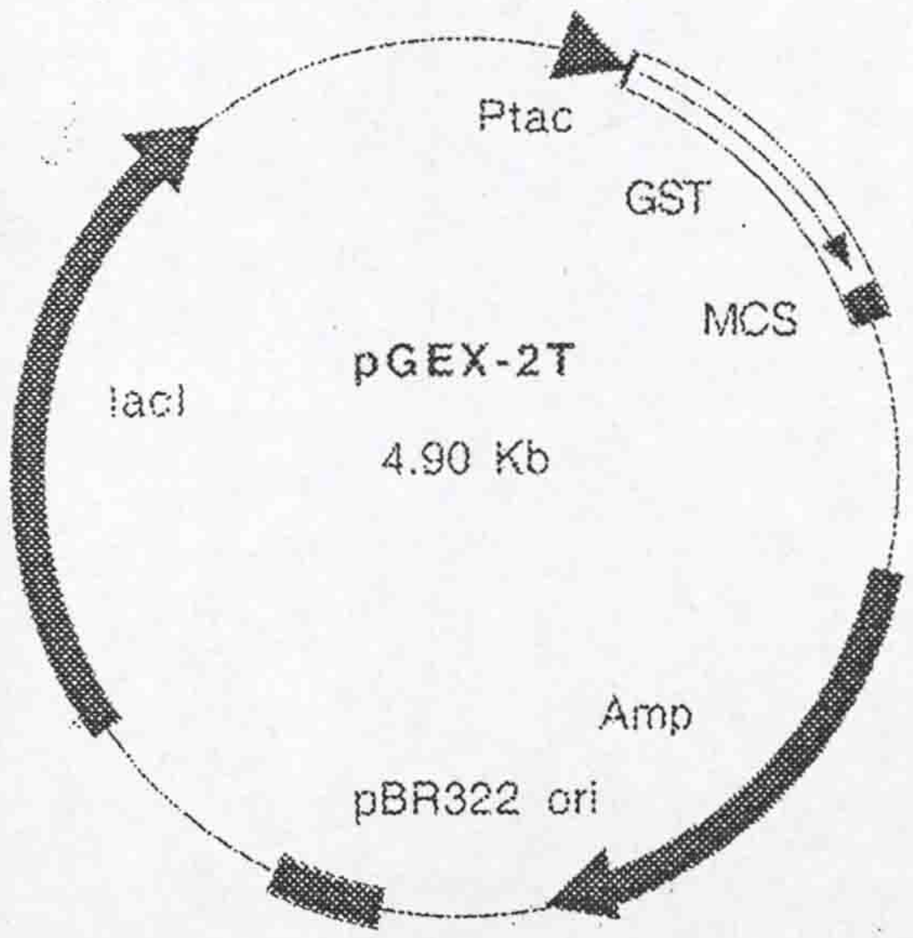

MCS

END OF GST

*Bam*HI *Sma*I *Eco*RI

```
CTG GTT CCG CGT GGA TCC CCG GGA ATT CAT
Leu Val Pro Arg Gly Ser Pro Gly Ile His
```

Thrombin

```
CGT GAC TGA C TGA CG
Arg Asp stop  stop
```

Figure 2.13 pGEX-2T vector. Ptac: tac promotor(183-211); GST: glutathione S-transferase region (258-918); Thrombin: thrombin cleavage site (918-935); Amp: ampicillin resistance gene (1309-2214); *lacI*: $lacI^q$ gene region(3297-4377); pBR322 oi: plasmid replication origin (2974-2977); MCS: multiple cloning site region (930-945). This vector is for expressing GST or GST-target fusion proteins in *E coli.*

The GST protein is a 26 kDa enzyme (Smith & Johnson 1988), which can be easily purified on affinity columns (Kaelin *et al.*, 1992). The Ptac promotor is designed for inducible and high level of expression in *E.coli* strain BL21, which has an internal $LacI^q$ gene for expression control. The $LacI^q$ product binds to the operator region in the Ptac promotor to prevent transcription until induction by IPTG. This maintains a tight control over background expression. When IPTG is added to cell culture, the IPTG will bind to LacI and release the repression of the Ptac promotor.

For construction of pGEX-S100A1, the S100A1 coding frame was amplified by PCR with the primers: 5' S100A1 *Bam*HI primer GCT GGA TCC ATG GGC TCT GAG CTG G and 3' S100A1 *Eco*RI primer AGT GAA TTC TCA ACT GTT CTC GGA GAA G. The PCR fragment was extracted from the gel, digested with restriction enzymes, *Eco*RI and *Bam*HI and subcloned into the pGEX-2T vector at *Bam*HI and *Eco*RI sites. The whole of S100A1coding sequence and the junctions between S100A1 and the vector were sequenced to rule out the possibility of mutations resulting from the PCR reaction.

For large-scale expression, the BL21 DE3 competent cells were transformed with pGEX-S100A1 and pGEX-2T vectors. A single colony from each transformation was cultured in 5 ml LB overnight at 37 °C. The overnight culture was transferred to 500 ml 2 x YT medium and cultured to OD_{600nm} of 0.5. Then 1mM IPTG was added and the culture was incubated for a further 90 min with constant shaking at 37°C. The cell was harvested by centrifugation.

2.5.8 GST and GST-S100A1 purification

The cell pellet from above was resuspended in 1x GST-binding buffer (Section 2.2.11) with 100 μg/ml lysozyme and 1mM PMSF. After incubation on ice for 15min, 5mM DTT was added and the cell extract was sonicated. Triton X-100 was added to the extract to a final concentration of 1%(v/v) and the extract was centrifuged at 15,000rpm at 4°C for 20 min in Sorvall centrifuge. The supernatant was applied to a Glutathione-S-Sepharose column (Section 2.5ml) equilibrated with PBS. The unbound proteins were washed away with 25

ml PBS. The GST or GST-tagged protein was eluted from the column with normal elution buffer or extreme elution buffer (Section 2.2.11). The proteins were analysed on SDS-PAGE. The column was regenerated with regeneration buffer A and B (Section 2.2.11). The GST and GST-S100A1 were normally over 95% pure but the GST-S100A1 always showed some evidence of degradation (Figure 2.14). The proteins were then dialysed against PBST (Section 2.2.21) for 24 h with two buffer changes. Concentrations of the proteins were determined by the Bradford method (Section 2.6.1) and the dialysate was aliquoted and stored at –80 °C.

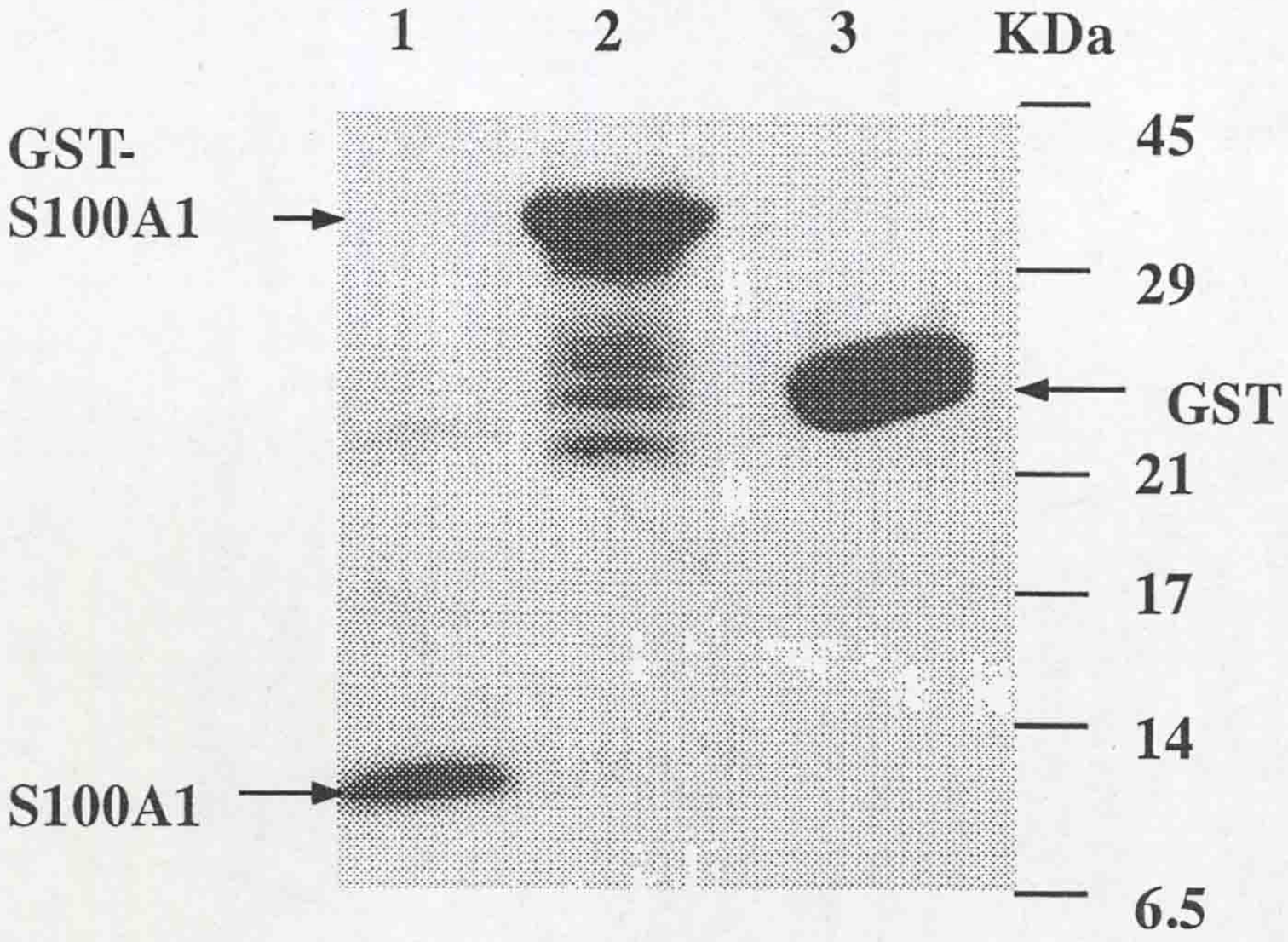

Figure 2.14 Purification of GST-S100A1 and GST proteins. The GST and GST-S100A1 fusion protein were expressed in *E coli* and purified by affinity chromatography on Glutathione-Sepharose columns. The purified proteins were analysed on 15% (w/v) of SDS-PAGE and the gel was stained by Coomassie blue (Section 2.6.3). *Lane 1*, non-tagged S100A1 protein (Section 2.5.7), the weak band with higher molecular weight (about 22 kDa) than the major band (10kDa) is the S100A1dimer as it can be recognised by anti-S100A1 antibody; *lane 2,* GST-S100A1 fusion protein, the weaker, smaller bands than the major band (36 kDa) are thought to be degradation products of GST-S100A1; lane 3, GST (26kDa).

2.5.9 Expression S100A4 protein using pJLA vector

The pJLA 602-S100A4-expression vector was generated originally by Gibbs (Gibbs *et al.*, 1995). The map of the construct is shown in Figure 2.15. The transcription of S100A4 mRNA is initiated at the bacteriophage major left (P_L) and right promoters (P_R) in tandem and terminated by the bacteriophage fd-terminator. Transcriptional activity is very effectively repressed at 28°C-30°C by the temperature-sensitive product of the bacteriophage cI^{ts857} gene, and induced by inactivating the cI gene by raising the incubation temperature to 42 °C.

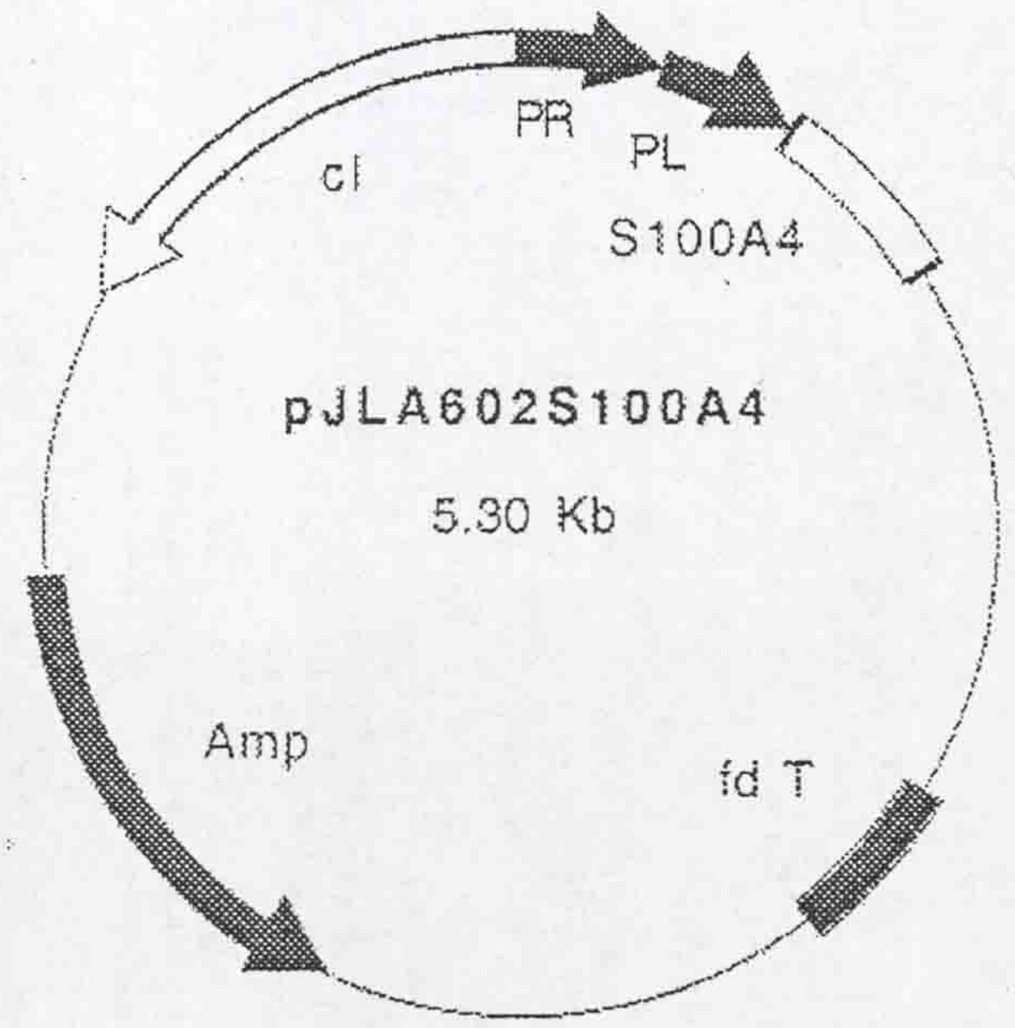

Figure 2.15 pJLA602S100A4 expression vector. pL and pR: bacteriophage major left and right promotors. fd T: bacteriophage fd-terminator. cI: bacteriophage cI^{ts857} gene, which can be inactivated by raising temperature to 42°C. Amp: ampicillin resistance gene. S100A4: rat S100A4 coding sequence.

R1180 competent bacteria were transformed with the expression plasmid, pJLA602S100A4. A single transformant was cultured in 30 ml Terrific Broth (Section 2.2.2) containing ampicillin and tetracycline overnight at 30°C with shaking at 200rpm.Thirty ml of the overnight culture was diluted to 3,000ml Terrific Broth (Section 2.2.2), divided into 6 x 2L flasks and incubated at 30°C with shaking at 200 rpm. When the culture reached OD_{600nm} 0.5, the temperature of the incubator was raised to 42°C and the culture was incubated for a further 22 h. The bulk bacterial culture was harvested by centrifugation for 10 min at 4,000 rpm and the pellet was washed with 50 ml buffer B (Section 2.2.12). The pellet was resuspended in 30 ml buffer B and frozen at -80°C. The cells were thawed at 37°C and PMSF was added to a final concentration of 1 mM. The cells were then sonicated on ice and centrifuged at 15,000 rpm for 30min and the resultant supernatant was collected for purification. The remainder of the procedures was exactly the same as that described in Section 2.5.7.

2.6 General protein biochemistry methods

Protein concentration determination

The concentrations of the purified recombinant protein preparations were determined using the methods of Bradford (1976) using the Coomassie reagent from Bio-Rad conducted according to the supplier's instructions.

For S100A4, a sample of purified S100A4 was extensively dialysed against ddH_2O to remove any salt, freeze-dried and weighed. The sample was then used as a standard for measuring S100A4 at the absorption of 280nm in a spectrophotometer.

2.6.1 Protein electrophoresis

Protein samples and standards for SDS-PAGE analysis were dissolved in SDS-PAGE sample buffer (Section 2.2.13) and boiled for 5 min before being subjected to SDS-PAGE (Laemmli 1970) using the Bio-Rad Mini Protean Gel System. The concentrations of the resolving gels were 7.5% to 15%(w/v) in acrylamide depending on the protein analysed whilst that of the stacking gel was always 4 % in acrylamide. Gels were run at 160 V.

2.6.2 Coomassie brilliant blue staining of protein gel

The gels after electrophoresis were stained with Coomassie blue staining solution (Section 2.2.14) containing Coomassie brilliant blue 250R for over 3 h or overnight, rocking at room temperature and destained with destaining buffer (Section 2.2.14) until clear protein bands were revealed.

2.6.3 Silver staining of protein gel

Silver staining was carried out in a clean glass or plastic container with constant gentle rocking at room temperature. The gels after electrophoresis were fixed in Fixation Buffer (Section 2.2.16) for 30 min and sensitised in Sensitising Buffer (Section 2.2.16) for 30 min. After washing twice with ddH_2O for 5 min, silver reaction was carried out in silver nitrate solution (Section 2.2.16) for 20 min. The gel was washed twice with ddH_2O, for 1 min each time and then incubated in developing buffer (Section 2.2.16). When clear bands appeared, the reaction was terminated with Stop Buffer (Section 2.2.16) for 10 min. The stained gel was finally preserved in gel preserving buffer (Section 2.2.16).

2.6.4 Western blotting

Proteins were separated by SDS-PAGE using the Bio-Rad Mini Protean Gel System and electrophoretically transferred to a PVDF membrane (Milipore) using the method of Towbin (Towbin *et al.*, 1992) using a Bio-Rad mini transblot apparatus at 70V for 2 h.

After transfer, the membrane was incubated with blocking buffer (Section 2.2.17) for at least 1 h at room temperature or overnight at 4°C. The membrane was incubated with primary antibody in the Antibody Dilution Buffer (Section 2.2.17) for over 2 h at room temperature or overnight at 4°C. After washing with Washing Buffer (Section 2.2.17) four times, 10 min each time, the membrane was incubated a further hour at room temperature with a peroxidase-conjugated secondary antibody (1:2,000-1:8,000). After washing, the antibodies bound to the membrane were visualised by incubation with ECL reagents for 2 min at room temperature and recorded on X-ray film with 1-10 min exposure.

2.6.5 Gel overlay with S100A4 protein

The gel overlay method used in this study is a modification of a previously published procedure (Burgess *et al.*, 1984). The recombinant proteins were subjected to SDS-PAGE using the buffer system of Laemmli (Laemmli 1970) and electroblotted onto PVDF membranes (Towbin *et al.*, 1979). The membranes were incubated overnight with Overlay Buffer (Section 2.2.18) containing 3 μg/ml rat rS100A4 and 0.5 mM $CaCl_2$ and washed four times, 5 min each time with gel overlay wash buffer (Section 2.2.18). Membranes were then incubated with overlay blocking buffer (Section 2.2.18) for 1 hour and washed three times, 5 min each time with wash buffer (Section 2.2.17). The membranes were incubated for 2 h with 2.5 ml of the Antibody Dilution Buffer (Section 2.2.17) containing a 500-fold dilution of the rabbit anti-rat S100A4 serum. After washing in buffer six times, 5 min each time, the filters were incubated for 1 hour in a 4,000-fold dilution of a secondary antibody (HRP-conjugated anti-rabbit IgG, Sigma). After a final wash with TBST (Section 2.2.17) for 30 min, bound antibody was detected using the ECL system with exposure against Kodak XAR-5 film.

2.6.6 GST-pull down assay

For the detection of binding of S100A1 and S100A4 proteins *in vitro*, the GST-S100A1 fusion protein or GST alone was attached to glutathione S-Sepharose slurries (Amersham Pharmacia Biotech) at a concentration of 0.5 mg/ml of slurry. One hundred μl of a solution of 0.1mg/ml rS100A4 protein in KTT buffer (Section 2.2.19) was incubated with 100μl aliquots of the GST or GST-S100A1 slurries for 3 h at 4°C. The mixtures were applied to spin columns and centrifuged in a microcentrifuge at 800 rpm for 1 min. The columns were spun-washed with the KTT buffer at least 10 times. Unbound proteins were eluted with at least 50 bed volumes of KTT, until no further protein was eluted. Bound proteins were eluted with GST Elute Buffer (Section 2.2.19). Eluted S100A4 was analyzed by SDS-PAGE, followed by transfer onto PVDF filters (Immobilon, Millipore, France), and incubation with a 1:500 dilution of an affinity-purified rabbit polyclonal antibody to rat rS100A4. Bound antibodies were detected using the ECL system (Amersham Pharmacia Biotech).

2.6.7 PKC phosphorylation

The PKC was purchased from Upstate Biotechnology (purified, having α, β, γ–PKC activities) and the phosphorylation reactions were carried out according to the manufacturer's instructions. The reaction mixture was prepared as follows: 5.2 μg of MH-IIAF21 or 4.2 μg MHC-IIBF17 (to make a final concentration of 5 μM), 10 μl PKA inhibitor, 10 μl PKC activator mixture (Section 2.2.20), 10 μl [r-P^{32}] ATP mixture (Section 2.2.20) and 3 μl PKC enzyme (25ng), ADB buffer (Section 2.2.20) to a total volume of 50 μl. To test the effect of S100A4 on MHC phosphorylation, 0 to 3.2 μg (to make a final concentration of 5 μM) S100A4 was pre-incubated with MHC at room temperature for 40 min. To test the effect of S100A4/S100A1 on MHC phosphorylation, 3.2 μg S100A4 was pre-incubated overnight with 0 to 5.3 μg S100A1 (to make a final concentration of 10 μM) in the ADB buffer containing 0.5mM $CaCl_2$ at 4°C. The mixture was then incubated with MHC-IIAF21 or MHCIIBF17 at room temperature for 40 min. The phosphorylation reactions were incubated at 30°C for 10min and were stopped by adding 12 μl of 5x SDS loading buffer (Section 2.2.13). After boiling for 10 min, 15 μl of sample was loaded on 10% SDS-PAGE. The gel was then dried with a Bio-Rad gel drier and phosphorylation signals were recorded on X-ray film by an overnight exposure.

For the phosphorylation of immobilised MHC-IIAF21 or MHC-IIBF17 on biosensor surface, the [r-P^{32}] ATP was substituted by same amount (in molar) of cold ATP and the reaction mixture was incubated at 30°C for 30 min. The reaction was stopped by removal of the reaction mixture and a thorough wash using PBST.

2.6.8 Myosin sedimentation

The semi-quantitative method was adapted from Murakami (Murakami *et al.*, 1995). 10.5 μM of MHC-IIAF21 or 8.5 μg of MHC-IIBF17 (to make a final concentration of 5μM) was incubated at 4°C overnight in the bundling buffer: imidazole-HCl (pH 7.5), 100 mM NaCl, 2.5 mM $MgCl_2$ in a total volume of 100 μl. After centrifugation at 13600g for 30 min, 20 μl of the supernatant was analysed on SDS-PAGE. For detection of MHC IIA, Western blotting was used with a polyclonal anti-MHC IIA *C*-terminal antibody whilst for detection

of MHC IIB, silver staining or anti-His tag antibody was used.

To test the effect of some S100 proteins on myosin II self-assembly, 6.3μg of S100A4, 5.3 μg of S100A1, and 5.9 μg of S100A2 proteins (to make a final concentration of 5 μM) were pre-incubated for 8 h at 4°C with MHC-IIAF21 or IIBF17 in the presence or absence of 0.5 mM $CaCl_2$. To test the effect of S100A4/S100A1 on the MHC IIA self-assembly, 6.3 μg S100A4 (to make a final concentration of 5 μM) was pre-incubated overnight at 4°C with 0 to 5.3 μg S100A1 (to make a final concentration of 5 μM) in the presence of 0.5 mM $CaCl_2$. The mixture was then incubated with MHC IIA for 8 h at 4°C. Bundling buffer was then added to the mixture and incubated overnight at 4°C. The rest of the procedures are same as above.

2.7 Optical biosensor

2.7.1 Introduction

Since the introduction of a commercial surface plasmon resonance (SPR) biosensor in 1990 (Fagerstam *et al.*, 1990), SPR has become increasingly popular for the qualitative and quantitative characterization of the specific binding of a mobile reactant to a binding partner immobilized on the sensor surface (Szabo *et al.*, 1995). This new technique can measure the binding affinities and the kinetic constants of reversible interactions between biological macromolecules. SPR biosensor is attractive, in part, because the measured physical quantity is a refractive index change and therefore no chromophoric group or labeling of macromolecules is required. The SPR can be applied to interactions within a range of affinities from μM to sub-nM. The SPR uses only small sample volumes and can provide a large amount of real-time information on the course of binding. With this information, the equilibrium constants of association and dissociation of the reactants can be determined (Schuck 1997)

2.7.2 Protein preparation and immobilization

The purified S100 proteins were extensively dialysed against the Pi buffer (Section 2.2.21) and the protein solutions were concentrated with ULTRAFREE-15 Centrifugal Filter

Devices (Millipore). The concentrations of the recovered protein were determined as described in Section 2.6.1. The MHC-IIAF21 and IIBF17 proteins were dissolved in Pi buffer with 0.2 % (w/v) SDS after final step of purification (Section 2.5.7) to keep them in a soluble form.

A dual beam manual biosensor machine (Affinity Sensor) was used in all the related experiments. The dual well cuvettes with an amino silane surface were purchased from Affinity Sensor and the immobilisation was carried out according to the protocol supplied by the company as follows: (1) wash the surface with Pi buffer 50 µl x 3; (2) to activate the surface, 3 x 30 µl of BS3 solution (Section 2.2.21) were added and removed, the last solution was left for 8min and a binding curve was viewed on the window of IAsys Auto programme; (3) wash the surface with Pi buffer 50 µl x 3; (4) add 25 µl Pi buffer and 5 µl of prepared protein solution with 10-20 µg protein, leave for about 30 min for binding and a binding curve was displayed; (5) wash the surface with Pi 50 µl x 3 and the binding response generated should be between 150-300 arc seconds. If less than 150 arc seconds, step (4) was repeated; (6) to block the excess binding sites on the surface, 3x50 µl of 3M Tris-HCl (pH 8.0) were added and the last solution was left for 10 min. After washing with PBST (Section 2.2.21) 50 µl x3, the surface was ready for use. All the procedures were carried out at 20 °C with frequent stirring at 100 times per second.

2.7.3 Determination of the binding affinity with the biosensor

The ligates, S100 proteins, were in Pi buffer and diluted to different concentrations with PBST buffer (Section 2.2.21). For each binding cycle, the surface was first washed with PBST 3 x 50 µl and the last wash was left for 5-10 min, until a stable base line was achieved. Then 26 to 29.5 µl PBST (Section 2.2.21) with or without $CaCl_2$ (depending on the experiment) was added and left for 3 min and from 0.5 to 4 µl of ligate was added to make a total reaction volume of 30 µl. The binding phase lasted 5 min. The surface was then washed with 3 x 50 µl of PBST. The last wash was left for 3 min to determine the dissociation rate. The last step in the cycle was to regenerate the surface with 3 x 50 µl washes of 20 mM HCl followed by 3 x 50 µl washes of PBST. For measuring the binding

affinity of each pair of proteins, a series of concentrations of ligate were used and a set of binding cycles were generated. Their Kds were then calculated using Fastfit software provided by the company (IAsys sensor).

2.8 Cell culture

2.8.1 Routine culture of cells

Rat mammary (Rama) cells and human mammary cells were seeded into 9 cm diameter tissue culture dishes and grown in monolayer culture in Routine Medium for Rama cells (Section 2.2.22) at 37°C in a humidified atmosphere of 10% CO_2: 90% air. The cells were washed twice with PBS and incubated in 5 ml Versene (Gibco) at 37°C for 10 min and then washed twice with PBS before each passaging. The human mammary cell lines, MCF-7A, MDA-MB-231, and SKBr-3, were grown in a specific culture medium for each individual cell line (Section 2.2.22). The cultured cells were transferred or passaged when the cell monolayer was 80% confluent.

2.8.2 Counting cells

The number of cells in suspension was determined using a particle counter (Coulter Electronics). A sample of cell suspension (0.5 ml) was mixed with 9.5 ml of Isoton II (Coulter Electronics, Luton, UK). Replicate counts were performed upon each suspension of cells and the mean was used to calculate the number of cells in the original suspension.

2.8.3 Freezing cells

When cell monolayers were ready for passaging, they were detached as described in Section 2.8.1. The resuspended cells were transferred to a 25 ml plasticUniversal tube and the total number of cells determined (Section 2.8.2). The cell suspension was centrifuged at 800 rpm. for 5 min in a bench centrifuge, and the supernatant removed by aspiration. The cell pellet was resuspended in an appropriate volume of Freezing Medium (Section 2.2.22) to produce a final cell density of 1 x 10^6 cells/ml and 1 ml aliquots were transferred to cryotubes. The cryotubes were placed on dry ice for 2 h and then stored at –70°C for 2-3 days before being transferred to a –140°C freezer for long-term storage.

2.8.4 Thawing cells

Cryotubes were removed from –140°C storage and thawed by being placed in a 37°C water bath. The cells were transferred to a 25 ml plastic Universal tube to which 10 ml of Routine Medium (Section 2.2.22) was added slowly. The cell suspension was then centrifuged at 800 rpm for 5 min. The supernatant was discarded and the cell pellet was resuspended in 9 ml Routine Medium (Section 2.2.22). The cell suspension was transferred to three 9 cm dishes and suitable culture medium was added to give a final volume of 10 ml per dish.

2.8.5 Cell transfection

For transient transfection of GFP or dsRED fusion plasmids, cells were routinely cultured and passaged into 35 mm diameter glass-bottomed microwell dishes (p35G-1.5-7c, Matek Corporation) at a density of 2 x 10^4 cells/dish. After 24 h incubation at 37°C in an atmosphere of 10% CO_2, the medium was changed to 1.5ml of normal medium without antibiotics (penicillin and streptomycin). Two µl of Fugene 6 (Roche) was used for each transfection, which was mixed with 100 µl serum free medium and incubated for 5 min. One µg DNA was added and the resultant mixture was incubated at room temperature for 20 min. Finally the mixture was added to the dish. After 24 h of incubation at 37°C in an atmosphere of 10% CO_2, the dish was checked in a confocal microscope with excitation at 488 nm for GFP and 543 nm for dsRED.

For generating stably transfected cell lines, the Rama 37 and KP1-Rama 37 cell lines (Davies *et al.*, 1993b) were seeded at a density of 8 x 10^4 cells per well in 6-well dishes and incubated, routinely overnight. The cell monolayer was washed twice with PBS and 800µl serum-free and antibiotics-free medium was added. For each transfection, 100 µl of serum-free and antibiotics-free medium was mixed with 6 µl of lipofectamine (Life Technologies) in a sterile tube and then 0.5 µg pCDNA4-S100A1 DNA was added and mixed. After 45 min of incubation at room temperature to allow DNA-liposome complexes to form, 100 µl of serum-free and antibiotics-free medium was added and the resultant mixture was transferred to one well in a 6-well dish with gentle mixing. The cell culture was then incubated for 5 h and then 1 ml antibiotics-free medium containing 20% FCS was

added. After a further 19 h of incubation, this medium was replaced by Routine Medium and Zeocin at a final concentration of 750 μg/ml was added for selection. Cells were cultured in the Selective Medium for a further 2-3 weeks until the cells in control mock transfection wells all died and healthy cell clones had formed in the transfected wells. The clones surviving in Zeocin-containing medium were isolated and transferred using a ring cloning technique (McFarland 2000). These clones were grown in culture under selective condition for a further 7 days. For each clone, a fraction of the cells was frozen for future use and the remainder were used to prepare total RNA. After analysis using Northern blotting, the clones with high level, medium level and undetectable level of expression of S100A1 mRNA were selected and used for the following experiments.

2.8.6 Immunofluorescent staining of cells

About 500 cells were seeded per well of chambered slides and grown in culture for 24 h. The cells were fixed with 4% (w/v) paraformadehyde (Section 2.2.23) in PBS for 10 min. and then permeabilized with Permeabilisation Buffer (Section 2.2.23) for 5 min. After a 30-minute incubation in Blocking Buffer (Section 2.2.23), the cells were incubated with primary antibody, either rabbit anti-S100A4 (1:50 dilution) or mouse anti-S100A1 (1:20 dilution) in Blocking Buffer (Section 2.2.23). After washing four times with PBS, the cells were incubated for 1 hour with the appropriate secondary antibody. Fluorescein isothiocyanate (FITC)-conjugated anti-mouse IgG was used for staining with anti-S100A1 while tetramethylrhodamine-isothiocyanate (TRITC)-conjugated anti-rabbit IgG was used for staining with anti-S100A4. After washing, the slides were dried and mounted. Photographs were taken using a Zeiss LSM 510 confocal microscope.

2.8.7 Soft Agar Assay

To prepare pre-coated agar dishes, 35 mm diameter culture dishes were coated with 2 ml of 0.6% (w/v) agar in Routine Culture Medium with 10% (v/v) FCS. The cells were routinely grown to 80% confluence, detached by trypsinisation and counted as described in Section 2.8.1. The cells were washed once by centrifugation and resuspended in Routine Culture Medium with 10% FCS at 2×10^5/ml. One hundred μl of the cell suspension (2×10^4 cells),

750 µl routine culture medium and 250 µl 1.2% (w/v) agar were mixed and the resultant mixture were added to one pre-coated dish. Triple dishes were used for each cell line. The dishes containing agar were then incubated at 37 °C in the atmosphere of 10% CO_2 for 4 weeks. During this period, 2 drops of routine culture medium were added to each dish twice a week to keep them moist. The resultant clones, > 0.06 mm in diameter, were counted using a microscope. This is because the cell mass < 0.06mm was dying and too small to be counted as a clone that survived in the semi-solid medium. Ten microscopic fields were randomly selected and the average number of clones in each field was calculated. The statistical significance of number of clones between different cell lines was determined using a Fisher Exact test.

2.8.8 Migration assays

Migration assays for Rama 37, KP1-Rama 37 and cells transfected with pCDNA4-S100A1 were carried out using Boyden Chamber units with 6.5 mm diameter polycarbonate membrane inserts with 8 μm pores (Corning Costar). 1 x10^5 cells was added to the upper compartment in 200 µl of BM (Section 2.2.22) with 2% (v/v) FCS. Four hundred µl BM with 10% FCS were added to the lower compartment. At the same time the cells were also seeded into 24 well dishes, 1x10^5 cells in 200 µl BM with 2% (v/v) FCS were added to each well of 3 wells for each cell line analysed. The cells were then incubated at 37°C in an atmosphere of 10% (v/v) CO_2 for 20 h. The filters were then washed with PBS. The cells on the upper surface of the inserts were removed by wiping with a cotton swab, and the cells on the lower surface of the filter were fixed and stained with DiffQuik reagent (Dade Behring). The number of cells of per field that migrated to the lower surface of the filters was determined microscopically. Six to ten randomly chosen fields, 0.5 x 0.5 mm, were counted per filter. The total number of cells per filter was calculated as follows: the average number per 0.25mm^2 x 4 x area (3.25 x 3.25 x 3.14 mm^2) of the filter. The migration ability of each cell line was expressed as a percentage of total cell seeded, which shows how many cells migrated to the lower side of the membrane of each hundred cells added. The results were finally normalized by the cell number in the 24 well plates after 20 h incubation. This is based on the fact that the cells after trypsinisation may vary in viability. In this way, the

cell motilities measured from different cell lines are more comparable.

Chapter Three

The effects of interaction of S100A4 with the *C*-terminal regions of non-muscle myosin IIA and IIB heavy chain

3.1 Introduction

It has been recognized that cell motility by non-muscle cells requires virtually continuous restructuring of the cytoskeleton (Wilson *et al.*, 1992). It is also clear that cell motility requires a mechanism for converting chemical energy into mechanical work. Actin and myosin, two important constituents of the cytoskeleton, have been postulated to act as the chemicomechanical transducer in motile cells. Central to their role as a force generating mechanism in motile cells is the ability of myosin to hydrolyse ATP when it interacts with actin (Collins & Matsudaira 1991).

Myosins constitute a superfamily of actin-dependent molecular motors. Phylogenetic analysis currently places myosins into 15 classes. The conventional myosins that form filaments in muscle and non-muscle cells are grouped as class II myosins. There has been extensive characterization of these myosins and much is known about their functions (Sellers 2000).

Myosin II is an ubiquitous actin-based motor protein and directly involved in regulating cytokinesis, cell motility and cell morphology. All vertebrate cells, including muscle cells, contain a form of myosin II (DeLozanne *et al.*, 1985). Myosin II is composed of a pair of heavy chains, a pair of essential light chains and a pair of regulatory light chains. The two myosin heavy chains are self-associated in their intermediate regions and form a helical coiled coil (rod-like domain). To its *N*-terminus are two heads. Each head can be divided into a globular motor domain of approximately 770 amino acids that contains the catalytic and actin binding sites, and a neck region of approximately 70 amino acids which binds one essential and one regulatory light chain (ELC and RLC). The neck region with its

associated ELC plays both structural and regulatory roles. In the absence of calcium, the RLC is not phosphorylated and the myosin cannot interact with actin. Calcium activates the specific calmodulin-dependent kinase, myosin light chain kinase (MLCK), which phosphorylates the RLC, initiating actin-myosin interaction (Scholey *et al.*, 1980). RLC is the only known substrate for MLCK (Gallagher *et al.*, 1997). To the *C*-terminus of the rod region is a non-helical tailpiece of approximately 34–44 amino acids (Korn *et al.*, 1988), which was shown to regulate filament formation and localization of myosin II (Sabry *et al.*, 1997).

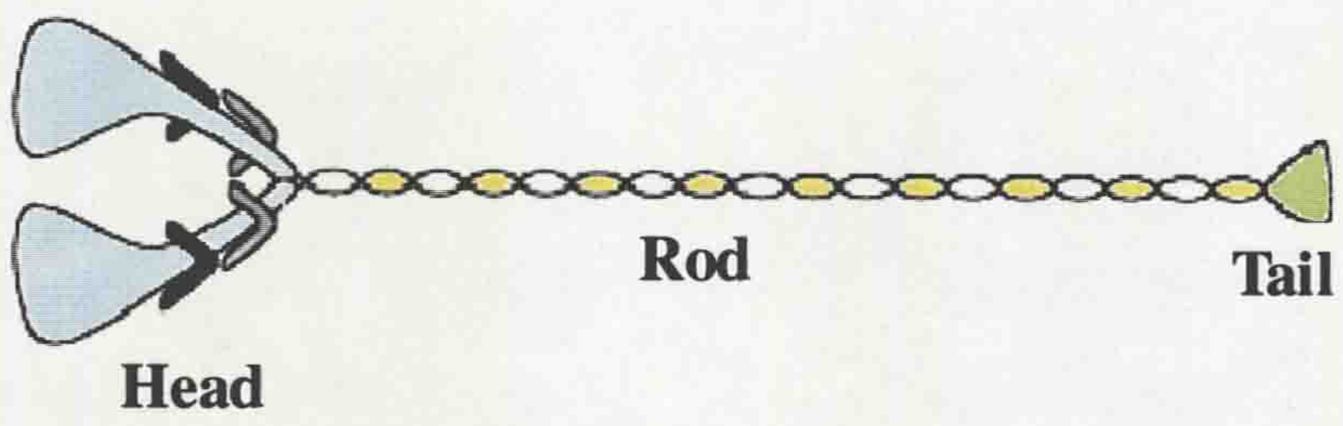

Figure 3.1 A diagram of myosin II molecules. The Myosin II molecule is shown consisting of a pair of essential light chains (in black), a pair of regulatory light chains (in grey) and a pair of heavy chains (in color) which form the basic structure of the molecule, head (blue), rod (white and yellow) and tail (green)

Vertebrates express at least two non-muscle myosin-II heavy chain isoforms, myosin IIA (MHC-IIA) and myosin IIB (MHC-IIB) (Simons *et al.*, 1991; Saez *et al.*, 1990). These two isoforms exhibit 85% amino acid identity in the motor domain and 72% identity in the rod, with most of the differences clustered in the nonhelical tailpiece. Most tissues express various ratios of MHC-IIA and MHC-IIB; however, the relative amount of the two isoforms in a given tissue is species-dependent, and some tissues and individual cell types within a specific tissue express only a single isoform (Cheng *et al.*, 1992). For example, chicken intestinal epithelium, platelets and rat basophilic leukemia cells express exclusively MHC-IIA, whereas embryonic cardiac myocytes only express MHC-IIB and brain is highly enriched in MHC-IIB. The isoforms of non-muscle myosin II have different

distributions *in vivo*, even within individual cells. Cultured bovine aortic endothelia contained both MHC-IIA and IIB. Both isoforms are distributed along stress fibres, in linear or punctate aggregates within lamellipodia, and diffusely around the nucleus. The MHC-IIA isoform was preferentially located toward the leading edge of migrating cells while the MHC-IIB isoform was enriched in structures at the trailing edges of cells (Cheng *et al.*, 1992). The MHC-IIA isoform appeared in newly formed structures more rapidly than the MHC-IIB isoform, and was also lost more rapidly when structures disassembled. These observations suggest that the different localizations of MHC-IIA and IIB reflect different rates at which the isoforms transit through self-assembly, movement and disassembly within the cell. The relative proportions of different myosin II isoforms within a particular cell type may determine the lifetimes of various myosin II-based structures in that cell (Kolega 1998).

The biochemical properties of the two isoforms are also consistent with the premise that MHC-IIA and MHC-IIB are functionally distinct. MHC-IIA has a maximal actin-activated ATPase activity that is 2.6-fold greater than that of MHC-IIB, and moves actin filaments at velocities 3.4- fold faster than those observed with myosin-IIB (Kelley *et al.*, 1996). The identification of a single isoform in some cell types suggests that in certain contexts MHC-IIA and MHC-IIB may be functionally interchangeable; however, the localization of the two isoforms to different actin-rich structures suggests that myosin-II molecules with different biochemical activities are required at specific subcellular sites. The proposal that MHC-IIA and MHC-IIB have unique functions *in vivo* is further supported by the observation that inhibition of MHC-IIB expression in neurons diminishes the length of neuritic extensions without affecting the number of neurites per cell or the extension of small protrusions (Wylie *et al.*, 1998). These findings suggest that MHC-IIB mediates neurite growth and growth cone advancement, and that MHC-IIA cannot compensate for MHC-IIB in these processes.

Three additional MHC-IIB splice variants have been identified in neuronal tissue, which result in the insertion of 10(B1a), 16(B1b) or 21(B2) amino acids within the motor domain

(Itoh *et al.*, 1995). In the cloning of MHC-IIB cDNA from the chicken brain, two exon cassettes that undergo alternative splicing have been identified. One insert encoding 10 amino acids (termed a B1 cassette) is located near the ATP binding region, and another insert encoding 21 amino acids (termed a B2 cassette) is located near the actin binding region (Takahashi *et al.*, 1992;Takahashi *et al.*, 2001). B1 and B2 cassettes are inserted into flexible structures loop 1 and loop 2, respectively, which are thought to be important in regulating actin motor activities. The expression of these two exon cassettes is specific to the central nervous system. In the chicken brain, MHC-IIB with the B1 cassette (MHC-IIB (B1)) is highly expressed during early embryonic stages, while that with the B2 cassette (MHC-IIB (B2)) begins to be expressed around birth (Itoh K 1995). Further study of the *C*-terminus of rabbit brain MHC-IIB, two different MIIB clones containing closely related, but distinct, cDNA sequences were identified (Murakami *et al.*, 1998). These two species of MHC-IIB were designated MHC-IIB$^{\alpha}$ and MHC-IIB$^{\beta}$. The two isoforms showed differences in filament self-assembly properties in the presence of various concentrations of salt. PKC incorporated 1 mol of phosphate/ mol peptide to MHC-IIB$^{\alpha}$ but 2 mols to MHC-IIB$^{\beta}$. However, PKC had very similar effects on the filament self-assembly properties of the two isoforms. Casein kinase II incorporated 4 mol of phosphate/mol peptide to MHC-IIB$^{\alpha}$ but 2 to MHC-IIB$^{\beta}$ and this caused strong inhibition of self-assembly to MHC-IIB$^{\alpha}$ but only slight inhibition to MHC-IIB$^{\beta}$. The human MIIB identified is more similar to the rabbit MIIB$^{\alpha}$ than to MIIB$^{\beta}$ according to their amino acid sequences (see figure 3.1).

Figure 3.2 Comparison of the amino acid sequences of human MHC-IIB *C*-terminus with rabbit MHC-IIB$^{\alpha}$ and MHC-IIB$^{\beta}$. In this region, there are 6 amino acids in human MHC-IIB (in purple) different from both MHC-IIB$^{\alpha}$ and MHC-IIB$^{\beta}$of rabbit. There are 6 different amino acids between rabbit MHC-IIB$^{\alpha}$ (in red) and MHC-IIB$^{\beta}$ (in blue), among them, 4 amino acids in MHC- IIB$^{\beta}$ are different from human MHC-IIB and only 2 amino acids in MHC- IIB$^{\alpha}$ are different from human MHC-IIB. Therefore, human MHC-IIB is more similar to rabbit MHC-IIB$^{\alpha}$ than MHC-IIB$^{\beta}$ in identical amino acids in the *C*-terminal region of 366 amino acids.

Cells lacking myosin II appear to be incapable of generating or maintaining 3D shape independent of a substrate. When a substrate is available, these MHC II^{-} (lack of myosin II) cells can attach and spread on the surface in a myosin-independent manner but cannot maintain their normal 3D cell shapes that require myosin II (Shelden & Knecht 1996).

Myosin II is important to cell motility. Amongst the remarkable variety of motility that cells display, cytokinesis (cell division) is particularly striking. Dramatic changes in cell shape occur before, during and after cytokinesis. Myosin II is implicated in the 'rounding up' of cells prior to cytokinesis, and is essential in the formation of the contractile cleavage furrow during cytokinesis (Maciver 1996).

Phosphorylation is an important factor in regulating the functions of myosin II. Phosphorylation occurs not only on its regulatory light chains (RLC), essential light chains and also on heavy chains. During cellular events, such as mitosis (Yamakita *et al.,* 1994) and secretion (Choi 1994), multiple residues on the RLC and myosin-II heavy chain are phosphorylated. These phosphorylation events have been attributed to several different kinases, including protein kinase C, the Ca^{2+}/calmodulin-dependent myosin light chain kinase (MLCK) (Scholey *et al.,* 1980), Rho kinase (Amano *et al.,* 1998), p21-activated kinase (Chew *et al.,* 1998) or casein kinase II. This suggests that myosin II may be subjected to regulation by multiple phosphorylation signals. Equally important for the regulation of myosin II function will be the activities of the phosphatases that mediate dephosphorylation of the heavy and light chains, although at present very little is known about these activities (Somlyo *et al.,* 2000).

Although most research has been carried out on the phosphorylation of myosin light chains, distinct phosphorylation sites for PKC and casein kinase II on MHC-IIA and MHC-IIB have also been identified. *In vitro*, PKC phosphorylates MHC-IIA on a single serine residue near the carboxy-terminal end of the predicted helical domain (Conti *et al.*, 1991), and MHC-IIB on multiple serines in the non-helical tailpiece (Murakami *et al.,* 1998). Casein kinase II phosphorylates both isoforms on the non-helical tailpiece (Murakami *et al.,* 1998; Murakami *et al.*, 1990). Importantly, phosphorylation of the heavy chain is also observed *in vivo* (Moussavi 1993). In resting T lymphocytes, MHC-IIA is phosphorylated on the casein kinase II site; however, following treatment with phorbol esters, the heavy chain is also phosphorylated on the PKC site *in vivo* (Moussavi 1993). MHC-IIA heavy chain phosphorylation at the PKC site is also observed following phorbol ester-induced

activation of PKC in platelets (Kawamoto *et al.*, 1989) and rat basophilic leukaemia cells (Ludowyke *et al.*, 1989). MHC-IIB purified from bovine brain is phosphorylated on a single casein kinase II site (Murakami *et al.*, 1990). The *Drosophila* myosin II tail was also phosphorylated *in vitro* by PKC at serines 1936 and 1944, which are located in the non-helical globular tailpiece. These sites are close to a conserved serine that is phosphorylated in vertebrate, non-muscle myosin-IIs. If the two serines are mutagenized to alanine or aspartic acid, phosphorylation no longer occurs (Su & Kiehart 2001). The non-muscle myosin heavy chain in *Drosophila* appears to be similar to rabbit non-muscle myosin-IIA in having phosphorylation sites on *C*-terminus. Conservation during 530-1,000 million years of evolution suggests that regulation by heavy chain phosphorylation may contribute to non-muscle myosin-II function in some real way (Su & Kiehart 2001).

In the case of MHC-IIA, it is known that the non-helical tailpiece contributes to filament formation. Heavy chain phosphorylation by either PKC or casein kinase II inhibits the self-assembly of MHC-IIB into filaments; whereas, the self-assembly of MHC-IIA is unaffected by this phosphorylation (Murakami *et al.*, 1998). Inhibition of MHC-IIB filament self-assembly by casein kinase II requires phosphorylation of multiple sites on the non-helical tailpiece. In contrast, even though PKC is observed to phosphorylate the non-helical tailpiece of MHC-IIB on multiple sites, PKC phosphorylation on only a single residue is sufficient to inhibit the self-assembly of myosin-IIB into filaments (Murakami *et al.*, 1998).

Conversion of the three mapped threonine phosphorylation sites in the myosin II heavy chain tail to alanines results in a mutant in Dictyostelium discoideum, which displays constitutive myosin overassembly in the cytoskeleton and increased cortical tension (Stites *et al.*, 1998). Myosin II localization in dividing cells is also regulated by myosin heavy chain phosphorylation (Sabry *et al.*, 1997). The myosin II heavy chain (MHC)-specific protein kinase C (MHC-PKC) isolated from Dictyostelium discoideum has been implicated in the regulation of myosin II self-assembly in response to the chemo-attractant, cAMP

(Ravid & Spudich 1989). Cells devoid of MHC-PKC exhibit substantial myosin II over-assembly, as well as aberrant cell polarization, chemotaxis, and morphological differentiation. Cells over-expressing the MHC-PKC contain highly phosphorylated MHC and exhibit impaired myosin II localization and no apparent cell polarization and chemotaxis (Abu-Elneel *et al.*, 1996). Self-assembly of MHC-IIB F47 (C-terminal 47KDa), but not MHC-IIAF46 (C-terminal 46KDa fragment), was significantly inhibited by PKC phosphorylation (Murakami *et al.*, 1995), suggesting that the self-assembly of MHC-IIA and IIB is regulated by different mechanisms.

The interaction of S100A4 and natural MHC-IIA was first revealed by co-immunoprecipitation (Kriajevska *et al.*, 1994) and Ca^{2+}-dependent association between mouse S100A4 protein and recombinant MHC-IIA was confirmed by gel overlay technique (Kriajevska *et al.*, 1994). The mouse S100A4-binding site on MHC-IIA was mapped to a 29-amino acid region at the *C* -terminal end of MHC-IIA (between amino acids 1909-1937;Kriajevska *et al.*, 1998). Co-sedimentation analysis and electron microscopy suggested that mouse S100A4 destabilizes myosin filaments (Ford *et al.*, 1997) In the presence of Ca^{2+}, mouse S100A4 has been reported to inhibit the actin-activated MgATPase activity of myosin *in vitro* (Ford *et al.*, 1997), suggesting the interaction has functional effects. Further investigation found that mouse S100A4 binding to MHC-IIA inhibits the phosphorylation of the myosin heavy chain by PKC and protein kinase CK2 *in vitro* (Kriajevska *et al.*, 2000). Two-dimensional phosphopeptide analysis showed that Mouse S100A4 protein inhibits PKC phosphorylation of the platelet myosin A heavy chain at Ser-1917 (Kriajevska *et al.*, 1998), which is within mouse S100A4 binding site.

As outlined before, overexpression of S100A4 can increase cell motility and cause tumour metastasis (Sherbet & Lakshmi 1998;Davies *et al.*, 1996) and the mechanism is still unclear. Therefore the interaction of S100A4 with the motor molecule in non-muscle cells provides a window to look deep inside the molecular mechanism of metastasis. Thus, in this chapter, the binding of S100A4 on the heavy chain of the other non-muscle myosin II isoform, MHC-IIB and its effects, have been investigated and compared to that of MHC-IIA.

3.2 Results

3.2.1 Preparation of recombinant MHC-IIAF21 and MHC-IIBF17

The constructs, pET16-MHC-IIAF21 and pET16-MHC-IIBF17, which express MHC-IIA *C*-terminal 21 kDa fragment and MHC-IIB *C*-terminal 17 kDa fragment, respectively, were described in Section 2.5.3. The plasmids were transferred into host strain, BL21 DE3, induced with IPTG (Section 2.5.4), and the resulting recombinant myosin fragments purified with His-Binding columns (Section 2.5.5). The purified proteins were analysed on SDS-PAGE (Section 2.6.2) and the gel was stained with Coomassie Brilliant Blue (Section 2.6.3). Both MHC-IIAF21 and IIBF17were over 95% pure (Figure 3.3), based upon scanning of stained gels.

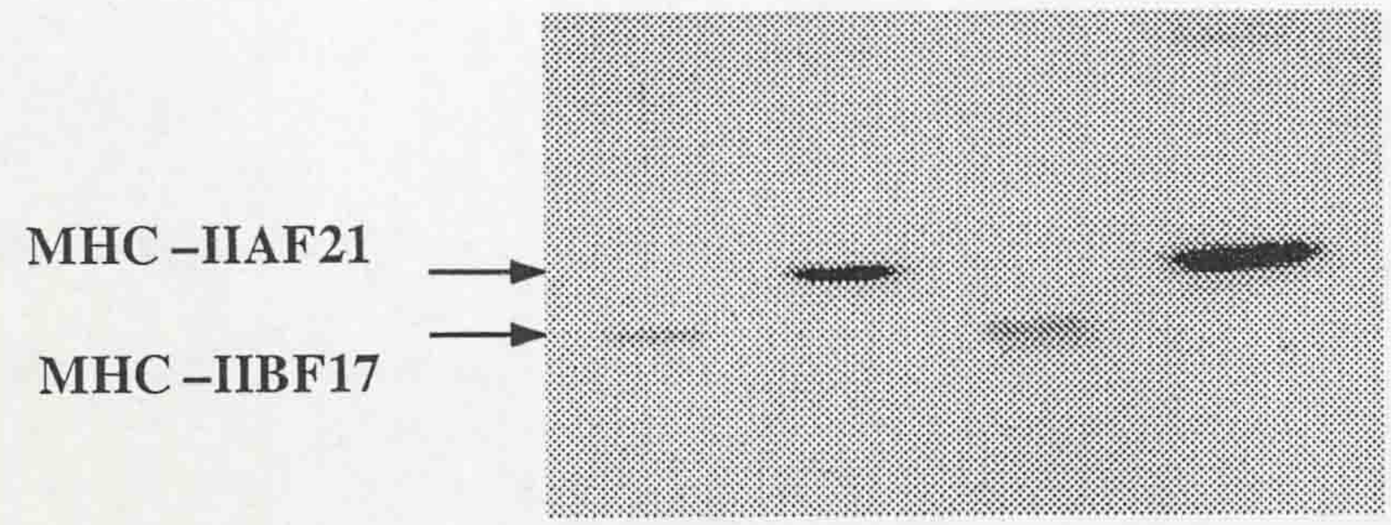

Figure 3.3 Purified MHC-IIAF21 and MHC-IIBF17 recombinant proteins. *Lane 1* and *lane 3*, 2μg and 4μg of MHC-IIBF17 *(C*-terminal 17kDa fragment); *lane 2 and lane 4*, 6μg and 12μg of MHC-IIAF21 (*C*-terminal 21kDa fragment).

3.2.2 The interaction of S100A4 with MHC-IIAF21 and IIBF17 revealed by gel overlay experiments

To confirm the ability of S100A4 to bind to the MHC-IIAF21 and II BF17 recombinant proteins, gel overlay experiments (Section 2.6.6) were performed. In these experiments, varying amounts of MHC-IIAF21 (from 0.05μg to 4.5μg) and IIBF17 (from 0.07μg to 6μg) were loaded onto SDS polyacrylamide gels and subjected to electrophoresis. Known amounts of the proteins were loaded so that the binding of S100A4 to MHC-IIAF21 and MHC-IIBF17 could be quantified. The S100A4 was shown to bind to both MHC-IIAF21 and IIBF17 (Figure 3.4). However, the binding to MHC-IIAF21 appeared stronger than that to MHC-IIBF17 because the binding signal was detected from 0.5μg/lane or above on MHC-IIAF21 while the binding signal was only detected from 2μg/lane or above on MHC-IIBF17 (Figure 3.4). To achieve the same intensity of signal, about 5 times more (in moles) MHC-IIBF17 than MHC-IIAF21 on the gel was needed. This result suggests that S100A4 has a higher affinity for MHC-IIAF21 than for MHC-IIBF17. The control proteins and molecular marker have no background signals, suggesting that the binding is specific for MHC-IIAF21 and MHC-IIBF17.

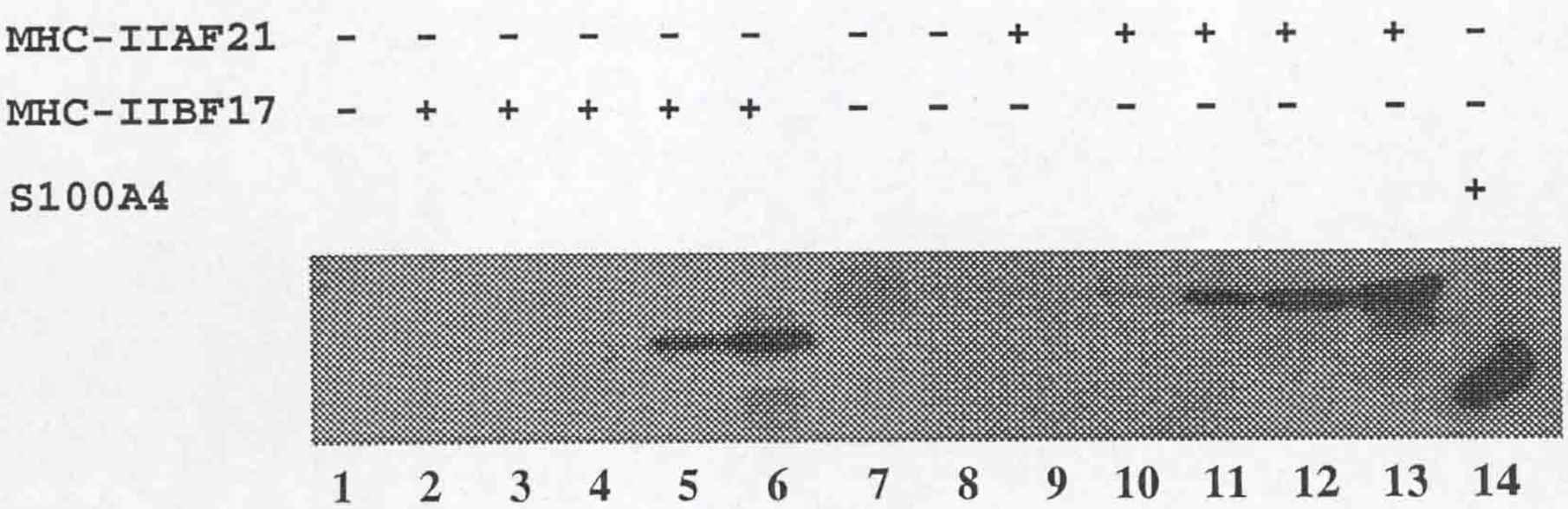

Figure 3.4 S100A4 binding to both MHC IIAF21 and IIBF17 revealed by gel overlay assay (Section 2.6.6). Varying amounts of MHC-IIAF21 and IIBF17 were loaded on SDS-PAGE and blotted onto Immobilon P membrane. The membrane was overlaid with S100A4 in overlay buffer containing 0.5mM $CaCl_2$. The binding of S100A4 to MHC-IIAF21 and IIBF17 was detected by an anti-S100A4 antibody. *Lanes 1 and 8*, bacterial lysate (50μg) of *BL21 DE3* for negative control. *Lanes 2-6*, different amounts of recombinant MHC-IIBF17: 0.07μg (*lane 2*); 0.22μg (*lane 3*); 0.66μg (*lane 4*); 2μg (*lane 5*); 6μg (*lane 6*). *Lane 7*, molecular weight marker. *Lanes 9-13* different amounts of MHC-IIAF21: 0.05μg (*lane 9*); 0.16μg (*lane 10*); 0.5μg (*lane11*); 1.5μg (*lane 12*); 4.5μg (*lane 13*). *Lane 14*, 2μg of S100A4 was used as a positive control for the binding of the S100A4 antibody.

3.2.3 Characterisation of the binding properties of S100A4 to MHC-IIAF21 and IIBF17using an optical biosensor

The recombinant proteins of MHC-IIAF21 or MHC-IIBF17 were separately immobilized onto the amino silane surfaces of the biosensor (Section 2.7.2). The binding properties of S100A4 to immobilized MHC-IIAF21 or MHC-IIBF17 were characterized by fast association kinetics in 0.5 mM calcium buffer. The binding of S100A4 to MHC-IIAF21 or MHC-IIBF17 was always homogenous; there was no evidence for the presence of more than one binding site for S100A4 in MHC-IIAF21 or MHC-IIBF17. Plots of k_{on} against ligand concentration for the binding of S100A4 to immobilized MHC-IIAF21 or to immobilized MHC-IIBF17 in the presence of Ca^{2+} were plotted using FastPlot software

(Figure 3.5) and yielded straight lines (r = 0.96-0.99; Table 3.1). In the presence of 0.5 mM Ca^{2+}, the association rate constant for the S100A4/MHC-IIAF21 interaction (k_{ass} = 53,000 $\pm$ 300 $M^{-1}s^{-1}$) was much higher than for the S100A4/MHC-IIBF17 interaction (k_{ass} = 790 $\pm$10 $M^{-1}s^{-1}$) (Table 3.1). The dissociation rate constant of S100A4 from MHC-IIAF21 (k_{diss} = 0.035 $\pm$0.007 s^{-1}) was much faster than that of S100A4 from MHC-IIBF17 (k_{diss} = 0.005 $\pm$ 0.001 s^{-1}) (Table 3.1). Thus, when the kinetic parameters were used to calculate affinities, the interaction between S100A4 and MHC-IIAF21 had a much higher affinity (Kd 660 $\pm$20 nM) than the interaction between S100A4 and MHC-IIBF17 (Kd 6,300$\pm$ 100nM). The Kd values calculated from the extent of binding observed at equilibrium were very similar to those calculated from the kinetic binding parameters (Table 3.1).

Table 3.1, Kinetics of S100A4 binding to immobilized MHC-IIAF21 and MHC-IIBF17 in 0.5mM Ca^{2+} buffer.

Proteins immobilised	k_{ass} $M^{-1}s^{-1}$ [a]	r [b]	K_{diss} s^{-1} [c]	K_d nM [d] (Kinetics)	K_d nM [e] (Equilibrium)
MHC-IIAF21	$0.53 \pm 0.003 \times 10^5$	0.99	0.035 ± 0.007	660 ± 20	250 ± 20
MHC-IIBF17	$0.79 \pm 0.01 \times 10^3$	0.96	0.005 ± 0.001	$6,300 \pm 100$	$4,000 \pm 300$

a. The S.E. of each determination of k_{ass} is derived from the deviation of the data from a one-site binding model, calculated by matrix inversion using the FastFit software provided with the instrument. No evidence was found for a two-site model of association.

b. The correlation coefficient of the linear regression through the k_{on} values used for obtaining k_{ass}.

c. The k_{diss} is the mean ±S.E. of at least 6 values, obtained at different concentrations of S100A4. No evidence was found for a two-site model of dissociation.

d. The Kd (kinetics) was calculated from the ratio of k_{diss}/k_{ass}, and the S.E. is the combined S.E. of the two kinetic parameters.

e. Kd (equilibrium) were calculated from the extent of binding observed at five or more different concentrations of ligate (S100A4) in two independent experiments. The S.E. is the combined error of the two experiments.

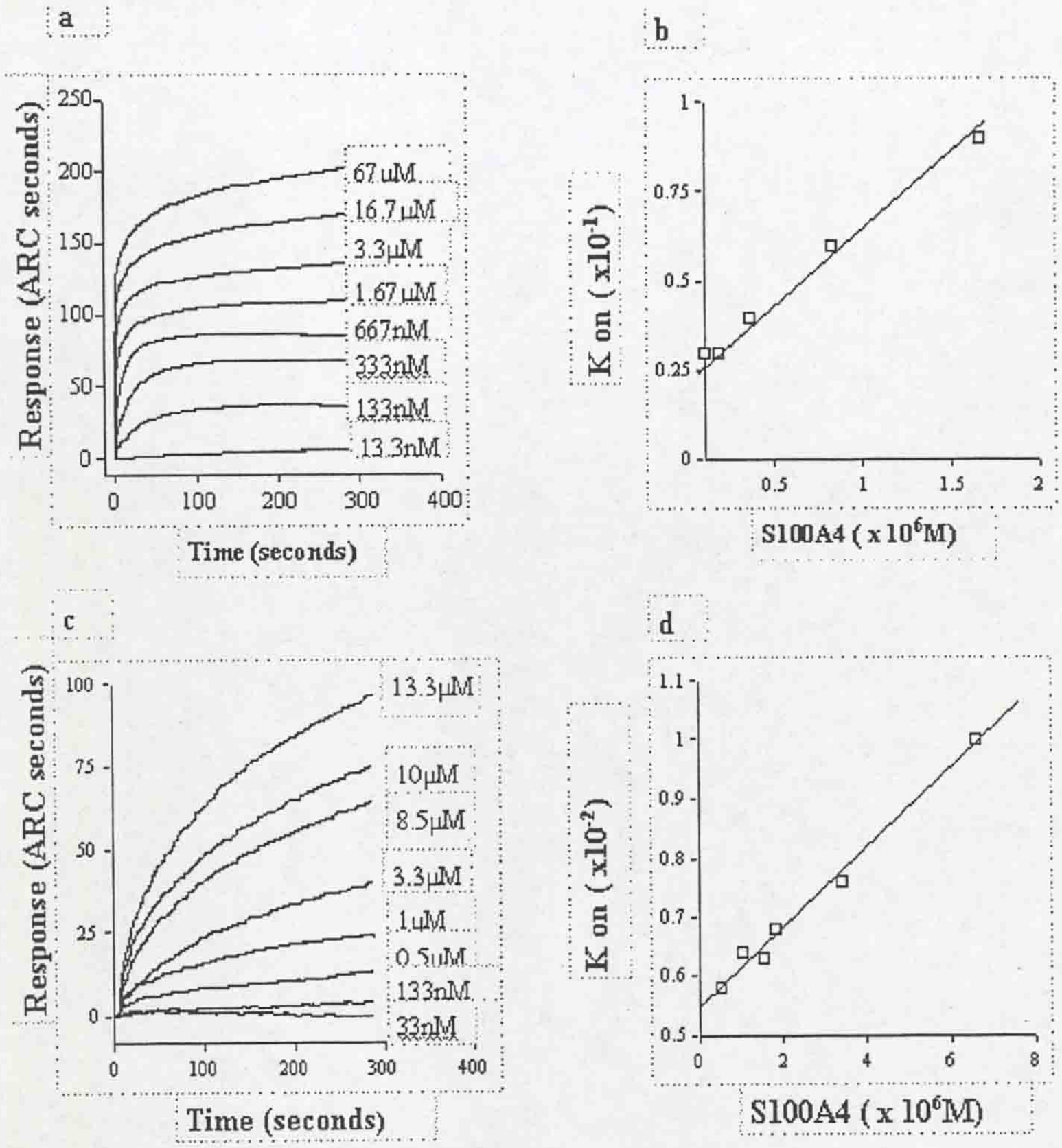

Figure 3.5 S100A4-MHC-IIAF21 and S100A4-MHC-IIBF17 interactions using an optical biosensor. Recombinant MHC-IIAF21 *(panels a-b)* and MHC-IIBF17 *(panels c-d)* were immobilized on an aminosilane surface (Section 2.7.3). Varying concentrations of recombinant S100A4 were added in the presence of calcium ions (0.5mM). The extents of binding were observed for 300-400 seconds (*panels a and c*). The concentration of added S100A4 was plotted against k_{on} using FastPlot software (*panels b and d*) and yielded a straight line (r = 0.96 -0.99) in each case.

3.2.4 Calcium influence on the interaction of S100A4 with MHC-IIAF21 and MHC-IIBF17

Using the biosensor assay, the effects of Ca^{2+} on the binding of S100A4 to MHC-IIAF21 and IIBF17 can be quantified. In a Ca^{2+}-free buffer, S100A4 binds to either immobilised MHC-IIAF21 or MHC-IIBF17 (Figure 3.6). When 0.5mM Ca^{2+} is added to the reaction buffer, the binding responses are obviously increased (Figure 3.6 a, b and c). However, the effect of Ca^{2+} on the binding of S100A4 to immobilised MHC-IIAF21 is much more dramatic than that to immobilised MHC-IIBF17. The binding response (extent) of S100A4 to MHC-IIBF17 increases about 40% whilst the binding response of S100A4 to MHC-IIAF21 increases about 600% relative to the no-added-calcium control after the addition of 0.5 mM Ca^{2+}(Figure 3.6d).

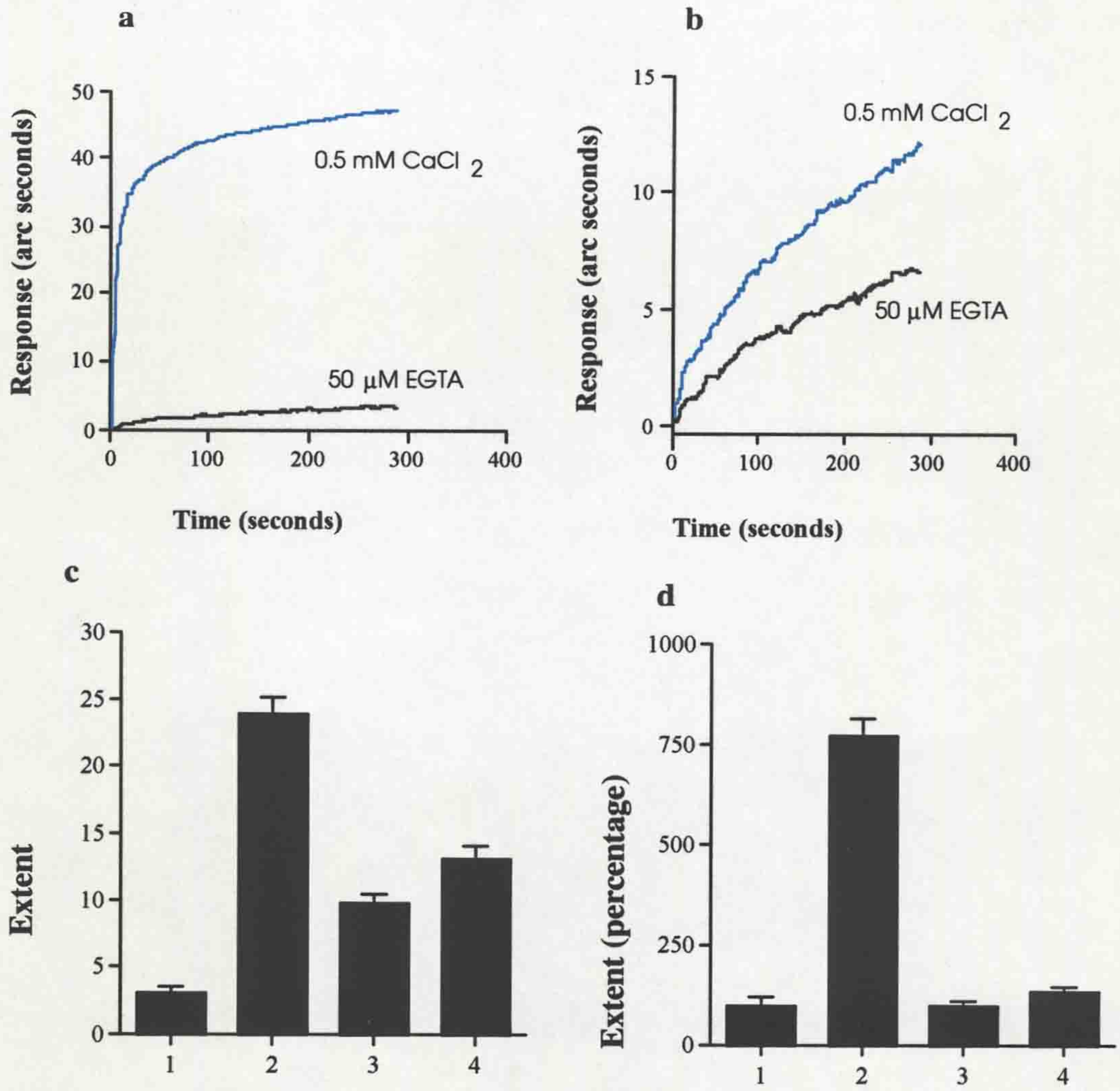

Figure 3.6. Effects of Ca^{2+} on the binding of S100A4 to immobilised MHC-IIAF21 and MHC-IIBF17 detected using biosensor. *Panels a and b:* examples of the binding curves of S100A4 (300nM) on either immobilised MHC-IIAF21 (*panel a*) or MHC-IIBF17 (*panel b*) in the presence or absence of added Ca^{2+}. *Panels c and d*: the extents of each binding cycle were calculated using Fastfit software (Affinity Sensor) (*panel c*) and the extent expressed as percentages with the extent in Ca^{2+}-free buffer shown as 100% (*panel d*), for S100A4 binding to MHC-IIAF21 (*columns 1 and 2*) or MHC-IIBF17 (*columns 3 and 4*) in Ca^{2+}-free buffer (*columns 1 and 3*) and in the presence of 0.5 mM $CaCl_2$ (*columns 2 and 4*).

From the results of the above experiments, S100A4 was shown to bind both MHC-IIA and

IIB *in vitro*. The binding is not Ca^{2+}-dependent but can be enhanced by added Ca^{2+}. The next step of this study is to find out whether the interactions have some biological effects or not.

3.2.5 S100A4 inhibits the phosphorylation of the *C*-terminus of MHC-IIAF21 and IIBF17 by PKC

As outlined above, natural MHC-IIA and MHC-IIB can be phosphorylated by PKC. To show that the recombinant MHC-IIAF21 and IIBF17 can also be phosphorylated by PKC, phosphorylation reactions *in vitro* were carried out as described in Section 2.6.8. The results show that both MHC-IIAF21 and IIBF17 can be phosphorylated by PKC (Fig. 3.7).

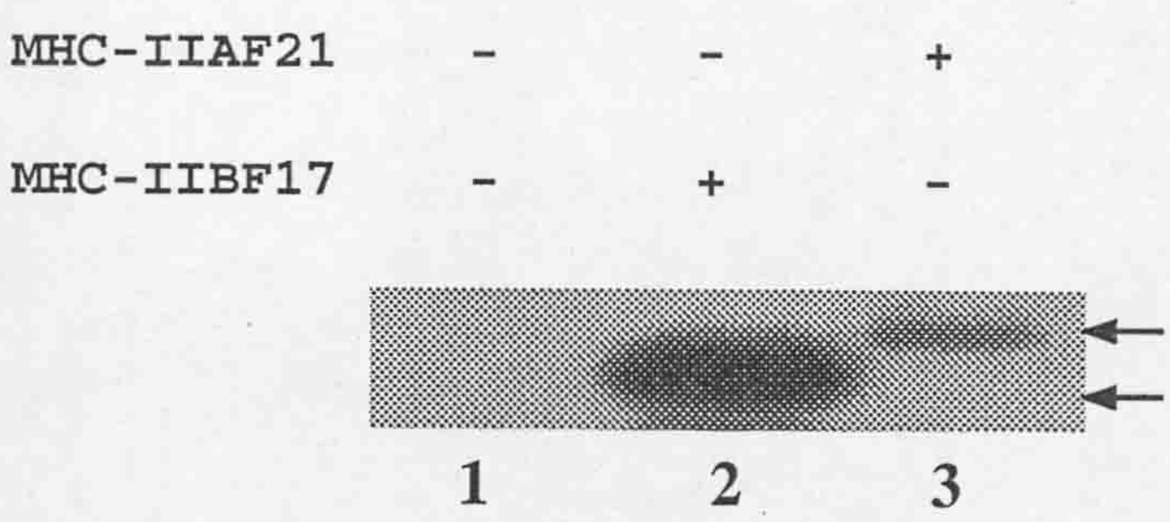

Figure 3.7. Phosphorylation of MHC-IIAF21 and MHC-IIBF17 by PKC *in vitro*. The purified MHC-IIAF21 (5.2 μg) and MHC-IIBF17 (4.2 μg) recombinant fragments were used as the substrate for PKC. The phosphorylated MHC-IIAF21 and IIBF17 were analysed on SDS-PAGE and radioactive phosphate was detected by autoradiography. *Lane 1*, negative control without substrate; *lane 2*, MHC-IIBF17; *lane 3*, MHC-IIAF21.

To investigate the effects of S100A4 on the PKC phosphorylation of MHC-IIAF21 and MHC-IIB, S100A4 was pre-incubated with non-phosphorylated MHC-IIAF21 and MHC-IIBF17 to allow S100A4 to bind to MHC-IIAF21 and IIBF17 before *in vitro* PKC phosphorylation as described in Section 2.6.8. S100A4 greatly reduced the phosphorylation of MHC-IIAF21 but little effect was observed with the same molar ratio of BSA as S100A4 (Figure 3.8).

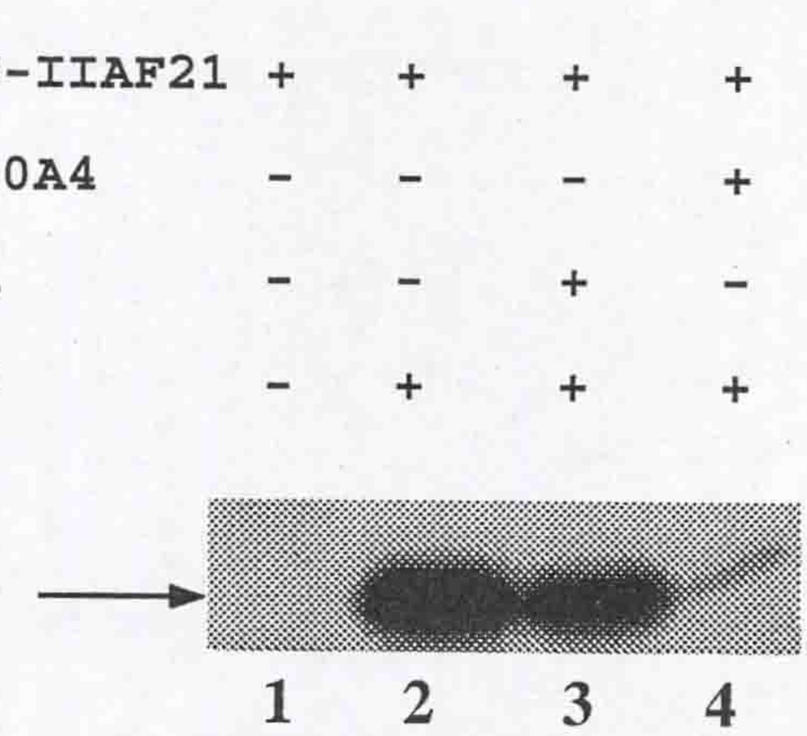

Figure 3.8. S100A4 inhibits the PKC phosphorylation of MHC-IIAF21. Five μM MHC-IIAF21 was used as the substrate of PKC in each reaction. *Lane 1,* PKC was omitted as a negative control, *lane 2,* MHC-IIAF21 alone as a positive control, *lane 3,* 5 μM BSA and *lane 4,* 5 μM S100A4 protein were pre-incubated with MHC-IIAF21 in the presence of 0.5mM Ca^{2+} at room temperature for 40 min and the mixtures were used in the phosphorylation reactions. Arrow indicates the phosphorylated MHC-IIAF21.

To rule out the possibility, that S100A4 could directly inhibit the activity of PKC, the effect of S100A4 was tested on another substrate of PKC, histone 3 (Figure. 3.9). S100A4, from 0.5 μM to 16 μM, was pre-incubated with 5 μM histone 3, but there was no obvious effect on the phosphorylation of histone 3. These results suggest that S100A4 specifically inhibits the phosphorylation of MHC-IIAF21. This may result from its specific binding to MHC-IIA. However, there is a slight inhibitory effect on histone 3 phosphorylation when 16 μM of S100A4 was used. This could be due to non-specific effect of high concentration of proteins in the reaction.

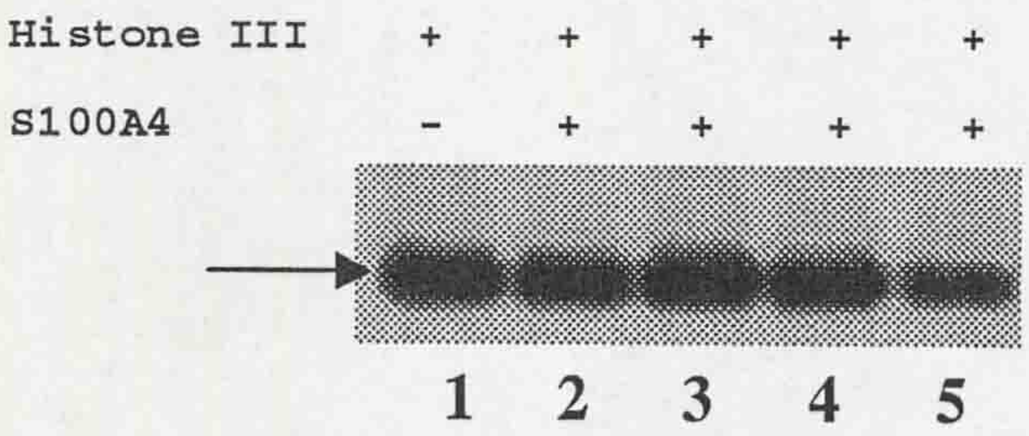

Figure 3.9. The effects of S100A4 on the phosphorylation of histone 3 by PKC. Two μM of histone 3 was used as the substrate of PKC in each reaction. The histone 3 was pre-incubated at room temperature for 40 min in the presence of 0.5mM Ca^{2+} with varying concentrations of S100A4, 0 μM (*Lane 1*), 0.5 μM (*lane 2*), 2 μM (*lane 3*), 8 μM (*lane 4*), 16 μM (*lane 5*). Arrow indicates the phosphorylated histone 3.

To confirm the inhibitory effect of S100A4 on the MHC-IIA phosphorylation by PKC, varying concentrations of S100A4 were pre-incubated with MHC-IIAF21 and the mixtures were used in phosphorylation reactions. The results show that S100A4 inhibited the phosphorylation of MHC-IIAF21 by PKC in a dosage dependent manner (Figure 3.10).

a

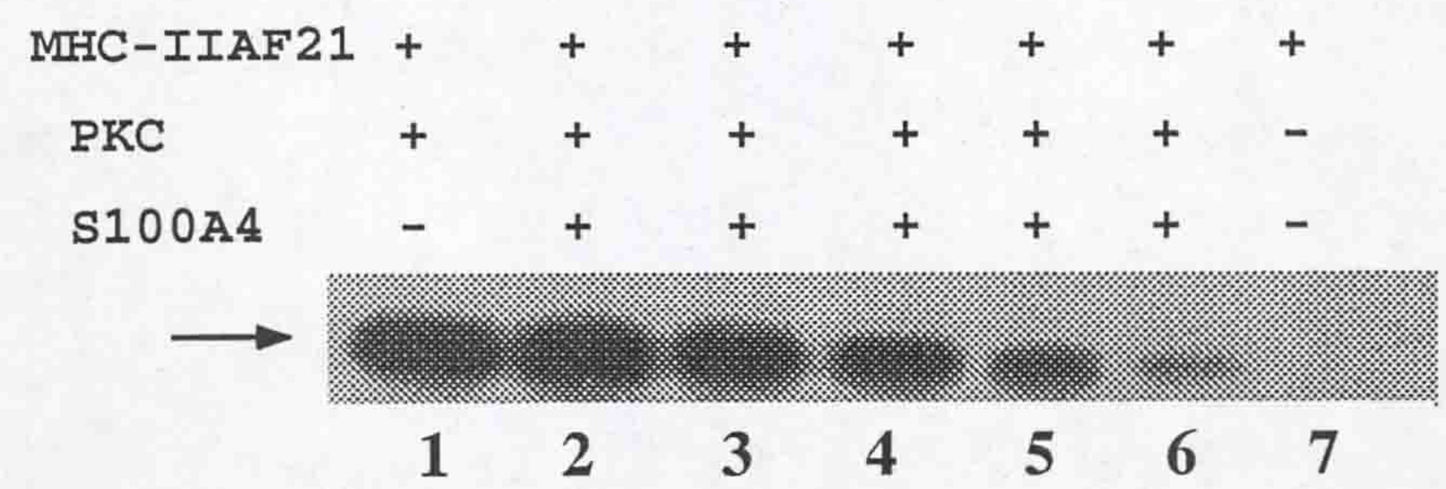

b

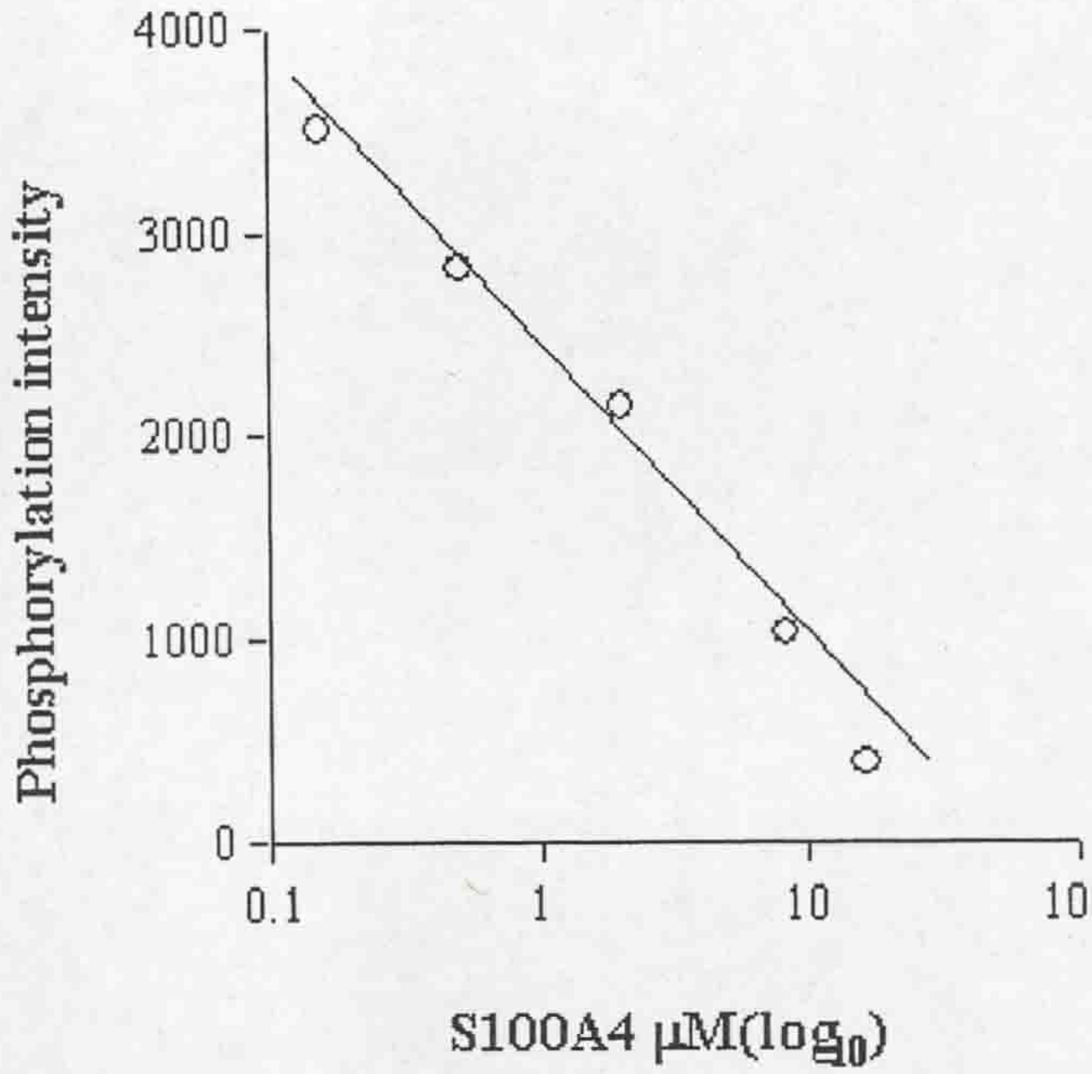

Figure 3.10 The dosage dependent inhibition of S100A4 on the phosphorylation of MHC-IIAF21 by PKC. *Panel A*. Five μM MHC-IIAF21 was used as the substrate of PKC in each reaction. The MHC-IIAF21 was pre-incubated at room temperature for 40 min in the presence of 0.5mM Ca^{2+} with varying concentrations of S100A4, 0 μM (*lane 1*), 0.15 μM (*lane 2*), 0.5 μM (*lane 3*), 2 μM (*lane 4),* 8 μM (*lane 5*), 16 μM (*lane 6*). *Lane 7*, a negative control with PKC omitted. Arrow indicates phosphorylated MHC-IIAF21. *Panel B*. A plot of MHC-IIAF21 phosphorylation intensities against Log S100A4 concentrations in the PKC phosphorylation reaction yielded a straight line ($r = 0.89$, $p < 0.01$).

To investigate if S100A4 has a similar effect on MHC-IIB, the same experiments were carried out, except that MHC-IIBF17 was used as the substrate for PKC. S100A4, from 0.1 μM to 16 μM, was pre-incubated with 5 μM MHC-IIB. Only the high concentrations of S100A4, 8 μM and 16 μM, showed an inhibitory effect.

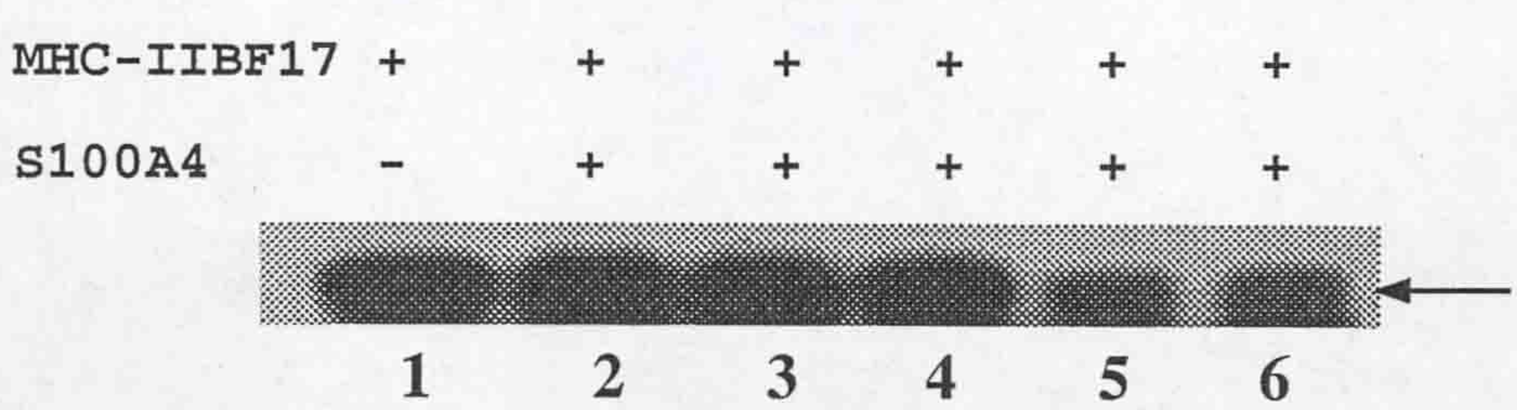

Figure 3.11. S100A4 inhibits the phosphorylation of MHC-IIBF17 by PKC. Five μM of MHC-IIBF17 was used as the substrate of PKC in each reaction. The MHC-IIAF17 was pre-incubated at room temperature for 40 min in the presence of 0.5 mM Ca^{2+} with varying concentrations of S100A4, 0 μM (*lane 1*), 0.1 μM (*lane 2*), 0.5 μM (*lane 3*), 2 μM (lane *4*), 8 μM (*lane 5*); 16 μM (*lane 6*). Arrow indicates phosphorylated MHC-IIBF17.

3.2.6 PKC phosphorylation of MHC-IIAF21 and IIBF17 influences their binding to S100A4

To investigate whether the PKC phosphorylation of MHC-IIAF21 and MHC-IIBF17 has any influence on their binding to S100A4, two independent *in vitro* methods were employed: gel overlay assay and biosensor assay.

3.2.6.1 Gel overlay assay

In these experiments, the recombinant MHC-IIAF21 and MHC-IIBF17 fragments were first phosphorylated with PKC as described in Section 2.6.8 and then subjected to gel overlay assay. Phosphorylated MHC-IIAF21 proteins were subjected to electrophoresis in two SDS-PAGE gels and one was dried and exposed to X-ray film, the other was transferred to PVDF membrane. The membrane was overlaid with S100A4 and the binding of S100A4 to immobilised MHC-IIAF21 was detected by an anti-S100A4 antibody as

described in Section 2.6.6. The result shows that the phosphorylation was increased with increasing PKC in reactions and the binding of S100A4 to MHC-IIAF21 was gradually reduced with the increasing of MHC-IIAF21 phosphorylation ($r = -0.85$, $P<0.05$) (Pearson Correlation in SPSS), suggesting that phosphorylation of MHC-IIAF21 by PKC reduced its ability to interact with S100A4.

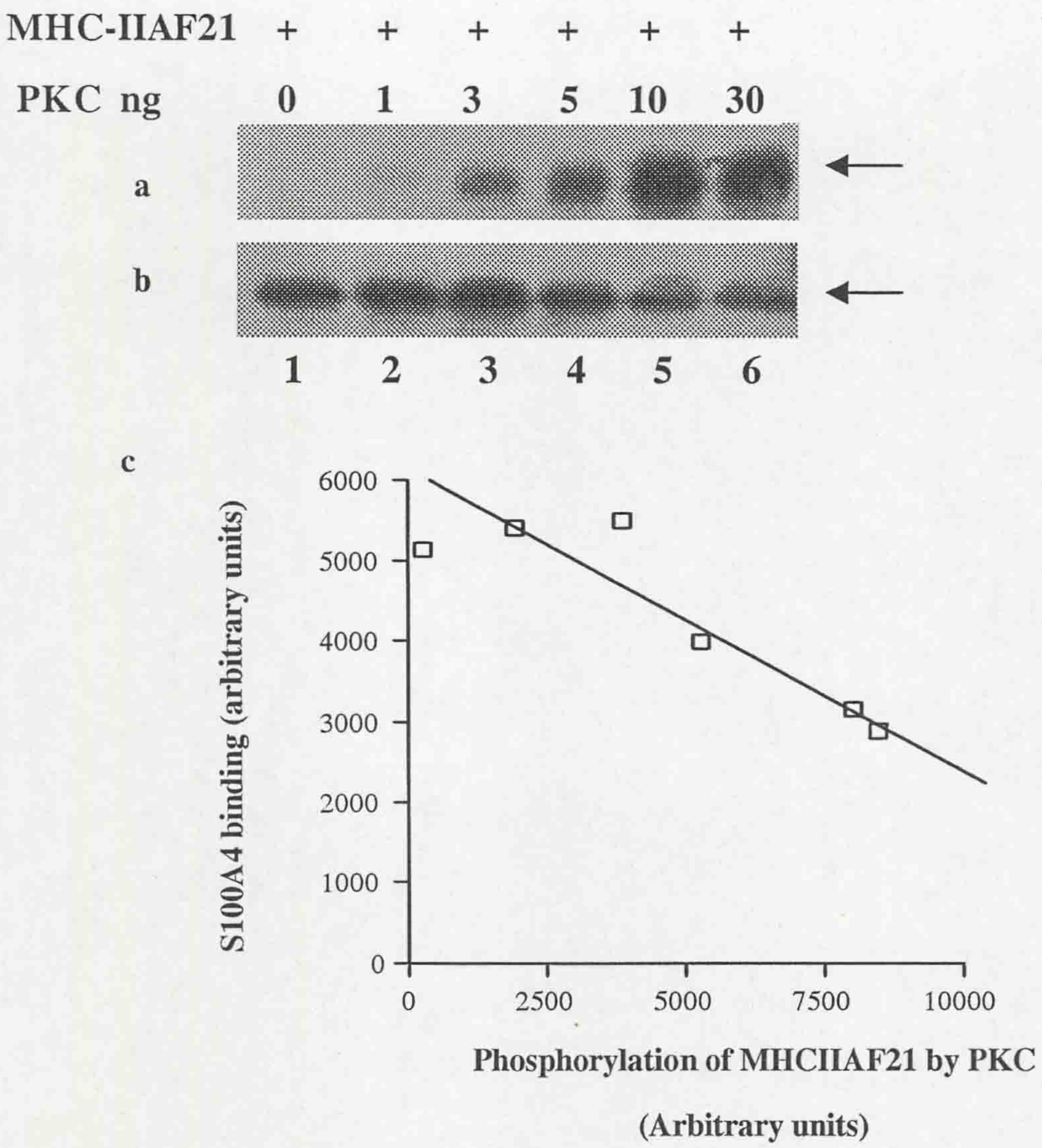

Figure 3.12. Phosphorylation of MHC-IIAF21 with ^{32}P by PKC reduced its ability to interact with S100A4. *Panel a*: autoradiography of phosphorylated MHC-IIAF21 with varying amounts of PKC (from 0 to 30ng in a 50µl reaction) at 30 ℃ for 15 min. Arrow indicates phosphorylated MHC-IIAF21. *Panel b*: The same samples of phosphorylated MHC-IIAF21 as those used in *panel b* were analysed by gel overlay assay with S100A4. The binding of S100A4 onto the MHC-IIAF21 was detected with anti-S100A4 antibody (DAKO). The arrow indicates the position of MHC-IIAF21. *Panel c*, the plot shows the relationship between MHC-IIAF21 phosphorylation by PKC and S100A4 binding from the data in *panel a and b.*

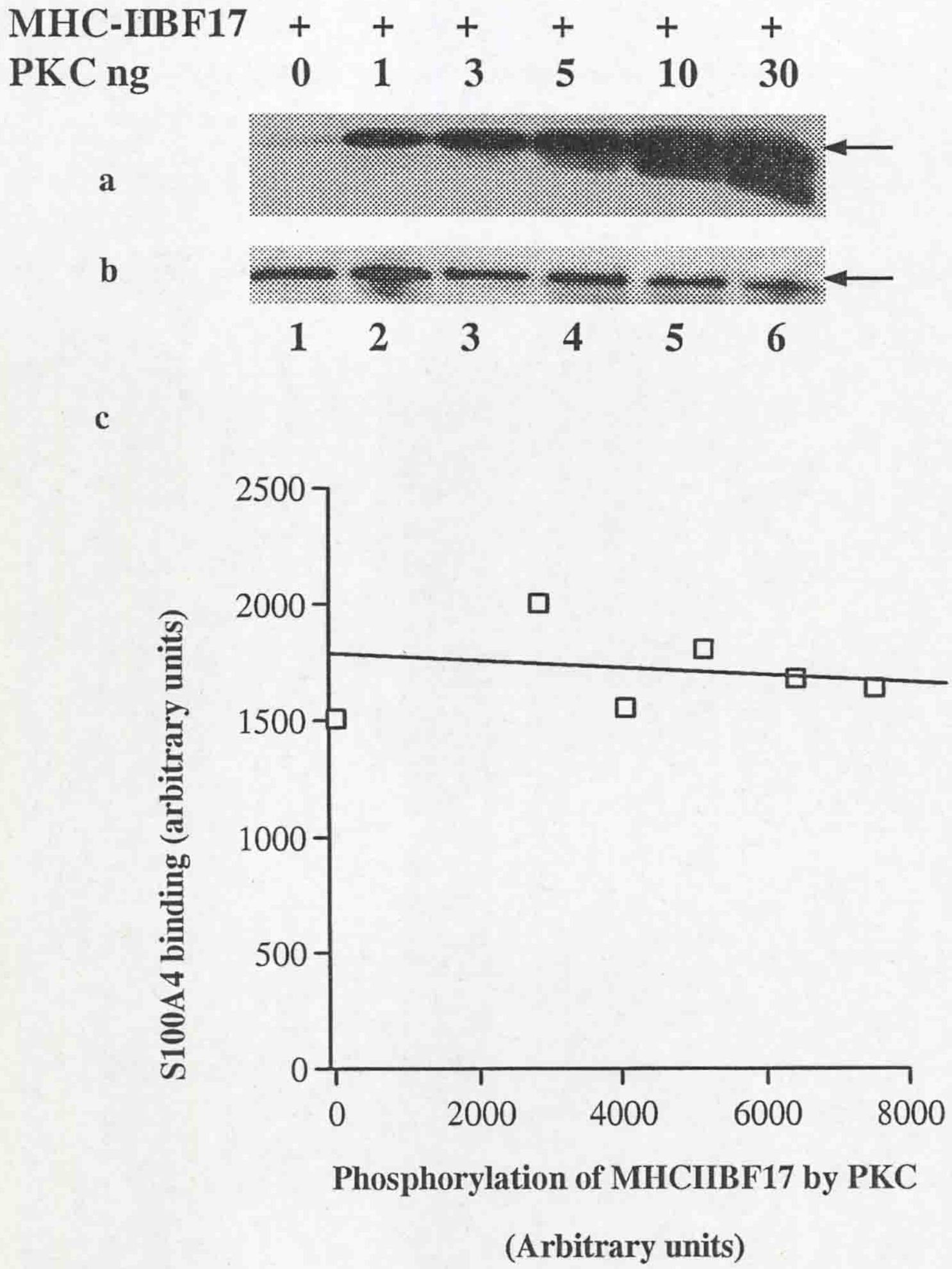

Figure 3.13. The effect of PKC phosphorylation of MHC-IIBF17 *C*-terminus on its ability to interact with S100A4. *Panel a*: autoradiography of PKC phosphorylation. Five μg of MHC-IIBF17 was used in each reaction and about 2μg was loaded on SDS-PAGE. The gel was dried and X-ray film was exposed for 4 h. *Lanes 1-6* used different amount of PKC, from 0 to 30ng in each 50μl reaction. Arrow indicates phosphorylated MHC-IIBF17. *Panel b*: same samples as that used in *Panel a* were analysed by gel overlay assay with S100A4. The binding of S100A4 was detected by anti-S100A4 antibody (DAKO). The arrow indicates the position of MHC-IIBF17. *Panel c*, the plot shows the relationship between MHC-IIBF17 phosphorylation by PKC and S100A4 binding from the data in *panel a and b*.

When the experiments were repeated with MHC-IIBF17, the reduction of binding of S100A4 was not observed associated with the increase of MHC-IIBF17 phosphorylation ($r = 0.02$, $p>0.05$) (Pearson Correlation in SPSS) (Figure 3.13).

3.2.6.2 Biosensor assay

In these assays, the recombinant MHC-IIAF21 and MHC-IIBF17 were separately immobilized on to aminosilane surfaces. The binding of S100A4 to the immobilised MHC-IIAF21 and IIBF17 on the surfaces was analysed as described in Section 2.7.3. Then the immobilised MHC-IIAF21 and IIBF17 on the surfaces were phosphorylated with PKC as described in Section 2.6.8. The binding of S100A4 to the surfaces after phosphorylation was analysed and compared with the binding before phosphorylation. The result shows that phosphorylation of MHC-IIAF21 by PKC reduced by about 30% its binding to S100A4, but the phosphorylation of MHC-IIBF17 by PKC did not obviously reduce its binding to S100A4 (Figure 3.14). The mock phosphorylations without PKC of the MHC-IIAF21 and IIBF17 on the surfaces had no effect on the binding of S100A4 (data not shown).

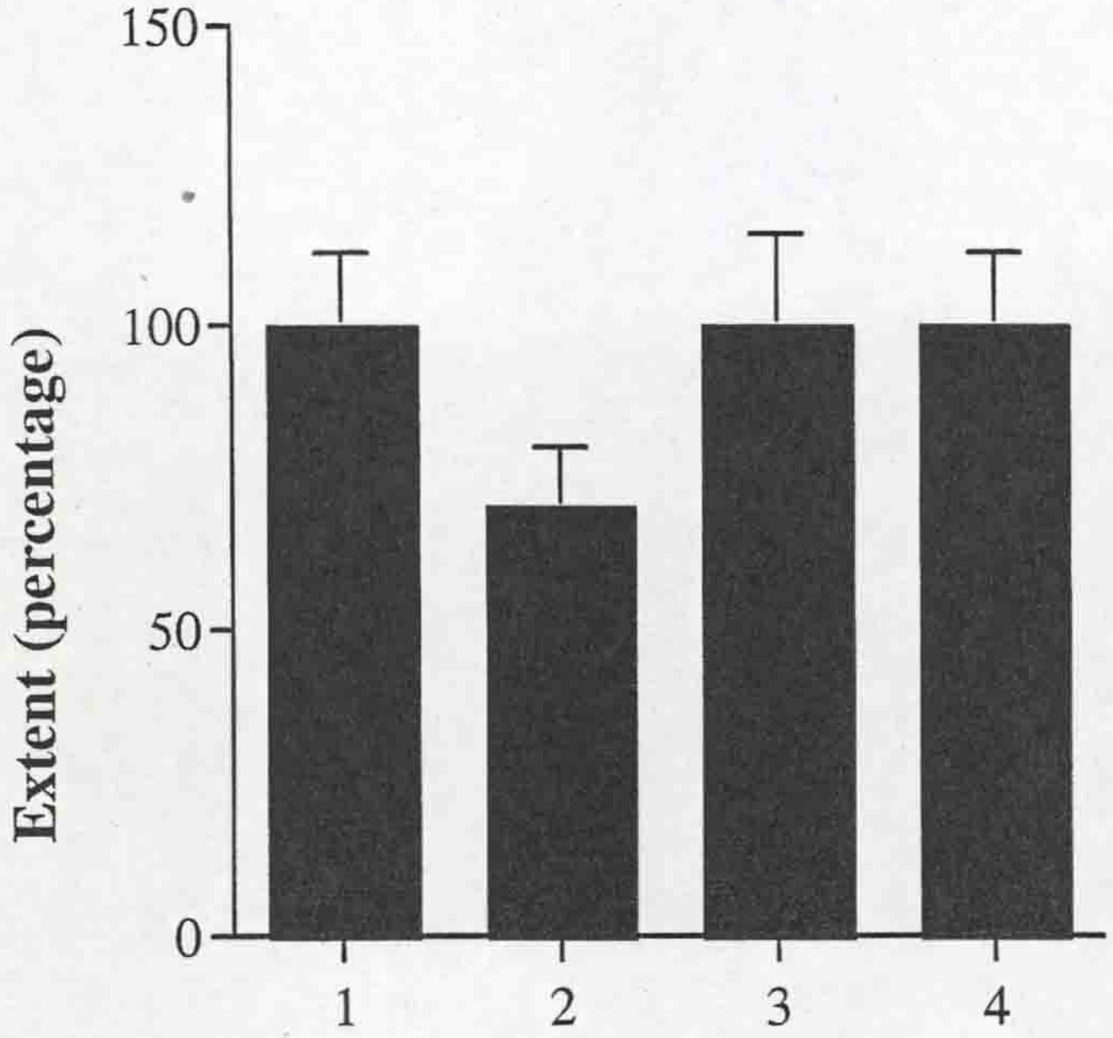

Figure 3.14 The effects of PKC phosphorylation of MHC-IIAF21 and IIBF17 on their binding to S100A4 revealed by biosensor assay. MHC-IIAF21 and IIBF17 were immobilised onto the aminosilane surfaces and the PKC phosphorylation reactions were carried out on the surfaces. The binding of S100A4 to the immobilised MHC-IIAF21 (*column 1 and 2*) and IIBF17 (*column 3 and 4*) were analysed before (*column 1 and 3*) and after (*column 2 and 4*) the phosphorylation. The extents calculated with Fastfit software were used to measure the binding changes before and after phosphorylation. The average extent before phosphorylation was designated as 100%. The values shown in this figure are the averages of three separate measurements $\pm$ SD.

3.2.7 S100A4 inhibits the sedimentation of MHC-IIAF21 but not MHC-IIBF17

Since the S100A4 binding site partly overlaps the assembly site on the MHC II heavy chain (Figure 3.18), the binding of S100A4 may affect the self-assembly of MHC-IIAF21 and MHC- IIBF17. In these experiments, S100A4 was pre-incubated with MHC-IIAF21 or MHC-IIBF17 as described in Section 2.6.9.Then sedimentation assays were carried out. The results showed that S100A4, but not S100A1, inhibited sedimentation of MHC-IIAF21 (Figure 3.15) in a Ca^{2+} dependent manner. However, S100A4 showed no effect on the

sedimentation of MHC-IIBF17 (Figure 3.15b).

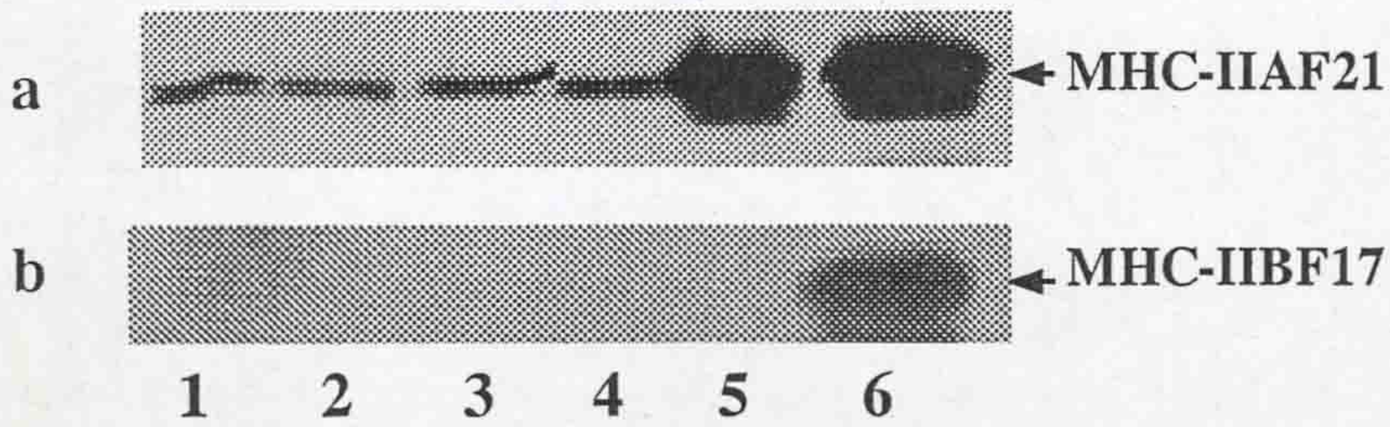

Figure 3.15 Effects of S100A4 on the sedimentation of MHC-IIAF21 and MHC-IIBF17. Five μM MHC-IIAF21 (*Panel a*) and 5μM MHC-IIBF17 (*Panel b*) were preincubated with S100A4 or S100A1 in the presence or absence of Ca^{2+} at 4°C for 8 h. MHC-IIAF17 (*panel a*) or MHC-IIBF17 (*panel b*) alone in the presence of 0.5 mM Ca^{2+} (*lane 1*), or in the absence of Ca^{2+} (*lane 2*); with 5 μM S100A1 in the presence of 0.5 mM Ca^{2+}(*lane 3*); with 5 μM S100A4 in the absence of Ca^{2+} (*lane 4*); with 5μM S100A4 in the presence of 0.5 mM Ca^{2+} (*lane 5*); MHC-IIAF21 (*Panel a*) or MHCIIBF17 (*Panel b*) alone without centrifugation (*lane 6*). Then the mixtures were incubated in bundling buffer (Section 2.6.9) at 4 °C overnight and centrifuged at 13,500 x g in a microcentrifuge for 30 min. Twenty μl of the resultant supernatant was analysed by SDS-PAGE. The MHC-IIAF21 and MHC-IIBF17 were detected by Western blotting using anti-MHC-IIAF21 antibody (*Panel a*) and anti-His tag antibody (*Panel b*), respectively.

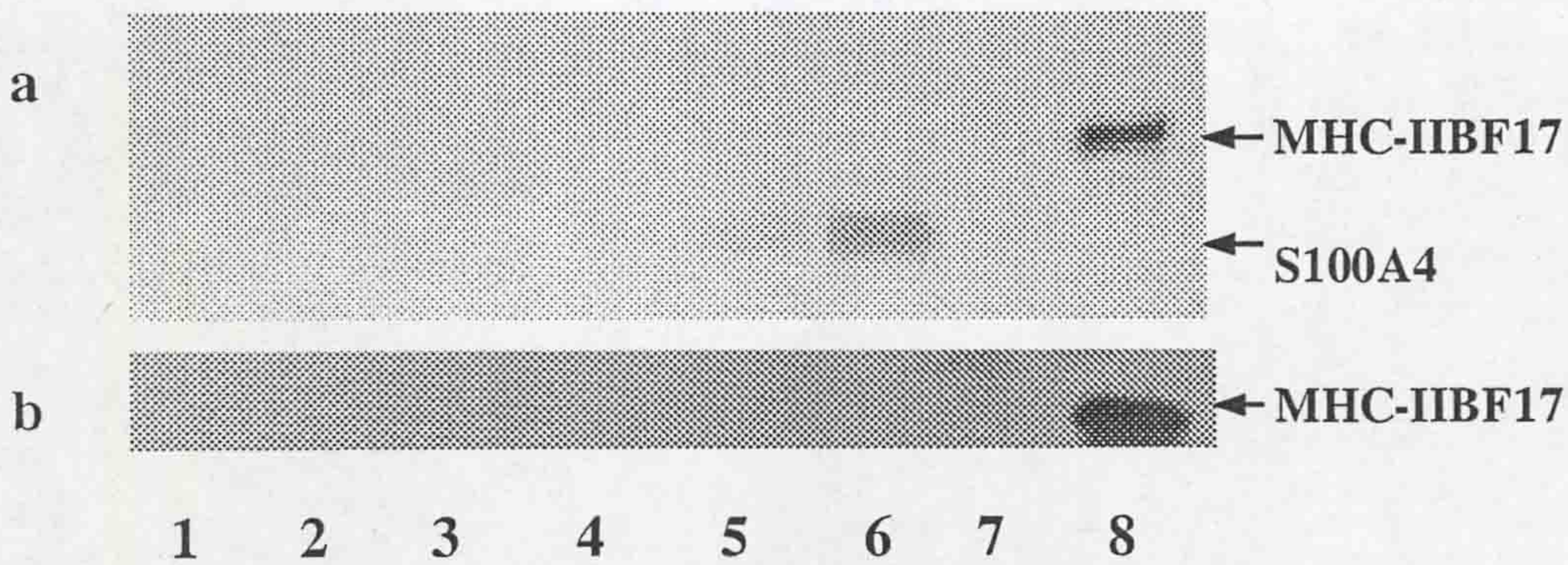

Figure 3.16 Dosage dependent effect of S100A4 on the sedimentation of MHC-IIBF17. Five μM of MHC-IIBF17 was pre-incubated at 4°C for 8 h with varying concentrations of S100A4, MHB only (*lane 1*), 0.25 μM S100A4 (*lane 2*), 1 μM S100A4 (*lane 3*), 4 μM S100A4 (*lane 4*), 8 μM S100A4 (*lane 5*), 16 μM S100A4 (*lane 6*), 4 μM S100A4 (*lane 7*), MHC-IIBF17 alone without centrifugation (*lane 8*). Except *lane 7*, in which MHC-IIBF17 was pre-incubated in the absence of Ca^{2+}, the remaining reactions were all carried out in the presence of 0.5mM Ca^{2+}. The mixtures were then incubated overnight in bundling buffer (Section 2.6.9) at 4 °C. The mixtures were centrifuged at 13,500 x g for 30 min in a micro-centrifuge. Twenty μl of the resultant supernatants were analysed on SDS-PAGE. The gel was stained with silver nitrate (Section 2.6.4) (*panel a*) or blotted to membrane (*panel b*) and the MHC-IIBF17 was detected by Western blotting with anti-His tag antibody.

To confirm the negative result with MHC-IIBF17, varying concentrations of S100A4 from 0 to 16μM were preincubated with MHC-IIBF17 in the presence of 0.5mM $CaCl_2$. The MHC-IIBF17 remaining in the supernatant was detected both by silver staining (Figure 3.16a) and by Western blotting with anti-His tag antibody (Figure 3.16b). The S100A4 showed no effect on the sedimentation of MHC-IIB. For MHC-IIAF21 there is always a detectable amount of protein in the supernatant in the sedimentation experiment while the MHC-IIBF17 could not be detected in the supernatants at all by silver staining or by Western blotting. The reason is not clear.

3.2.8 Exploration of the interactions *in vivo* of S100A4 with MHC-IIA and MHC-IIB using the yeast two-hybrid system

The experiments described above were all carried out *in vitro* thus the yeast two-hybrid system was used to explore the interaction of S100A4 with MHC-IIA and IIB *in vivo*.

3.2.8.1 Constructs used in this work

BD constructs in pBD-GAL4 Cam vector (bait),

PBD-S100A4 (full length of human S100A4 fused with GAL4 BD).
PBD-MHC-IIBc823 (*C*-terminal 823 amino acids (aa) of MHC-IIA fused with GAL4 BD).
PBD-MHC-IIAc105 (*C*-terminal 105 aa of MHC-IIA fused with GAL4 BD).
PBD-MHC-IIBc115 (*C*-terminal 115 aa of MHC-IIB fused with GAL4 BD).

AD constructs in pAD-GAL4-2.1 vector (prey)

pAD-S100A4 (full length of human S100A4 fused with GAL4 AD),
pAD-MHC-IIBc823 (*C*-terminal 823 aa of MHC-IIB fused with GAL4 AD)
pAD-MHC-IIBc204 (*C*-terminal 204 aa of MHC-IIB fused with GAL4 AD).
pAD-MHC-IIBc115 (*C*-terminal 115 aa of MHC-IIB fused with GAL4 AD).
pAD-MHC-IIBc72 (*C*-terminal 72 aa of MHC-IIB fused with GAL4 AD).
pAD-MHC-IIAc105 (*C*-terminal 105 aa of MHC-IIA fused with GAL4 AD).

LexA (bait) and pYES-trp2 (prey) constructs for LexA-B42 yeast two-hybrid system

LexA-S100A4 (full length of human S100A4 fused with LexA)
LexA-MHC-IIBc115 (*C*-terminal 115 aa of MHC-IIB fused with LexA
LexA-MHC-IIAc105 (*C*-terminal 105 aa of MHC-IIA fused with LexA)
YES-S100A4 (full length of human S100A4 fused with B42)
YES-MHC-IIBc115 (*C*-terminal 115 aa of MHC-IIB fused with B42)
YES-MHC-IIAc105 (*C*-terminal 105 aa of MHC-IIA fused with B42)

3.2.8.2 MHC-IIA, MHC-IIB and S100A4 are self-associated in yeast cells.

In the yeast two-hybrid system, constructs yielding proteins containing 105 amino acids at the *C*-terminus of MHC-IIA were shown to self-associate. Similarly, constructs containing 823, 204 or 115 amino acids from the *C*-terminus of MHC-IIB were also shown to self-associate (Table 3.2). However, a construct containing 72 amino acids failed to associate with a construct yielding protein containing the *C*-terminal 115 amino acids of MHC-IIB, suggesting that the self-association of MHC-IIB requires a certain length of helical region (Table 3.2).

The S100A4 self associates in the yeast two-hybrid systems (Table 3.2) although the interaction signal (reporter gene expression) is not as strong as that of the self-association of MHC-IIA or MHC-IIB based on the intensity of the colour in lift assay.

Table 3.2 Self-associations of MHC-IIA, IIB and S100A4, and the interactions of S100A4 with MHC-IIA or IIB in yeast two-hybrid systems

Bait	Prey	Growth[a] in His$^-$ plate	β-galactosidase activity[b] (Lift assay)
pBDMHC-IIBc823	pAD-MHC-IIBc823	+++	+++
pBD-MHC-IIBc115	pAD-MHC-IIBc72	+	-
pBD-MHC-IIAc105	pAD-MHC-IIAc105	+++	+++
LexA-MHC-IIBc115	YES-MHC-IIBc115	+++	+++
LexA-MHC-IIAc105	YES-MHC-IIAc105	+++	+++
pBD-S100A4	pAD-S100A4	+++	++
LexA-S100A4	YES-S100A4	++	++
pBD-S100A4	pAD-MHC-IIBc823	+	-*
pBD-S100A4	PAD-MHC-IIBc204	+	-*
pBD-S100A4	pAD-MHC-IIBc115	+	-*
pBD-S100A4	pAD-MHC-IIBc72	+	-*
pBD-S100A4	pAD-MHC-IIAc105	+	-*
pBD-MHC-IIBc823	pAD-S100A4	+	-*
pBD-MHC-IIBc115	pAD-S100A4	+	-*
pBD-MHC-IIBc115	pAD-S100A4	+	-*
pBD-MHC-IIAc105	pAD-S100A4	+	-*
LexA-S100A4	YES-MHC-IIBc115	+	-*
LexA-S100A4	YES-MHC-IIAc105	+	-*
LexA-MHC-IIBc115	YES-S100A4	+	-*
LexA-MHC-IIAc105	YES-S100A4	+	-*
pBD-MHC-IIBc823		+++**[c]	-
pBD-MHC-IIBc115		+++**	-
pBD-MHC-IIBc115		+++**	-
pBD-MHC-IIAc105		+++**	-
LexA-MHC-IIBc115		+++**	-
LexA-MHC-IIAc105		+++**	-
pBD-S100A4		+++**	-
LexA-S100A4		+++**	-
	pAD-MHC-IIBc823	+++**	-
	PAD-MHC-IIBc204	+++**	-
	pAD-MHC-IIAc105	+++**	-
	pAD-MHC-IIBc72	+++**	-
	YES-MHC-IIBc115	+++**	-
	YES-MHC-IIAc105	+++**	-

pAD-S100A4	+++**	-
YES-S100A4	+++**	-

a. The growth of transfected yeast with Bait and/or Prey vectors in selective plate (His-). +++: Grows well. +: Only a few tiny clones grow.

b. The lift assay was carried out as described in Section 2.4.3. The intensity and speed of the development of the blue colour developed in most of clones are grouped as: -, no blue colour developed within 16 h. ++: blue colour developed within 16 h, +++: blue colour developed within 3 h and very intense.

c. +++** indicates that the yeast grows in selective plates with sufficient histidine.

Table 3.3. MHC-IIA/IIB constructs and their self-associations/interactions with S100A4 in yeast two-hybrid systems

MHC-IIB/IIA constructs and length (amino acid)	Diagram[a]	Self association[b]	Interaction with S100A4[c]
MHC-IIBc 823	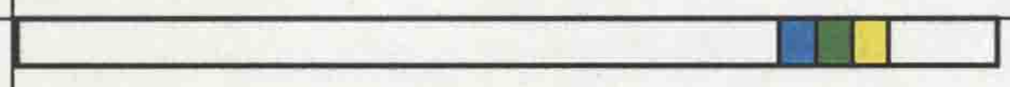	Yes	No
MHC-IIBc 204		Yes	No
MHC-IIBc 115		Yes	No
MHC-IIBc 72	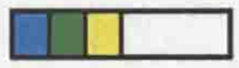	No	No
MHC-IIAc 105		Yes	No

a. The diagram of MHC-IIA and IIB *C*-terminal region. Blocks in blue and green represent the assembly site and blocks in yellow and green represent the S100A4 binding site. Block in green is the overlapped region of the assembly site and the S100A4 binding site.

b. MHC-IIB self-association or MHC-IIA self-association in yeast determined by lift assay.

c. The interaction of each MHC-IIA or IIB *C*-terminal fragment with wild type S100A4 in yeast determined by lift assay.

3.2.8.3 S100A4 does not interact with MHC-IIA or IIB in the yeast two-hybrid system

To check the interaction of S100A4 with non-muscle myosins *in vivo,* a construct containing the *C*-terminal 823 amino acids of MHC-IIB in the Gal4 BD-AD system was first used. However, no interactions were detected in this experiment. The first factor that might cause this negative result was the rod structure of MHC-IIB, as it might prevent the close interaction of the DNA binding and activation domains in the yeast two-hybrid system. Thus, constructs containing 204, 115 and 72 amino acids of MHC-IIB *C*-terminus were generated but none of them was shown to interact with S100A4 (Table 3.2 and 3.3). The MHC-IIA containing 105 *C*-terminal amino acids did not interact with S100A4 either. The fact that the 105 and 115 or 72 amino acids *C*-terminal fragments of MHC-IIA and IIB, which contains a very short rod region, also failed to interact, suggests that the rod shape of MHC-IIA or IIB is not the cause of the negative results. In order to rule out the second possibility that this negative result was due to a specific property of the Gal4 yeast two-hybrid system, the experiments were repeated using the LexA-B42 yeast two-hybrid system and S100A4 did not interact with MHC-IIA containing *C*-terminal 105 amino acids nor MHC-IIB containing *C*-terminal 115 amino acids in the system (Table 3.2).

The third factor that might be important is that the low level of free Ca^{2+} in yeast might be insufficient to support a calcium-dependent binding phenomenon. To test this possibility, a mutant yeast strain, K610 with the pmr1 null mutation, was used. The PMR1 gene is a member of a Ca^{2+} ATPase family (Rudolph *et al.,* 1989), which serves as a Ca^{2+} pump in the Golgi and Golgi-like membranes to maintain the homeostasis of ions. It was found that exposure to moderately high Ca^{2+} concentrations led to elevated levels of Ca^{2+} in cells of pmr1 null mutant, in comparison with cells of wild type (Halachmi & Eilam 1996). The highest cytosolic free Ca^{2+} that has been observed is about 1500nM.

In this thesis, the K610 strain was transfected with a yeast two-hybrid reporter plasmid, pSH18-34 (Invitrogen), which has 8 LexA operator sites upstream of the *lac*Z reporter gene.

When bait and prey proteins bind, the LexA and B42 are brought together and then the transcription of LacZ reporter gene is triggered. Stable transformants were selected by URA3 marker after transformation of K610 strain with pSH18-34 and was used in the LexA-B42 yeast two-hybrid system. Although, the interactions of S100A4 with MHC-IIA or IIB were detected using the system (data not shown), no conclusion can be made without a full characterization of the system, which needs to be done in the near future.

3.3 Discussion

S100A4 binding site, assembly site, and PKC phosphorylation site are all mapped to their *C*-terminus of MHC-IIA and IIB (Kriajevska *et al.,* 1998; Mitsuo, *et al.,* 2001). Since it is much more convenient to use *C*-terminal fragments than the large and less soluble MHC-IIA and MHC-IIB whole molecules (Niederman & Pollard 1975) for *in vitro* assays, the recombinant *C*-terminal tails of MHC-IIA and MHC-IIB, named MHC-IIACF21 (21 kDa fragment) and MHC-IIBCF17 (17kDa fragment), which contain the functional sites listed above, were produced for the binding, PKC phosphorylation, and sedimentation assays. The protein sequences of MHC-IIAF21 and MHC-IIBF17, along with the functional sites indicated, are shown in Figure 3.18.

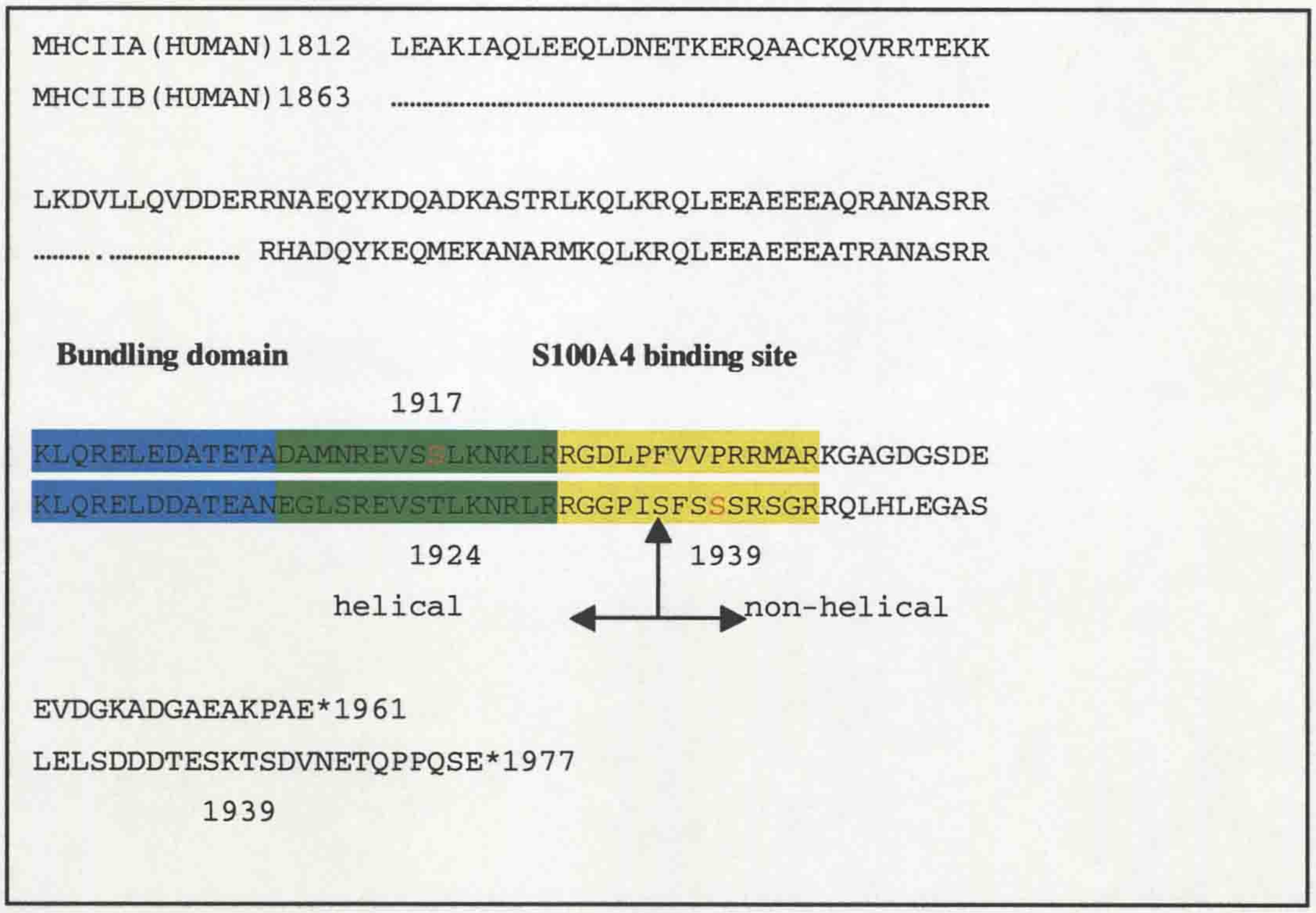

Figure 3.18. The assembly site, S100A4 binding site and PKC phosphorylation site in MHC-IIA and IIB. S100A4 binding site (29 amino acids) is highlighted in yellow and green. Assembly site (28 amino acids), which is essential for myosin self-assembly and filament formation, is highlighted in blue and green. The green region is the overlapped region of S100A4 binding site and the assembly site. The possible PKC phosphorylation sites (S1917 in MHC-IIA and S1939 in MHC-IIB) are in red. The up-right arrow indicates the boundary of the helical domain and non-helical tail. The S100A4 binding site is located on the junction of the helical domain and non-helical tail. The assembly site is located in the *C*-terminal end of the rod region of MHC-IIA and IIB.

Both MHC-IIAF21 and MHC-IIBF17 are soluble in buffers with NaCl concentration over 0.3M. Both fragments can be phosphorylated by PKC in normal reaction conditions suggested by the supplier of PKC. Both fragments are shown to be able to bind to S100A4 and both fragments can self-assembly in Bundling Buffer (Section 2.6.9) with 100mM NaCl and 2.5 mM $MgCl_2$. Therefore these fragments are suitable to substitute for MHC-IIA

and IIB for the experiments carried out in this project. Murakami (Murakami, *et al.,* 2000) used the *C*-terminal MHC-IIA (46kDa) and MHC-IIB (47kDa) for bundling and phosphorylation experiments *in vitro*. Although these fragments are longer than the fragments used in this project, the results from the different lengths of myosin II fragments are very similar, which will be discussed later. Similar results were also reported using the full length of MHC-IIA. For example, S100A4 was shown to bind to and inhibit the PKC phosphorylation of full length of MHC-IIA (Ford *et al.,* 1997). Therefore, the short fragments, MHC-IIAF21 and MHC-IIBF17, may well represent the whole molecules for the functional assays employed in this work.

In this study, S100A4 has been shown to bind to both MHC-IIAF21 and IIBF17. Although the binding of S100A4 to MHC-IIA was already reported (Kriajevska *et al.,* 1994), this is the first time that the binding of S100A4 to MHC-IIB has been studied in detail *in vitro*. In gel overlay experiments, S100A4 was shown to bind more strongly to MHC-IIAF21 than that to MHC-IIBF17, but the binding strengths are not fully quantifiable using this technique. Their binding affinities were determined in the biosensor assays. S100A4 showed a 10-fold faster binding to MHC-IIAF21 than to MHC-IIBF17 in the presence of 0.5mM Ca^{2+}. Moreover, the interaction between S100A4 and MHC-IIAF21 is more sensitive to added Ca^{2+} in the concentration range of 5μM to 0.5mM than that between S100A4 and MHC-IIB as shown in the biosensor assay. Although the effective range of Ca^{2+} in the assay is over the physiological range of cytosolic free Ca^{2+}, which is about 100nM to 500nM in mammalian cells, the possibility exists that higher local Ca^{2+} level upon stimuli may appear in some cells. Therefore, the effect of Ca^{2+} on the interactions of S100A4 with MHC-IIA and IIB may occur *in vivo*. Further investigation needs to be carried out in the future.

S100A4 does bind to MHC-IIB with a Kd = 4-6 μM. However, it is still unknown what is the molar concentration of S100A4 in different breast cancer cell lines and S100A4 transfected cell lines. Therefore it is difficult to predict if the interaction of S100A4 with MHC-IIA and MHC-IIB occurs in physiological or pathological conditions in cells. Further

studies will need to be carried out to determine the concentrations of S100A4 in different cell lines and to directly show that these interactions occur *in vivo*. As MHC-IIB was shown to have a tumour suppressive effect (Yam *et al.*, 2001), the binding of S100A4 to MHC-IIB, if it occurs *in vivo*, may be a key link to tumour progression. In addition, the S100A4-induced metastasis only occurs when S100A4 was greatly up-regulated in cell lines. Therefore the lower affinity binding of S100A4 to MHC-IIB may play a more important role in tumour metastasis than its binding to MHC-IIA in carcinoma cells with very high levels of S100A4.

In this work, S100A4 has been shown to inhibit the phosphorylation of MHC-IIAF21 in a dose dependent manner and this result is the same as reported previously (Kriajevska *et al.*, 1998). In contrast, S100A4 at the same concentrations has much less effect on the PKC phosphorylation of MHC-IIBF17 than that of MHC-IIAF21. Only a very high concentration of S100A4 could affect the PKC phosphorylation of MHC-IIBF17.

The PKC phosphorylation site on human platelet myosin was mapped previously to Serine-1917 (Conti *et al.*, 1991;Kriajevska *et al.*, 1998) (Figure 3.18), which is within the S100A4 binding site of the MHC-IIAF21 fragment. Although the PKC phosphorylation site(s) in human MHC-IIB is not clear, the mapping on rabbit MHC-IIB by Murakami and his colleagues (Murakami *et al.*, 1998) could be helpful in predicting the possible site(s) on human MHC-IIBF17. On rabbit MHC-IIB^{a}, a closer isoform to human MHC-IIB than rabbit MHC-IIB$^{\beta}$, PKC only phosphorylated serine, but not threonine residues. PKC phosphorylation sites in rabbit MIIB^{aF47} were mapped to a region containing a cluster of serine residues near the predicted junction of the helical and nonhelical domains: P-I-S(PO4)-F-S(PO4)-S(PO4)-S(PO4)-R-S(PO4)-. It was reported from quantitative data that out of these five potential PKC sites, only one site seemed to be phosphorylated per peptide (Murakami *et al.*, 1998). As outlined before, the MHC-IIBF17 is similar to rabbit MIIB^{a} in amino acid sequence and the predicted PKC phosphorylation sites are identical between human MHC-IIB and rabbit MIIB^{a}. If only one site can be phosphorylated, *PhosphoBase v*2.0 predicts it to be Ser-1939 (-P-I-S-F-S-S(PO4)-S-R-S-) in human

MHC-IIB.

There is not a PKC phosphorylation site in MHC-IIA corresponding to the Ser-1939 in MHC-IIB and the corresponding site in MHC-IIB to the site Ser-1917 in MHC-IIA is threonine (Thr-1924) instead of serine. In this case, the MHC-IIB is different from MHC-IIA. According to a previous report (Murakami *et al.*, 1998) that no threonine is phosphorylated in rabbit MHC-IIB, Thr-1924 in human MHC-IIB may not be phosphorylated by PKC. Although a detailed peptide mapping of the PKC phosphorylation sites in human MHC-IIB has not been carried out yet, it is highly probable that PKC phosphorylates different sites in human MHC-IIA and MHC-IIB.

Both Ser-1917 in MHC-IIA and Ser-1939 in MHC-IIB are within the S100A4 binding region predicted by alignment with the S100A4 binding site in MHC-IIA (Figure 3.18) so S100A4 binding may compete with PKC for binding to the sites and thus inhibit the phosphorylation. The fact that S100A4 has a stronger effect on PKC phosphorylation of MHC-IIA than that of MHC-IIB is consistent with the fact that S100A4 has a much higher affinity with MHC-IIA than that with MHC-IIB. This argument supports a competition model. Therefore, another question has been raised: does the phosphorylation of MHC-IIA and MHC-IIB by PKC affect their binding to S100A4? To answer this question, the binding of S100A4 to pre-phosphorylated MHC-IIA and MHC-IIB was analysed using gel overlay experiment and an optical biosensor.

The results show that PKC phosphorylation of MHC-IIAF21 did reduce the S100A4 binding in both experiments. In a biosensor assay, the S100A4 binding to the immobilised MHC-IIA was reduced about 30% after PKC phosphorylation (Figure 4.5). However, phosphorylation of MHC-IIBF17 by PKC showed no obvious effect on its binding to S100A4 in both gel overlay experiment and biosensor assay. The different results from MHC-IIAF21 and IIBF17 may be explained by the sequence alignment of the two peptides (Figure 3.18). The PKC phosphorylation site, Ser-1917 in MHC-IIA is within the conserved region of S100A4 binding site. Therefore the addition of a phosphate group may

cause enough change to affect the binding of S100A4. However, the 5 potential PKC phosphorylation sites, including Ser-1939, in MHC-IIB (Murakami *et al.,* 1998) are located in the non-conserved region of S100A4 binding site based on the sequence alignment of MHC-IIA and IIB (Figure 3.18), so phosphorylation of Ser 1939 may not be sufficient to affect the binding of S100A4.

The binding of S100A4 also showed differential effects on the self-assembly of MHC-IIAF21 and MHC-IIBF17. The binding of S100A4 inhibited the self-assembly of MHC-IIA filaments in calcium dependent manner. However, the binding of S100A4 did not reduce the self-assembly of MHC-IIBF17. This result is same as a previous report (Murakami *et al.,* 2000). The assembly sites for both MHC-IIA and MHC-IIB self-assembly are highly conserved between the two isoforms and both located at *C*-terminal ends and overlap the S100A4 binding sites (Figure 3.18). The binding of S100A4 may change the conformation of the *C*-terminal tails and block the process of self-assembly. As the affinity of S100A4 to MHC-IIB is lower, and probably much lower than that of self-assembly of MHC-IIB in low salt condition, so S100A4 could not compete for the shared site with MHC-IIB itself and thus had no effect on the self-assembly of MHC-IIB. These differential effects of S100A4 on MHC-IIA and IIB *in vitro* suggest that the two isoforms of non-muscle myosins might be modulated by S100A4 *in vivo* in a very different way.

There is, however, no direct evidence to show that S100A4 interacts with either MHC-IIAF21 or IIBF17 *in vivo*. Although, the co-immunoprecipitation and co-localization of MHC-IIAF21 and S100A4 were reported, these experiments have their limitations and cannot fully represent the interaction *in vivo* because immuno-precipitation might precipitate a complex, which formed after cell lysis, and co-localization does not indicate direct molecular interactions. As the yeast two-hybrid system is a simple method to test protein-protein interaction *in vivo*, it was used to detect the interactions between S100A4 and MHC-IIA or MHC-IIB. However, S100A4 does not interact with MHC-IIAF21 and IIBF17in two separate yeast two-hybrid systems (Table 3.1), although the S100A4 self-association and MHC-IIA or IIB self-assembly were well detected in the same

conditions. The reason why S100A4 could interact with MHC-IIA and IIB in many experiments *in vitro* but not in the yeast two-hybrid assay is not clear. It is unlikely that the rod shape of myosin is responsible for the negative results in yeast two-hybrid system because no interaction occurs even when the short constructs that do not have rod region were used. The low Ca^{2+} concentration in yeast may be the major reason for the negative results. The interactions of S100A4 with MHC-IIAF21 and IIBF17 *in vitro* are Ca^{2+} independent but are sensitive to added Ca^{2+}. In most experiments, 500μM Ca^{2+} was used. In biosensor assays, the Ca^{2+} started to have an effect on binding at the concentration of 4-6 μM (data not shown) and obtained maximum effect at about 500μM. However, in yeast, the cytosolic free Ca^{2+} is only in the range of 50nM to 200nM. In most situations, the nuclear Ca^{2+} changes follow the Ca^{2+} changes in cytosol although the Ca^{2+} changes in nucleoplasm and cytoplasm are different upon some stimuli (Lin *et al.*, 1994;Badminton *et al.*, 1996). Therefore, there is the possibility that the nuclear Ca^{2+} in yeast could be too low to support the calcium-sensitive interaction of S100A4 with MHC-IIAF21 or IIBF17 and no detectable reporter gene product (beta-galactosidase) was produced in the assay.

Although some preliminary results from the yeast two-hybrid system with nmr1 mutant yeast support the hypothesis, this question is still left open because the system has not been fully validated yet. Alternative means to detect interactions *in vivo* are the mammalian two-hybrid system, and fluorescence resonance energy transfer (FRET). However, these techniques are beyond the scope of this thesis.

Chapter Four

Interaction of S100A4 with S100A1

4.1 Introduction

Since S100A4 has been shown to play an important role in tumour metastasis, it is very important to fully understand the mechanism of S100A4 in this process. One of the approaches has been to find possible target proteins of S100A4. As outlined earlier, S100A4 was shown to interact with number of proteins, such as MHC-IIA and IIB, actin, tropomysin, p53, (Kriajevska *et al.,* 1994;Takenaga *et al.,* 1994c;Ford & Zain 1995; Grigorian *et al.,* 2001) and most recently, the metastasis-associated protein II (MetAP2) (Endo *et al.,* 2002) all *in vitro*. In this project, the yeast two-hybrid system was employed to screen a yeast two-hybrid library of breast cancer cells in order to identify interacting partners of S100A4 *in vivo*. Unexpectedly, S100A4 was found to interact with S100A1 (Wang *et al.,* 2000). The nature of the interaction, the co-expression and co-localization of S100A4 with S100A1 is now reported.

4.2 Results

4.2.1 Yeast two-hybrid screen

More than 2 x 10^6 yeast cell transformants from a yeast two-hybrid cDNA library, constructed from mRNA isolated from a human breast cancer specimen, were transfected with the S100A4 (p9Ka) cDNA bait vector. Target plasmids were recovered from 14 independent blue colonies, and purified plasmid DNAs were co-transformed individually into L40 yeast cells along with the S100A4 (p9Ka) bait plasmid. Reisolation of plasmid DNA and cotransformation were repeated serially three times, during which only four colonies showed the blue colour in lift assay on each occasion. Plasmid DNA was isolated from these four transformants, and the nucleotide sequences of the cDNAs in the target vectors were determined. The sequence of each of the four target plasmids was precisely that of human S100A1. The four colonies containing both the

S100A4 bait and S100A1 prey plasmids exhibited β-galactosidase activities that were 20-70-fold higher than colonies containing only bait plasmid or only a prey plasmid (Figure 4.1). However, the prey constructs in the library (Invitrogen) contained an additional 19 amino acids (AICPEPAPTSGPGQPCTAA) of protein sequence inserted between the B42 activating domain and the *N*-terminus of the target protein. To rule out the possibility that this extra sequence might be interacting directly with the S100A4 protein, the extra sequence was deleted from one of the isolated target clones. L40 strain yeast transformants containing both the pYESTrp2ExS100A1 prey construct, bearing the deletion, and the S100A4 bait construct LexA-S100A4, yielded a blue colour within 3 h in the lift assay, and the β-galactosidase activity of the deleted clone was greater than that of the original clone containing the additional 19 amino acids insert (data not shown). Thus, the β-galactosidase activity was not caused by the presence of these additional amino acids at the NH_2 terminus of the cloned S100A1 protein in the yeast cells from the breast cancer library. The above experiments suggest that, at least in yeast cells, S100A4 can interact in a heterologous manner with S100A1.

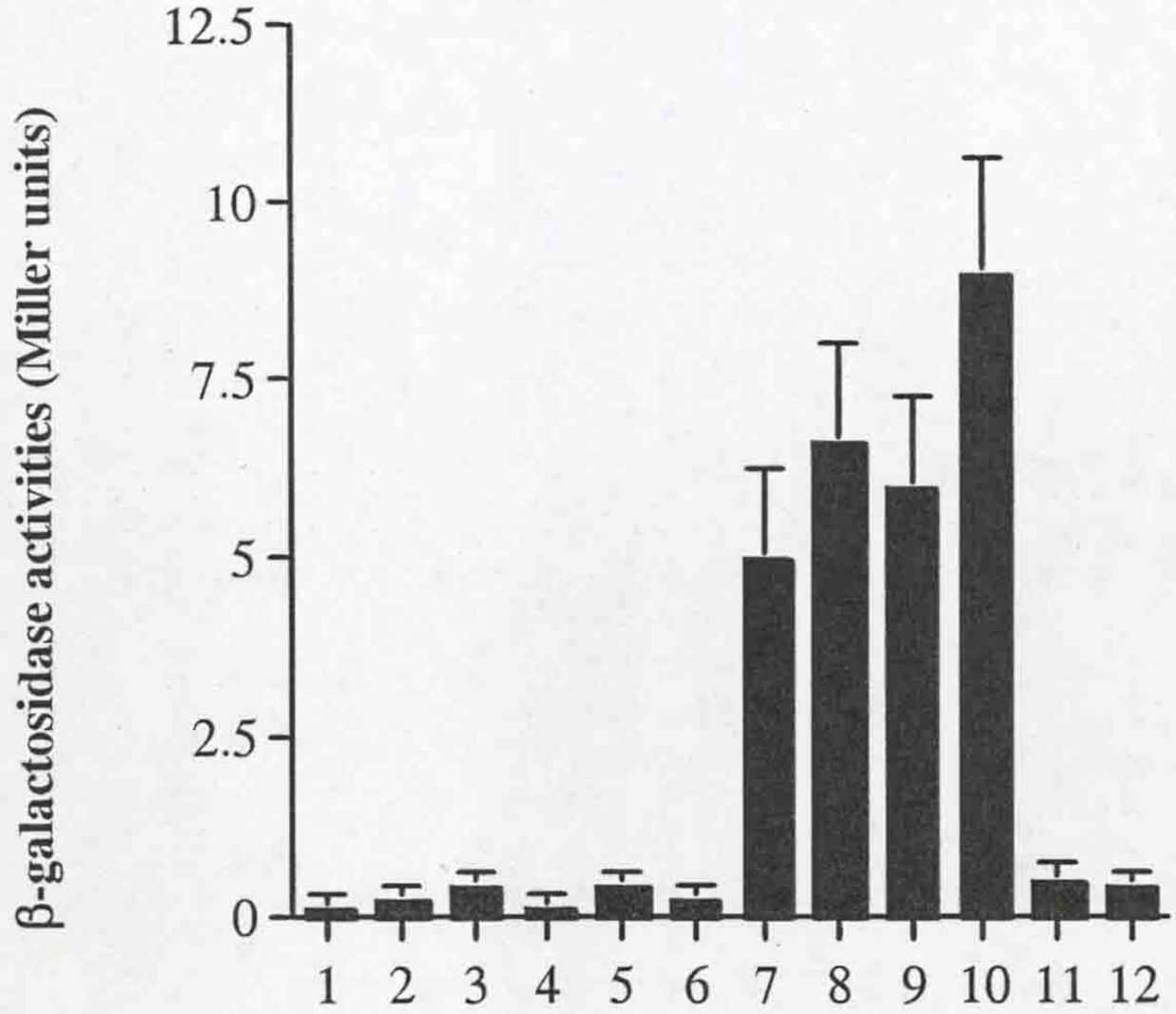

Figure 4.1 β-Galactosidase activities of yeast clones bearing S100A4 bait and/or target vectors isolated from the breast cancer two-hybrid library. Clones of yeast strain L40 were transformed with the DNA constructs indicated below, grown up, and β-galactosidase activity determined in Miller units as described under in section 2.4.4. *column 1*, bait plasmid LexA-S100A4 alone; *columns 2-5*, each of four recovered target plasmids, alone; *column 6*, bait vector, LexA-S100A4, and target vector pYESTrp2 without insert; *columns 7-12*, bait vector LexA-S100A4 and each of six recovered target vectors, A-F, four of which contained S100A1 cDNA (*columns 7-10*).

4.2.2 Point mutation disrupts the heterodimerisation of S100A4 and S100A1 in yeast

Two single nucleotide point mutations of the S100A4 cDNA were generated which yielded amino acid substitutions in residues involved in the dimer interface reported previously for S100A6 (Potts *et al.*, 1995b). These changes, which resulted in conversion of phenylalanine 72 and tyrosine 75 of the S100A4 protein sequence to glutamine, individually fully (Phe-72), or partially (Tyr-75), disrupted S100A4 dimer formation with wt S100A4 in the yeast two-hybrid system (not shown). Bait plasmids containing cDNAs bearing either of these mutations completely failed to yield blue colonies when co-transfected with S100A1 prey plasmids under the same conditions that yielded blue colonies within 6 h when un-mutated S100A4 was used. These specific mutations individually abolished the interaction between S100A4 and S100A1 in the yeast cells as determined by β-galactosidase activity (Figure 4.2). The mutation, F15A in S100A1 disrupted both S100A1 homodimerisation and the heterodimerisation with S100A4 (Figure 4.2). The β-galactosidase activity produced by S100A4wt/S100A1wt interaction is similar to that produced by S100A1/S100A1 interaction in yeast.

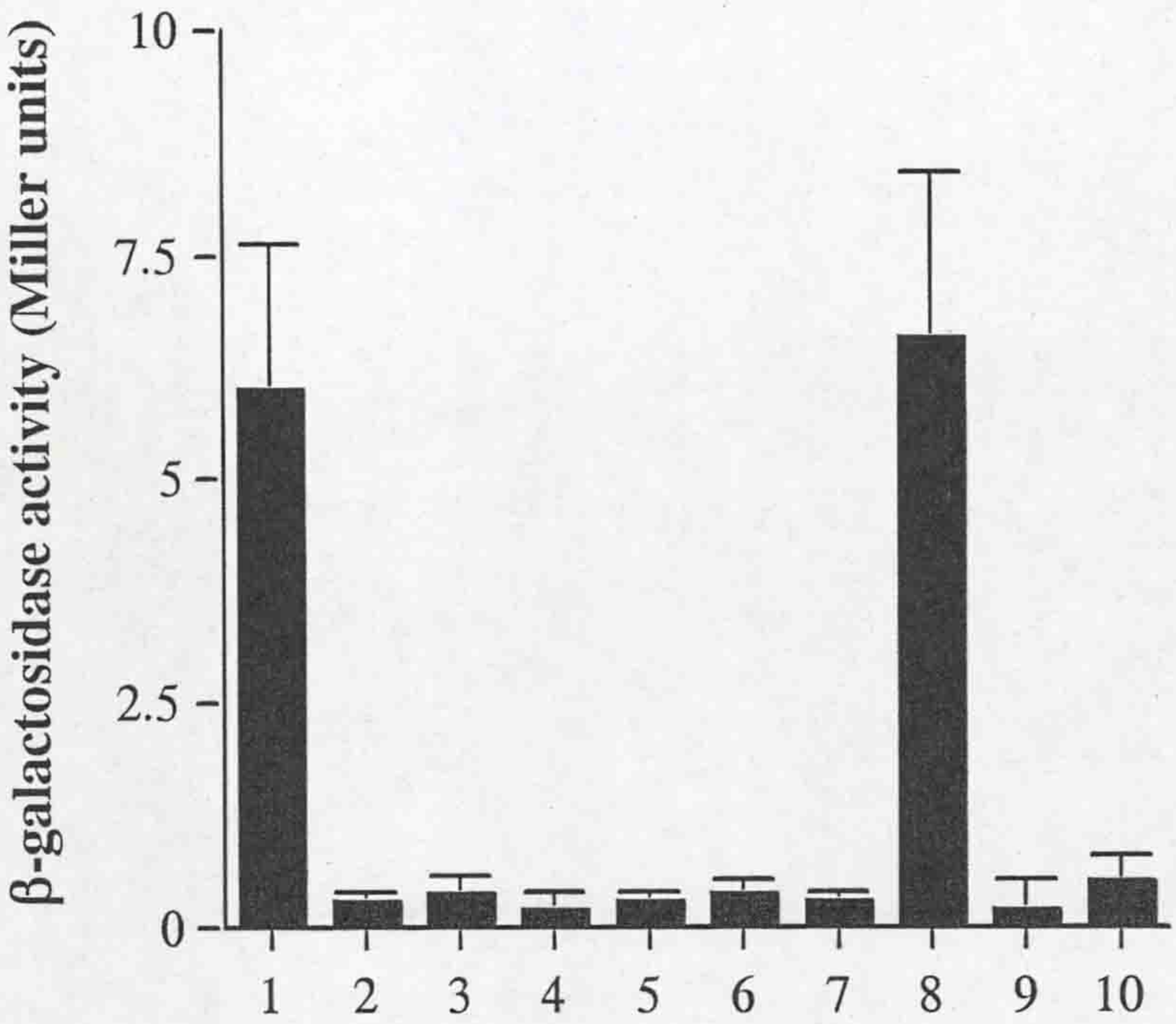

Figure 4.2 β-Galactosidase activities of yeast clones bearing S100A4 and S100A1 mutants. LexA-S100A4wt and YESTrp2-S100A1wt (column *1)*; LexA-S100A4wt and YESTrp2 vector (*column 2*); LexA vector and YESTrp2-S100A1wt *(column 3*); LexA-S100A4 F72Q mutation and YESTrp2-S100A1wt *(column 4)*; LexA-S100A4 Y75Q mutation and YESTrp2-S100A1wt *(column 5*); *column 6*, YESTrp2-S100A1wt alone; LexA-S100A4wt alone (*column 7*); bait LexA-S100A1wt and YESTrp2-S100A1wt *(column 8*); LexA-S100A1F15A and YESTrp2-S100A1wt (column 9); LexA-S100A1F15A and YESTrp2-S100A4wt (column 10). The means ± S.D. of at least three experiments are shown.

4.2.3 S100A4 prefers to form heterodimer with S100A1 in the yeast two-hybrid

system

To show that the interaction between S100A4 and S100A1 was specific, interactions of S100A1/S100A1 (bait/prey), S100A4/S100A1, S100A4/S100A4, S100A4/S100P, S100A4/S100A2 and S100A4/ pYEStrp2 vector were tested using the yeast two-hybrid system (Figure 4.3). The β-galactosidase activities were measured (Section 2.4.4) and used to represent the relative strength of interaction of each pair of fusion proteins. In order to reveal that the various levels of β-galactosidase activities are of statistical significance, the non-paired *t* test (using SPSS software) was employed (Table 4.1). The β-galactosidase activities from the yeast cells expressing S100A4/S100A1 fusion proteins are significantly higher than that of S100A4/ S100A4 ($p<0.01$) S100A4/S100A2 ($p<0.01$) and S100A4/S100P ($p<0.01$) but shows no significant difference from that of S100A1/S100A1 ($p>0.05$) in the yeast two-hybrid system (Table 4.1), indicating stronger interactions of S100A1/S100A1, S100A1/S100A4 occurred in yeast cells. These results suggest that S100A4 might preferentially bind to S100A1 at least in the fusion forms in yeast.

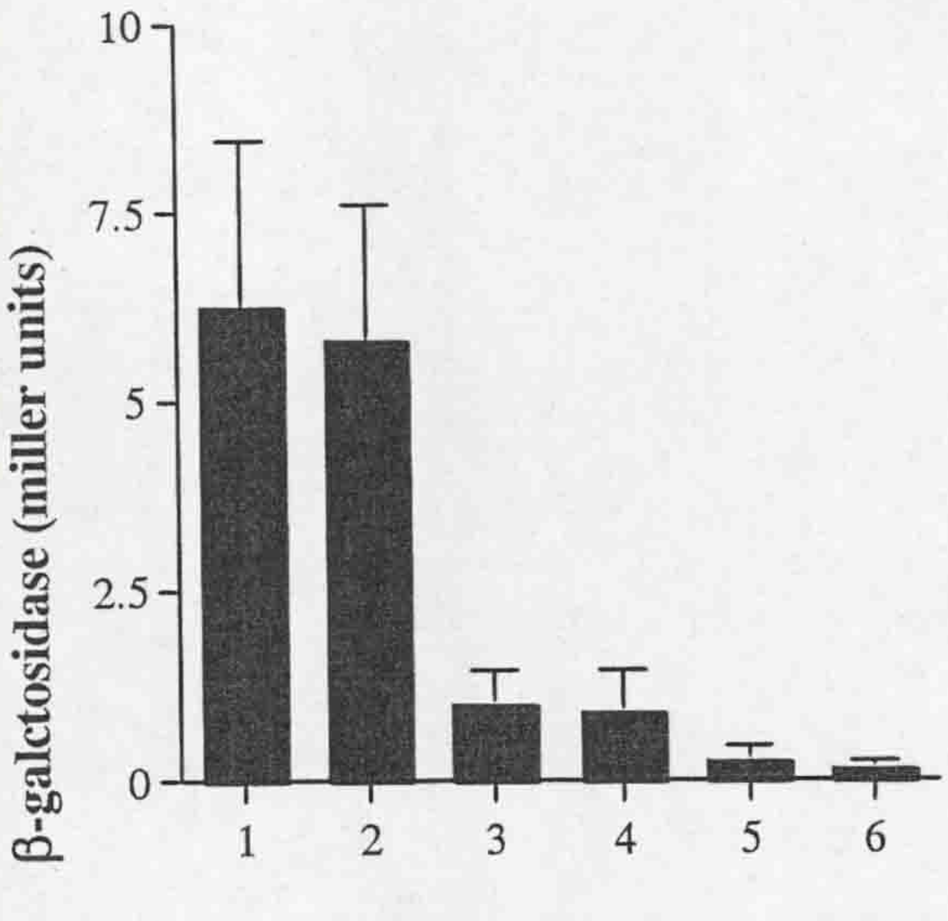

Figure 4.3. Comparison of β-galactosidase activities produced by the interactions of S100A4 with S100A1, S100A4, S100P and S100A2 in yeast. LexA-S100A1wt + YESTrp2-S100A1wt (*column 1*), LexA-S100A4wt + YESTrp2-S100A1wt (*column 2*); LexA-S100A4wt + YESTrp2-S100A4wt (*column 3*); LexA-S100A4wt + YESTrp2-S100Pwt (*column 4*); LexA-S100A4wt + YESTrp2-S100A2wt (*column 5*); LexA-S100A4wt + YESTrp2 vector (*column 6*).

Table 4.1 The statistical analysis of the interactions of S100A4 with other S100 proteins in yeast two-hybrid system

Bait	Prey	β-galactosidase activities Means ± SD[a] (Miller units)
LexA-S100A1wt	YESTrp2-S100A1wt	6.23 ±2.21[b]
LexA-S100A4wt	YESTrp2-S100A1wt	5.78±1.82[c]
LexA-S100A4wt	YESTrp2-S100A4wt	0.99±0.45[d]
LexA-S100A4wt	YESTrp2-S100Pwt	0.87± 0.54
LexA-S100A4wt	YESTrp2-S100A2wt	0.23±0.12[e]
LexA-S100A4wt	YESTrp2	0.14± 0.11

d. Means and SD calculated form more than 6 samples from at least two individual experiments. Non-paired *t* test (in SPSS software) was used for the statistical analysis.

e. The β-galactosidase activity in the S100A1/S100A1-containing yeast cells is significantly higher than that in S100A4/S100A2, or S100A4/S100A4, or S100A4/S100P containing yeast cells ($p<0.01$) but has no significant difference from that in S100A1/S100A4-containing yeast cells ($p>0.05$).

f. The β-galactosidase activity in S100A1/S100A4-containing yeast cells is significantly higher than that in S100A4/S100A2, S100A4/S100A4 and S100A4/S100P-containing yeast cells ($p<0.01$).

g. The β-galactosidase activity in S100A4/S100A4-containing yeast cells is significantly higher than that in S100A4/S100A2-containing yeast cells ($p<0.05$) but has not significantly different from that in S100A4/S100P-containing yeast cells ($p>0.05$).

h. The β-galactosidase activity in S100A4/S100A2-containing yeast cells is not significantly different from that in the negative control (S100A4/control vector) ($p>0.05$).

4.2.4 Interaction of S100A4 with S100A1 *in vitro*

To confirm the interaction by methods *in vitro*, the recombinant proteins of S100A4,

S100A1, GST and GST-S100A1 were produced (Section 2.5.8). GST-pull down assays and gel overlay assays were employed, where anti-S100A4 was used. As S100A1 and S100A4 are similar in protein sequence and 3D structure (Vallely *et al.*, 2002; Rustandi *et al.*, 2002), it is possible that the anti-body to one protein may cross react with the other. To role out the possibility and make the assays valid, the binding of anti-S100A4 to His-S100A1, GST, and GST-S100A1 recombinant proteins was checked by Western blotting (Figure 4.4). The results showed that the anti-S100A4 does not cross-react with S100A1, nor GST and GST-S100A1 fusion protein. In addition, anti-S100A1 does not cross-react with S100A4 recombinant protein.

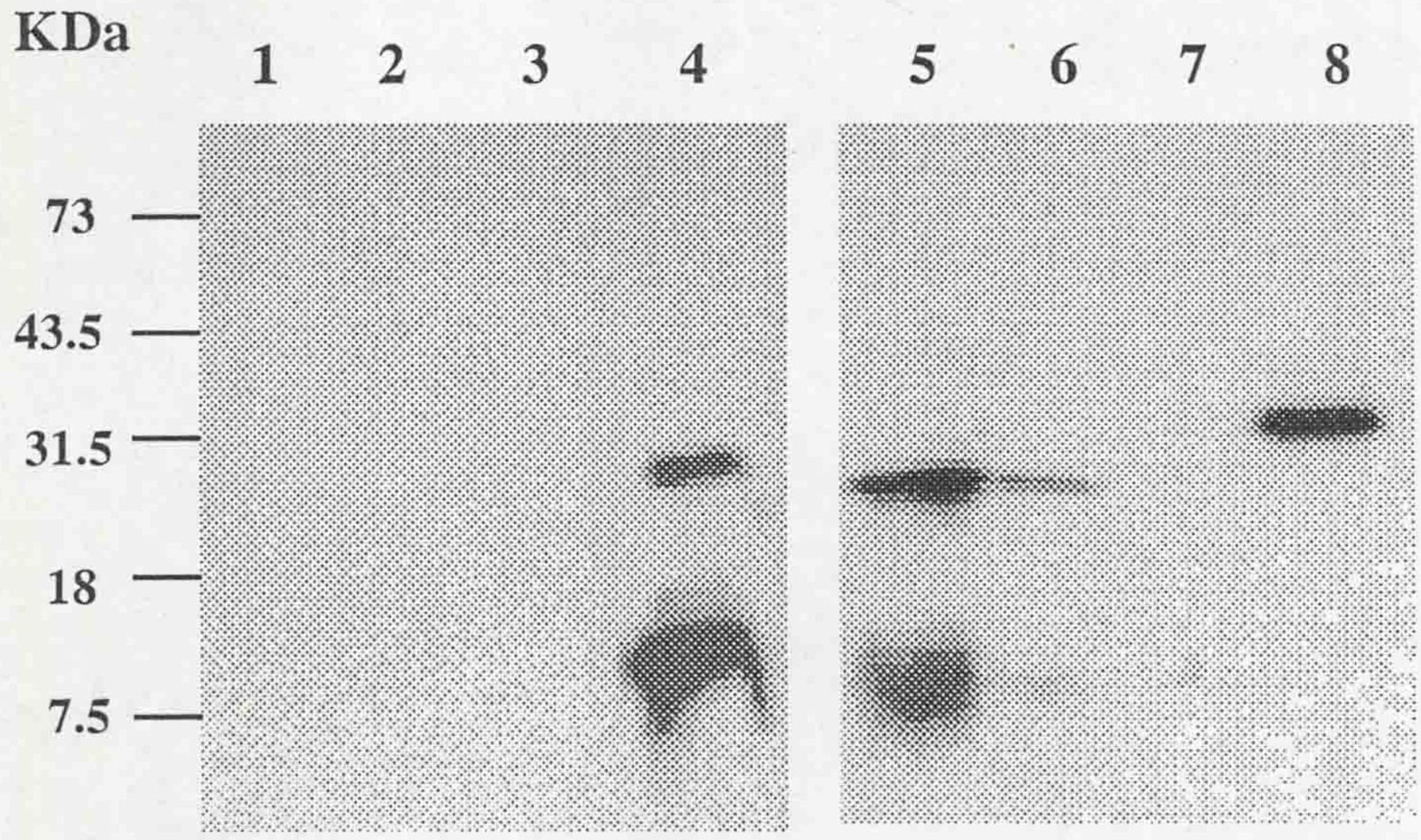

Figure. 4.4. The specificity of antibodies directed against recombinant S100A1 and S100A4 proteins. Samples of proteins, 5 μg His-S100A1 (*lane 1*), 5 μg GST-S100A1 (*lane 2*), 5 μg GST (*lane 3*), 5 μg S100A4 (*lane 4*), purified 5 μg His-S100A1 (*lane 5*), 20 μg cell lysate with induced His-S100A1 (*lane 6*), 5 μg S100A4 (*lane 7*), and 5 μg GST-S100A1 (*lane 8*) were subjected to SDS-PAGE and transferred to PVDF membranes. The membranes were incubated with rabbit polyclonal anti-S100A4 (*left panel*, *lanes 1-4*) or mouse monoclonal anti-S100A1 (*right panel*, *lanes 5-8*) and then with a second antibody that was detected in turn using the ECL system as described in Section 2.6.5. The lower band of S100A1 or S100A4 is the monomer and the upper band is an SDS-resistant

multimer arising from storage of the recombinant proteins.

4.2.4.1 Interactions *in vitro* revealed by affinity chromatography (GST-pull down assay)

To find out whether it is possible to detect interaction between S100A4 and S100A1 *in vitro*, the GST-S100A1 fusion protein and the control GST were immobilized on Sepharose-glutathione columns. The interaction *in vitro* with recombinant S100A4 was detected by the retention of the S100A4 on the Sepharose-glutathione-GST-S100A1 column. After extensive washing, the bound proteins were eluted from the columns with excess glutathione, and the proteins in the resulting fractions were analysed by SDS-PAGE and Western blotting with anti-S100A4 antibody. When a sample of recombinant S100A4 was passed through a column containing bound recombinant GST, no reduced glutathione-elutable S100A4 was retained on the column beyond the wash fraction (Figure. 4.5a). However, when the S100A4 was passed through a similar column but containing immobilized GST-S100A1 fusion protein, S100A4 was retained on the column, even after extensive washing with buffer, and was eluted, along with the GST-S100A1 fusion protein, with reduced glutathione. This result suggests strongly that S100A4 can bind to GST-S100A1 fusion protein but not to the GST control *in vitro*. Exactly the same result was obtained when the experiment was carried out with a cell lysate of *Escherichia coli* BL-21 cells, which had been induced to produce S100A4 with IPTG (Figure. 4.5*b*). The interaction *in vitro* of purified recombinant GST-S100A1 with S100A4 (purified or non-purified) was detected in the presence of 0.5 mM calcium ions and could be reversed in the presence of 1.0 mM EGTA (Figure. 4.5*b*).

a

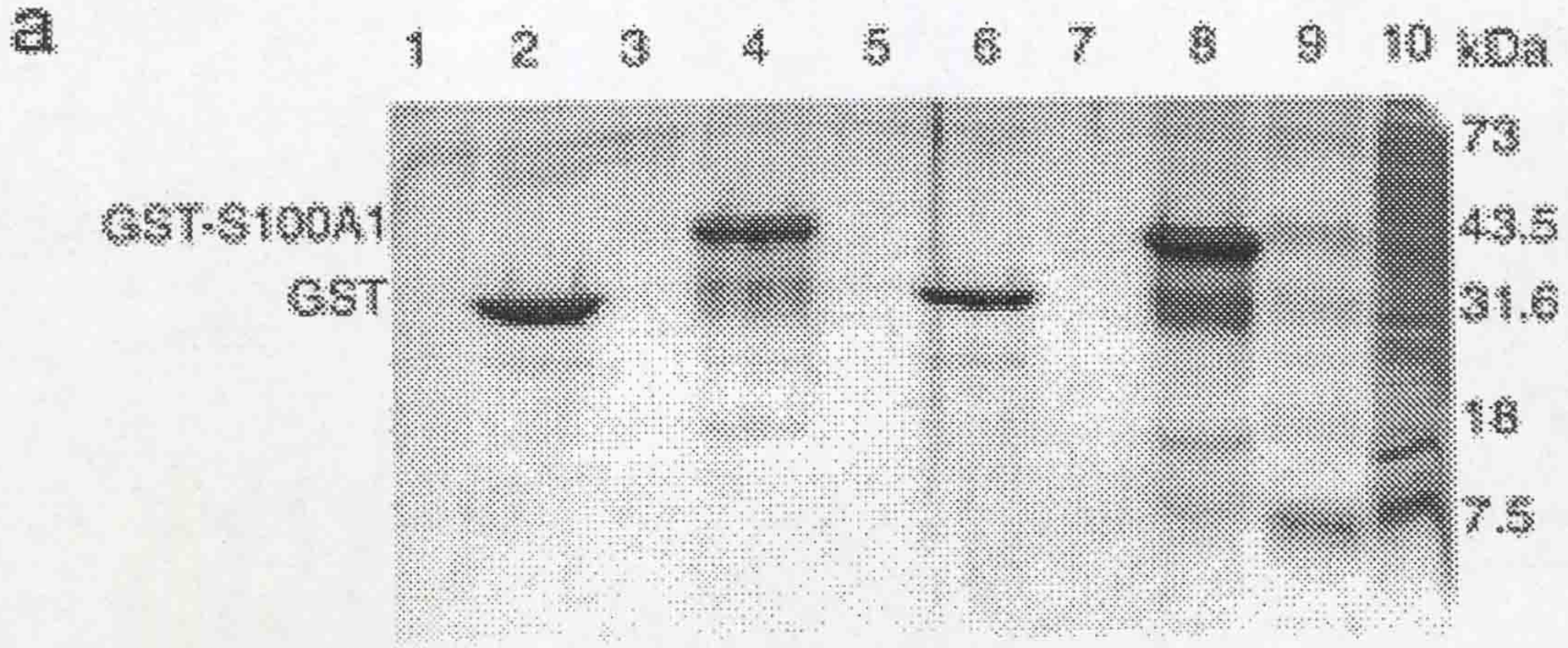

	1	2	3	4	5	6	7	8
GST-S100A1	–	–	+	+	–	–	+	+
GST	+	+	–	–	+	+	–	–
Calcium	+	+	–	–	–	–	+	+
EGTA	–	–	+	+	+	+	–	–
Fraction	W	E	W	E	W	E	W	E

b

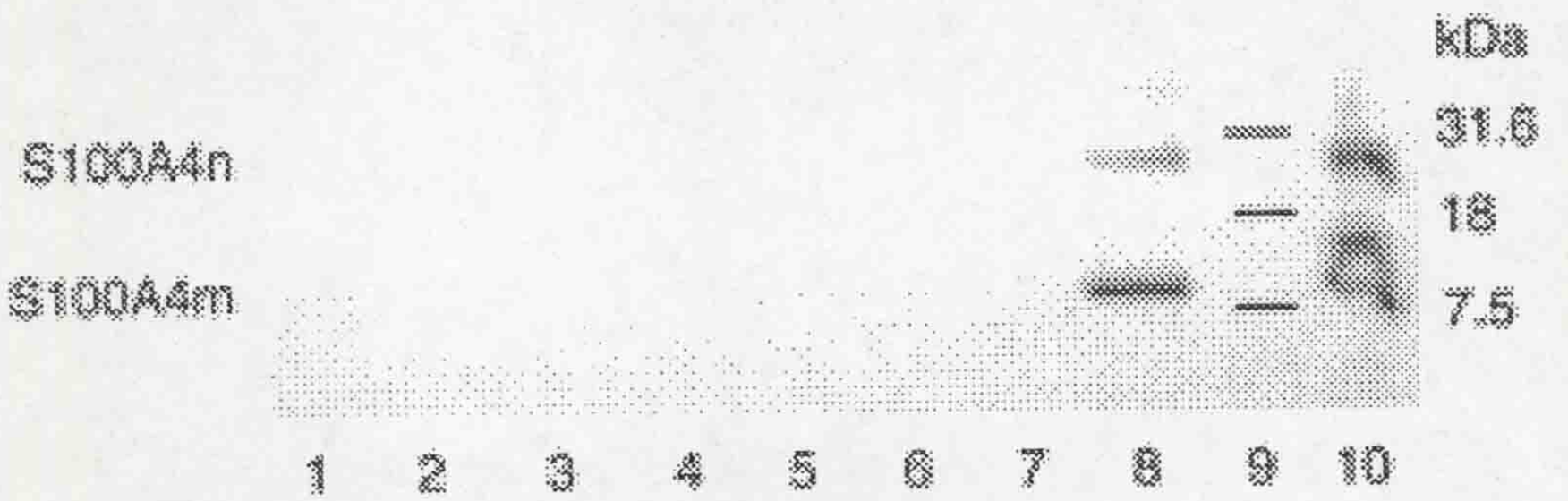

c

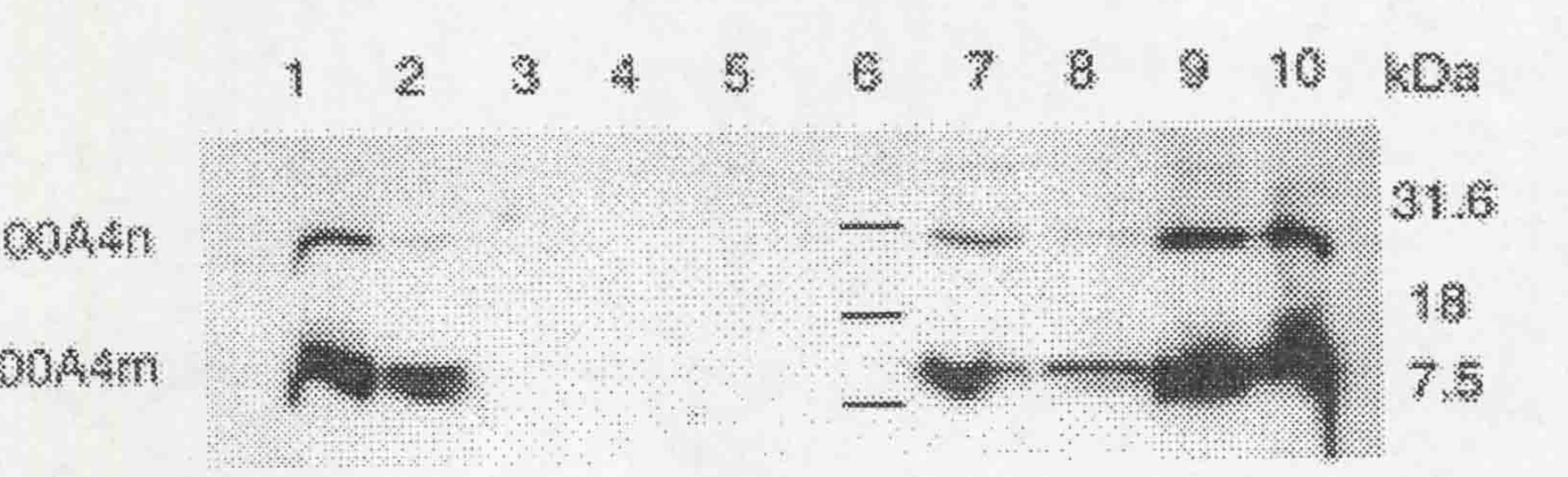

	1	2	3	4	5	6	7	8	9	10
GST-S100A1	–	–	–	–	+		+	+	+	
GST	+	+	+	+	–		–	–	–	
S100A4	+	+	+	–	–		+	+	+	
Calcium	+	+	+	n/a	n/a		+	+	+	
Fraction	PT	MW	E	PP	PP	Mr	E	MW	PT	A4

Figure 4.5 Interaction between S100A4 and S100A1 *in vitro*. Recombinant GST (*panels a and b*, *lanes 1*, *2*, *5*, and *6*; *panel c*, *lanes 1-4*) or GST-S100A1 recombinant fusion protein (*panels a and b*, *lanes 3*, *4*, *7*, and *8*; *panel c*, *lanes 5*, *7*, *8*, and *9*) were purified and immobilized on glutathione-Sepharose columns. Either a bacterial extract containing recombinant S100A4 (*panels a* and *b*; shown in *lane 10*) or purified S100A4 (*panel c*; shown in *lane 10*) was passed through the columns using a Tris buffer (*panels a* and *b*) or a phosphate-buffered solution (*panel c*), as described in Section 2.6.7. In *panels a* and *b*, the buffer contained either calcium (*lanes 1*, *2*, *7*, and *8*) or EGTA (*lanes 3-6*). The proteins that passed through the columns (designated *PT*) were collected (*panel c*, *lanes 1* and *9*). The columns were washed until no more protein was eluted, and the washes were either pooled (*panel c*, *lanes 2* and *8*, designated *MW* for mixed wash), or a final wash fraction was passed through (*panels a* and *b*, *lanes 1*, *3*, *5*, and *7*, designated *W*). Proteins remaining bound to the columns were eluted, designated by *E* (*panels a* and *b*, *lanes 2*, *4*, *6*, and *8*; *panel c*, *lanes 3* and *7*), as described in Section 2.6.7. Samples of the fractions were subjected to SDS-PAGE as described in Section 2.6.2 and a gel was stained (*panel a*) or the proteins were transferred onto membranes (*panels b* and *c*). S100A4 was detected by a rabbit anti-S100A4, which did not cross-react with S100A1 (*panels b* and *c)*. The molecular masses of marker proteins (*panel a*, *lane 9*, designated M_r) are indicated in kDa alongside *panel a*. On *panel c* the markers on the original stained gel (*lane 6*, designated M_r) are not visible on the autoradiograph but have been drawn in to indicate their position. On *panel c*, samples of pure proteins (*PP*) of the recombinant glutathione *S*-transferase (*lane 4*), the GST-S100A1 recombinant fusion protein (*lane 5*), and recombinant S100A4 (*lane 10*, designated *A4*) were also subjected to electrophoresis and Western blotting. *m*, monomeric; *n*, multimeric; *n/a*, not applicable. The multiple weak bands in *panel a*, *lanes 4* and *8*, arise from degradation of the GST-S100A1 fusion protein, and the apparent doublet for S100A4m in *panel b* is an overloading artefact.

4.2.4.2 Interaction revealed by gel overlay

Interaction between S100A1 and S100A4 was demonstrated using a gel overlay technique with purified S100A1 and S100A4 proteins (Figure. 4.6). S100A4 protein binding to the proteins on the membrane was detected by anti-S100A4. The results showed that S100A4 could bind to both His-S100A1 and GST-S100A1, but not GST protein.

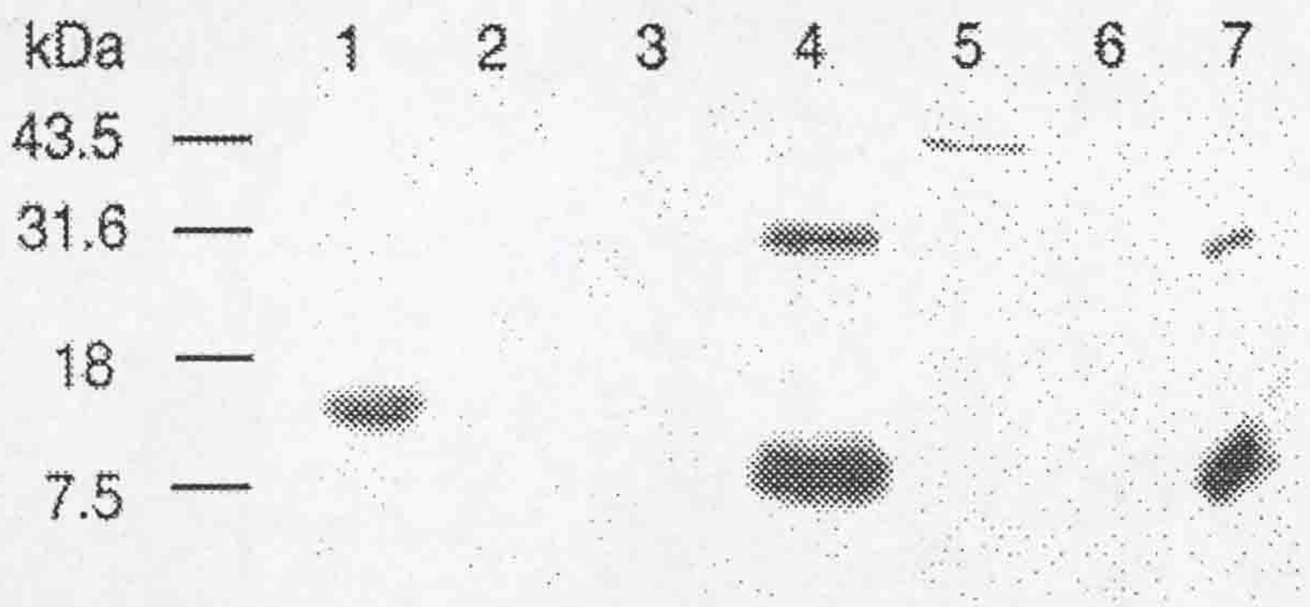

Figure. 4.6 Interaction *in vitro* between S100A1 and S100A4 using gel overlay. Purified recombinant proteins, His-S100A1 (*lane 1*), GST (*lane 3*), rat S100A4 (*lane 4*), GST-S100A1 (*lane 5*), GST (*lane 6*), and human S100A4 (*lane 7*) were separated by SDS-PAGE (15% (w/v)) and blotted onto PVDF membranes. The membranes were incubated with S100A4, and any binding of S100A4 was detected by anti-S100A4 (see Section 2.6.6). The banding pattern of molecular masses of markers in kDa is shown on the *left side* of the image. *Lane 2* contained no protein.

4.2.5 Binding affinities of S100A4 to S100A1 characterised by an optical biosensor

The binding strengths of S100A1/S100A4 and S100A4/S100A4 detected in yeast two-hybrid system were represented by β-galactosidase activities and may not be proportional to their binding affinities. Moreover, the interactions detected in yeast two-hybrid system are the interactions of fusion proteins and their binding strength may be different from that of the native proteins. Therefore non-tagged S100A1 and S100A4 recombinant proteins were produced and their binding affinities were detected using a biosensor. The binding properties of S100A4 to immobilised S100A4 and immobilised S100A1 were characterized by fast association kinetics (Section 2.7.3). In the presence of

0.5mM Ca^{2+}, the association rate constant for the S100A4/S100A1 (homodimer) interaction (k_{ass} = 0.20 ± 0.03 x 10^5 $M^{-1}s^{-1}$) was slightly higher than that for the S100A4/S100A4 interaction (k_{ass} = 0.12 ± 0.01 x10^5 $M^{-1}s^{-1}$) (Table 4.2), indicating that the interaction of S100A4 with immobilized S100A1 is slightly faster than that with immobilized S100A4. The dissociation rate constant of S100A4 from S100A4 was similar to that of S100A4 from S100A1 (Table 4.2). The affinity calculated from the kinetic parameter between S100A4 and S100A1 (Kd 300 ± 60 nM) was similar to that between S100A4 and S100A4 (Kd 670 ± 80nM). The Kd values calculated from the extents of binding observed at equilibrium were Kd 500 ± 140nM for S100A4/S100A1 interaction and Kd 1,000 ± 300nM for S100A4/S100A4 interaction, which are similar to these calculated from the kinetic binding parameters.

The binding of S100A4 to immobilized S100A4 or S100A1 was always homogenous; there was no evidence for the presence of more than one binding site for S100A4 with immobilized S100A4 or S100A1. This result supports the monomer-monomer interaction model. Plots of k_{on} against ligand concentrations yield straight lines in both S100A4/S100A4 (Figure 4.7a, r = 0.94) and S100A4/S100A1 (Figure 4.7b, r = 0.98) interactions. The binding of different concentrations of S100A4 to immobilized S100A1 or S100A4 were also plotted using FastPlot software (Figure 4.7c and d).

Table 4.2. Kinetics of S100A4 binding to immobilized S100A4 and S100A1 in the presence of 0.5mM $CaCl_2$

Immobilised protein	k_{ass} $M^{-1}s^{-1}$[a]	r[b]	k_{diss} s^{-1}[c]	K_d nM[d] (kinetics)	K_d nM[e] (equilibrium)
S100A4	$0.12\pm0.01 \times 10^5$	0.94	0.008 ± 0.0005	670 ± 80	$1{,}000\pm300$
S100A1	$0.20\pm0.03 \times 10^5$	0.98	0.006 ± 0.001	300 ± 60	500 ± 140

a. The S.E. of each determination of k_{ass} is derived from the deviation of the data from a one-site binding model, calculated by matrix inversion using the FastFit software provided with the instrument. No evidence was found for a two-site model of association.

b. The correlation coefficient of the linear regression through the k_{on} values used for obtaining k_{ass}.

c. The k_{diss} is the mean ± S.E. of at least 6 values, obtained at different concentrations of S100A4. No evidence was found for a two-site model of dissociations

d. The Kd (kinetics) was calculated from the ratio of k_{diss}/k_{ass}, and the S.E. is the combined S.E. of the two kinetic parameters.

e. Kd (equilibrium) values were calculated from the extent of binding observed at five or more different concentrations of ligate in two independent experiments. The S.E. is the combined error of the two experiments.

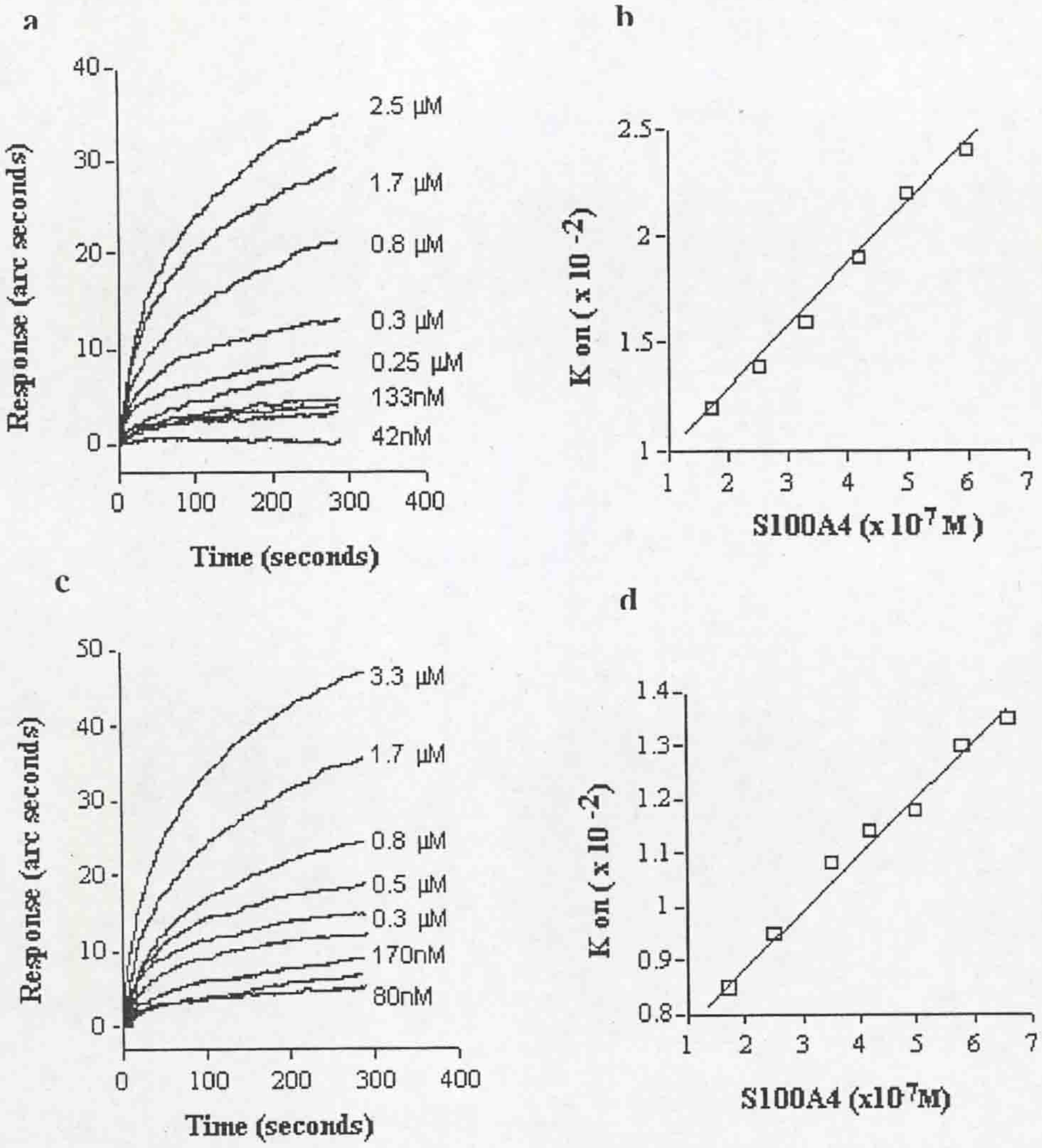

Figure 4.7 Measurement of S100A4-S100A4 and S100A4-S100A1 interactions using an optical biosensor. The plot of the response (arc seconds) of different concentrations of S100A4 binding to the S100A1 surface (*panel a*) and S100A4 surface (*panel c*). The plot of k_{on} against the concentration of ligand: S100A4 recombinant protein binding to S100A1 surface (*panel b*) and S100A4 surface (*panel d*).

4.2.6 Calcium influence on the interaction of S100A4 and S100A1

To investigate in more detail the influence of calcium ions on the interaction between S100A4 and S100A1, the GST-S100A1 columns described above were utilized, with buffers containing between 0 and 1.0 mM calcium ions or 0.5 and 1.0 mM EGTA. Interaction between S100A1 and S100A4 could be detected using the buffer with no added calcium; however, the amount of S100A4 retained on the Sepharose-glutathione-GST-S100A1 column increased as the

concentration of calcium in the buffer was increased (Figure. 4.8). 0.5 mM EGTA reduced the amount of S100A4 retained on the Sepharose-glutathione-GST-S100A1, and no detectable S100A4 was retained with 1.0 mM EGTA. These results suggest that although the interaction of S100A4 with S100A1 can occur in the presence of a low Ca^{2+}ion concentration, high Ca^{2+} can promote the interaction. However, a high concentration of EGTA creates conditions that reduce the retained S100A4 to an undetectable level.

To quantify the Ca^{2+} enhancements of the binding of S100A4 to S100A4 and S100A1, biosensor assays in the presence and absence of Ca^{2+} were carried out. In Ca^{2+} free buffer (with 50μM EGTA), S100A4 can bind to both immobilised S100A4 and immobilised S100A1. However, in the presence of 0.5mM Ca^{2+}, the binding responses increased about 50-60 % relative to that in Ca^{2+} free buffer (Figure 4.9).

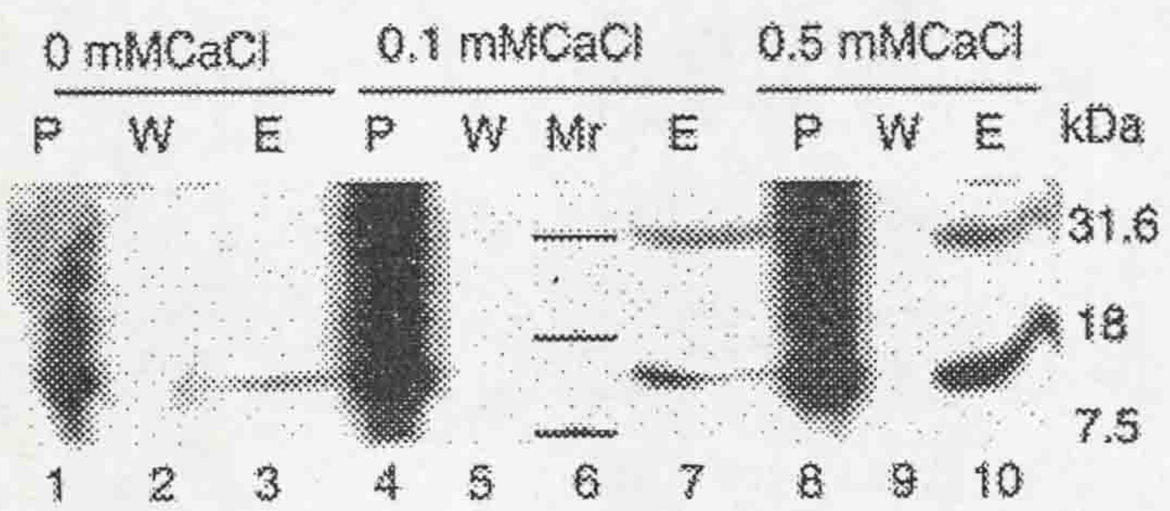

Figure. 4.8. Effect of calcium ions on the interaction *in vitro* between S100A4 and S100A1. GST-S100A1 fusion recombinant protein was purified and immobilized on glutathione-Sepharose beads. The beads were incubated at 4 °C overnight with S100A4 protein in Tris buffer containing no added $CaCl_2$ (*lanes 1-3*) or added $CaCl_2$ to 0.1 mM (*lanes 4*, *5*, and *7*), 0.5 mM (*lanes 8-10*), 1.0 mM (*lanes 11-13*) or EGTA added to 0.5 mM (*lanes 14-16*) or 1.0 mM (*lanes 17-19*). The mixtures were then applied to spun columns. After extensive washing, the GST-S100A1 was eluted from the beads with glutathione. The fractions, *P* (pass-through), *W* (last wash), and *E* (elute) were subjected to SDS-PAGE and Western blotting. The S100A4 that had been retained on the column was detected with anti-S100A4. The smear in the pass-through fractions arises from aggregation of the excess recombinant S100A4 protein. Molecular mass markers (M_r) of standard proteins on the stained gel are shown in *lanes 6* and *20*.

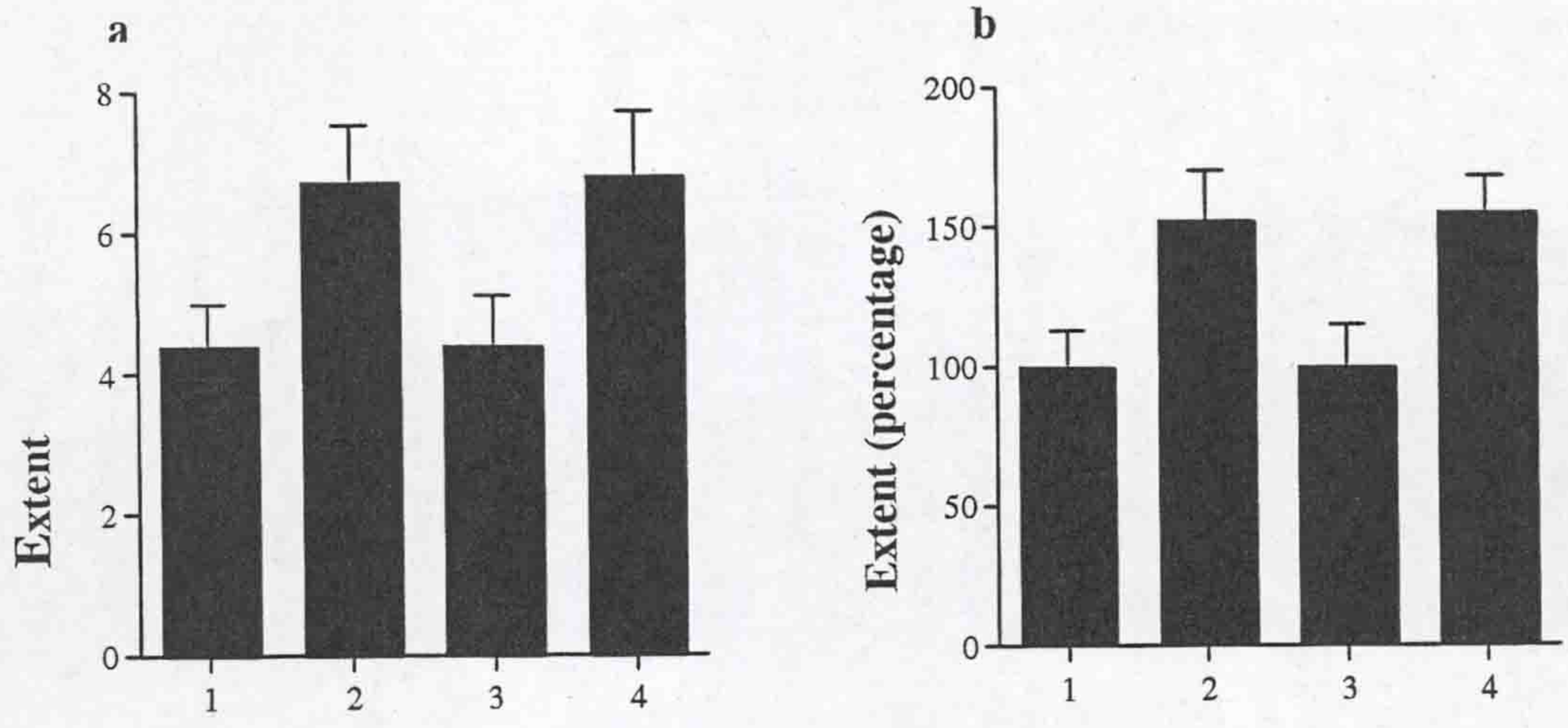

Figure 4.9 The effects of Ca^{2+} on the binding of S100A4 to immobilised S100A4 and S100A1 in the biosensor assay. S100A4 and S100A1 were immobilised onto the aminosaline surfaces of the biosensor cells separately. Freshly thawed S100A4 in Pi buffer (Section 2.2.21) was used as the ligate in the assay. Each binding assay was repeated 4 times with the same reaction conditions. The extent from each cycle was calculated with the Fastfit software and average extent and standard deviation (*panel a*) was obtained using the computer programme Excel. The average extent in the absence of Ca^{2+} was designated as 100% and the average extent in the presence of Ca^{2+} were shown as the percentage (*panel b*) of that in the absence of Ca^{2+}. S100A4 binds to immobilised S100A4 in the absence of Ca^{2+} (*columns 1*) and in the presence of 0.5mM Ca^{2+}(*columns 2*), and S100A4 binds to immobilised S100A1in the absence of Ca^{2+} (*columns 3*) and in the presence of 0.5mM Ca^{2+}(*columns 4*).

4.2.7 Co-expression of S100A4 and S100A1 in MDA-MB-231 cell line

To find out whether S100A1 and S100A4 coexist in the same cells naturally, the presence of S100A1 mRNA was sought in breast tumour cell lines of known S100A4 status using a PCR-based assay. A correctly sized ethidium bromide-stained band of DNA on agarose gels was obtained following RT-PCR using human S100A1-specific primers on RNA from human mammary cell lines, MCF-7, MDA-MB-231, and SKBr-3 (Figure. 4.10). The latter two cell lines have been shown previously to contain high levels of S100A4 mRNA. Sequencing of the PCR products confirmed that their sequences corresponded to the human S100A1 mRNA. No bands were obtained with any of the RNAs when RT-PCRs were carried out in the absence of the Superscript reverse transcriptase. Thus, the mRNAs for

both S100A1 and S100A4 were present in MDA-MB-231 and SKBr-3 cell lines. The presence of both S100A1 and S100A4 proteins in the same cells has also been shown by Western blotting (Figure. 4.11).

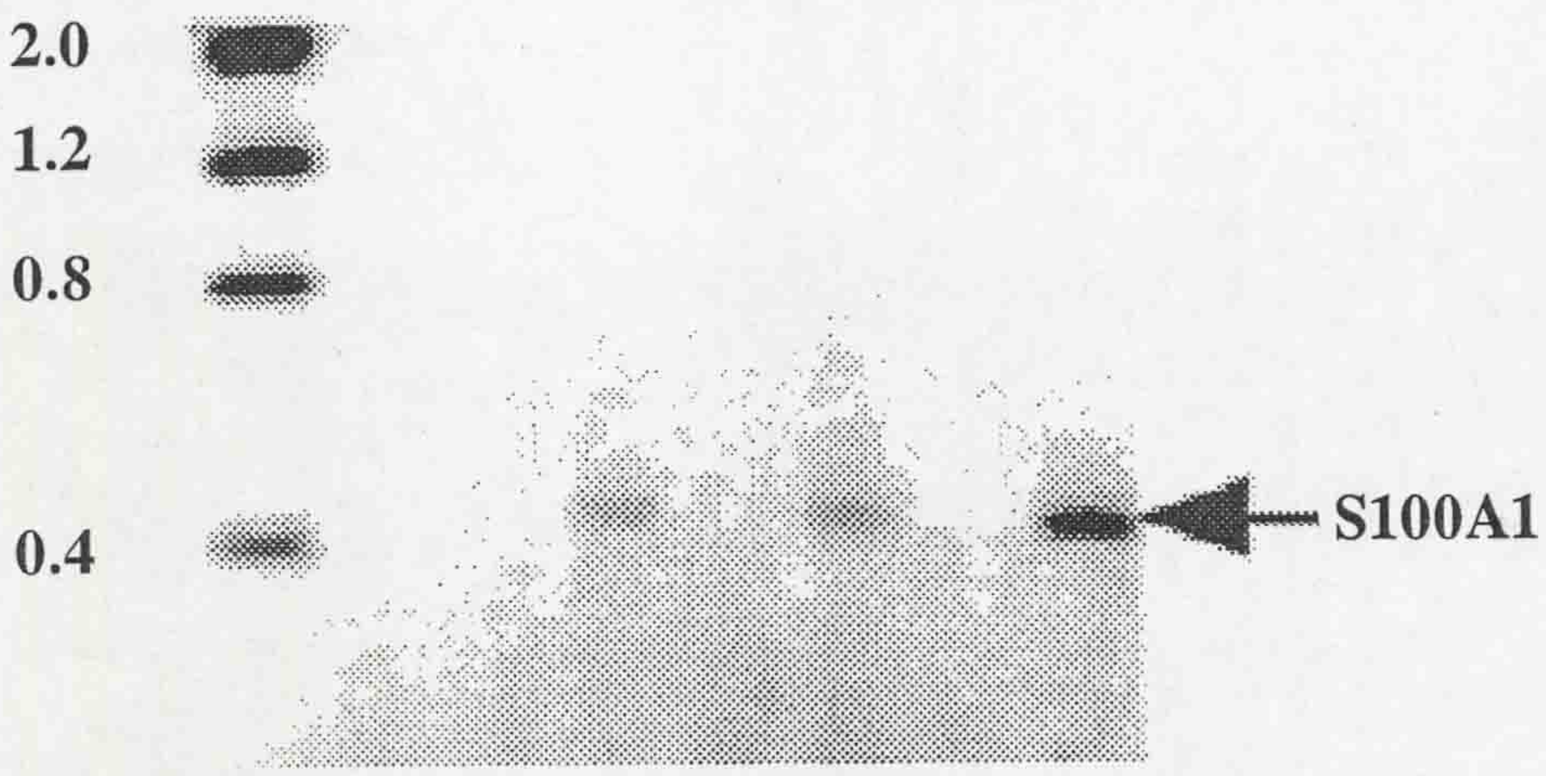

Figure. 4.10 Detection of mRNA for S100A1 in breast tumour cell lines. RNA from the malignant human breast cancer cloned cell lines, MCF-7 (*lanes 3* and *4*), SK-Br-3 (*lanes 5* and *6*), and MDA-MB-231 cells (*lanes 7* and *8*) was subjected to RT-PCR (*lanes 4*, *6*, and *8*) or control amplification in which the reverse transcriptase was omitted (*lanes 3*, *5*, and *7)*, using primers specific for human S100A1, as described in Section 2.3.14. A PCR reaction without template was also carried out (*lane 2*). The resulting PCR products were subjected to agarose gel electrophoresis along with molecular size markers (*lane 1*), and the gel was stained with ethidium bromide. The image has been reversed. The band of S100A1 amplification product is indicated by the *arrow*.

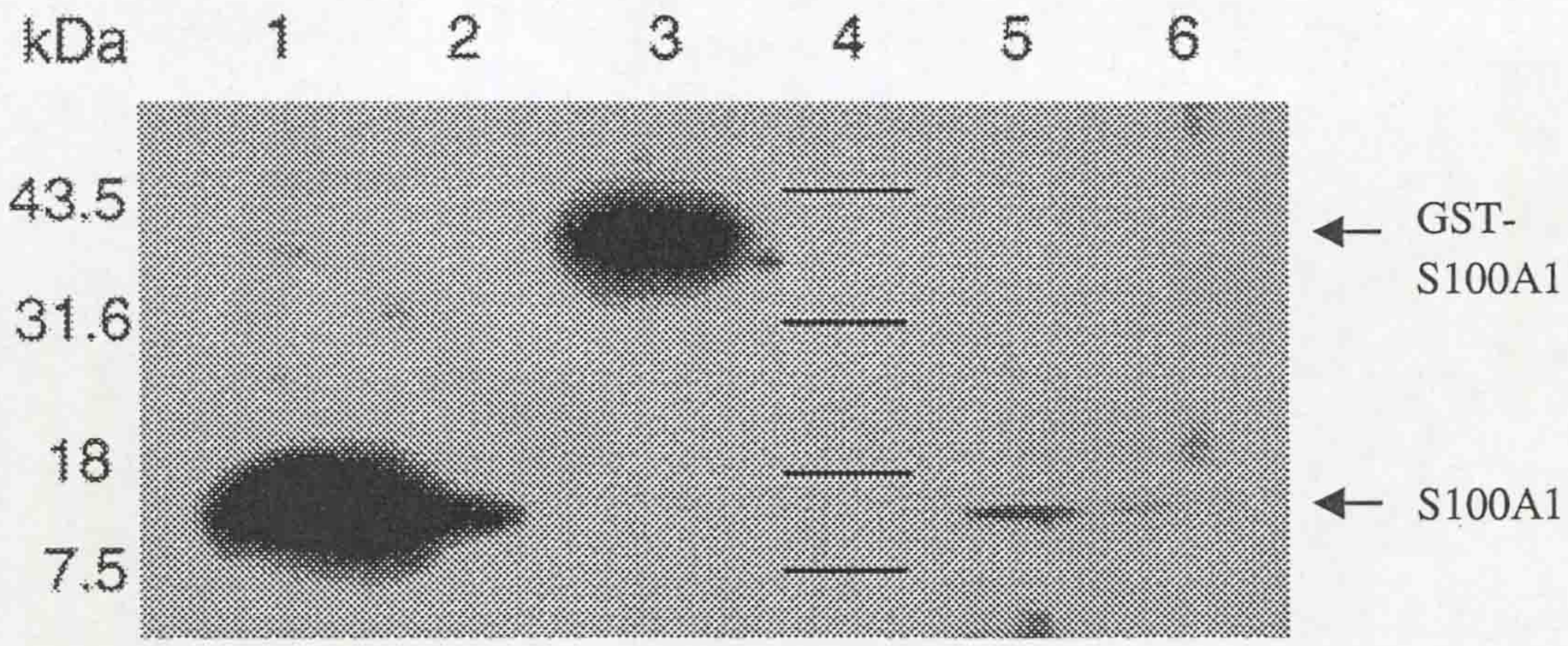

Figure. 4.11 Western blotting of S100A1 and S100A4 proteins in cell lines. Recombinant proteins His-S100A1 (*lane 1*, 15 μg and *lane 2*, 2 μg), GST-S100A1 (*lane 3*, 5 μg), and lysates from cell lines SK-Br-3 (*lane 5*, 40 μg) and MDA-MB-231 (*lane 6*, 40 μg) were separated by SDS-PAGE (15% (w/v)) and blotted onto PVDF membranes. The S100A1 was detected by polyclonal anti-S100A1 (Section 2.6.5). Molecular weight markers are shown diagrammatically (*lane 4*), with their molecular masses indicated in kDa on the *left side*.

4.2.8 Co-localisation of S100A4 and S100A1

By dual labeling immunofluorescence on MDA-MB-231 cells, both S100A1 and S100A4 were localized to the perinuclear region and to the cytoskeleton, and the fluorescence of each could be removed by preincubating each antibody separately with its cognate, but not the other recombinant protein (Figure. 4.12). Superimposition of the staining shows their partial co-localization on stress fibres and in the perinuclear region.

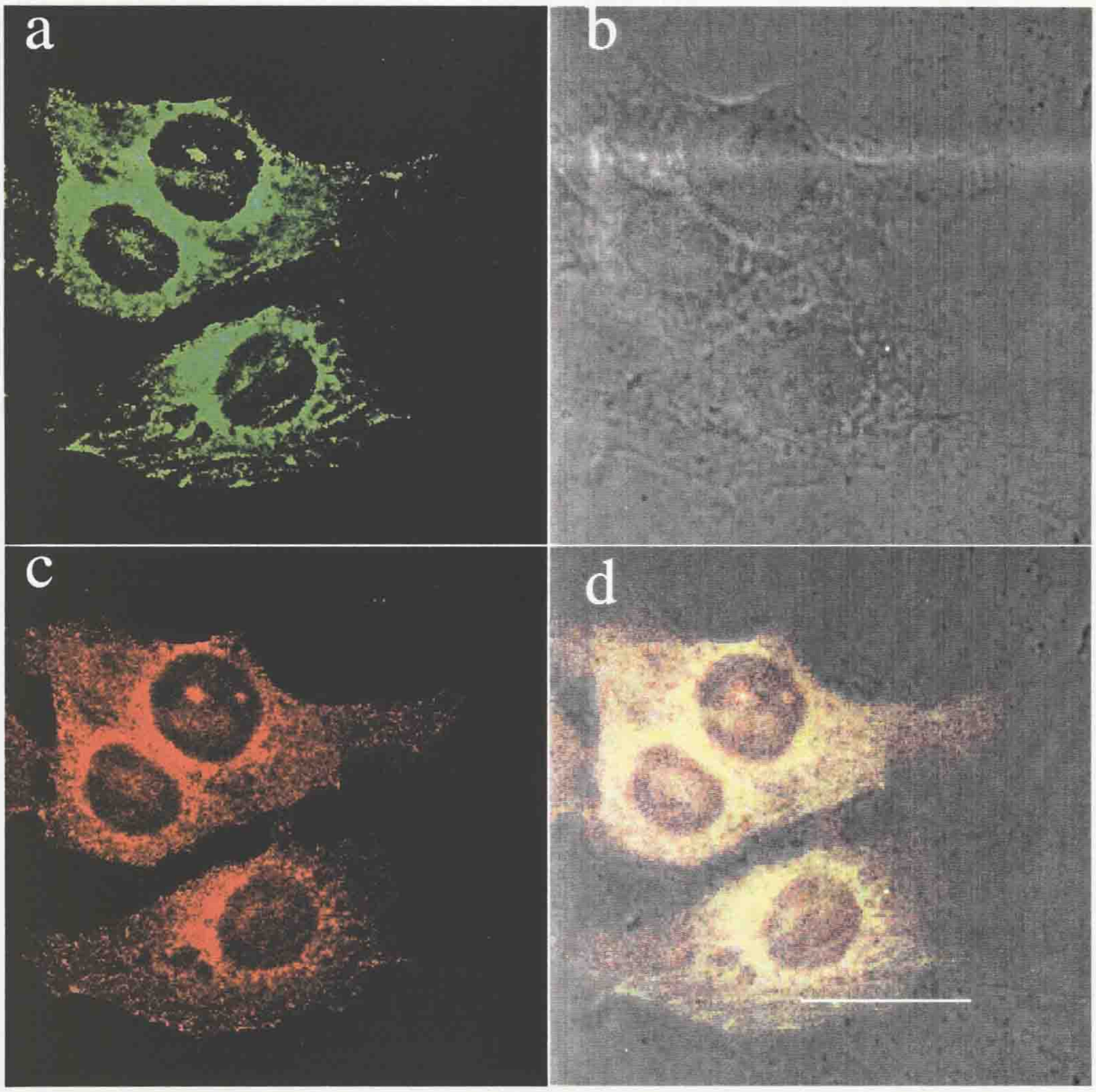

Figure. 4.12 Immunofluorescent localization of S100A1 and S100A4 in human mammary cells in culture. MDA-MB-231 cells were grown in chambered slides, fixed, and incubated with a mouse monoclonal anti-S100A1 and fluorescein isothiocyanate-conjugated anti-mouse IgG (*panel A*) or with a rabbit polyclonal anti-S100A4 and tetramethylrhodamine -isothiocyanate conjugated anti-rabbit IgG (*panel C*) (Section 2.8.6). Superimposition of the images in *A* and *C* indicates partial co-localization of the two S100A proteins around the nucleus and on stress fibres. *Panels A-C* and the phase-contrast image (*panel B*) are of the same field. *bar* = 20 µm.

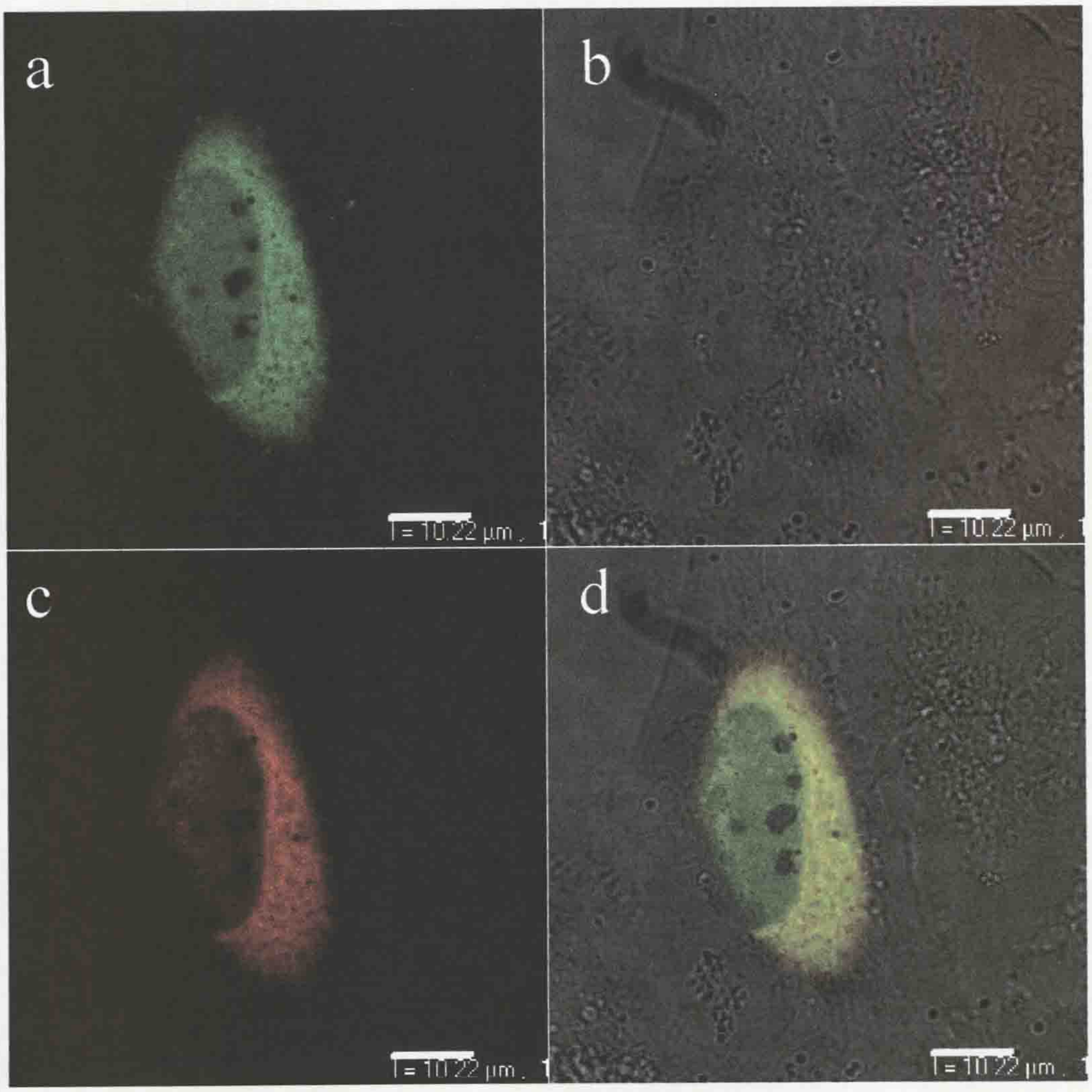

Figure. 4.13 Co-localization of S100A1 and S100A4 in Hela cells. HeLa cells were grown in 3.5 cm culture dishes and transfected with pCDNA4-dsREDS100A1-GFPS100A4 plasmid. 24 h after transfection, the cells were examined under a confocal microscope. GFP-S100A4 (*panel A),* dsRED S100A1 (*panel C*). Superimposition of the images in *A* and *C* indicates partial colocalization of the two S100A proteins around the nucleus and in cytoplasm (*panel D*). *Panel A, C, D* and the phase-contrast image (*panel B*) are of the same field.

The localisation of GFP-tagged human S100A1 and human S100A4 in HeLa cells (Figure 4.13) were very similar to the pattern observed by immunofluorescent staining (Figure 4.12). Both S100A4 (*panel A*) and S100A1 *(panel C*) fusion proteins were located in the peri-nuclear region. Superimposition of *panels a and c* showed co-localisation of S100A4 and S100A1 fusion proteins (*panel D*). This experiment confirmed the observations of the immunofluorescent staining with anti-S100A4 and anti-S100A1 and also ruled out the possibility of cross-reactions

of the antibodies used for immunofluorescent staining.

4.3 Discussion

S100A1 is the first S100 protein isolated from bovine brain in 1965 and has been extensively studied since then. The S100A1 gene is located in the same S100 gene cluster (human chromosome 1q21) (Ridinger *et al.,* 1998) as the S100A4 gene. Human S100A1 protein has 93 amino acids with a typical structure of S100 proteins (Baudier *et al.,* 1986). Although it has been reported previously that both S100A1 and S100A4 form homodimeric forms (Tarabykina *et al.,* 2001; Ilg *et al.,* 1996; Pedrocchi *et al.,* 1994), this is the first report of S100A4 interacting with S100A1. The interaction of S100A4 with S100A1 was found in yeast two-hybrid system and confirmed by experiments *in vitro*, including GST-pull down experiments and gel overlay assays. The Ca^{2+} influence on the interaction was also investigated. Using the GST-pull down assay, the interaction was not Ca^{2+}-dependent and could occur in the buffer with 0.5mM EGTA (a Ca^{2+}-free environment). However, increasing the concentration of Ca^{2+} in the reaction buffer dramatically promoted the binding of S100A4 to the GST-S100A1 fusion protein. In biosensor assays, the extents of the binding of S100A4 to immobilised S100A1 increased 50-60% when the Ca^{2+} in the buffer was changed from 0 (with 50μM EGTA) to 0.5mM. The result is similar to that observed in the interactions of S100B with S100A6 and S100A1, which are calcium-independent in co-immunoprecipitation experiments, and Ca^{2+} only strengthens the interactions (Deloulme *et al.,* 2000a). Using an optical biosensor, the Kd of S100A4 binding to immobilised S100A1 is about 300-500nM in the presence of 0.5 mM Ca^{2+}, which is similar to the Kd of S100A4 binding to immobilised S100A4, about 700-1,000nM.

In the screening of the yeast two-hybrid library constructed from a human breast cancer specimen (Invitrogen), only S100A1 was found to interact with the S100A4 bait. This could be because of the low Ca^{2+} environment in yeast, which was suitable for the Ca^{2+}-independent interactions but not for Ca^{2+}-dependent interactions, such as the

interaction with MHC-IIA and IIB as discussed in Chapter 3. To explore if the way of interaction of S100A4/S100A1 is similar to that of the previously characterised homodimerisations of S100A1/S100A1 and S100A4/S100A4 (Osterloh *et al.,* 1998; Rustandi *et al.,* 2002; Tarabykina *et al.,* 2001; Vallely *et al.,* 2002), S100A4 and S100A1 molecules had been specifically mutated. The conserved amino acid residues, Y72 and Y75, were reported previously to be associated with the dimer interface of S100A6 (calcyclin) (Potts *et al.,* 1995a) and it was also shown in yeast two-hybrid system that these two conserved residues are important to the homodimerisation of S100A4. In this study, the mutation of Y72Q and Y75Q, which prevented S100A4 homodimerization in the yeast two-hybrid system, also prevented interaction of S100A4 with S100A1. The dimer interface of apo-mouse S100A4 (Ca^{2+}-free state) defined by NMR involves residues in helix 1 (P4, L5, E6, A8, L9, V11, M12, T15, and F16), helix 2 (L38), loop 3 (L42), helix 4 (F72, Q73, V77, L79, S80, and A83), and loop 5 (F89) (Vallely *et al.,* 2002). F72 is on the interface while F75 is not. The reason of F75Q interrupting the S100A4 homodimerisation and S100A4/S100A1 heterodimerisation could be due to a conformation change in the hydrophobic core.

The dimer interface of apo-S100A1 determined by NMR involves (E3, L4, E5, A7, M8, L11, V14, and F15 in helix 1, L41 in loop 2, Q72, V76, V78, A79, and T82 in helix 4, and F88 in loop 4) (Rustandi *et al.,* 2002). F15 in S100A1 is on the dimer interface and was also shown to be important for S100A1 homodimerisation. The F15A mutation in this study interrupted both S100A1 homodimerisation and the heterodimerisation of S100A1/S100A4. All these results strongly suggest that the S100A4/S100A1 interaction resembles the natural association of other S100 proteins into homo- (Potts *et al.,* 1995a) and hetero- (Teigelkamp *et al.,* 1991) dimeric forms. This result is also supported by the observation that $Ca2^{+}$ influences the S100A4/S100A1 interaction, which is consistent with the fact that homodimers of many S100 proteins can be formed in the presence or in the absence of Ca^{2+} (Otterbein *et al.,* 2002).

Based upon the time taken for the blue dye arising from β-galactosidase activity to become visible, the interaction between S100A4 and S100A1 *in vivo* was more effective at stimulating reporter gene activity than the homodimeric interaction of S100A4 in the same yeast two-hybrid system (Figure 4.3). In the biosensor assay, the binding affinity of S100A4 to immobilised S100A4 is similar to that of S100A4 to immobilised S100A1. This result suggests that the S100A1/S100A4 heterodimer could be formed as efficiently as that of the S100A4 homodimer in cells if the two proteins co-existed.

To check the possible co-existence of S100A1 and S100A4 in cell lines, RT-PCR and Western blotting were used to detect the mRNA and protein of S100A1 in S100A4 expressing cells, MDA-MB-231 and SKBr-3. The results showed that both mRNAs and proteins of S100A1 and S100A4 are present in these cell lines. Immunofluorescent staining and living colour GFP fusion proteins showed that S100A1 and S100A4 partially co-localised in the perinuclear and cytoplasmic regions of individual cells. Co-expression of S100A1 and S100A4 has also been reported previously in primary cultures and cell lines of human vascular smooth muscle cells (Mandinova *et al.,* 1998). Localization of S100A4 (Mandinova *et al.,* 1998; Davies *et al.,* 1993b; Gibbs *et al.,* 1994), and of S100A1 to the cytoskeleton (Mandinova *et al.,* 1998) has been reported previously. These observations suggest that S100A1 and S100A4 might also be interacting inside the cell at these same locations.

The distribution of S100A1 and S100A4 proteins in normal cells is much more diverse. Although S100A1 was originally found in brain, where it interacts with S100B, it is also found in heart, slow twitch skeletal muscle, smooth muscle, and kidney (Zimmer *et al.,* 1995). In contrast, S100A4 is not found in significant quantities in brain, but it is distributed widely and specifically elsewhere in the body, including kidneys, lungs, thymus, and muscle tissues, at least in the rat (Gibbs *et al.,* 1995). The observation that S100A1 interacts with S100A4 as well as with S100B, but that S100B, but not S100A4 (Gibbs *et al.,* 1995), is found widely in brain tissue, raises the possibility that S100A1 has different S100 partners depending upon the S100 proteins that are expressed in the particular cells concerned.

Chapter Five

The effects of S100A1 on S100A4 activities *in vitro* and *in vivo*

5.1 Introduction

The homodimerisation and heterodimerisation of S100 proteins have been well documented. The first two S100 proteins identified were S100A1 homodimer and S100A1/S100B heterodimer. Further studies found that most S100 proteins exist in dimeric or multimeric states except calbindin D9k, which is always a monomer (Kordel, *et al.,* 1990). This has been proved for S100A1, S100A4, S100A6, S100A7, S100A8, S100A10, S100A11, S100P and S100B by nuclear magnetic resonance (NMR), X-ray crystallography or multiple anomalous wavelength dispersion (Donato 2001). Although S100A12 was shown in a hexameric form (Moroz *et al.,* 2002), dimeric states are more common at least *in vitro*. Some S100 proteins were also shown to form heterodimers, such as the S100A1/S100B, the S100A8/S100A9, the S100B/S100A6, the S100A1/S100A4, the S100B/S100A11, and the S100A1/S100P (Deloulme *et al.,* 2000b; Baudier & Gerard 1983; Bhardwaj *et al.,* 1992; Isobe, *et al.,* 1983).

Some S100 dimeric states seem to exist *in vivo*. S100A8/S100A9 heterodimer has been shown to be the prefered form within cells and was shown to be involved in inflammatory processes, fatty acid transportation and the metabolism of arachidonic acid in human neutrophils (Kerkhoff *et al.,* 1999; Roulin *et al.,* 1999; Kerkhoff *et al.,* 2001; Siegenthaler *et al.,* 1997; Kerkhoff *et al.,* 1998). S100B forms several heterodimeric forms although S100B2 homodimer is the prevalent form (Donato 1986; Drohat *et al.,* 1997). S100A1/S100B heterodimer was also detected in the serum of patients during cardiac surgery (Anderson *et al.,* 2001). Therefore, some cellular functions of S100A1 and S100B may be performed in the S100B/S100A1 heterodimer form, suggesting that heterodimerisations of S100 proteins do have some biological functions.

In Chapter 4, the interaction of S100A4 with S100A1, most probably heterodimerisation has been characterised. Evidence is also provided that S100A1 and S100A4 interact in yeast cells and co-expressed and co-localised in some breast cancer cells. Does the interaction have any biological functions? In this Chapter, the possible effects of S100A1 on some activities of S100A4 are investigated.

5.2 Results

5.2.1 S100A1 partially reverses the inhibitory effect of S100A4 on the phosphorylation of MHC-IIAF21

S100A4 was shown to have an inhibitory effect on the phosphorylation of MHC-IIAF21 by PKC in Chapter 3. To investigate the possible effect of S100A1 on S100A4, the two proteins were pre-incubated and the mixture was added into PKC phosphorylation reactions of MHC-IIA (Section 2.6.8). S100A4 has obvious inhibitory effect on MHC-IIAF21 phosphorylation reaction as shown in Chapter 3, while S100A1 has no obvious effect on the phosphorylation (Figure 5.1). If the two proteins were pre-incubated, the inhibitory effect of S100A4 on the phosphorylation was reduced (Figure 5.1) and the overall phosphorylation of MHC-IIAF21 was increased. However, S100A1 could not fully abolish the inhibitory effect of S100A4 on the PKC phosphorylation of MHC-IIAF21.

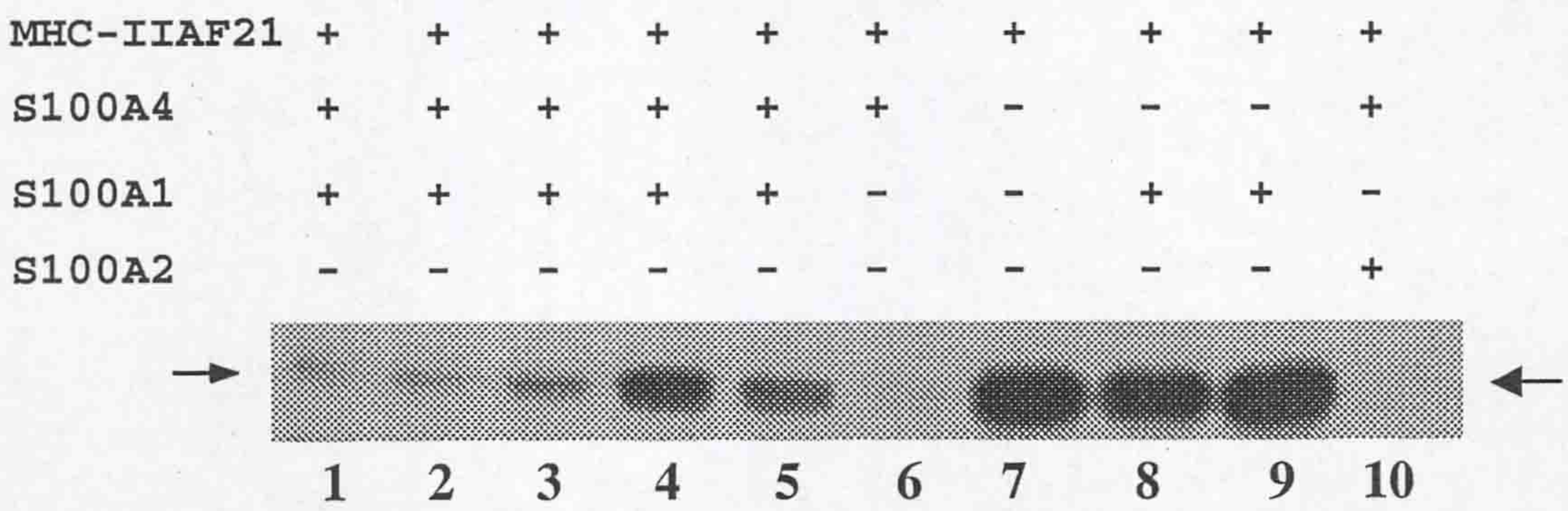

Figure 5.1. S100A1 partially reversed the inhibitory effect of S100A4 on the phosphorylation of MHC-IIAF21 by PKC. Five μM MHC-IIAF21 was used as the substrate for PKC in each reaction. In the experiment, S100 proteins were pre-incubated first and then the mixtures were incubated with MHC-IIAF21 prior to PKC phosphorylation reaction. *Lanes 1-6*, 5 μM S100A4 was pre-incubated overnight at 4°C in the presence of 0.5mM $CaCl_2$ with varying concentrations of S100A1, 0.1 μM (*lane1*), 0.3 μM (*lane 2*), 1 μM (*lane 3*), 3 μM (*lane 4*), 10 μM (*lane 5*), 0 μM (*lane 6*). *Lane 7*, MHC-IIAF21 only. *Lane 8*, 1 μM S100A1 and *lane 9*, 10 μM S100A1 were pre-incubated with MHC-IIAF21. *Lane 10*, 3 μM S100A2 was pre-incubated with S100A4 in the presence of 0.5 mM $CaCl_2$. The arrow indicates phosphorylated MHC-IIAF21.

5.2.2 S100A1 reverses the inhibitory effect of S100A4 on the sedimentation of MHC-IIAF21

In Chapter 3, S100A4 was shown to inhibit the self-assembly of MHC-IIAF21 in Ca^{2+}-dependent manner. To investigate effects of S100A1 on S100A4 in the sedimentation assay of MHC-IIAF21, 5 μM S100A4 was pre-incubated with varying concentrations of S100A1 ranging from 43 nM to 4.28 μM. The amount of MHC-IIAF21 in the supernatant of the sedimentation assay decreased with the increasing of S100A1 concentration and reached a low level at an S100A1 concentration of 4.28 μM, which is similar to that without S100A4 in the reaction. S100A1 itself (4.28μM) had no obvious effect on the self-assembly of MHC-IIAF21. However, S100A2 seems to co-operate with S100A4 to

enhance the inhibitory effect on the self-assembly of MHC-IIAF21 into a pelletable form.

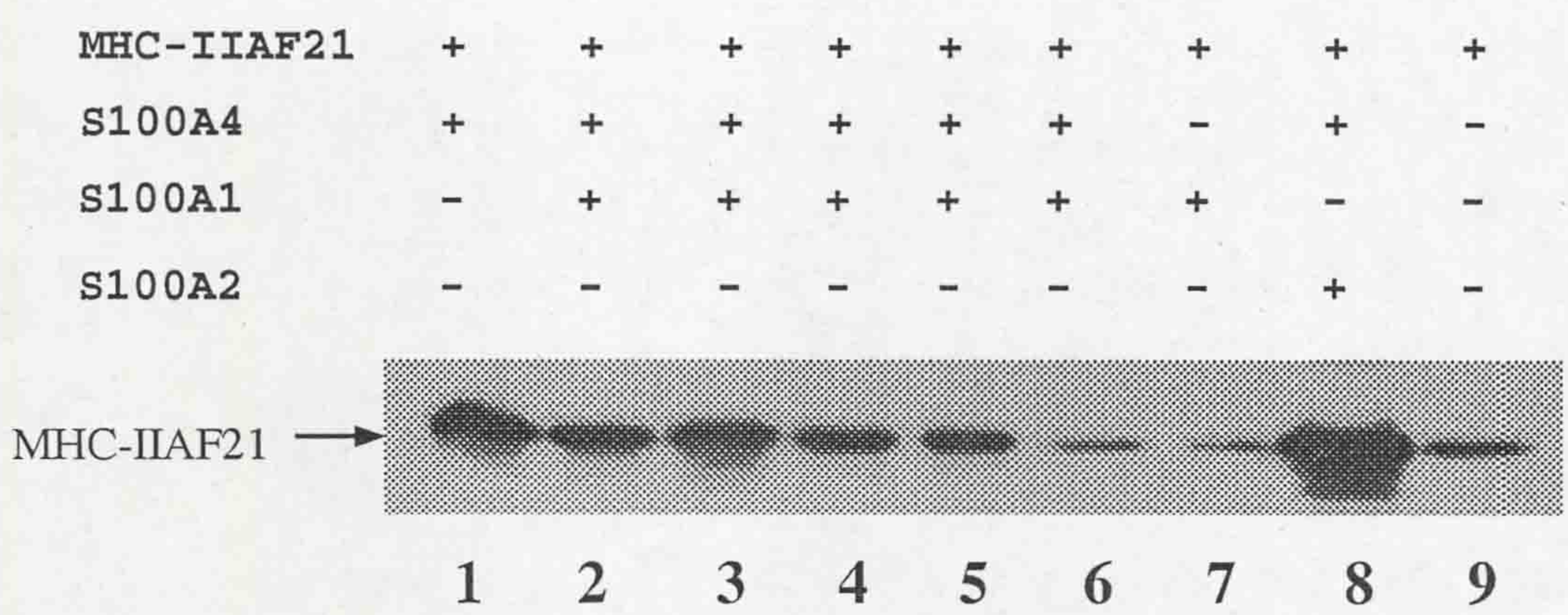

Figure 5.2 Effects of S100A4/S100A1 on the sedimentation of MHC-IIAF21. 5 μM of S100A4 was preincubated overnight at 4°C in the presence of 0.5mM Ca^{2+} with varying concentrations of S100A1, 0 μM (*lane 1*), 43nM (*lane 2*), 128nM (*lane 3*), 428nM (*lane 4*), 1.28 μM (*lane 5*), 4.28 μM (*lane 6*) or S100A2 (*lane 8*, 4,28 μM). Then 5μM MHC-IIAF21 were added to the mixture and incubated for another 8 h. Finally the mixtures were incubated in Bundling Buffer for a sedimentation assay (Section 2.6.9). Twenty μl of the resultant supernatant was analysed on SDS-PAGE. The MHC-IIAF21 retained in the supernatant was detected by Western blotting with anti-MHC-IIA antibody. *Lane 7*, 4.28 μM S100A1 was pre-incubated with 5 μM MHC-IIAF21 and S100A4 was omitted. *Lane 9*, 5 μM of MHC-IIA alone.

5.2.3 S100A1 reduced the motility and cloning formation of a high S100A4-containing rat mammary cell line

To investigate the possible effect of S100A1 on S100A4 *in vivo*, the expression of S100A1 was up-regulated in the rat mammary cell lines, Rama 37 and KP1-Rama 37, by transfection of an S100A1-encoding expression vector. The Rama 37 is a benign tumour cell line with very low level (undetectable by Northern or Western blotting) of S100A4 and S100A1. KP1-Rama 37 cell line was derived from the Rama 37 cell line by transfection of

S100A4. The KP1-Rama 37 cells were shown to have higher motility than its parental cell line, Rama 37 (Davies *et al.,* 1993) and to have metastatic ability when it was injected into syngeneic rats while the Rama 37 cell line does not. The increased motility and metastatic ability in KP1-Rama 37 cells is believed to arise from the up-regulation of S100A4 (Davies *et al.,* 1993a). S100A4 was also shown to positively correlate with the motility of mice cell lines isolated from a tumour of an S100A4 transgenic mouse strain (Jenkinson *et al.,* 2002). In this experiment, the effect of S100A1 on S100A4 induced cell motility was checked.

5.2.3.1 Construction of S100A1 expression construct

The S100A4 expressing plasmid, pCDNA4-S100A1, was constructed as follows. The PCR fragment of S100A1-coding sequence was ligated to the pCDNA4 vector at *Hind* III and *BamH*I sites and the pCDNA4-S100A1 expression vector was generated (Figure 5.3). The whole insert and the sequences around its junctions were sequenced.

A. **S100A1 coding sequence amplified by PCR**

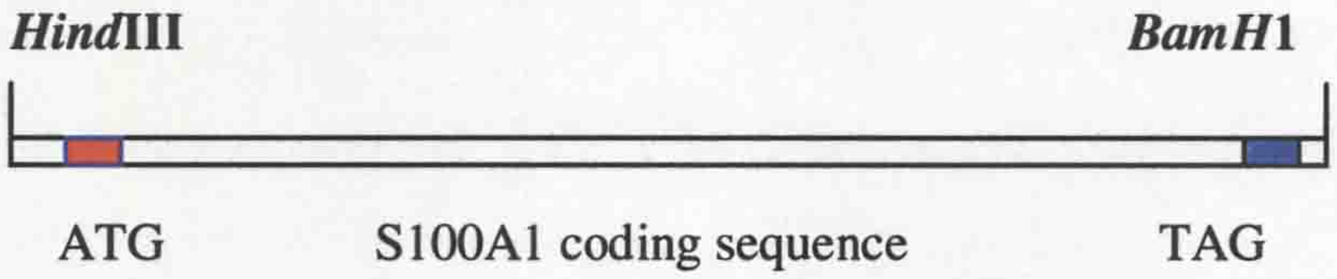

B. **Final construct of S100A1 expression vector, pCDNA4-S100A1**

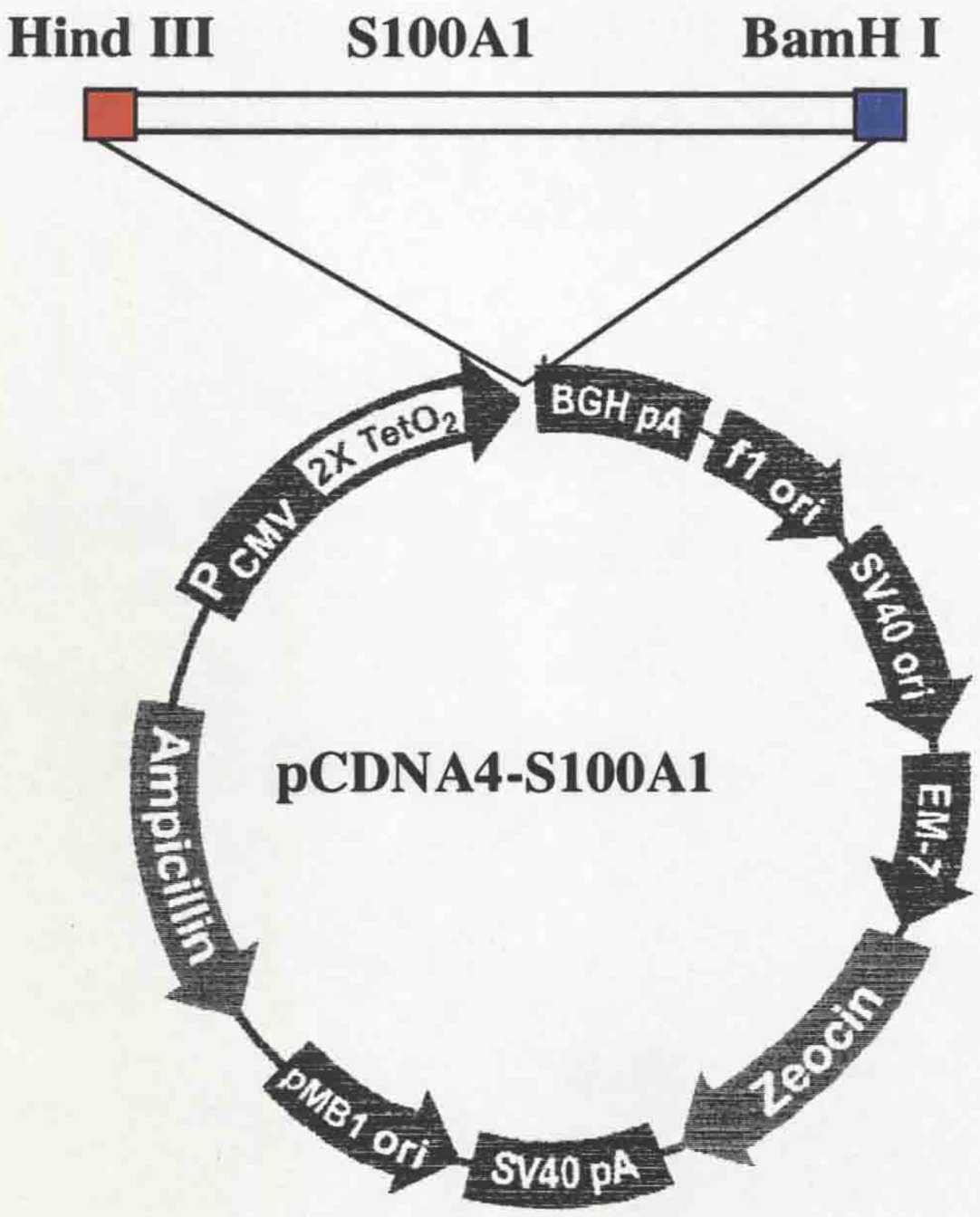

Figure 5.3 The diagram of the construction of pCDNA4-S100A1 expression vector. *Panel A*, the PCR product of S100A1 coding sequence flanking with restriction enzymes: 5' *Hind*III and 3' *BamH*I. *Panel B*, the final construct of pCDNA4-S100A1. The red block represents ATG, the translation start of S100A1 and the blue block represents the translation stop code of S100A1.

5.2.3.2 Transfection of Rama 37 and KP1-Rama 37 cells and selection of stable transfected cell lines

The pCDNA4-S100A1 and pCDNA4 (as a control plasmid) were first linearised with *Fsp* I restriction enzyme, which does not cut any of the expression cassettes in the constructs. The Rama 37 cells and KP1-Rama 37 cells were transfected with linearised pCDNA4-S100A1 or pCDNA4, using lipofectamine (Gibco) as described in Section 2.8.5. The cells were then grown under selection with 750μg/ml Zeocin (Invitrogen) for 4 weeks. The Zeocin resistant clones transfected with pCDNA4-S100A1 were isolated and cultured. The Zeocin-resistant clones transfected with pCDNA4 control plasmid were pooled. Total RNA was extracted from the cells derived from each individual clone as described in Section 2.3.13.

To detect the expression of genes delivered by transfection in isolated clones, 10 μg of the extracted RNA were analysed by Northern blotting as described in Section 2.3.16. Some transfected cell lines were chosen according to the similar mRNA levels of S100A1 and S100A4, which were normalised by the mRNA levels of beta-actin (Figure 5.4). One clone selected from transfected KP1-Rama 37 cells (KT6), has a high and similar level of S100A1 mRNA and S100A4 mRNA. One clone isolated from transfected Rama 37 cells (RT4) has a similar level of S100A1 mRNA to that of KT6. Both the parental cell lines and the cells transfected with pCDNA4 vector (Rama 37V and KP1V) have an undetectable level of S100A1 mRNA (Figure 5.4).

S100A4 mRNA levels in the selected clones and in parental cell lines were checked by Northern blotting. In Rama 37 cells, RT4 and Rama 37V cells, S100A4 mRNA is undetectable. In KP1-Rama 37 cells, KT6 and KP1V cells, high levels of S100A4 mRNA were detected. The transfected cells were then passaged 7 times without Zeocin selection and the S100A1 and S100A4 levels did not change through the passaging (data not shown). This indicated that these selected clones have stable levels of S100A1 and S100A4.

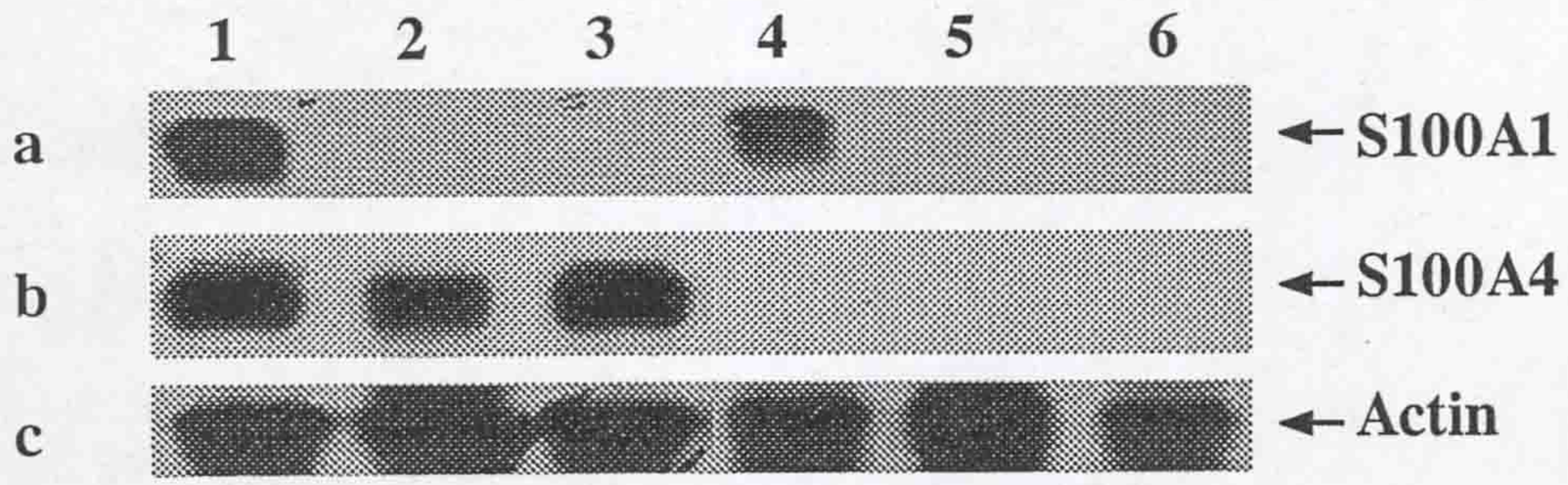

Figure 5.4. Northern blotting analysis of S100A1 and S100A4 transfected cell lines. Ten μg of total RNA extracted from parental and transfected cell lines were analysed by Northern blotting with ^{32}P dCTP-labelled probes. *Panel a*, filter incubated with S100A1 probe; *panel b*, filter incubated with S100A4 probe; *panel c*, filter incubated with beta-actin probe. RNA extracted from KT6 (*Lane 1*), RNA extracted from KP1V (*lane 2*, KP1-Rama 37 cells transfected with pCDNA4 control plasmid), KP1-Rama37 cells (*lane 3*), RNA isolated from RT4 (*lane 4*), RNA extracted from Rama37V (*lane 5*, Rama 37 cells transfected with pCDNA4 control vector) and RNA extracted from Rama 37 cells (*lane 6*).

To detect the levels of S100A1 and S100A4 proteins, Western blotting was carried out (Figure 5.5). The results show that S100A4 is present in the KP1 cell line and its derivatives. S100A1 is expressed in S100A1expression plasmid transfected cell lines, RT4 and KT6. S100A4 levels are very similar in all S100A4 expressing cell lines. S100A1 levels are also very similar in the two S100A1 expressing cell lines.

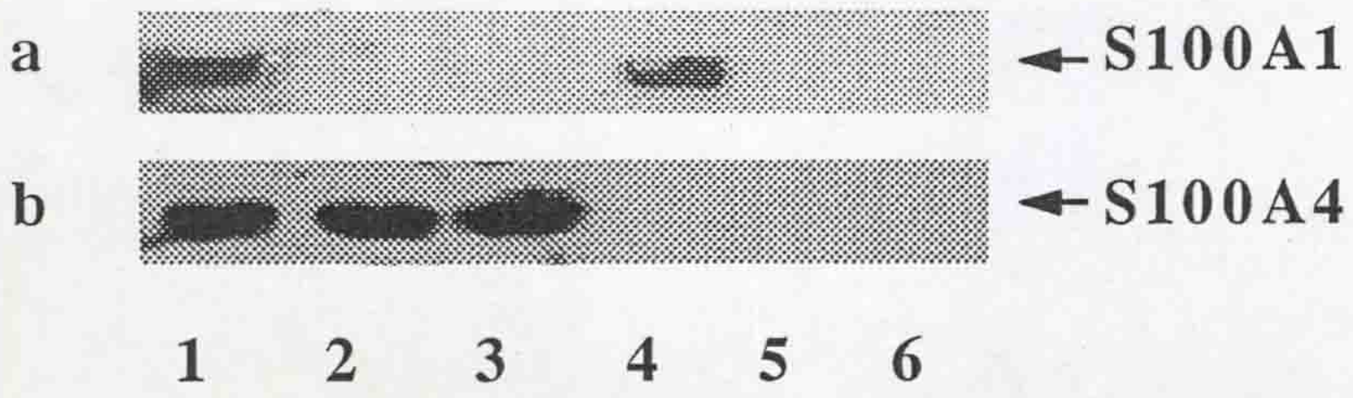

Figure 5.5 Detection of S100A1 and S100A4 proteins in parental and S100A1 expression plasmid transfected cell lines using Western blotting. Forty μg of total protein from each cell lysate was analysed on a 15% SDS-PAGE. The mouse anti-human S100A1 monoclonal antibody (DAKO) and rabbit anti-human S100A4 polyclonal antibody (DAKO) were used to detect S100A1 (*panel a*) and S100A4 (*panel b*) respectively. *Lanes1-6*, cell lysates from cell lines: KT6 (*lane 1*); KP1V (*lane 2*); KP1-Rama37 cells (*lane 3*); RT4 (*lane 4*); Rama37V (*lane 5*); Rama 37 cells (*lane 6*).

As the Western blotting only checks the total amount of S100A1 and S100A4 proteins in a given number of cells, it does not show the proportion of cells expressing the proteins in the cell population. To check whether the S100A4 and S100A1 are uniformly expressed in each cell line, immunofluorescent staining was carried out. The results showed that S100A1 and S100A4 are uniformly expressed in all the S100A4 or S100A1 expression cell lines (Figure 5.6). In the Rama 37 cells, neither S100A1 nor S100A4 was detected. In the KP1 Rama 37 cells, no S100A1 was detected while S100A4 was detected in all the cells examined. In the RT4 cells, no S100A4 was detected while S100A1 was detected in all the cells examined. In the KT6 cells, all the cells examined expressed both S100A1 and S100A4. However, only about 90% of the cells examined expressed both S100A1 and S100A4 at similar levels, about 5% expressed more S100A1 than S100A4 and about 5% expressed more S100A4 than S100A1. This was determined by the colour of superimposed image (Figure 5.6 column 3) of each cell examined (200 cells in total were examined), yellow colour indicates similar amounts of S100A1 and S100A4, green colour indicates more S100A1 than S100A4, and red colour indicates more S100A4 than S100A1.

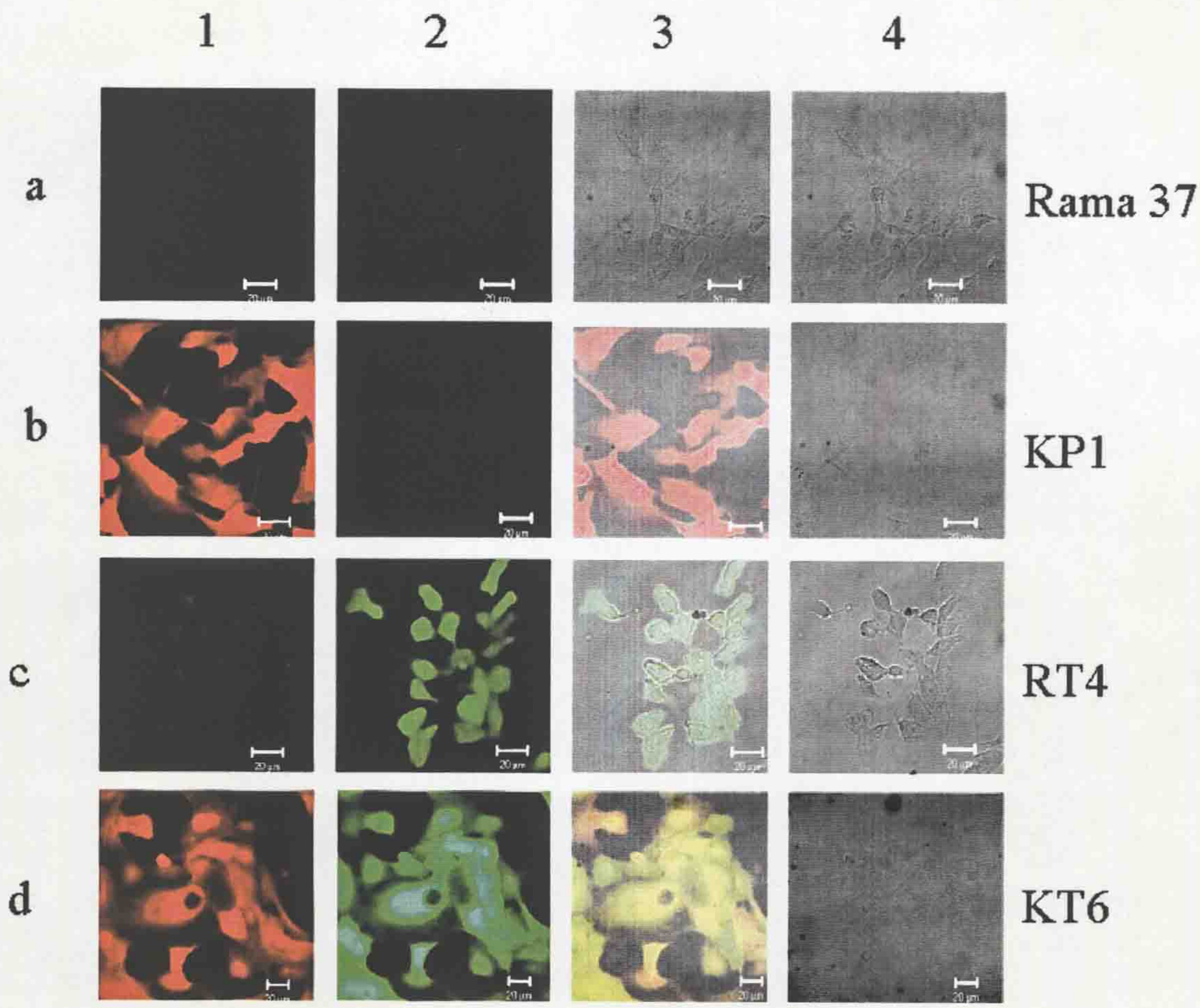

Figure 5.6. Immunofluorecent staining of S100A1 and S100A4 in parental and transfected cell lines. The same primary antibodies as those used in Western blotting were mixed and incubated overnight with paraformadehyde fixed cells at 4°C. After washing, two secondary antibodies, FITC-conjugated goat anti-rabbit IgG to detect rabbit anti-S100A4 and Texas Red conjugated goat anti-mouse IgG to detect mouse anti-S100A1, were mixed and incubated with the cells for 1h at room temperature. The images were captured with a confocal microscope with excitation wavelength, 488 nm for FITC and 543nm for Texas RED. *Column 1* is image from the staining of anti-S100A4 antibody and *column 2* is the image from the staining of anti-S100A1 antibody. *Column 3* is the superimposed images of *column 1* and 2 of each cell line. *Column 4* is the phase construct.

At higher magnification, the immunofluorescence experiments also show that S100A1 and S100A4 were co-localised mainly in the perinuclear region and small amounts of the proteins co-localisation on the cell surface of the KT6 cell too (Figure 5.7).

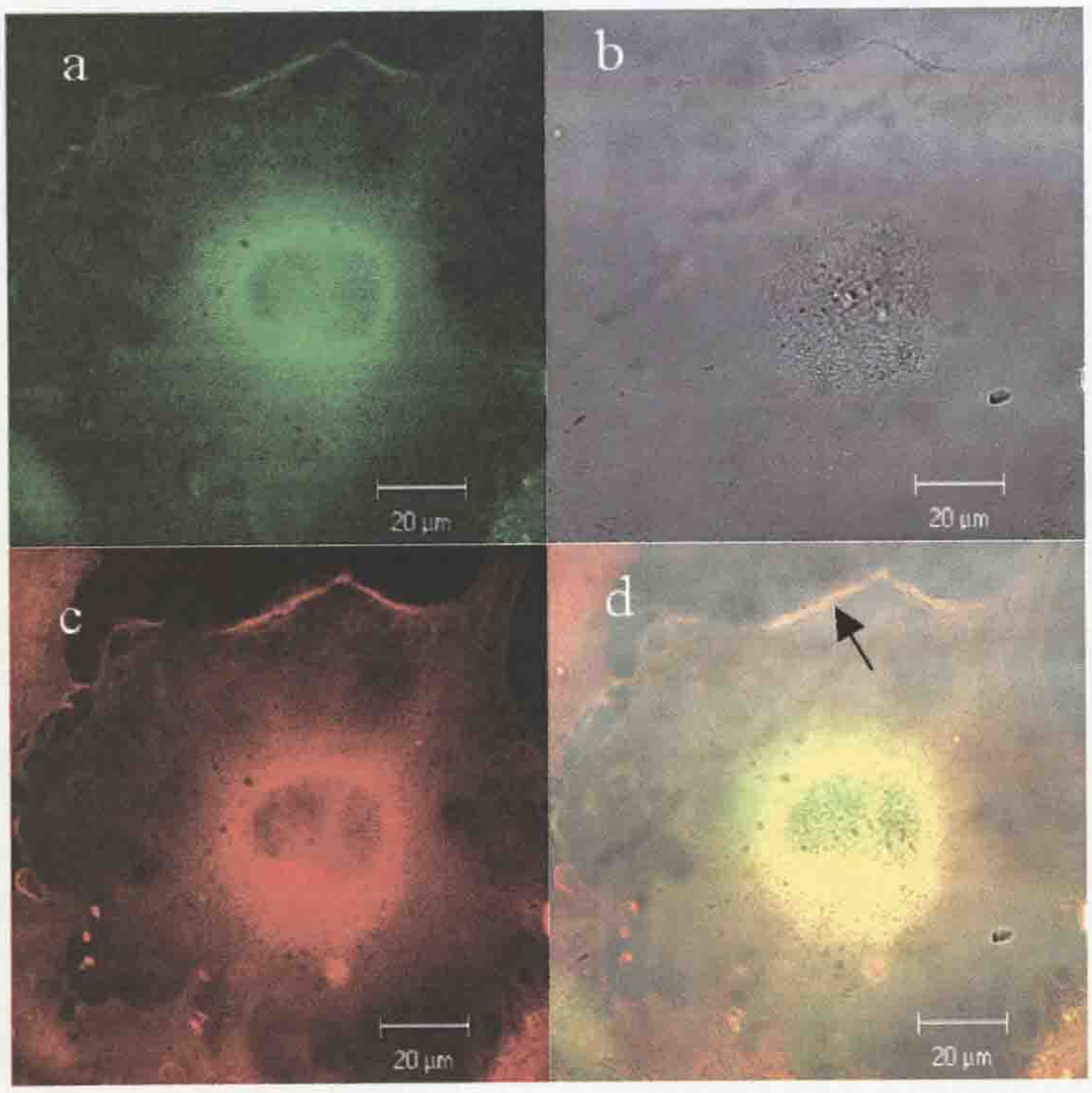

Figure 5.7 The co-localisation of S100A1 and S100A4 in a KT6 cell revealed by immunofluorescent staining. The experimental conditions were exactly the same as those in Figure 5.6. *Panels a-d* are same field. *Panel a* is the image from the staining of anti-S100A1, *panel b* is the phase contrast. *Panel c* is the images from the staining of anti-S100A4. *Panel d* is the superimposed image of a and c. Arrow indicates the co-localisation of S100A1 and S100A4 in the cell membrane.

5.2.3.3 Over expression of S100A4, but not S100A1, increased the motility and cloning formation ability of Rama 37 cells

The cell motility assay with the Boyden Chamber has been widely used. The conditions for testing the motility of the Rama 37 cells were also fully characterised in this lab (Jenkinsson *et al.*, unpublished data). Therefore, the method was chosen to measure the motilities of these S100A4

and S100A1 transfected cell lines. The results show that KP1-Rama 37 cell line is more motile than its parental cell line, Rama 37($p<0.05$), while the RT4 cell line (Rama 37 cell line transfected with S100A1 expression plasmid) has similar motility rate to that of Rama 37 cells (Table 5.1). This suggests that a high level of S100A4 was able to promote cell motility, while the high level of S100A1 did not affect the motility of Rama 37 cells (Table 5.1).

The cloning formation ability in soft agar of the transfected cells and their parental cells were also examined. The Rama 37 cells and S100A1 transfected Rama 37 cells, RT4, grew poorly in soft agar assay (Table 5.1). However, KP1-Rama 37 cells have shown much stronger ability to grow in soft agar than that of its parental cells, Rama 37. This result suggests that up-regulation of S100A4 promotes the anchorage-independent growth of Rama 37 cells.

5.2.3.4 Up-regulation of S100A1 reduced the motility and cloning formation ability of KP1-Rama 37 cells but not Rama 37 cells

Cells (KT6) expressing S100A1 in addition to S100A4 had a lower motility rate than the cells (KP1 Rama 37 or KP1V) expressing S100A4 alone ($P<0.001$) (Table 5.1), suggesting that up-regulated S100A1 could reduce the cell motility induced by up-regulated S100A4 in Rama 37 cells.

The KT6 cells, expressing both S100A1 and S100A4, also showed lower ability to grow in soft agar than the cells, KP1-Rama 37 or KP1V, expressing S100A4 alone ($p< 0.05$) (Table 5.1). This suggests that up-regulation of S100A1 may interact with S100A4 and reduce the ability of anchorage-independent growth promoted by S100A4.

Table 5.1 Cell motility and soft agar assays

Cell lines	S100A1 mRNA[a]	S100A4 mRNA[b]	Motility X±SD (%) [c]	Cloning formation Per microscope field[d]
Rama 37	-	-	15.8±1.0	0[i]
Rama 37V	-	-	16.0±1.7[e]	0[i]
RT4	+	-	15.6±1.0[e]	0[i]
KP1-Rama 37	-	+	19.5±0.7[f]	9.2±3.0[j]
KP1V	-	+	18.6±2.1[g]	8.7±2.9[k]
KT6	+	+	9.4±1.6[h]	2.1±1.5[l]

a. and b . S100A1/S100A4 mRNA level was detected by Northern blotting and normalised with beta-actin.
   - indicates that no mRNA was detected.
   + indicates that a strong signal of mRNA was detected.

c. Motility assay using the Boyden Chamber. Each cell line was subjected to at least 3 independent experiments. Motility is the mean percentage of cells that moved through the filter in a period of 20 h against the total number of cells seeded in a 24 well plate and cultured in the same medium and under same conditions as that used in the upper Chamber (Section 2.8.8). The mean% ±standard deviation (SD) are shown.

d. The cloning formation in soft agar. 2 x 10^4 cells were seeded in a 35mm culture dish. Each cell line was subjected to at least 3 independent experiments. After 4 weeks of routine culture, clones with diameter larger than 0.06mm were counted under microscope. Clone formation efficiency is the mean± standard deviation (SD) is shown in this column.

e. No significant differences (Non-paired *t* test) were shown between the transfected cell lines and their parental cell line, Rama 37.

f. KP1-Rama 37 cell line shows significantly higher motile ability than that of its parental cell line, Rama 37 ($p<0.05$) (Non-paired *t* test).

g. The KP1V cell line is not significantly different from KP1-Rama 37 cell line ($p>0.05$) (Non-paired *t* test).

h. KT6 cell line shows statistically-significantly lower motility than KP1-Rama 37 cell line ($p<0.001$), Rama 37 ($p<0.001$) and RT4 ($p<0.001$) (Non-paired *t* test).

i. These cell lines did not form clones in soft agar.

j. KP1 Rama 37 cell line formed more clones in soft agar than KT6 cells ($p<0.001$) (Non-paired *t* test).

k. KP1V formed similar number of clones in soft agar assay to that of its parental cell line, KP1-Rama 37 and there is no significance in statistical analysis (Non-paired *t* test).

l. KT6 cells also formed clones in soft agar but the number of the clones is statistically less than that of KP1 Rama 37 cells ($p<0.001$) (Non-paired *t* test).

5.3 Discussion

In the experiments *in vitro*, the inhibitory effects of S100A4 on both PKC phosphorylation and self-assembly of MHC-IIA were greatly reduced if the S100A4 was pre-incubated with S100A1. S100A1 itself showed no obvious effects on either PKC phosphorylation or the self-assembly of MHC-IIA. As the S100A1 showed no obvious binding to immobilised MHC-IIA in a biosensor assay (data not shown), the *in vitro* effect of S100A1 is unlikely to be due to the competition of the binding sites on MHC-IIA with S100A4. From a previous study, recombinant S100A1 and S100A4 proteins were shown to form a heterodimer in solution (Tarabykina *et al.*, 2000). The biosensor assay in this Chapter also showed that S100A4 binds to the immobilised S100A1 in the manner of monomer-monomer interaction, suggesting the effects of S100A1 on S100A4 in the *in vitro* experiments resulted from S100A1 and S100A4 heterodimerisation.

In the experiments *in vivo*, up-regulation of S100A1 in the KP1-Rama 37 cells, a cell line with S100A4 up-regulated, showed inhibitory effects on the motility and cloning formation abilities of the cells. However, up-regulation of S100A1 in the Rama 37 cells, a cell line with undetectable S100A4, showed no effect on the motility and cloning formation of the cells. The results suggest that S100A1 may exert its effect through direct interaction with S100A4 in these rat breast cell lines.

The reason for using the Rama 37 and KP1-Rama 37 cell lines in the experiments is that the Rama 37/KP1 cell system has been well characterised both *in vitro* and *in vivo* in this laboratory (Davies *et al.*, 1993a). The Rama 37 cell line is a near-diploid, genetically stable epithelial cell line, which has been derived from a benign 7,12-dimethylbenz-2[a]anthracene-induced rat mammary tumour (Dunnington *et al.*,., 1983). This cell line produces benign, non-metastatic encapsulated tumours when injected into the mammary fat pads of its syngeneic rat host (Dunnington *et al.*, 1983). KP1 Rama 37 cell line is one of the cell lines derived from Rama 37 by transfection with S100A4 and selected through the rat breast cancer model. KP1-Rama 37 cells have gained the metastatic

ability.

mRNAs and proteins of S100A1 and S100A4 could not be detected by Northern and Western blotting in the Rama 37 cell line. In the KP1-Rama 37 cell line, S100A1 is undetectable by Western blotting, but a high level of S100A4 can be detected. Therefore the two cell lines are suitable for the up-regulation of S100A1 by transfection. The new cell lines isolated after transfection with pCDNA4-S100A1 or empty vector pCDNA4 , RT4, KT6, Rama37V, and KP1V have very similar growth rates to their parental cell lines (data not shown). S100A1 is stably expressed in transfected cell lines, RT4 and KT6. S100A4 is stably expressed in KP1-Rama 37 and its derivatives, KT6 and KP1V. Moreover, no endogenous S100A4 was detected in RT4 and Rama37V and no endogenous S100A1 was detected in KP1V through 6-10 passages after transfection. Therefore, the cell lines are reliable for further analysis.

The motility assays were carried out with the Boyden Chamber system (Albini *et al.*, 1987). In this system, the percentage of the cells migrating from upper-chamber to the lower side of the membrane or the lower compartment in a given time period represents the ability of the cells to migrate. The Rama 37 cells were shown to be very motile (Rudland unpublished data). However, the KP1-Rama 37 cells were shown to be statistically significantly more motile than its parental cell line, Rama 37. The increased motility of KP1-Rama 37 cells was linked to the increased expression of S100A4 in the transfected cell line. The results are consistent with previous studies using fibroblasts. Transfectants expressing large amounts of the S100A4 protein showed significantly higher cell motility than their parental cells, src 3Y1-H, a normal rat fibroblast (Takenaga *et al.*, 1994a). The expression of S100A4 was also correlated with motile and invasive abilities in various clones derived from Lewis lung carcinoma (Takenaga *et al.*, 1994a). These results suggest that the S100A4 protein plays a role in regulating cell motility and tumour cell invasiveness. CSML0 cells, a nonmetastatic mouse mammary adenocarcinoma cell line, transfected with S100A4 were assessed in *in vitro* motility and invasion assays, as well as in *in vivo* metastasis assays. Cell lines expressing S100A4 displayed an altered morphology as well as increased motility in

modified Boyden chemotaxis chambers (Ford *et al.*, 1995). However, no significant increase in *in vitro* invasion or in *in vivo* metastasis was observed, suggesting that the presence of S100A4 may be important for metastasis by increasing motility, but may not be sufficient for invasion *in vitro* or metastasis *in vivo* (Ford *et al.*, 1995), a view supported by results of Jenkinson (unpublished data).

In the present experiments, the Rama 37 cells transfected with S100A1 showed no obvious change in cell motility compared to untransfected R37 cells although the S100A1 level in the cells was up-regulated to a similar level to that of S100A4 in KP1-Rama 37 cells. However, up-regulated S100A1 in KP1-Rama 37 cells to the similar level to S100A4 dramatically reduced the cell motility in the Boyden chamber assay. The effect of S100A1 on the motility of KP1-Rama 37 cells could be partly the result of heterodimerisation of S100A1 and S100A4 in the cells. However, the heterodimerisation could not explain the result that the motility rate of KT6 is significantly lower than that of Rama 37. Therefore, some unknown effects may contribute to the reduction of the motility rate in KT6 cells where both S100A1 and S100A4 were up-regulated.

In the soft agar assay, Rama 37 cells did not form clones in our experimental conditions. However, the KP1-Rama 37 did form clones in soft agar, indicating that the KP1-Rama 37 cells gained the ability of anchorage-independent growth. This ability is most likely correlated to the higher level of S100A4 expression, suggesting that S100A4 may have the ability to promote the anchorage independent growth of cells. S100A4 was shown to be a metastasis-promoting gene but this is the first time its effect on the anchorage-independent growth has been shown. In contrast, the Rama 37 cells with S100A1 up-regulated did not gain the ability of anchorage independent growth. The KP1-Rama 37 cells with S100A1 up-regulated by transfection significantly reduced their anchorage-independent growth activity, which may result from the antagonism of S100A1 to S100A4 possibly through direct interaction in the cells. The results suggest that S100A1 might effectively reduce any S100A4-induced anchorage-independent growth activity *in vivo*.

The soft agar assay is also used to estimate the changes of cell malignancy as the non-malignant cell growth is prevented by the semisolid medium. The ability of cells to grow in the semi-solid medium is the ability of anchorage-independent growth where cancer cells need to survive without cell-substratum interaction. It was reported that the highly metastatic cell lines showed a high anchorage-independent growth (Nakanishi *et al.*, 2002). In the multistep process of metastasis, anchorage-independent growth might be important. Other metastasis inducing or related gene products, such as metastasis-associated gene 1 (MTA1), can enhance anchorage-independent growth (Mahoney *et al.*, 2002) whereas tumour suppressor genes such as p53 suppress anchorage-independent growth (Rauth *et al.*, 1998). S100A1 was shown to reduce both S100A4 induced cell motility and anchorage-independent growth, which are two major factors relating to tumour metastasis, it is thus possible that S100A1 may have the ability to reduce S100A4-induced metastasis.

So far, the experiments discussed above have shown that S100A1 has antagonistic effects on the activities of S100A4 both *in vitro* and *in vivo*. The effects most probably result from their direct interaction although this has yet to be proven. The interaction of S100A1 and S100A4 *in vivo* was first shown in the yeast two-hybrid system (Wang *et al.*, 2000; Tarabykina *et al.*, 2000). S100A4 was also shown to be more likely to form a heterodimer with S100A1 than an S100A4 homodimer in the yeast two-hybrid system (Chapter 4). In this Chapter, S100A1 was shown to co-localise with S100A4 in KT6 cells, a mammalian cell line. Therefore, the heterodimerisation of S100A1 and S100A4 may occur in the KT6 cells but there is no direct evidence for this at present. Fluorescence resonance energy transfer (FRET) may provide more direct evidence of interaction in the mammalian cells and this work will be done in the near future.

If the interaction which occurred *in vitro* and *in vivo* is heterodimerisation, the results from the experiments *in vitro* and *in vivo* indicate that the S100A1/S100A4 heterodimer might function differently from an S100A4 homodimer. Up-regulated S100A1 could greatly reduce the S100A4 homodimer in KT6 cells and decrease the cell motility and

anchorage-independent growth induced by S100A4. Since S100A1 has many other interacting partners, up-regulation of S100A1 in the cells may also have effects on other S100A1 target proteins and cause other changes in the cells. Therefore further investigation will need to be carried out in order to understand fully the relationship between S100 proteins and tumour metastasis.

Although S100A1 and S100A4 were shown to co-exist in some human breast cancer cell lines, such as MDA-MB-231, SKBR3 and MCF-7, the levels of S100A4 in these cell lines were much higher than that of S100A1. The effect of S100A1 on S100A4 could be unnoticeable. When the S100A1 was up-regulated to the level similar to that of S100A4 in KP1-Rama 37 cells, the effects of S100A1 on S100A4 became obvious, suggesting a balance model between S100 proteins. The possible heterodimerisation of S100A1 and S100A4 may serve as a regulatory mechanism in balancing the effects of one S100 protein by another.

Chapter Six

General discussion and future works

This thesis has examined interactions of S100A4 with three potential protein targets *in vitro* and *in vivo*. A comparative study on the interactions of S100A4 with MHC-IIA and MHC-IIB as well as the resultant effects has been carried out. A new interacting partner of S100A4, S100A1, has been discovered by yeast two-hybrid screening and its effects on the activities of S100A4 *in vitro* and *in vivo* have also been investigated.

The interaction of S100A4 with myosin A heavy chains has been studied in some detail previously (Kriajevska *et al.*, 1994, Ford *et al.*, 1997) and it is thus known that S100A4 binds to MHC-IIA and shows inhibitory effects on its phosphorylation and self-assembly *in vitro* (Kriajevska, et al 1998; Murakami et al 2000). However, this thesis reports the first detailed examination of MHC-IIB as a target of S100A4. Although, MHC-IIA and MHC-IIB are very closely related isoforms, their binding affinities for S100A4 and resultant effects are quite different. The Kd for S100A4 and MHC-IIA is about 10 times lower than that for S100A4 and MHC-IIB. The inhibitory effects on the phosphorylation of MHC-IIB could only occur when a much higher concentration of S100A4 was used than that for MHC-IIA. S100A4 inhibits the sedimentation of MHC-IIA but not of MHC-IIB. These results indicate that the effects of S100A4 on MHC-IIA are different from those on MHC-IIB *in vitro*. It is possible that these effects might reflect to some extent some differences in biological function between the MHC isoforms in *vivo*.

Non-muscle myosins were shown to be important in cell motility, cell morphology and cell division (Bresnick 1999). Much less is known about the function of individual MHC isoforms. From previous studies, it is known that the biology of MHC-IIA and MHC-IIB is different in several respects. In most cell types, myosin-IIA and myosin-IIB co-localise to perinuclear stress fibers, but in cortical regions, the two isoforms exhibit cell specific

differences in their patterns of localization. MHC-IIA is preferentially located towards the leading edge of migrating cells when compared with MHC-IIB by double immunofluorescence staining (Kolega 1998) while the MHC-IIB is enriched in structures at the cells' trailing edges in neurons (Cheng *et al.*, 1992). Time-lapse imaging of injected fluorescently labelled MHC-IIA and MHC-IIB in bovine aortic endothelial cells revealed differences in the rates at which the two isoforms rearranged during cell movement. MHC-IIA appears in newly formed structures more rapidly than the MHC-IIB and is also lost more rapidly when structures disassembled (Kolega 1998). The maximal actin-activated ATPase activity of non-muscle myosin-IIA is 2.6-fold greater than that of non-muscle myosin-IIB, and the velocity of actin filaments moved by non-muscle myosin-IIA is 3.4-fold faster than those observed with non-muscle myosin-IIB (Kelley *et al.*, 1996). These observations indicate differences in both distributions and kinetic properties of the two isoforms. Notwithstanding, the differential effects of S100A4 on MHC-IIA and IIB may have diverse biological functions if the interactions occur *in vivo*. High levels of S100A4 in cancer cells may interact with both MHC-IIA and MHC-IIB and the overall outcome might affect the patterns of cytoskeletal dynamics and favour cell motility, invasion, anchorage-independent growth and tumour metastasis in these cancer cells.

Interestingly, MHC-IIB has been proposed to have a tumour suppressor effect (Yam et al 2001). Down-regulation of MHC-IIB but not MHC-IIA was found in rat 6 embryo fibroblast cells transfected with a temperature-sensitive mutant $p53^{val135}$, an inactivating mutant for normal p53 function. The down-regulation of MHC-IIB was also found in the rat 6 cells transfected with c-H-ras or v-myc oncogenes but not in the mouse SVT2 cells expressing a high level of the normal p53 gene (Yam et al 1999). The overexpression of transfected MHC-IIB but not MHC-IIA was shown to be very effective in suppressing the anchorage-independent growth in soft agar assay and the tumourigenicity of the T2 cells, (a transformed cell line isolated from rat 6 embryo fibroblast cell line transfected with mutant $p53^{val135}$), when tested in nude mice (Yam et al 2001), raising the possibility that MHC-IIB has a tumour suppressor function. It is not yet known whether the anchorage-independent

growth-promoting capability of S100A4 in KP1 Rama 37 cells has any relationship with its effect on MHC-IIB. However, interruption of the function of MHC-IIB by a high level of S100A4 might be more important in promoting tumour progression than that of MHC-IIA.

As outlined before, both MHC-IIA and MHC-IIB can be phosphorylated by PKC *in vitro*. *In vivo*, following treatment with phorbol esters, MHC-IIA is also phosphorylated on the PKC site at Serine-1917 in human T lymphocytes (Moussavi *et al.*, 1993), platelets (Kawamoto *et al.*, 1989) and rat basophilic leukaemia cells (Ludowyke *et al.*, 1989). There are presently no published reports showing that MHC-IIB is phosphorylated by PKC in *vivo*. In this work, S100A4 was shown to bind to MHC-IIB and to inhibit its phosphorylation by PKC but not to affect its self-assembly *in vitro*. It is not known whether S100A4 binds to MHC-IIB *in vivo* and what is the outcome if they do interact with each other in cells.

To investigate the interaction *in vivo*, the yeast two-hybrid system was used. However, the interactions of S100A4 with MHC-IIA and IIB were not detected although the self-associations of MHC-IIA, MHC-IIB and S100A4 were detected in the yeast two-hybrid system. One reason for the failure to detect the calcium-dependent interaction between S100A4 and MHC could be the low level of Ca^{2+} in yeast, which only support the calcium-independent interactions, such as S100A4 homodimerisation and S100A4/S100A1 heterodimerisation, and cannot support the Ca^{2+}-dependent interactions, such as the interaction of S100A4 with MHC-IIA. Further evidence supporting this argument is that the calcium-dependent interaction of S100A4 with p53, which was revealed by some experiments *in vitro* (Grigorian et al 2001), also cannot be detected in the yeast two-hybrid system (data not shown). Therefore, a calcium-sensitive two-hybrid system needs to be developed in future to identify and test the Ca^{2+} dependent interactions. Although a suitable yeast strain was identified, further extensive work to develop the system was outside the scope of the present work. In addition, some available techniques, such as the mammalian two-hybrid system or FRET as discussed in Chapter 3 might be usefully employed to overcome the limitation of the present yeast two-hybrid system.

At present, it is difficult to evaluate any role of S100A4 on the activities of MHC isoforms *in vivo*, based on existing knowledge of non-muscle myosin isoforms. Once S100A4 interaction with MHC isoforms *in vivo* has been shown, up-regulation of S100A4 or MHC isoforms *in vivo* might provide a means to probe the effects of S100A4 on cell activities like motility and division. Further investigation on the regulatory effects of S100A4 on non-muscle myosins *in vivo* will need to be carried out in future.

More importantly, work carried out for this thesis led to the first identification of an interaction with S100A1 (Wang *et al.*, 2000). This observation was confirmed shortly afterwards (Tarabykina *et al.*, 2000). These results have been extended in this thesis to show that S100A1 affects some activities of S100A4 both *in vitro* and *in vivo*. . S100A1 has been known to be an important molecule in regulating cytoskeletal fibres, including microtubules, type III intermediate filament and actin (Garbuglia et al 1999). S100A1 is mainly expressed in muscle cells and neurones. In the present study, a low level of expression of S100A1 can be detected in some breast tumour cell lines, such as MDA-MB-231, which express high levels of S100A4. S100A4 and S100A1 are also found to co-localise mainly in the perinuclear region but also in stress fibres and near the cell surface in MDA-MB-231 cells and in the S100A1 transfected rat mammary cell line, RT6. In the yeast two-hybrid assay, the relative binding strength indicated by the ability to activate reporter gene transcription seems stronger for the interaction of S100A4 with S100A1 than that for S100A4 self-assembly. In biosensor assays, the binding affinity of S100A4 to immobilised S100A1 is similar to, at least not lower than, the affinity of S100A4 to immobilised S100A4. Moreover, the interactions of S100A4 with S100A1 and with itself are not Ca^{2+}-dependent although these interactions can be enhanced by high Ca^{2+} concentrations. Therefore, these interactions are very likely to occur in some mammalian cells, such as human muscle cells expressing high level of S100A1 and S100A4 (Engelkamp *et al.*, 1992) and the high-S100A4-expressing breast carcinoma cell line, MDA-MB-231 cells as outlined above. The data from biosensor assays support a model of monomer-monomer interaction of both S100A4/S100A4 and S100A1/S100A4. From the

point mutation analysis in the yeast two-hybrid system, the residues, which are important for homodimerisation of S100A1 or S100A4 are also important for the interaction of S100A1 with S100A4, suggesting that the structural elements associated with the interaction of S100A1 with S100A4 are very similar to those of S100A4/S100A4 or S100A1/S100A1 dimerisation The involvement of similar residues indicates that S100A1 might compete with S100A4 for interaction with S100A4 molecule and affect the dimerisation of S100A4. Therefore, this observation may provide an explanation for the effect of S100A1 on S100A4 activities.

In the experiments *in vitro*, S100A1 can reduce the inhibitory effect of S100A4 on both the self-assembly of and PKC-dependent phosphorylation of MHC-IIA. A high level of S100A1 in high S100A4-expressing KP1-Rama 37 cells reduced both cell motility and the capability for anchorage-independent growth, indicating that S100A1 is able to modulate the activities of S100A4, both *in vitro* and *in vivo* and suggesting a possibility that S100A1 might inhibit S100A4-induced metastasis. To clarify this important latter point, experiments to check the possible effect of S100A1 on S100A4 induced metastasis in our rat breast cancer model are presently being carried out.

The evidence presented in this thesis demonstrates that S100A1 can antagonise some activities induced by S100A4. The effects of S100A1 on S100A4 may result from the direct interaction of the two proteins, probably, but not certainly, as heterodimers. Although heterodimerisations of various S100 proteins have been described previously (Heizmann, 2002), the antagonistic modulation model, proposed here, not only provides a new mechanism for regulating the kinetics of the cytoskeleton and cell motility but may also suggest a general modulatory mechanism amongst many S100 proteins.

Reference

Abu-Elneel, K., Karchi, M., Ravid, S. 1996. Dictyostelium myosin II is regulated during chemotaxis by a novel protein kinase C. *J Biol Chem* 271:977-84.

Agnihotri, R., Crawford, H. C., Haro, H., Matrisian, L. M., Havrda, M. C., Liaw, L. 2001. Osteopontin, a novel substrate for matrix metalloproteinase-3 (stromelysin-1) and matrix metalloproteinase-7 (matrilysin). *J Biol Chem* 276:28261-7.

Aguirre-Ghiso, J. A., Liu, D., Mignatti, A., Kovalski, K., Ossowski, L. 2001. Urokinase receptor and fibronectin regulate the ERK(MAPK) to p38(MAPK) activity ratios that determine carcinoma cell proliferation or dormancy *in vivo*. *Mol Biol Cell* 12:863-79.

Albertazzi, E., Cajone, F., Leone, B. E., Naguib, R. N., Lakshmi, M. S., Sherbet, G. V. 1998. Expression of metastasis-associated genes h-mts1 (S100A4) and nm23 in carcinoma of breast is related to disease progression. *DNA Cell Biol* 17:335-42.

Albini, A., Iwamoto, Y., Kleinman, H. K., Martin, G. R., Aaronson, S. A., *et al.* 1987. A rapid *in vitro* assay for quantitating the invasive potential of tumour cells. *Cancer Res* 47:3239-45.

Allore, R., O'Hanlon, D., Price, R., Neilson, K., Willard, H. F., *et al.* 1988. Gene encoding the beta subunit of S100 protein is on chromosome 21: implications for Down syndrome. *Science* 239:1311-3.

Amano, M., Chihara, K., Nakamura, N., Fukata, Y., Yano, T., *et al.* 1998. Myosin II activation promotes neurite retraction during the action of Rho and Rho-kinase. *Genes Cells* 3:177-88.

Ambartsumian, N. S., Grigorian, M. S., Larsen, I. F., Karlstrom, O., Sidenius, N., *et al.* 1996. Metastasis of mammary carcinomas in GRS/A hybrid mice transgenic for the mts1 gene. *Oncogene* 13:1621-30.

Anderson, R. E., Hansson, L. O., Nilsson, O., Liska, J., Settergren, G., Vaage, J. 2001. Increase in serum S100A1-B and S100BB during cardiac surgery arises from extracerebral sources. *Ann Thorac Surg* 71:1512-7.

Arii, S., Mori, A., Uchida, S., Fujimoto, K., Shimada, Y., Imamura, M. 1999. Implication of vascular endothelial growth factor in the development and metastasis of human cancers. *Hum Cell* 12:25-30.

Ashby, M. C., Tepikin, A. V. 2001. ER calcium and the functions of intracellular organelles. *Semin Cell Dev Biol* 12:11-7.

Averboukh, L., Liang, P., Kantoff, P. W., Pardee, A. B. 1996. Regulation of S100P expression by androgen. *Prostate* 29:350-5.

Badminton, M. N., Campbell, A. K., Rembold, C. M. 1996. Differential regulation of nuclear and cytosolic Ca^{2+} in HeLa cells. *J Biol Chem* 271:31210-4.

Barraclough, R. 1998. Calcium-binding protein S100A4 in health and disease. *Biochim Biophys Acta* 1448:190-9.

Barraclough, R., Chen, H. J., Davies, B. R., Davies, M. P., Ke, Y., *et al.* 1998. Use of DNA transfer in the induction of metastasis in experimental mammary systems. *Biochem Soc Symp* 63:273-94.

Barraclough, R., Dawson, K. J., Rudland, P. S. 1982. Control of protein synthesis in cuboidal rat mammary epithelial cells in culture. Changes in gene expression accompany the formation of elongated cells. *Eur J Biochem* 129:335-41.

Barraclough, R., Kimbell, R., Rudland, P. S. 1988. The identification of a normal rat gene located close to the gene for the potential myoepithelial cell calcium-binding protein, p9Ka. *J Biol Chem* 263:14597-600.

Barraclough, R., Savin, J., Dube, S. K., Rudland, P. S. 1987. Molecular cloning and sequence of the gene for p9Ka. A cultured myoepithelial cell protein with strong homology to S-100, a calcium-binding protein. *J Mol Biol* 198:13-20.

Barry, S. T., Ludbrook, S. B., Murrison, E., Horgan, C. M. 2000. A regulated interaction between alpha5beta1 integrin and osteopontin. *Biochem Biophys Res Commun* 267:764-9.

Barwise, J. L., Walker, J. H. 1996a. Annexins II, IV, V and VI relocate in response to rises in intracellular calcium in human foreskin fibroblasts. *J Cell Sci* 109:247-55.

Barwise, J. L., Walker, J. H. 1996b. Subcellular localization of annexin V in human foreskin fibroblasts: nuclear localization depends on growth state. *FEBS Lett* 394:213-6.

Baudier, J., Bergeret, E., Bertacchi, N., Weintraub, H., Gagnon, J., Garin, J. 1995. Interactions of myogenic bHLH transcription factors with calcium-binding calmodulin and S100a (alpha alpha) proteins. *Biochemistry* 34:7834-46.

Baudier, J., Cole, R. D. 1988. Interactions between the microtubule-associated tau proteins and S100b regulate tau phosphorylation by the Ca^{2+}/calmodulin-dependent protein kinase II. *J Biol Chem* 263:5876-83.

Baudier, J., Cole, R. D. 1988. Interactions between the microtubule-associated tau proteins and S100b regulate tau phosphorylation by the Ca^{2+}/calmodulin-dependent protein kinase II. *J Biol Chem* 263:5876-83.

Baudier, J., Delphin, C., Grunwald, D., Khochbin, S., Lawrence, J. J. 1992. Characterization of the tumour suppressor protein p53 as a protein kinase C substrate and a S100b-binding protein. *Proc Natl Acad Sci U S A* 89:11627-31.

Baudier, J., Gerard, D. 1983. Ions binding to S100 proteins: structural changes induced by calcium and zinc on S100a and S100b proteins. *Biochemistry* 22:3360-9.

Baudier, J., Glasser, N., Gerard, D. 1986. Ions binding to S100 proteins. I. Calcium- and zinc-binding properties of bovine brain S100 alpha alpha, S100a (alpha beta), and S100b (beta beta) protein: Zn^{2+} regulates Ca^{2+} binding on S100b protein. *J Biol Chem* 261:8192-203.

Bayless, K. J., Davis, G. E. 2001. Identification of dual alpha 4beta1 integrin binding sites within a 38 amino acid domain in the N-terminal thrombin fragment of human osteopontin. *J Biol Chem* 276:13483-9.

Bayless, K. J., Meininger, G. A., Scholtz, J. M., Davis, G. E. 1998. Osteopontin is a ligand for the alpha4beta1 integrin. *J Cell Sci* 111:1165-74.

Becker, D., and Fikes, J. 1993. Oxford: IRL press. 295-319 pp.

Bennett, D. L., Bootman, M. D., Berridge, M. J., Cheek, T. R. 1998. Ca^{2+} entry into PC12 cells initiated by ryanodine receptors or inositol 1,4,5-trisphosphate receptors. *Biochem J* 329:349-57.

Berman, A. E., Kozlova, N. I. 2000. Integrins: structure and functions. *Membr Cell Biol* 13:207-44.

Berridge, M. J. 1990. Temporal aspects of calcium signalling. *Adv Second Messenger Phosphoprotein Res* 24:108-14.

Berridge, M. J., Cobbold, P. H., Cuthbertson, K. S. 1988. Spatial and temporal aspects of cell signalling. *Philos Trans R Soc Lond B Biol Sci* 320:325-43.

Berridge, M. J., Lipp, P., Bootman, M. D. 2000a. Signal transduction. The calcium entry pas de deux. *Science* 287:1604-5.

Berridge, M. J., Lipp, P., Bootman, M. D. 2000b. The versatility and universality of calcium signalling. *Nat Rev Mol Cell Biol* 1:11-21.

Berridge, M., Lipp, P., Bootman, M. 1999. Calcium signalling. *Curr Biol* 9:R157-9.

Bertram, J., Palfner, K., Hiddemann, W., Kneba, M. 1998. Elevated expression of S100P, CAPL and MAGE 3 in doxorubicin-resistant cell lines: comparison of mRNA differential display reverse transcription-polymerase chain reaction and subtractive suppressive hybridization for the analysis of differential gene expression. *Anticancer Drugs* 9:311-7.

Bhardwaj, R. S., Zotz, C., Zwadlo-Klarwasser, G., Roth, J., Goebeler, M., *et al.* 1992. The calcium-binding proteins MRP8 and MRP14 form a membrane-associated heterodimer in a subset of monocytes/macrophages present in acute but absent in chronic inflammatory lesions. *Eur J Immunol* 22:1891-7.

Bianchi, R., Garbuglia, M., Verzini, M., Giambanco, I., Donato, R. 1994. Calpactin I binds to the glial fibrillary acidic protein (GFAP) and cosediments with glial filaments in a $Ca(^{2+})$-dependent manner: implications for concerted regulatory effects of calpactin I and S100 protein on glial filaments. *Biochim Biophys Acta* 1223:361-7.

Birnboim, H. C., Doly, J. 1979. A rapid alkaline extraction procedure for screening recombinant plasmid DNA. *Nucleic Acids Res* 7:1513-23.

Borsig, L., Wong, R., Feramisco, J., Nadeau, D. R., Varki, N. M., Varki, A. 2001. Heparin and cancer revisited: mechanistic connections involving platelets, P-selectin, carcinoma mucins, and tumour metastasis. *Proc Natl Acad Sci U S A* 98:3352-7.

Borsig, L., Wong, R., Hynes, R. O., Varki, N. M., Varki, A. 2002. Synergistic effects of L- and P-selectin in facilitating tumour metastasis can involve non-mucin ligands and implicate leukocytes as enhancers of metastasis. *Proc Natl Acad Sci U S A* 99:2193-8.

Bradford, M. M. 1976. A rapid and sensitive method for the quantitation of microgram quantities of protein utilizing the principle of protein-dye binding. *Anal Biochem* 72:248-54.

Brodt, P., Fallavollita, L., Bresalier, R. S., Meterissian, S., Norton, C. R., Wolitzky, B. A. 1997. Liver endothelial E-selectin mediates carcinoma cell adhesion and promotes liver metastasis. *Int J Cancer* 71:612-9.

Bronckart, Y., Decaestecker, C., Nagy, N., Harper, L., Schafer, B. W., *et al.* 2001. Development and progression of malignancy in human colon tissues are correlated with expression of specific $Ca^{(2+)}$-binding S100 proteins. *Histol Histopathol* 16:707-12.

Brooks, P. C., Clark, R. A., Cheresh, D. A. 1994. Requirement of vascular integrin alpha v beta 3 for angiogenesis. *Science* 264:569-71.

Brooks, P. C., Stromblad, S., Sanders, L. C., von Schalscha, T. L., Aimes, R. T., *et al.* 1996. Localization of matrix metalloproteinase MMP-2 to the surface of invasive cells by interaction with integrin alpha v beta 3. *Cell* 85:683-93.

Brownstein, C., Falcone, D. J., Jacovina, A., Hajjar, K. A. 2001. A mediator of cell surface-specific plasmin generation. *Ann N Y Acad Sci* 947:143-55; discussion 155-6.

Brummendorf, T., Rathjen, F. G. 1995. Cell adhesion molecules 1: immunoglobulin superfamily. *Protein Profile* 2:963-1108.

Brunner, N., Pyke, C., Hansen, C. H., Romer, J., Grondahl-Hansen, J., Dano, K. 1994. Urokinase plasminogen activator (uPA) and its type 1 inhibitor (PAI-1): regulators of proteolysis during cancer invasion and prognostic parameters in breast cancer. *Cancer Treat Res* 71:299-309.

Burgess, W. H., Watterson, D. M., Van Eldik, L. J. 1984. Identification of calmodulin-binding proteins in chicken embryo fibroblasts. *J Cell Biol* 99:550-7.

Chambers, A. F., MacDonald, I. C., Schmidt, E. E., Morris, V. L., Groom, A. C. 2000. Clinical targets for anti-metastasis therapy. *Adv Cancer Res* 79:91-121.

Cheng, T. P., Murakami, N., Elzinga, M. 1992. Localization of myosin IIB at the leading edge of growth cones from rat dorsal root ganglionic cells. *FEBS Lett* 311:91-4.

Chew, T. L., Masaracchia, R. A., Goeckeler, Z. M., Wysolmerski, R. B. 1998. Phosphorylation of non-muscle myosin II regulatory light chain by p21-activated kinase (gamma-PAK). *J Muscle Res Cell Motil* 19:839-54.

Chien, C. T., Bartel, P. L., Sternglanz, R., Fields, S. 1991. The two-hybrid system: a method to identify and clone genes for proteins that interact with a protein of interest. *Proc Natl Acad Sci U S A* 88:9578-82.

Choi OH, Adelstein RS, Beaven MA. 1994. Secretion from rat basophilic RBL-2H3 cells is associated with diphosphorylation of myosin light chains by myosin light chain kinase as well as phosphorylation by protein kinase C. *J Biol Chem* 269:536-541

Collins, K., Matsudaira, P. 1991. Differential regulation of vertebrate myosins I and II. *J Cell Sci Suppl* 14:11-6

Conti, M. A., Sellers, J. R., Adelstein, R. S., Elzinga, M. 1991. Identification of the serine residue phosphorylated by protein kinase C in vertebrate nonmuscle myosin heavy chains. *Biochemistry* 30:966-70.

Davies, B. R., Barraclough, R., Davies, M. P., Rudland, P. S. 1993a. Production of the metastatic phenotype by DNA transfection in a rat mammary model. *Cell Biol Int* 17:871-9.

Davies, B. R., Davies, M. P., Gibbs, F. E., Barraclough, R., Rudland, P. S. 1993b. Induction of the metastatic phenotype by transfection of a benign rat mammary epithelial cell line with the gene for p9Ka, a rat calcium-binding protein, but not with the oncogene EJ-ras-1. *Oncogene* 8:999-1008.

Davies, B. R., O'Donnell, M., Durkan, G. C., Rudland, P. S., Barraclough, R., *et al.* 2002. Expression of S100A4 protein is associated with metastasis and reduced survival in human bladder cancer. *J Pathol* 196:292-9.

Davies, M. P., Rudland, P. S., Robertson, L., Parry, E. W., Jolicoeur, P., Barraclough, R. 1996. Expression of the calcium-binding protein S100A4 (p9Ka) in MMTV-neu transgenic mice induces metastasis of mammary tumours. *Oncogene* 13:1631-7.

Davies, M., Harris, S., Rudland, P., Barraclough, R. 1995. Expression of the rat, S-100-related, calcium-binding protein gene, p9Ka, in transgenic mice demonstrates different patterns of expression between these two species. *DNA Cell Biol* 14:825-32.

de Launoit, Y., Chotteau-Lelievre, A., Beaudoin, C., Coutte, L., Netzer, S., *et al.* 2000. The PEA3 group of ETS-related transcription factors. Role in breast cancer metastasis. *Adv Exp Med Biol* 480:107-16.

Dedhar, S. 1999. Integrins and signal transduction. *Curr Opin Hematol* 6:37-43.

Deloulme, J. C., Assard, N., Mbele, G. O., Mangin, C., Kuwano, R., Baudier, J. 2000a. S100A6 and S100A11 are specific targets of the calcium- and zinc-binding S100B protein *in vivo*. *J Biol Chem* 275:35302-10.

Deloulme, J. C., Assard, N., Mbele, G. O., Mangin, C., Kuwano, R., Baudier, J. 2000b. S100A6 and S100A11 are specific targets of the calcium- and zinc-binding S100B protein *in vivo*. *J Biol Chem* 275:35302-10.

DeLozanne, A., Lewis, M., Spudich, J. A., Leinwand, L. A. 1985. Cloning and characterization of a nonmuscle myosin heavy chain cDNA. *Proc Natl Acad Sci U S A* 82:6807-10.

Delphin, C., Ronjat, M., Deloulme, J. C., Garin, G., Debussche, L., *et al.* 1999. Calcium-dependent interaction of S100B with the *C*-terminal domain of the tumour suppressor p53. *J Biol Chem* 274:10539-44.

Denhardt, D. T., Lopez, C. A., Rollo, E. E., Hwang, S. M., An, X. R., Walther, S. E. 1995. Osteopontin-induced modifications of cellular functions. *Ann N Y Acad Sci* 760:127-42.

Denhardt, D. T., Noda, M. 1998. Osteopontin expression and function: role in bone remodeling. *J Cell Biochem Suppl* 30-31:92-102.

Dolmetsch, R. E., Xu, K., Lewis, R. S. 1998. Calcium oscillations increase the efficiency and specificity of gene expression. *Nature* 392:933-6.

Donato, R. 1986. S-100 proteins. *Cell Calcium* 7:123-45.

Donato, R. 2001. S100: a multigenic family of calcium-modulated proteins of the EF-hand type with intracellular and extracellular functional roles. *Int J Biochem Cell Biol* 33:637-68.

Doussiere, J., Bouzidi, F., Vignais, P. V. 2002. The S100A8/A9 protein as a partner for the cytosolic factors of NADPH oxidase activation in neutrophils. *Eur J Biochem* 269:3246-55.

Drohat, A. C., Nenortas, E., Beckett, D., Weber, D. J. 1997. Oligomerization state of S100B at nanomolar concentration determined by large-zone analytical gel filtration chromatography. *Protein Sci* 6:1577-82.

Dunican, D. J., Doherty, P. 2000. The generation of localized calcium rises mediated by cell adhesion molecules and their role in neuronal growth cone motility. *Mol Cell Biol Res Commun* 3:255-63.

Dunnington, D. J., Hughes, C. M., Monaghan, P., Rudland, P. S. 1983. Phenotypic instability of rat mammary tumour epithelial cells. *J Natl Cancer Inst* 71:1227-40.

El-Rifai, W., Frierson, H. F., Jr., Harper, J. C., Powell, S. M., Knuutila, S. 2001. Expression profiling of gastric adenocarcinoma using cDNA array. *Int J Cancer* 92:832-8.

El-Tanani, M., Barraclough, R., Wilkinson, M. C., Rudland, P. S. 2001. Metastasis-inducing dna regulates the expression of the osteopontin gene by binding the transcription factor Tcf-4. *Cancer Res* 61:5619-29.

Endo, H., Takenaga, K., Kanno, T., Satoh, H., Mori, S. 2002. Methionine aminopeptidase 2 is a new target for the metastasis-associated protein, S100A4*. *J Biol Chem* 6:6

Engelkamp, D., Schafer, B. W., Mattei, M. G., Erne, P., Heizmann, C. W. 1993. Six S100 genes are clustered on human chromosome 1q21: identification of two genes coding for the two previously unreported calcium-binding proteins S100D and S100E. *Proc Natl Acad Sci U S A* 90:6547-51.

Europe-Finner, G. N., Newell, P. C. 1985. Inositol 1,4,5-trisphosphate induces cyclic GMP formation in Dictyostelium discoideum. *Biochem Biophys Res Commun* 130:1115-22.

Fagerstam, L. G., Frostell, A., Karlsson, R., Kullman, M., Larsson, A., *et al.* 1990. Detection of antigen-antibody interactions by surface plasmon resonance. Application to epitope mapping. *J Mol Recognit* 3:208-14.

Feinberg, A. P., Vogelstein, B. 1984. "A technique for radiolabeling DNA restriction endonuclease fragments to high specific activity". Addendum. *Anal Biochem* 137:266-7.

Felding-Habermann, B., Fransvea, E., O'Toole, T. E., Manzuk, L., Faha, B., Hensler, M. 2002. Involvement of tumour cell integrin alpha v beta 3 in hematogenous metastasis of human melanoma cells. *Clin Exp Metastasis* 19:427-36.

Felding-Habermann, B., O'Toole, T. E., Smith, J. W., Fransvea, E., Ruggeri, Z. M., *et al.* 2001. Integrin activation controls metastasis in human breast cancer. *Proc Natl Acad Sci U S A* 98:1853-8.

Fisher, J. L., Field, C. L., Zhou, H., Harris, T. L., Henderson, M. A., Choong, P. F. 2000. Urokinase plasminogen activator system gene expression is increased in human breast carcinoma and its bone metastases--a comparison of normal breast tissue, non-invasive and invasive carcinoma and osseous metastases. *Breast Cancer Res Treat* 61:1-12.

Fogh, J., and Trempe, G., 1975. New human tumour cell lines. In: J. Fogh (ed.), Human Tunour cells in vitro, pp. 115-153. New York: Plenum Publishing Corp.

Ford, H. L., Salim, M. M., Chakravarty, R., Aluiddin, V., Zain, S. B. 1995. Expression of Mts1, a metastasis-associated gene, increases motility but not invasion of a nonmetastatic mouse mammary adenocarcinoma cell line. *Oncogene* 11:2067-75.

Ford, H. L., Silver, D. L., Kachar, B., Sellers, J. R., Zain, S. B. 1997. Effect of Mts1 on the structure and activity of nonmuscle myosin II. *Biochemistry* 36:16321-7.

Ford, H. L., Zain, S. B. 1995. Interaction of metastasis associated Mts1 protein with nonmuscle myosin. *Oncogene* 10:1597-605.

Frandsen, T. L., Holst-Hansen, C., Nielsen, B. S., Christensen, I. J., Nyengaard, J. R., *et al.* 2001. Direct evidence of the importance of stromal urokinase plasminogen activator (uPA) in the growth of an experimental human breast cancer using a combined uPA gene-disrupted and immunodeficient xenograft model. *Cancer Res* 61:532-7.

Gahmberg, C. G., Tolvanen, M., Kotovuori, P. 1997. Leukocyte adhesion--structure and function of human leukocyte beta2-integrins and their cellular ligands. *Eur J Biochem* 245:215-32.

Gallagher PJ, Herring BP, Stull JT. 1997. Myosin light chain kinases. *J Mus Res Cell Motil* 18:1-16

Garbuglia, M., Verzini, M., Hofmann, A., Huber, R., Donato, R. 2000. S100A1 and S100B interactions with annexins. *Biochim Biophys Acta* 1498:192-206.

Garbuglia, M., Verzini, M., Sorci, G., Bianchi, R., Giambanco, I., *et al.* 1999. The calcium-modulated proteins, S100A1 and S100B, as potential regulators of the dynamics of type III intermediate filaments. *Braz J Med Biol Res* 32:1177-85.

Garcia, M., Derocq, D., Pujol, P., Rochefort, H. 1990. Overexpression of transfected cathepsin D in transformed cells increases their malignant phenotype and metastatic potency. *Oncogene* 5:1809-14.

Garcia, M., Platet, N., Liaudet, E., Laurent, V., Derocq, D., *et al.* 1996. Biological and clinical significance of cathepsin D in breast cancer metastasis. *Stem Cells* 14:642-50.

Gasparini, G. 2000. Prognostic value of vascular endothelial growth factor in breast cancer. *Oncologist* 5 Suppl 1:37-44.

Geisow, M. J., Ali, S. M., Boustead, C., Burgoyne, R. D., Taylor, W. R., Walker, J. H. 1990. Structures and functions of a supergene family of calcium and phospholipid binding proteins. *Prog Clin Biol Res* 349:111-21.

Gerke, V., Moss, S. E. 2002. Annexins: from structure to function. *Physiol Rev* 82:331-71.

Gibbs, F. E., Barraclough, R., Platt-Higgins, A., Rudland, P. S., Wilkinson, M. C., Parry, E. W. 1995. Immunocytochemical distribution of the calcium-binding protein p9Ka in normal rat tissues: variation in the cellular location in different tissues. *J Histochem Cytochem* 43:169-80.

Gibbs, F. E., Wilkinson, M. C., Rudland, P. S., Barraclough, R. 1994. Interactions *in vitro* of p9Ka, the rat S-100-related, metastasis-inducing, calcium-binding protein. *J Biol Chem* 269:18992-9.

Gillan, L., Matei, D., Fishman, D. A., Gerbin, C. S., Karlan, B. Y., Chang, D. D. 2002. Periostin secreted by epithelial ovarian carcinoma is a ligand for alpha(V)beta(3) and alpha(V)beta(5) integrins and promotes cell motility. *Cancer Res* 62:5358-64.

Goodison, S., Urquidi, V., Tarin, D. 1999. CD44 cell adhesion molecules. *Mol Pathol* 52:189-96.

Gotoh, M., Sakamoto, M., Kanetaka, K., Chuuma, M., Hirohashi, S. 2002. Overexpression of osteopontin in hepatocellular carcinoma. *Pathol Int* 52:19-24.

Grigorian, M., Ambartsumian, N., Lykkesfeldt, A. E., Bastholm, L., Elling, F., *et al.* 1996. Effect of mts1 (S100A4) expression on the progression of human breast cancer cells. *Int J Cancer* 67:831-41.

Grigorian, M., Andresen, S., Tulchinsky, E., Kriajevska, M., Carlberg, C., *et al.* 2001. tumour suppressor p53 protein is a new target for the metastasis-associated Mts1/S100A4 protein: functional consequences of their interaction. *J Biol Chem* 276:22699-708.

Groves, P., Finn, B. E., Kuznicki, J., Forsen, S. 1998. A model for target protein binding to calcium-activated S100 dimers. *FEBS Lett* 421:175-9.

Groves, P., Palczewska, M. 2001. Cation binding properties of calretinin, an EF-hand calcium-binding protein. *Acta Biochim Pol* 48:113-9.

Guerreiro Da Silva, I. D., Hu, Y. F., Russo, I. H., Ao, X., Salicioni, A. M., *et al.* 2000. S100P calcium-binding protein overexpression is associated with immortalization of human breast epithelial cells *in vitro* and early stages of breast cancer development *in vivo*. *Int J Oncol* 16:231-40.

Habelhah, H., Okada, F., Kobayashi, M., Nakai, K., Choi, S., *et al.* 1999. Increased E1AF expression in mouse fibrosarcoma promotes metastasis through induction of MT1-MMP expression. *Oncogene* 18:1771-6.

Halachmi, D., Eilam, Y. 1996. Elevated cytosolic free Ca^{2+} concentrations and massive Ca^{2+} accumulation within vacuoles, in yeast mutant lacking PMR1, a homolog of Ca^{2+} -ATPase. *FEBS Lett* 392:194-200.

Hanahan, D. 1985. *DNA cloning: A Practical Approach* Vol. 1. Oxford: IRL Press. 109-135 pp.

Hanzawa, M., Shindoh, M., Higashino, F., Yasuda, M., Inoue, N., *et al.* 2000. Hepatocyte growth factor upregulates E1AF that induces oral squamous cell carcinoma cell invasion by activating matrix metalloproteinase genes. *Carcinogenesis* 21:1079-85.

Heierhorst, J., Kobe, B., Feil, S. C., Parker, M. W., Benian, G. M., *et al.* 1996. Ca^{2+}/S100 regulation of giant protein kinases. *Nature* 380:636-9.

Heizmann, C.W. 2002. The multifunctional S100 protein family.
Methods Mol Biol. 172:69-80.

Hesketh, J., Baudier, J. 1986. Evidence that S100 proteins regulate microtubule self-assembly and stability in rat brain extracts. *Int J Biochem* 18:691-5.

Hida, K., Shindoh, M., Yoshida, K., Kudoh, A., Furaoka, K., *et al.* 1997. Expression of E1AF, an ets-family transcription factor, is correlated with the invasive phenotype of oral squamous cell carcinoma. *Oral Oncol* 33:426-30.

Hiroumi, H., Dosaka-Akita, H., Yoshida, K., Shindoh, M., Ohbuchi, T., *et al.* 2001. Expression of E1AF/PEA3, an Ets-related transcription factor in human non-small-cell lung cancers: its relevance in cell motility and invasion. *Int J Cancer* 93:786-91.

Hoffmann, A., Roeder, R. G. 1991. Purification of his-tagged proteins in non-denaturing conditions suggests a convenient method for protein interaction studies. *Nucleic Acids Res* 19:6337-8.

Hofmann, M. A., Drury, S., Fu, C., Qu, W., Taguchi, A., *et al.* 1999. RAGE mediates a novel proinflammatory axis: a central cell surface receptor for S100/calgranulin polypeptides. *Cell* 97:889-901.

Holly, S. P., Larson, M. K., Parise, L. V. 2000. Multiple roles of integrins in cell motility. *Exp Cell Res* 261:69-74.

Hotte, S. J., Winquist, E. W., Stitt, L., Wilson, S. M., Chambers, A. F. 2002. Plasma osteopontin: associations with survival and metastasis to bone in men with hormone-refractory prostate carcinoma. *Cancer* 95:506-12.

Hsieh, H. F., Yu, J. C., Ho, L. I., Chiu, S. C., Harn, H. J. 1999. Molecular studies into the role of CD44 variants in metastasis in gastric cancer. *Mol Pathol* 52:25-8.

Huttunen, H. J., Kuja-Panula, J., Sorci, G., Agneletti, A. L., Donato, R., Rauvala, H. 2000. Coregulation of neurite outgrowth and cell survival by amphoterin and S100 proteins through receptor for advanced glycation end products (RAGE) activation. *J Biol Chem* 275:40096-105.

Ilg, E. C., Schafer, B. W., Heizmann, C. W. 1996. Expression pattern of S100 calcium-binding proteins in human tumours. *Int J Cancer* 68:325-32.

Ish-Horowicz, D., Burke, J. F. 1981. Rapid and efficient cosmid cloning. *Nucleic Acids Res* 9:2989-98.

Isobe, T., Ishioka, N., Masuda, T., Takahashi, Y., Ganno, S., Okuyama, T. 1983. A rapid separation of S100 subunits by high performance liquid chromatography: the subunit compositions of S100 proteins. *Biochem Int* 6:419-26.

Isobe, T., Okuyama, T. 1988. [EF-hand proteins; an intracellular calcium sensor]. *Tanpakushitsu Kakusan Koso* 33:1955-68.

Itoh K, A. R. 1995. Cloning of the cDNA encoding human nonmuscle myosin heavy chain-B and analysis of human tissues with isoform-specific antibodies. *J Biol Chem* 270:14533¨C14540

Jing, C., Beesley, C., Foster, C. S., Chen, H., Rudland, P. S., *et al.* 2001. Human cutaneous fatty acid-binding protein induces metastasis by up-regulating the expression of vascular endothelial growth factor gene in rat Rama 37 model cells. *Cancer Res* 61:4357-64.

Jing, C., Beesley, C., Foster, C. S., Rudland, P. S., Fujii, H., *et al.* 2000. Identification of the messenger RNA for human cutaneous fatty acid-binding protein as a metastasis inducer. *Cancer Res* 60:2390-8.

Jinquan, T., Vorum, H., Larsen, C. G., Madsen, P., Rasmussen, H. H., *et al.* 1996. Psoriasin: a novel chemotactic protein. *J Invest Dermatol* 107:5-10.

John, A., Tuszynski, G. 2001. The role of matrix metalloproteinases in tumour angiogenesis and tumour metastasis. *Pathol Oncol Res* 7:14-23.

Jones, H., Moshtael, F., Simpson, R. H. 1992. Immunoreactivity of alpha smooth muscle actin in salivary gland tumours: a comparison with S100 protein. *J Clin Pathol* 45:938-40.

Kaczan-Bourgois, D., Salles, J. P., Hullin, F., Fauvel, J., Moisand, A., *et al.* 1996. Increased content of annexin II (p36) and p11 in human placenta brush-border membrane vesicles during syncytiotrophoblast maturation and differentiation. *Placenta* 17:669-76.

Kaelin, W. G., Jr., Krek, W., Sellers, W. R., DeCaprio, J. A., Ajchenbaum, F., *et al.* 1992. Expression cloning of a cDNA encoding a retinoblastoma-binding protein with E2F-like properties. *Cell* 70:351-64.

Kallenberg, L. A. 2000. Calcium signalling in secretory cells. *Arch Physiol Biochem* 108:385-90.

Katagiri, Y. U., Sleeman, J., Fujii, H., Herrlich, P., Hotta, H., *et al.* 1999. CD44 variants but not CD44s cooperate with beta1-containing integrins to permit cells to bind to osteopontin independently of arginine-glycine-aspartic acid, thereby stimulating cell motility and chemotaxis. *Cancer Res* 59:219-26.

Katayama, N., Murao, S., Ajiki, T., Kitazawa, S., Onoyama, H., *et al.* 2000. The role of S100A4 gene encoding an S100-related calcium-binding protein in human bile duct adenocarcinoma cell lines: correlation of S100A4 expression and invasive growth in Matrigel Matrix. *Int J Mol Med* 6:539-42.

Kawamoto S, Bengur AR, Sellers JR, Adelstein RS. 1989. In situ phosphorylation of human platelet myosin heavy and light chains by protein kinase C. *J Biol Chem* 264:2258-2265

Kaya, M., Yoshida, K., Higashino, F., Mitaka, T., Ishii, S., Fujinaga, K. 1996. A single ets-related transcription factor, E1AF, confers invasive phenotype on human cancer cells. *Oncogene* 12:221-7.

Kelley CA, Sellers JR, Gard DL, Bui D, Adelstein RS, Baines IC. 1996. Xenopus nonmuscle myosin heavy chain isoforms have different subcellular localizations and enzymatic activities. *J Cell Biol* 134:675¨C687

Kerkhoff, C., Klempt, M., Sorg, C. 1998. Novel insights into structure and function of MRP8 (S100A8) and MRP14 (S100A9). *Biochim Biophys Acta* 1448:200-11.

Kerkhoff, C., Klempt, M., Kaever, V., Sorg, C. 1999. The two calcium-binding proteins, S100A8 and S100A9, are involved in the metabolism of arachidonic acid in human neutrophils. *J Biol Chem* 274:32672-9.

Kerkhoff, C., Sorg, C., Tandon, N. N., Nacken, W. 2001. Interaction of S100A8/S100A9-arachidonic acid complexes with the scavenger receptor CD36 may facilitate fatty acid uptake by endothelial cells. *Biochemistry* 40:241-8.

Khatib, A. M., Fallavollita, L., Wancewicz, E. V., Monia, B. P., Brodt, P. 2002. Inhibition of hepatic endothelial E-selectin expression by *C*-raf antisense oligonucleotides blocks colorectal carcinoma liver metastasis. *Cancer Res* 62:5393-8.

Kilby, P. M., Van Eldik, L. J., Roberts, G. C. 1996. The solution structure of the bovine S100B protein dimer in the calcium-free state. *Structure* 4:1041-52.

Kim, J., Hajjar, K. A. 2002. Annexin II: a plasminogen-plasminogen activator co-receptor. *Front Biosci* 7:d341-8.

Kim, Y. W., Park, Y. K., Lee, J., Ko, S. W., Yang, M. H. 1998. Expression of osteopontin and osteonectin in breast cancer. *J Korean Med Sci* 13:652-7.

Kimura, K., Endo, Y., Yonemura, Y., Heizmann, C. W., Schafer, B. W., *et al.* 2000. Clinical significance of S100A4 and E-cadherin-related adhesion molecules in non-small cell lung cancer. *Int J Oncol* 16:1125-31.

Kinjo, M. 1978. Lodgement and extravasation of tumour cells in blood-borne metastasis: an electron microscope study. *Br J Cancer* 38:293-301.

Kirsch, M., Schackert, G., Black, P. M. 2000. Angiogenesis, metastasis, and endogenous inhibition. *J Neurooncol* 50:173-80.

Kolega, J. 1998. Cytoplasmic dynamics of myosin IIA and IIB: spatial 'sorting' of isoforms in locomoting cells. *J Cell Sci* 111:2085-95.

Komada, T., Araki, R., Nakatani, K., Yada, I., Naka, M., Tanaka, T. 1996. Novel specific chemtactic receptor for S100L protein on guinea pig eosinophils. *Biochem Biophys Res Commun* 220:871-4.

Komatsu, K., Andoh, A., Ishiguro, S., Suzuki, N., Hunai, H., *et al.* 2000a. Increased expression of S100A6 (Calcyclin), a calcium-binding protein of the S100 family, in human colorectal adenocarcinomas. *Clin Cancer Res* 6:172-7.

Komatsu, K., Kobune-Fujiwara, Y., Andoh, A., Ishiguro, S., Hunai, H., *et al.* 2000b. Increased expression of S100A6 at the invading fronts of the primary lesion and liver metastasis in patients with colorectal adenocarcinoma. *Br J Cancer* 83:769-74.

Kordel, J., Forsen, S., Drakenberg, T., Chazin, W. J. 1990. The rate and structural consequences of proline cis-trans isomerization in calbindin D9k: NMR studies of the minor (cis-Pro43) isoform and the Pro43Gly mutant. *Biochemistry* 29:4400-9.

Korn, E. D., Atkinson, M. A., Brzeska, H., Hammer, J. A., 3rd, Jung, G., Lynch, T. J. 1988. Structure-function studies on Acanthamoeba myosins IA, IB, and II. *J Cell Biochem* 36:37-50.

Kozlova, E. N., Lukanidin, E. 1999. Metastasis-associated mts1 (S100A4) protein is selectively expressed in white matter astrocytes and is up-regulated after peripheral nerve or dorsal root injury. *Glia* 27:249-58.

Krause, T., Turner, G. A. 1999. Are selectins involved in metastasis? *Clin Exp Metastasis* 17:183-92.

Kretsinger, R. H., Nockolds, C. E. 1973. Carp muscle calcium-binding protein. II. Structure determination and general description. *J Biol Chem* 248:3313-3326.

Kriajevska, M. V., Cardenas, M. N., Grigorian, M. S., Ambartsumian, N. S., Georgiev, G. P., Lukanidin, E. M. 1994. Non-muscle myosin heavy chain as a possible target for protein encoded by metastasis-related mts-1 gene. *J Biol Chem* 269:19679-82.

Kriajevska, M., Bronstein, I. B., Scott, D. J., Tarabykina, S., Fischer-Larsen, M., *et al.* 2000. Metastasis-associated protein Mts1 (S100A4) inhibits CK2-mediated phosphorylation and self-assembly of the heavy chain of nonmuscle myosin. *Biochim Biophys Acta* 1498:252-63.

Kriajevska, M., Tarabykina, S., Bronstein, I., Maitland, N., Lomonosov, M., *et al.* 1998. Metastasis-associated Mts1 (S100A4) protein modulates protein kinase C phosphorylation of the heavy chain of nonmuscle myosin. *J Biol Chem* 273:9852-6.

Krieg, P., Schuppler, M., Koesters, R., Mincheva, A., Lichter, P., Marks, F. 1997. Repetin (Rptn), a new member of the "fused gene" subgroup within the S100 gene family encoding a murine epidermal differentiation protein. *Genomics* 43:339-48.

Laemmli, U. K. 1970. Cleavage of structural proteins during the self-assembly of the head of bacteriophage T4. *Nature* 227:680-5.

Landar, A., Caddell, G., Chessher, J., Zimmer, D. B. 1996. Identification of an S100A1/S100B target protein: phosphoglucomutase. *Cell Calcium* 20:279-85.

Landar, A., Rustandi, R. R., Weber, D. J., Zimmer, D. B. 1998. S100A1 utilizes different mechanisms for interacting with calcium-dependent and calcium-independent target proteins. *Biochemistry* 37:17429-38.

Lawrance, I. C., Fiocchi, C., Chakravarti, S. 2001. Ulcerative colitis and Crohn's disease: distinctive gene expression profiles and novel susceptibility candidate genes. *Hum Mol Genet* 10:445-56.

Lesley, J., Hyman, R., English, N., Catterall, J. B., Turner, G. A. 1997. CD44 in inflammation and metastasis. *Glycoconj J* 14:611-22.

Levett, D., Flecknell, P. A., Rudland, P. S., Barraclough, R., Neal, D. E., *et al.* 2002. Transfection of S100A4 produces metastatic variants of an orthotopic model of bladder cancer. *Am J Pathol* 160:693-700.

Lewalle, J. M., Cataldo, D., Bajou, K., Lambert, C. A., Foidart, J. M. 1998. Endothelial cell intracellular Ca^{2+} concentration is increased upon breast tumour cell contact and mediates tumour cell transendothelial migration. *Clin Exp Metastasis* 16:21-9.

Lin, C., Hajnoczky, G., Thomas, A. P. 1994. Propagation of cytosolic calcium waves into the nuclei of hepatocytes. *Cell Calcium* 16:247-58.

Lloyd, B. H., Platt-Higgins, A., Rudland, P. S., Barraclough, R. 1998. Human S100A4 (p9Ka) induces the metastatic phenotype upon benign tumour cells. *Oncogene* 17:465-73.

Lloyd, B. H., Ruddell, C., Rudland, P. S., Barraclough, R. 1996. S100A3 mRNA expression displays an inverse correlation to breast cancer progression. *Biochem Soc Trans* 24:340S.

Ludowyke, R. I., Peleg, I., Beaven, M. A., Adelstein, R. S. 1989. Antigen-induced secretion of histamine and the phosphorylation of myosin by protein kinase C in rat basophilic leukemia cells. *J Biol Chem* 264:12492-501.

Maciver, S. K. 1996. Myosin II function in non-muscle cells. *Bioessays* 18:179-82.

Maelandsmo, G. M., Florenes, V. A., Mellingsaeter, T., Hovig, E., Kerbel, R. S., Fodstad, O. 1997. Differential expression patterns of S100A2, S100A4 and S100A6 during progression of human malignant melanoma. *Int J Cancer* 74:464-9.

Maelandsmo, G. M., Hovig, E., Skrede, M., Engebraaten, O., Florenes, V. A., *et al.* 1996. Reversal of the *in vivo* metastatic phenotype of human tumour cells by an anti-CAPL (mts1) ribozyme. *Cancer Res* 56:5490-8.

Mahoney, M. G., Simpson, A., Jost, M., Noe, M., Kari, C., *et al.* 2002. Metastasis-associated protein (MTA)1 enhances migration, invasion, and anchorage-independent survival of immortalized human keratinocytes. *Oncogene* 21:2161-70.

Mandinova, A., Atar, D., Schafer, B. W., Spiess, M., Aebi, U., Heizmann, C. W. 1998. Distinct subcellular localization of calcium binding S100 proteins in human smooth muscle cells and their relocation in response to rises in intracellular calcium. *J Cell Sci* 111:2043-54.

Mao, C., Kim, S. H., Almenoff, J. S., Rudner, X. L., Kearney, D. M., Kindman, L. A. 1996. Molecular cloning and characterization of SCaMPER, a sphingolipid Ca^{2+} release-mediating protein from endoplasmic reticulum. *Proc Natl Acad Sci U S A* 93:1993-6.

Markova, N. G., Marekov, L. N., Chipev, C. C., Gan, S. Q., Idler, W. W., Steinert, P. M. 1993. Profilaggrin is a major epidermal calcium-binding protein. *Mol Cell Biol* 13:613-25.

McAdory, B. S., Van Eldik, L. J., Norden, J. J. 1998. S100B, a neurotropic protein that modulates neuronal protein phosphorylation, is upregulated during lesion-induced collateral sprouting and reactive synaptogenesis. *Brain Res* 813:211-7.

McFarland, D. C. 2000. Preparation of pure cell cultures by cloning. *Methods Cell Sci* 22:63-6.

Medico, E., Gentile, A., Lo Celso, C., Williams, T. A., Gambarotta, G., *et al.* 2001. Osteopontin is an autocrine mediator of hepatocyte growth factor-induced invasive growth. *Cancer Res* 61:5861-8.

Mercurio, A. M., Rabinovitz, I., Shaw, L. M. 2001. The alpha 6 beta 4 integrin and epithelial cell migration. *Curr Opin Cell Biol* 13:541-5.

Miranda, L. P., Tao, T., Jones, A., Chernushevich, I., Standing, K. G., *et al.* 2001. Total chemical synthesis and chemotactic activity of human S100A12 (EN-RAGE). *FEBS Lett* 488:85-90.

Moore, B. 1965. Asoluble protein characteristic of the nervous system . *Biochem. Biophys.Res.Comm* 19:739-744

Moroz, O. V., Antson, A. A., Dodson, E. J., Burrell, H. J., Grist, S. J., *et al.* 2002. The structure of S100A12 in a hexameric form and its proposed role in receptor signalling. *Acta Crystallogr D Biol Crystallogr* 58:407-13.

Moussavi RS, K. C., Adelstein RS. 1993. Phosphorylation of vertebrate nonmuscle and smooth muscle myosin heavy chains and light chains. *Mol Cell Biochem* 127/128:219-227

Mousses, S., Bubendorf, L., Wagner, U., Hostetter, G., Kononen, J., *et al.* 2002. Clinical validation of candidate genes associated with prostate cancer progression in the CWR22 model system using tissue microarrays. *Cancer Res* 62:1256-60.

Muller, A., Homey, B., Soto, H., Ge, N., Catron, D., *et al.* 2001. Involvement of chemokine receptors in breast cancer metastasis. *Nature* 410:50-6.

Murakami N, H.-L. G., Elzinga M. 1990. Amino acid sequence around the serine phosphorylated by casein kinase II in brain myosin heavy chain. *J Biol Chem* 265:1041-1047

Murakami, N., Chauhan, V. P., Elzinga, M. 1998. Two nonmuscle myosin II heavy chain isoforms expressed in rabbit brains: filament forming properties, the effects of phosphorylation by protein kinase C and casein kinase II, and location of the phosphorylation sites. *Biochemistry* 37:1989-2003.

Murakami, N., Kotula, L., Hwang, Y. W. 2000. Two distinct mechanisms for regulation of nonmuscle myosin self-assembly via the heavy chain: phosphorylation for MIIB and mts 1 binding for MIIA. *Biochemistry* 39:11441-51.

Murakami, N., Singh, S. S., Chauhan, V. P., Elzinga, M. 1995. Phospholipid binding, phosphorylation by protein kinase C, and filament self-assembly of the COOH terminal heavy chain fragments of nonmuscle myosin II isoforms MIIA and MIIB. *Biochemistry* 34:16046-55.

Murao, S., Collart, F. R., Huberman, E. 1989. A protein containing the cystic fibrosis antigen is an inhibitor of protein kinases. *J Biol Chem* 264:8356-60.

Nabi, I. R., Watanabe, H., Raz, A. 1992. Autocrine motility factor and its receptor: role in cell locomotion and metastasis. *Cancer Metastasis Rev* 11:5-20.

Nakamura, T., Ajiki, T., Murao, S., Kamigaki, T., Maeda, S., *et al.* 2002. Prognostic significance of S100A4 expression in gallbladder cancer. *Int J Oncol* 20:937-41.

Nakanishi, K., Sakamoto, M., Yasuda, J., Takamura, M., Fujita, N., *et al.* 2002. Critical involvement of the phosphatidylinositol 3-kinase/Akt pathway in anchorage-independent growth and hematogeneous intrahepatic metastasis of liver cancer. *Cancer Res* 62:2971-5.

Nakayama N, Kawasaki H and Kretsinger R.2000. Evolution of EF-hand proteins. *Topics Biol Inorg Chem* 3:29-58

Naot, D., Sionov, R. V., Ish-Shalom, D. 1997. CD44: structure, function, and association with the malignant process. *Adv Cancer Res* 71:241-319.

Nelson, M. R., Chazin, W. J. 1998. An interaction-based analysis of calcium-induced conformational changes in Ca^{2+} sensor proteins. *Protein Sci* 7:270-82.

Nicolson, G. L., Custead, S. E. 1982. tumour metastasis is not due to adaptation of cells to a new organ environment. *Science* 215:176-8.

Niederman, R., Pollard, T. D. 1975. Human platelet myosin. II. *In vitro* self-assembly and structure of myosin filaments. *J Cell Biol* 67:72-92.

Ninomiya, I., Ohta, T., Fushida, S., Endo, Y., Hashimoto, T., *et al.* 2001. Increased expression of S100A4 and its prognostic significance in esophageal squamous cell carcinoma. *Int J Oncol* 18:715-20.

Oates, A. J., Barraclough, R., Rudland, P. S. 1996. The identification of osteopontin as a metastasis-related gene product in a rodent mammary tumour model. *Oncogene* 13:97-104.

O'Connor, K. L., Shaw, L. M., Mercurio, A. M. 1998. Release of cAMP gating by the alpha6beta4 integrin stimulates lamellae formation and the chemotactic migration of invasive carcinoma cells. *J Cell Biol* 143:1749-60.

O'Reilly, M. S., Holmgren, L., Chen, C., Folkman, J. 1996. Angiostatin induces and sustains dormancy of human primary tumours in mice. *Nat Med* 2:689-92.

Osterloh, D., Ivanenkov, V. V., Gerke, V. 1998. Hydrophobic residues in the *C*-terminal region of S100A1 are essential for target protein binding but not for dimerization. *Cell Calcium* 24:137-51.

Otterbein, L. R., Kordowska, J., Witte-Hoffmann, C., Wang, C. L., Dominguez, R. 2002. Crystal structures of S100A6 in the $Ca^{(2+)}$-free and $Ca^{(2+)}$-bound states: the calcium sensor mechanism of S100 proteins revealed at atomic resolution. *Structure (Camb)* 10:557-67.

Palecek, S. P., Loftus, J. C., Ginsberg, M. H., Lauffenburger, D. A., Horwitz, A. F. 1997. Integrin-ligand binding properties govern cell migration speed through cell-substratum adhesiveness. *Nature* 385:537-40.

Papamichael, D. 2001. Prognostic role of angiogenesis in colorectal cancer. *Anticancer Res* 21:4349-53.

Parker, C., Lakshmi, M. S., Piura, B., Sherbet, G. V. 1994. Metastasis-associated mts1 gene expression correlates with increased p53 detection in the B16 murine melanoma. *DNA Cell Biol* 13:343-51.

Pedrocchi, M., Schafer, B. W., Durussel, I., Cox, J. A., Heizmann, C. W. 1994. Purification and characterization of the recombinant human calcium-binding S100 proteins CAPL and CACY. *Biochemistry* 33:6732-8.

Petersen, O. H. 2000. The functional organisation of calcium signalling in exocrine acinar cells. *J Korean Med Sci* 15 Suppl:S44-5.

Philip, S., Bulbule, A., Kundu, G. C. 2001. Osteopontin stimulates tumour growth and activation of promatrix metalloproteinase-2 through nuclear factor-kappa B-mediated induction of membrane type 1 matrix metalloproteinase in murine melanoma cells. *J Biol Chem* 276:44926-35.

Potts, B. C., Smith, J., Akke, M., Macke, T. J., Okazaki, K., *et al.* 1995a. The structure of calcyclin reveals a novel homodimeric fold for S100 $Ca^{(2+)}$-binding proteins. *Nat Struct Biol* 2:790-6.

Potts, B. C., Smith, J., Akke, M., Macke, T. J., Okazaki, K., *et al.* 1995b. The structure of calcyclin reveals a novel homodimeric fold for S100 $Ca^{(2+)}$-binding proteins. *Nat Struct Biol* 2:790-6.

Rabbani, S. A., Xing, R. H. 1998. Role of urokinase (uPA) and its receptor (uPAR) in invasion and metastasis of hormone-dependent malignancies. *Int J Oncol* 12:911-20.

Radloff, R., Bauer, W., Vinograd, J. 1967. A dye-buoyant-density method for the detection and isolation of closed circular duplex DNA: the closed circular DNA in HeLa cells. *Proc Natl Acad Sci U S A* 57:1514-21.

Rauth, S., Green, A., Kichina, J., Shilkaitis, A. 1998. Suppression of tumourigenic and metastatic potentials of human melanoma cell lines by mutated (143 Val-Ala) p53. *Br J Cancer* 77:2215-22.

Ravid, S., Spudich, J. A. 1989. Myosin heavy chain kinase from developed Dictyostelium cells. Purification and characterization. *J Biol Chem* 264:15144-50.

Ray, J. M., Stetler-Stevenson, W. G. 1994. The role of matrix metalloproteases and their inhibitors in tumour invasion, metastasis and angiogenesis. *Eur Respir J* 7:2062-72.

Rety, S., Osterloh, D., Arie, J. P., Tabaries, S., Seeman, J., *et al.* 2000. Structural basis of the Ca($^{2+}$)-dependent association between S100C (S100A11) and its target, the N-terminal part of annexin I. *Structure Fold Des* 8:175-84.

Rickles, F. R., Shoji, M., Abe, K. 2001. The role of the hemostatic system in tumour growth, metastasis, and angiogenesis: tissue factor is a bifunctional molecule capable of inducing both fibrin deposition and angiogenesis in cancer. *Int J Hematol* 73:145-50.

Ridinger, K., Ilg, E. C., Niggli, F. K., Heizmann, C. W., Schafer, B. W. 1998. Clustered organization of S100 genes in human and mouse. *Biochim Biophys Acta* 1448:254-63.

Rimm, D. L., Koslov, E. R., Kebriaei, P., Cianci, C. D., Morrow, J. S. 1995. Alpha 1(E)-catenin is an actin-binding and -bundling protein mediating the attachment of F-actin to the membrane adhesion complex. *Proc Natl Acad Sci U S A* 92:8813-7.

Rochefort, H. 1991. [Mechanism of the overexpression of the cathepsin D gene in breast cancer and consequences in the metastatic process]. *C R Seances Soc Biol Fil* 185:415-21.

Rochefort, H., Capony, F., Garcia, M. 1990. Cathepsin D: a protease involved in breast cancer metastasis. *Cancer Metastasis Rev* 9:321-31.

Rodan, G. A. 1995. Osteopontin overview. *Ann N Y Acad Sci* 760:1-5.

Roldan, A. L., Cubellis, M. V., Masucci, M. T., Behrendt, N., Lund, L. R., *et al.* 1990. Cloning and expression of the receptor for human urokinase plasminogen activator, a central molecule in cell surface, plasmin dependent proteolysis. *Embo J* 9:467-74.

Rosty, C., Ueki, T., Argani, P., Jansen, M., Yeo, C. J., *et al.* 2002. Overexpression of S100A4 in Pancreatic Ductal Adenocarcinomas Is Associated with Poor Differentiation and DNA Hypomethylation. *Am J Pathol* 160:45-50.

Rothnagel, J. A., Rogers, G. E. 1986. Trichohyalin, an intermediate filament-associated protein of the hair follicle. *J Cell Biol* 102:1419-29.

Roulin, K., Hagens, G., Hotz, R., Saurat, J. H., Veerkamp, J. H., Siegenthaler, G. 1999. The fatty acid-binding heterocomplex FA-p34 formed by S100A8 and S100A9 is the major fatty acid carrier in neutrophils and translocates from the cytosol to the membrane upon stimulation. *Exp Cell Res* 247:410-21.

Rudland, P. S., Platt-Higgins, A., El-Tanani, M., De Silva Rudland, S., Barraclough, R., *et al.* 2002. Prognostic significance of the metastasis-associated protein osteopontin in human breast cancer. *Cancer Res* 62:3417-27.

Rudland, P. S., Platt-Higgins, A., Renshaw, C., West, C. R., Winstanley, J. H., *et al.* 2000. Prognostic significance of the metastasis-inducing protein S100A4 (p9Ka) in human breast cancer. *Cancer Res* 60:1595-603.

Rudolph, H. K., Antebi, A., Fink, G. R., Buckley, C. M., Dorman, T. E., *et al.* 1989. The yeast secretory pathway is perturbed by mutations in PMR1, a member of a Ca^{2+} ATPase family. *Cell* 58:133-45.

Rustandi, R. R., Baldisseri, D. M., Inman, K. G., Nizner, P., Hamilton, S. M., *et al.* 2002. Three-dimensional solution structure of the calcium-signaling protein apo-S100A1 as determined by NMR. *Biochemistry* 41:788-96.

Saad, Z., Bramwell, V. H., Wilson, S. M., O'Malley, F. P., Jeacock, J., Chambers, A. F. 1998. Expression of genes that contribute to proliferative and metastatic ability in breast cancer resected during various menstrual phases. *Lancet* 351:1170-3.

Saaristo, A., Karpanen, T., Alitalo, K. 2000. Mechanisms of angiogenesis and their use in the inhibition of tumour growth and metastasis. *Oncogene* 19:6122-9.

Sabry, J. H., Moores, S. L., Ryan, S., Zang, J. H., Spudich, J. A. 1997. Myosin heavy chain phosphorylation sites regulate myosin localization during cytokinesis in live cells. *Mol Biol Cell* 8:2605-15.

Saez, C. G., Myers, J. C., Shows, T. B., Leinwand, L. A. 1990. Human nonmuscle myosin heavy chain mRNA: generation of diversity through alternative polyadenylylation. *Proc Natl Acad Sci U S A* 87:1164-8.

Sambrook, J., Fritsch, E.F., and Maniatis, T. 1989. In *Molecular Cloning: A Laboratory Manual.* New York: Cold Spring Harbor Laboratory Press, Cold Spring Harbor, New York

Sato, H., Seiki, M. 1996. Membrane-type matrix metalloproteinases (MT-MMPs) in tumour metastasis. *J Biochem (Tokyo)* 119:209-15.

Scappaticci, F. A. 2002. Mechanisms and future directions for angiogenesis-based cancer therapies. *J Clin Oncol* 20:3906-27.

Schmidt, A. M., Stern, D. M. 2001. Receptor for age (RAGE) is a gene within the major histocompatibility class III region: implications for host response mechanisms in homeostasis and chronic disease. *Front Biosci* 6:D1151-60.

Schmitz-Peiffer, C., Browne, C. L., Walker, J. H., Biden, T. J. 1998. Activated protein kinase C alpha associates with annexin VI from skeletal muscle. *Biochem J* 330:675-81.

Scholey, J. M., Taylor, K. A., Kendrick-Jones, J. 1980. Regulation of non-muscle myosin self-assembly by calmodulin-dependent light chain kinase. *Nature* 287:233-5.

Schuck, P. 1997. Use of surface plasmon resonance to probe the equilibrium and dynamic aspects of interactions between biological macromolecules. *Annu Rev Biophys Biomol Struct* 26:541-66.

Selinfreund, R. H., Barger, S. W., Welsh, M. J., Van Eldik, L. J. 1990. Antisense inhibition of glial S100 beta production results in alterations in cell morphology, cytoskeletal organization, and cell proliferation. *J Cell Biol* 111:2021-8.

Sellers, J. R. 2000. Myosins: a diverse superfamily. *Biochim Biophys Acta* 1496:3-22.

Semprini, S., Capon, F., Tacconelli, A., Giardina, E., Orecchia, A., *et al.* 2002. Evidence for differential S100 gene over-expression in psoriatic patients from genetically heterogeneous pedigrees. *Hum Genet* 111:310-3.

Shelden, E., Knecht, D. A. 1996. Dictyostelium cell shape generation requires myosin II. *Cell Motil Cytoskeleton* 35:59-67.

Sheng, J. G., Mrak, R. E., Griffin, W. S. 1994. S100 beta protein expression in Alzheimer disease: potential role in the pathogenesis of neuritic plaques. *J Neurosci Res* 39:398-404.

Sherbet, G. V., Lakshmi, M. S. 1998. S100A4 (MTS1) calcium binding protein in cancer growth, invasion and metastasis. *Anticancer Res* 18:2415-21.

Sheu, F. S., Azmitia, E. C., Marshak, D. R., Parker, P. J., Routtenberg, A. 1994a. Glial-derived S100b protein selectively inhibits recombinant beta protein kinase C (PKC) phosphorylation of neuron-specific protein F1/GAP43. *Brain Res Mol Brain Res* 21:62-6.

Shibuya, M. 2001. Structure and function of VEGF/VEGF-receptor system involved in angiogenesis. *Cell Struct Funct* 26:25-35.

Shiozaki, H., Tahara, H., Oka, H., Miyata, M., Kobayashi, K., *et al.* 1991. Expression of immunoreactive E-cadherin adhesion molecules in human cancers. *Am J Pathol* 139:17-23.

Shrestha, P., Muramatsu, Y., Kudeken, W., Mori, M., Takai, Y., *et al.* 1998. Localization of $Ca(^{2+})$-binding S100 proteins in epithelial tumours of the skin. *Virchows Arch* 432:53-9.

Siegenthaler, G., Roulin, K., Chatellard-Gruaz, D., Hotz, R., Saurat, J. H., *et al.* 1997. A heterocomplex formed by the calcium-binding proteins MRP8 (S100A8) and MRP14 (S100A9) binds unsaturated fatty acids with high affinity. *J Biol Chem* 272:9371-7.

Simons, M., Wang, M., McBride, O. W., Kawamoto, S., Yamakawa, K., *et al.* 1991. Human nonmuscle myosin heavy chains are encoded by two genes located on different chromosomes. *Circ Res* 69:530-9.

Sjaastad, M. D., Angres, B., Lewis, R. S., Nelson, W. J. 1994. Feedback regulation of cell-substratum adhesion by integrin-mediated intracellular Ca^{2+} signaling. *Proc Natl Acad Sci U S A* 91:8214-8.

Smith, D. B., Johnson, K. S. 1988. Single-step purification of polypeptides expressed in Escherichia coli as fusions with glutathione S-transferase. *Gene* 67:31-40.

Somlyo, A. P., Somlyo, A. V. 2000. Signal transduction by G-proteins, rho-kinase and protein phosphatase to smooth muscle and non-muscle myosin II. J Physiol. 522 Pt 2:177-85.

Song, W., Zimmer, D. B. 1996. Expression of the rat S100A1 gene in neurons, glia, and skeletal muscle. *Brain Res* 721:204-16.

Sorg, C. 1992. The calcium binding proteins MRP8 and MRP14 in acute and chronic inflammation. *Behring Inst Mitt*:126-37.

Soule, H. D., vazques, J., Long, A., Albert, S., and Brennan, M. 1973. A human cell line from a pleural sffusion derived from a breast carcinoma. J. Natl. Cancer Inst., 51: 1409-1413.

Staudinger, J., Perry, M., Elledge, S. J., Olson, E. N. 1993. Interactions among vertebrate helix-loop-helix proteins in yeast using the two-hybrid system. *J Biol Chem* 268:4608-11.

Stites, J., Wessels, D., Uhl, A., Egelhoff, T., Shutt, D., Soll, D. R. 1998. Phosphorylation of the Dictyostelium myosin II heavy chain is necessary for maintaining cellular polarity and suppressing turning during chemotaxis. *Cell Motil Cytoskeleton* 39:31-51.

Strongin, A. Y., Collier, I., Bannikov, G., Marmer, B. L., Grant, G. A., Goldberg, G. I. 1995. Mechanism of cell surface activation of 72-kDa type IV collagenase. Isolation of the activated form of the membrane metalloprotease. *J Biol Chem* 270:5331-8.

Studier, F. W., Moffatt, B. A. 1986. Use of bacteriophage T7 RNA polymerase to direct selective high-level expression of cloned genes. *J Mol Biol* 189:113-30.

Su, Z., Kiehart, D. P. 2001. Protein kinase C phosphorylates nonmuscle myosin-II heavy chain from Drosophila but regulation of myosin function by this enzyme is not required for viability in flies. *Biochemistry* 40:3606-14.

Szabo, A., Stolz, L., Granzow, R. 1995. Surface plasmon resonance and its use in biomolecular interaction analysis (BIA). *Curr Opin Struct Biol* 5:699-705.

Takahashi, M., Kawamoto, S., Adelstein, R. S. 1992. Evidence for inserted sequences in the head region of nonmuscle myosin specific to the nervous system. Cloning of the cDNA encoding the myosin heavy chain-B isoform of vertebrate nonmuscle myosin. *J Biol Chem* 267:17864-71.

Takahashi, M., Takahashi, K., Hiratsuka, Y., Uchida, K., Yamagishi, A., *et al.* 2001. Functional characterization of vertebrate nonmuscle myosin IIB isoforms using Dictyostelium chimeric myosin II. *J Biol Chem* 276:1034-40.

Takenaga, K., Nakamura, Y., Endo, H., Sakiyama, S. 1994a. Involvement of S100-related calcium-binding protein pEL98 (or mts1) in cell motility and tumour cell invasion. *Jpn J Cancer Res* 85:831-9.

Takenaga, K., Nakamura, Y., Sakiyama, S. 1994b. Cellular localization of pEL98 protein, an S100-related calcium binding protein, in fibroblasts and its tissue distribution analyzed by monoclonal antibodies. *Cell Struct Funct* 19:133-41.

Takenaga, K., Nakamura, Y., Sakiyama, S. 1997a. Expression of antisense RNA to S100A4 gene encoding an S100-related calcium-binding protein suppresses metastatic potential of high-metastatic Lewis lung carcinoma cells. *Oncogene* 14:331-7.

Takenaga, K., Nakamura, Y., Sakiyama, S., Hasegawa, Y., Sato, K., Endo, H. 1994c. Binding of pEL98 protein, an S100-related calcium-binding protein, to nonmuscle tropomyosin. *J Cell Biol* 124:757-68.

Takenaga, K., Nakanishi, H., Wada, K., Suzuki, M., Matsuzaki, O., *et al.* 1997b. Increased expression of S100A4, a metastasis-associated gene, in human colorectal adenocarcinomas. *Clin Cancer Res* 3:2309-16.

Takino, T., Sato, H., Shinagawa, A., Seiki, M. 1995. Identification of the second membrane-type matrix metalloproteinase (MT-MMP-2) gene from a human placenta cDNA library. MT-MMPs form a unique membrane-type subclass in the MMP family. *J Biol Chem* 270:23013-20.

Tarabykina, S., Kriajevska, M., Scott, D. J., Hill, T. J., Lafitte, D., *et al.* 2000. Heterocomplex formation between metastasis-related protein S100A4 (Mts1) and S100A1 as revealed by the yeast two-hybrid system. *FEBS Lett* 475:187-91.

Tarabykina, S., Scott, D. J., Herzyk, P., Hill, T. J., Tame, J. R., *et al.* 2001. The dimerization interface of the metastasis-associated protein S100A4 (Mts1): *in vivo* and *in vitro* studies. *J Biol Chem* 276:24212-22.

Taylor, S., Herrington, S., Prime, W., Rudland, P. S., Barraclough, R. 2002. S100A4 (p9Ka) protein in colon carcinoma and liver metastases: association with carcinoma cells and T-lymphocytes. *Br J Cancer* 86:409-16.

Teigelkamp, S., Bhardwaj, R. S., Roth, J., Meinardus-Hager, G., Karas, M., Sorg, C. 1991. Calcium-dependent complex self-assembly of the myeloic differentiation proteins MRP-8 and MRP-14. *J Biol Chem* 266:13462-7.

Thiel, C., Osborn, M., Gerke, V. 1992. The tight association of the tyrosine kinase substrate annexin II with the submembranous cytoskeleton depends on intact p11- and $Ca(^{2+})$-binding sites. *J Cell Sci* 103:733-42.

Towbin, H., Staehelin, T., Gordon, J. 1992. Electrophoretic transfer of proteins from polyacrylamide gels to nitrocellulose sheets: procedure and some applications. 1979. *Biotechnology* 24:145-9.

Treves, S., Scutari, E., Robert, M., Groh, S., Ottolia, M., *et al.* 1997. Interaction of S100A1 with the Ca^{2+} release channel (ryanodine receptor) of skeletal muscle. *Biochemistry* 36:11496-503.

Tuck, A. B., Arsenault, D. M., O'Malley, F. P., Hota, C., Ling, M. C., *et al.* 1999. Osteopontin induces increased invasiveness and plasminogen activator expression of human mammary epithelial cells. *Oncogene* 18:4237-46.

Tzima, E., Trotter, P. J., Hastings, A. D., Orchard, M. A., Walker, J. H. 2000. Investigation of the relocation of cytosolic phospholipase A2 and annexin V in activated platelets. *Thromb Res* 97:421-9.

Tzima, E., Trotter, P. J., Orchard, M. A., Walker, J. H. 1999. Annexin V binds to the actin-based cytoskeleton at the plasma membrane of activated platelets. *Exp Cell Res* 251:185-93.

Ue, T., Yokozaki, H., Kitadai, Y., Yamamoto, S., Yasui, W., Ishikawa, T., Tahara, E. 1998. Co-expression of osteopontin and CD44v9 in gastric cancer. Int J Cancer. 17;79(2):127-32.

Vallely, K. M., Rustandi, R. R., Ellis, K. C., Varlamova, O., Bresnick, A. R., Weber, D. J. 2002. Solution structure of human Mts1 (S100A4) as determined by NMR spectroscopy. *Biochemistry* 41:12670-80.

van den Bos, C., Roth, J., Koch, H. G., Hartmann, M., Sorg, C. 1996. Phosphorylation of MRP14, an S100 protein expressed during monocytic differentiation, modulates $Ca(^{2+})$-dependent translocation from cytoplasm to membranes and cytoskeleton. *J Immunol* 156:1247-54.

Voura, E. B., Ramjeesingh, R. A., Montgomery, A. M., Siu, C. H. 2001. Involvement of integrin alpha(v)beta(3) and cell adhesion molecule L1 in transendothelial migration of melanoma cells. *Mol Biol Cell* 12:2699-710.

Wang, G., Rudland, P. S., White, M. R., Barraclough, R. 2000. Interaction *in vivo* and *in vitro* of the metastasis-inducing S100 protein, S100A4 (p9Ka) with S100A1. *J Biol Chem* 275:11141-6.

Weber, G. F., Ashkar, S., Glimcher, M. J., Cantor, H. 1996. Receptor-ligand interaction between CD44 and osteopontin (Eta-1). *Science* 271:509-12.

Wei, Y., Lukashev, M., Simon, D. I., Bodary, S. C., Rosenberg, S., *et al.* 1996. Regulation of integrin function by the urokinase receptor. *Science* 273:1551-5.

Weidner, K. M., Hartmann, G., Naldini, L., Comoglio, P. M., Sachs, M., *et al.* 1993. Molecular characteristics of HGF-SF and its role in cell motility and invasion. *Exs* 65:311-28.

Weinman, S. 1991. Calcium-binding proteins: an overview. *J Biol Buccale* 19:90-8.

Wilson, A. K., Pollenz, R. S., Chisholm, R. L., de Lanerolle, P. 1992. The role of myosin I and II in cell motility. *Cancer Metastasis Rev* 11:79-91.

Wojtukiewicz, M. Z., Sierko, E., Klement, P., Rak, J. 2001. The hemostatic system and angiogenesis in malignancy. *Neoplasia* 3:371-84.

Wylie SR, Wu P-J, Patel H, Chantler PD. 1998 A conventional myosin motor drives neurite outgrowth. *Proc Natl Acad Sci USA* 95:12967¨C12972

Xing, R. H., Rabbani, S. A. 1996. Overexpression of urokinase receptor in breast cancer cells results in increased tumour invasion, growth and metastasis. *Int J Cancer* 67:423-9.

Yam, J. W., Chan, K. W., Hsiao, W. L. 2001. Suppression of the tumourigenicity of mutant p53-transformed rat embryo fibroblasts through expression of a newly cloned rat nonmuscle myosin heavy chain-B. *Oncogene* 20:58-68.

Yamakita, Y., Yamashiro, S., Matsumura, F. 1994. *In vivo* phosphorylation of regulatory light chain of myosin II during mitosis of cultured cells. *J Cell Biol* 124:129-37.

Yana, I., Seiki, M. 2002. MT-MMPs play pivotal roles in cancer dissemination. *Clin Exp Metastasis* 19:209-15.

Yonemura, Y., Endou, Y., Kimura, K., Fushida, S., Bandou, E., *et al.* 2000. Inverse expression of S100A4 and E-cadherin is associated with metastatic potential in gastric cancer. *Clin Cancer Res* 6:4234-42.

Yu, A. E., Hewitt, R. E., Kleiner, D. E., Stetler-Stevenson, W. G. 1996. Molecular regulation of cellular invasion--role of gelatinase A and TIMP-2. *Biochem Cell Biol* 74:823-31.

Zhang, H. T., Craft, P., Scott, P. A., Ziche, M., Weich, H. A., *et al.* 1995. Enhancement of tumour growth and vascular density by transfection of vascular endothelial cell growth factor into MCF-7 human breast carcinoma cells. *J Natl Cancer Inst* 87:213-9.

Zhang, J., Takahashi, K., Takahashi, F., Shimizu, K., Ohshita, F., *et al.* 2001. Differential osteopontin expression in lung cancer. *Cancer Lett* 171:215-22.

Zhao, X. Q., Naka, M., Muneyuki, M., Tanaka, T. 2000. $Ca(^{2+})$-dependent inhibition of actin-activated myosin ATPase activity by S100C (S100A11), a novel member of the S100 protein family. *Biochem Biophys Res Commun* 267:77-9.

Zimmer, D. B., Dubuisson J.G. 1993. Identification of an S100 target protein: glycogen phosphorylase. Cell Calcium. 14(4):323-32

Zimmer, D. B., Cornwall, E. H., Landar, A., Song, W. 1995. The S100 protein family: history, function, and expression. *Brain Res Bull* 37:417-29.

THE JOURNAL OF BIOLOGICAL CHEMISTRY
Vol. 275, No. 15, Issue of April 14, pp. 11141–11146, 2000
Printed in U.S.A.

Interaction *in Vivo* and *in Vitro* of the Metastasis-inducing S100 Protein, S100A4 (p9Ka) with S100A1*

(Received for publication, November 10, 1999, and in revised form, December 9, 1999)

Guozheng Wang, Philip S. Rudland, Michael R. White‡, and Roger Barraclough§

From the Cancer and Polio Research Fund Laboratories and the ‡Centre for Cell Imaging, School of Biological Sciences, University of Liverpool, Liverpool L69 7ZB, United Kingdom

The calcium-binding protein S100A4 (p9Ka) has been shown to cause a metastatic phenotype in rodent mammary tumor cells and in transgenic mouse model systems. mRNA for S100A4 (p9Ka) is present at a generally higher level in breast carcinoma than in benign breast tumor specimens, and the presence of immunocytochemically detected S100A4 correlates strongly with a poor prognosis for breast cancer patients. Recombinant S100A4 (p9Ka) has been reported to interact *in vitro* with cytoskeletal components and to form oligomers, particularly homodimers *in vitro*. Using the yeast two-hybrid system, a strong interaction between S100A4 (p9Ka) and another S100 protein, S100A1, was detected. Site-directed mutagenesis of conserved amino acid residues involved in the dimerization of S100 proteins abolished the interactions. The interaction between S100A4 and S100A1 was also observed *in vitro* using affinity column chromatography and gel overlay techniques. Both S100A1 and S100A4 can occur in the same cultured mammary cells, suggesting that in cells containing both proteins, S100A1 might modulate the metastasis-inducing capability of S100A4.

S100 proteins are a family of low molecular weight, acidic proteins that contain two distinct EF-hands with different affinities for calcium (1). Elevated levels of one S100 protein, S100A4, are closely associated with the process of metastasis in breast and other cancer cells in rodent animal models and in human cancer specimens. S100A4 or its mRNA is found at an elevated level in metastatic relative to non-metastatic rat (2) and mouse (3) tumor cell lines and benign relative to malignant human breast tumors (4). Elevation of the level of rat (5) or human (6) S100A4 in benign rat mammary tumor cells results in the acquisition of metastatic capability by some of the cells. In transgenic mouse models of breast cancer, elevated levels of S100A4 in *neu* oncogene-induced (7), or in murine mammary tumor virus-induced (8), benign mammary tumors yield lung metastases. In colorectal adenocarcinoma specimens, elevated levels of immunocytochemically detected S100A4 are associated with the more malignant carcinomatous regions of the primary tumors and with liver metastases (9). The precise interactions whereby S100A4 induces metastasis are not fully understood.

S100A4, or its mRNA, is found in many normal cells, some of which are motile (10, 11), and S100A4 has been associated immunofluorescently with the actin/myosin cytoskeleton in fixed cells (5, 12–14). Calcium-dependent interaction of S100A4 with actin (15), tropomyosin (16), and non-muscle myosin (17–20) has been reported *in vitro*. S100 proteins form homodimers and heterodimers (21, 22); S100A4 forms calcium- and dithiothreitol-independent homodimers *in vitro* (23). The conditions employed for these interactions *in vitro* cannot match the conditions inside the cell, where functional interactions are likely to take place. Thus, the yeast two-hybrid system has been utilized to find interactions *in vivo* for the metastasis-inducing protein S100A4.

EXPERIMENTAL PROCEDURES

DNA Constructs for the Yeast Two-hybrid System—For screening a human breast tumor two-hybrid library constructed with pYESTrp2 vector (Invitrogen, Groningen, Netherlands), a bait vector was constructed by excising the LexA cassette from the pHybLex/Zeo vector (Invitrogen), and inserting it into the pAD-GAL4-2.1 vector (Stratagene, La Jolla, CA) to produce the LexA vector with the LEU2 selectable marker. A 303-base pair cDNA corresponding to the coding region of human S100A4 (p9Ka) mRNA was obtained by PCR[1] of an expression vector pET-p9Ka[2] and was subcloned into the LexA vector to produce the LexA-S100A4 bait construct. Nucleotide sequencing ensured the integrity of the cloning and sequences. Selection for this bait plasmid in yeast cells was on leucine-free plates or medium.

Yeast Transformation and Lift Assays and Liquid β-Galactosidase Assays—For the screening of the breast cancer two-hybrid library, yeast strain L40 (genotype: *MATa his3*Δ*200 trp1–901 leu2–3112 ade2 LYS2*::(4*lex*Aop-*HIS3*) *URA3*:: (8*lex*Aop-*lacZ*)*GAL4*) cells were transformed with LexA-S100A4 to produce a stable L40-LexA-S100A4 strain. A culture was transformed with the human breast cancer pYESTrp2 library DNA according to the lithium yeast transformation protocol (Invitrogen). Yeast transformants were selected by their growth on leucine-, tryptophan-, and histidine-free plates and media. Lift assays (according to Stratagene's protocol) were carried out 7 days after transformation, and colonies that gave a blue color within 16 h were isolated.

For each individual clone, both the bait plasmid, LexA-S100A4, and the target plasmid from the YESTrp2 library were isolated from the cells. The recovered YESTrp2 target plasmids were cotransformed into L40 yeast cells along with the original bait plasmid, LexA-S100A4, and lift assays were carried out to reconfirm the interaction in the yeast cells.

The activity of β-galactosidase of each positive transformant was determined using a liquid β-galactosidase assay (24). The number of Miller units of β-galactosidase activity was calculated using the formula: Miller units = (1,000 × optical density of the reaction)/(volume of cell assayed in ml × time in min × optical density of the culture at 600 nm).

Mutagenesis of S100A4—Amino acid residues phenylalanine 72 and tyrosine 75 of the human S100A4 protein sequence (25) were both altered to glutamine by changing the triplets from TTC and TAC to

* This work was supported by grants from Glaxo Wellcome, the Cancer and Polio Research Fund, the Medical Research Council, HEFCE, and Carl Zeiss Ltd. The costs of publication of this article were defrayed in part by the payment of page charges. This article must therefore be hereby marked "*advertisement*" in accordance with 18 U.S.C. Section 1734 solely to indicate this fact.

§ To whom correspondence should be addressed: School of Biological Sciences, Life Sciences Bldg., University of Liverpool, P.O. Box 147, Liverpool L69 7ZB, U. K. Tel.: 44-151-794-4327; Fax: 44-151-794-4349; E-mail: brb@liv.ac.uk.

[1] The abbreviations used are: PCR, polymerase chain reaction; rS100A4, recombinant S100A4; GST, glutathione *S*-transferase; PAGE, polyacrylamide gel electrophoresis; PVDF, polyvinylidene difluoride; RT-PCR, reverse transcript PCR.

[2] B. Lloyd and R. Barraclough, unpublished data.

CAG using the PCR extension method of site-directed mutagenesis (26). The two external primers used were: 5′-*Xho*I primer, TCTCTCGAGCTGCTGTCATGGCGTGC and 3′-*Pst*I primer, TGCGCCTGCAGTGGAGTTTTCATTTCTTC. The inner primers for the F72Q mutation were: 5′-GACCAGCAAGAGTACTGTGTCTTCC and 3′-CTCTTGCTGGTCCACCTCGTTGTCCC. The inner primers for the Y75Q mutation were: 5′-GAGCAGTGTGTCTTCCTGTCCTGC and 3′-GACACACTGCTCTTGGAAGTCCACC. The cDNAs with the point mutations were digested with *Xho*I and *Pst*I and inserted into the LexA vector. DNA sequencing confirmed the nucleotide changes and the coding frames for fusion protein expression.

Recombinant Proteins—Rat recombinant S100A4 (rat rS100A4) was produced and purified as described previously (12). A recombinant human S100A1 cDNA was obtained using PCR from a clone selected in the two-hybrid screen. The cDNA open reading frame, which encoded the 93 amino acids of human S100A1 protein, was subcloned into the expression vector pGEX-2T, and rS100A1 was produced as a fusion protein with 26 kDa of glutathione *S*-transferase (GST) protein at the NH_2 terminus (GST-S100A1). The fusion protein was purified to near homogeneity using glutathione-Sepharose 4B (Amersham Pharmacia Biotech). Histidine-tagged-rS100A1 (His-S100A1) was expressed in pET16b(+) vector and purified with histidine-binding resin (Novagen).

In Vitro Binding Assay for S100 Proteins—For the detection of binding of S100A1 and S100A4 proteins *in vitro*, the GST-S100A1 fusion protein or GST alone was attached to glutathione *S*-Sepharose (Amersham Pharmacia Biotech) slurries at a concentration of 0.5 mg/ml of slurry. 100 μl of a solution of 0.1 mg/ml rS100A4 protein in KTT buffer (140 mM KCl, 20 mM Tris-HCl, pH 7.4, 0.1% (w/v) Triton X-100, 5 mM dithiothreitol, with 1 mM $CaCl_2$, or 1 mM EGTA) was incubated with 100-μl aliquots of the GST or GST-S100A1 slurries for 3 h at 4 °C. The mixtures were applied to spin columns and centrifuged in a microcentrifuge at 800 rpm for 1 min. The columns were spun-washed with the KTT buffer at least 10 times. Unbound proteins were eluted with at least 50 bed volumes of KTT until no further protein was eluted. Bound proteins were eluted with 20 mM Tris-HCl, pH 8.0, 150 mM NaCl, 5 mM dithiothreitol, 10 mM reduced glutathione, and 0.1% (w/v) Triton X-100. Eluted S100A4 was analyzed by SDS-polyacrylamide gel electrophoresis (PAGE) (27) followed by transfer onto PVDF filters (Immobilon, Millipore, France), and incubation with a 1:500 dilution of an affinity-purified rabbit polyclonal antibody to rat rS100A4, produced as described previously (28). Bound antibodies were detected using the ECL system (Amersham Pharmacia Biotech).

For gel overlay, the recombinant GST-S100A1, His-S100A1, GST, and S100A4 proteins were subjected to SDS-PAGE (12.5% (w/v)) and electroblotted onto PVDF membranes. The membranes were incubated with overlay buffer (0.5% (w/v) bovine serum albumin, 0.25% (w/v) gelatin, 0.5% (w/v) detergent Nonidet P-40, 100 mM NaCl, 50 mM Tris, pH 7.5, containing 3 μg/ml rat rS100A4 plus either 0.5 mM calcium ions or 1 mM EGTA) for 4 h and washed four times for 5 min each in the same buffer without the bovine serum albumin, gelatin, or S100A4. Membranes were incubated with blocking buffer (3% (w/v) bovine serum albumin, 0.1% (w/v) Tween 20, 2% (w/v) Marvel in Tris-buffered saline). The membranes were washed three times for 5 min each in wash buffer (0.1% (w/v) Tween 20, 2% (w/v) Marvel in Tris-buffered saline). The membranes were incubated with 2.5 ml of the wash buffer containing a 500-fold dilution of the rabbit anti-rat S100A4 serum for 1.5 h. After being washed in buffer six times for 5 min each, the filters were incubated in a 2,500-fold dilution of a secondary antibody for 1 h. After a final wash with Tris-buffered saline for 30 min, bound antibody was detected using the ECL system with exposure against Kodak XAR-5 film.

Cell Culture, Isolation of RNA, and Reverse Transcript Polymerase Chain Reaction (RT-PCR)—The human malignant breast tumor cell lines MCF-7, SK-Br-3 and MDA-MB-231 (29) were cultured as described previously (30). Total RNA was isolated using the guanidinium isothiocyanate/CsCl method as described previously (31–33).

For RT-PCR, 1 μg of total RNA or 0.5 μg of poly(A)-containing RNA was reverse transcribed using Superscript according to the supplier's protocol (Life Technologies, Inc., Paisley, Scotland), and the resulting cDNA was amplified by 35 cycles of PCR using *Taq* polymerase (Life Technologies, Inc.) with the following human S100A1-specific primers: 5′-primer, ACAGGTCTCCACACACAGCTCC; 3′-primer, AGGCTCGAGAGGAAGGGCGCTGC. PCR products were analyzed by electrophoresis on 1.4% (w/v) agarose gels and stained with ethidium bromide. Control amplifications omitted the reverse transcriptase.

Immunofluorescent Detection of S100 Proteins—About 500 cells were plated per well of chambered slides and cultured for 24 h. The cells were fixed with 4% (w/v) paraformadehyde in phosphate-buffered saline for 10 min and permeabilized with 0.1% (w/v) Triton X-100 in phosphate-buffered saline for 5 min. After a 30-min incubation in blocking buffer (2% (w/v) bovine serum albumin in phosphate-buffered saline), the cells were incubated with primary antibody, either rabbit anti-S100A4 (1:50 dilution) or mouse anti-S100A1 (1:20 dilution) in blocking buffer. After being washed four times with phosphate-buffered saline, the cells were incubated with secondary antibody for 1 h. Fluorescein isothiocyanate-conjugated anti-mouse IgG for anti-S100A1 staining and tetramethylrhodamine β-isothiocyanate-conjugated anti-rabbit IgG for S100A4 staining were used. After washing, the slides were dried and mounted. Photographs were taken using a Zeiss LSM 510 confocal microscope.

RESULTS

Interaction of S100A4 in Yeast Cells—To identify heterologous interactions *in vivo* between S100A4 and components of malignant/metastatic cells, more than 2×10^6 yeast cell transformants from a two-hybrid cDNA library, constructed from mRNA isolated from a human breast cancer specimen, were transfected with the S100A4 (p9Ka) cDNA bait vector. Target plasmids were recovered from 14 independent blue colonies, and purified plasmid DNAs were cotransformed individually into L40 yeast cells along with the S100A4 (p9Ka) bait plasmid. Reisolation of plasmid DNA and cotransformation were repeated serially three times, after which only four colonies showed the blue color in lift assay on each occasion. Plasmid DNA was isolated from these four transformants, and the nucleotide sequences of the cDNAs in the target vectors were determined. The sequence of each of the four target plasmids was precisely that of human S100A1. The four colonies containing both the S100A4 bait and S100A1 prey plasmids exhibited β-galactosidase activities that were 20–70-fold higher than colonies containing only bait plasmid or only a prey plasmid (Fig. 1*a*). However, the prey constructs in the library (Invitrogen) contained an additional 19 amino acids of protein sequence inserted between the B42 activating domain and the NH_2 terminus of the target protein. To rule out the possibility that this extra sequence might be interacting directly with the S100A4 protein, the extra sequence was deleted from one of the isolated target clones. L40 strain yeast transformants containing both the pYESTrp2ExS100A1 prey construct, bearing the deletion, and the S100A4 bait construct LexA-S100A4, yielded a blue color within 3 h in the lift assay, and the β-galactosidase activity of the deleted clone was greater than that of the original clone containing the additional 19 amino acids insert (Fig. 1*b*). Thus, the β-galactosidase activity was not caused by the presence of these additional amino acids at the NH_2 terminus of the cloned S100A1 protein in the yeast cells from the breast cancer library. The above experiments suggest that, at least in yeast cells, S100A4 can interact in a heterologous manner with S100A1.

Point Mutation in the S100A4 cDNA Interrupts the Interaction between S100A4 and S100A1 in Vivo—Two single nucleotide point mutations of the S100A4 cDNA were generated which yielded amino acid substitutions in residues involved in the dimer interface reported previously for S100A6 (34). These changes, which resulted in conversion of phenylalanine 72 and tyrosine 75 of the S100A4 protein sequence to glutamine, individually fully (Phe-72), or partially (Tyr-75), disrupted S100A4 dimer formation in the yeast two-hybrid system (not shown). Bait plasmids containing cDNAs bearing either of these mutations completely failed to yield blue colonies when cotransfected with S100A1 prey plasmids under the same conditions that yielded blue colonies in 6 h when unmutated S100A4 was used. These specific mutations individually abolished the interaction between S100A4 and S100A1 in the yeast cells as determined by β-galactosidase activity (Fig. 1*c*).

Interaction between S100A4 and S100A1 in Vitro—Antibodies directed against recombinant S100A4 or S100A1 were

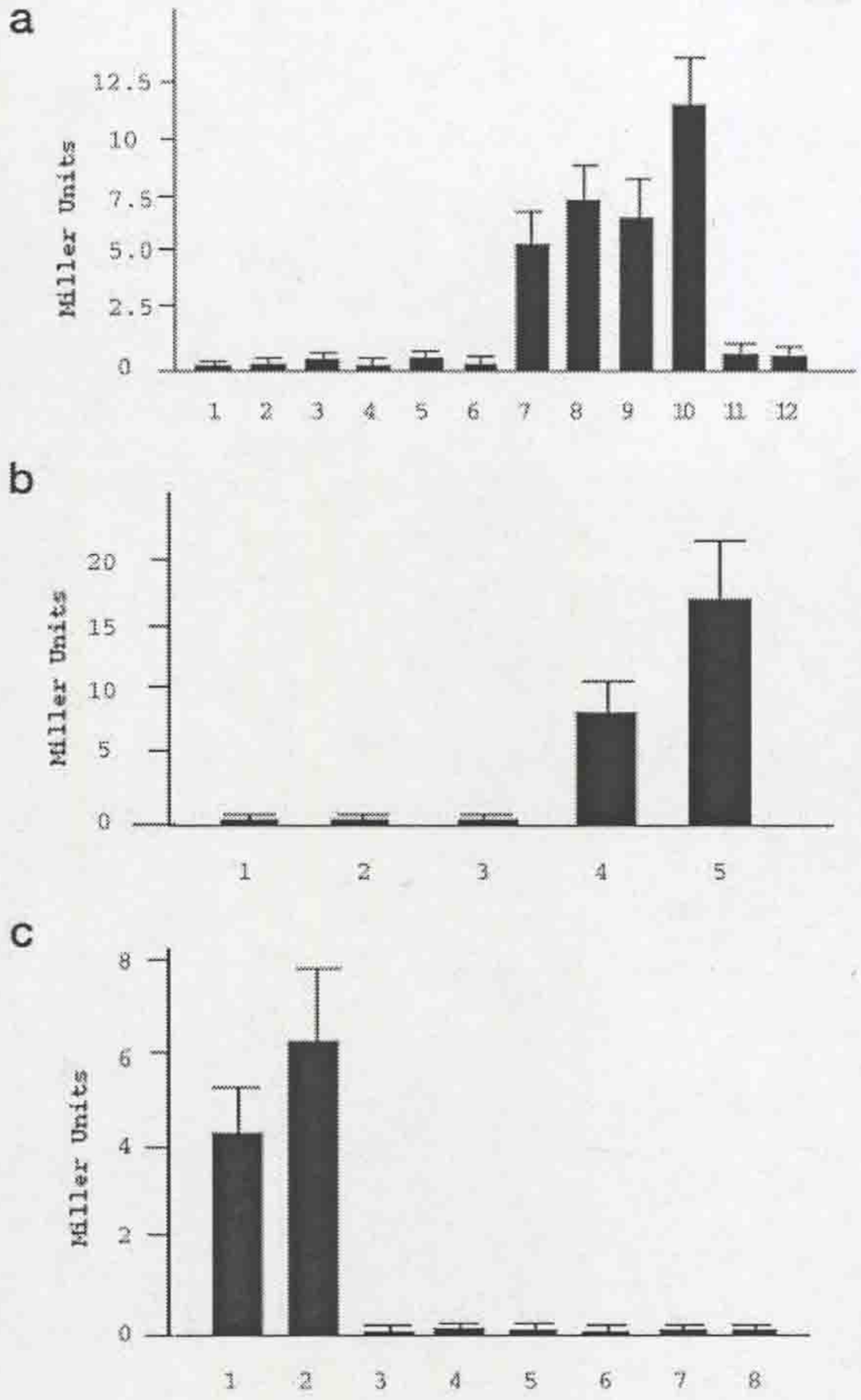

FIG. 1. **β-Galactosidase activity of yeast clones bearing S100A4 bait and/or target vectors isolated from the breast cancer two-hybrid library.** Clones of yeast strain L40 were transformed with the DNA constructs indicated below, grown up, and β-galactosidase activity determined in Miller units as described under "Experimental Procedures." *Panel a*, *column 1*, bait plasmid LexA-S100A4 alone; *columns 2–5*, each of four recovered target plasmids, alone; *column 6*, bait vector, LexA-S100A4, and target vector pYESTrp2 without insert; *columns 7–12*, bait vector LexA-S100A4 and each of six recovered target vectors, A-F, four of which contained S100A1 cDNA (*columns 7–10*). *Panel b*, *column 1*, LexA-S100A4 bait plasmid alone; *column 2*, with the original recovered target plasmid A alone; *column 3*, with the original recovered target plasmid A lacking the 19-amino acid region alone; *column 4*, with LexA-S100A4 bait plasmid and the original recovered target plasmid; *column 5*, with LexA-S100A4 bait plasmid and original recovered target plasmid lacking the 19-amino acid region. *Panel c*, *column 1*, bait LexA-S100A1 and YESTrp2-S100A4; *column 2*, LexA-S100A4 and YESTrp2-S100A1; *column 3*, LexA-S100A4 and YESTrp2 vector; *column 4*, LexA vector and YESTrp2-S100A1; *column 5*, LexA-S100A4 F72Q mutation and YESTrp2-S100A1; *column 6*, LexA-S100A4 Y75Q mutation and YESTrp2-S100A1; *column 7*, YESTrp2-S100A1 alone; *column 8*, LexA-S100A4 alone. The means ± S.D. of three experiments are shown.

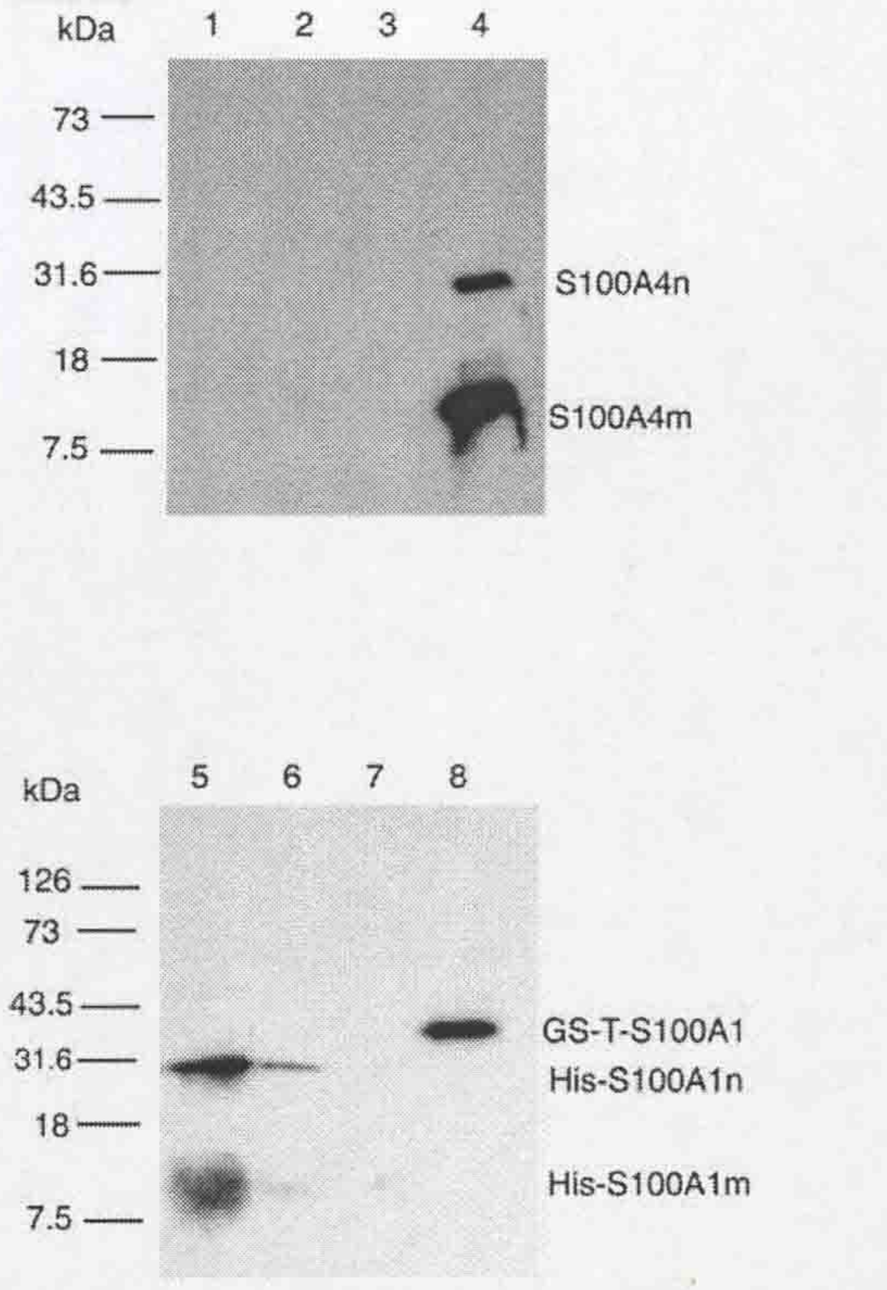

FIG. 2. **The specificity of antibodies directed against recombinant S100A1 and S100A4 proteins.** Samples of proteins, His-S100A1 (*lane 1*), GST-S100A1 (*lane 2*), GST (*lane 3*), S100A4 (*lane 4*), purified His-S100A1 (*lane 5*), cell lysate with induced His-S100A1 (*lane 6*), S100A4 (*lane 7*), and GST-S100A1 (*lane 8*) were subjected to SDS-PAGE and transferred to PVDF membranes. The membranes were incubated with rabbit polyclonal anti-S100A4 (*upper panel*, *lanes 1–4*) or mouse monoclonal anti-S100A1 (*lower panel*, *lanes 5–8*) and then with a second antibody that was detected in turn using the ECL system as described under "Experimental Procedures." *m*, monomer; *n*, multimer.

tested for their specificity toward their target recombinant proteins (Fig. 2). Using Western blotting, anti-S100A4 did not cross-react against NH_2-terminal polyhistidine-tagged S100A1, recombinant GST, nor against a GST-S100A1 fusion recombinant protein, but did recognize S100A4 protein at the same loading. Anti-S100A1 recognized the His-tagged S100A1 and the GST-S100A1 fusion protein but did not cross-react onto S100A4 protein at the same loading (Fig. 2).

To find out whether it is possible to detect interaction between S100A4 and S100A1 *in vitro*, the GST-S100A1 fusion protein and the control GST were immobilized on Sepharose-glutathione columns. The interaction *in vitro* with recombinant S100A4 was detected by the retention of the S100A4 on the Sepharose-glutathione-GST-S100A1 column. After extensive washing, the bound proteins were eluted from the columns with excess glutathione, and the proteins in the resulting fractions were analyzed by SDS-PAGE and Western blot with anti-S100A4 antibody. When a sample of recombinant S100A4 was passed through a column containing bound recombinant GST, no reduced glutathione-elutable S100A4 was retained on the column beyond the wash fraction (Fig. 3*c*). However, when the S100A4 was passed through a similar column but containing immobilized GST-S100A1 fusion protein, rS100A4 was retained on the column, even after extensive washing with buffer, and was eluted, along with the GST-S100A1 fusion protein, with reduced glutathione. This result suggests strongly that S100A4 can bind to GST-S100A1 fusion protein but not to the GST control *in vitro*. Exactly the same result was obtained when the experiment was carried out with a cell lysate of *Escherichia coli* BL-21 cells which had been induced to produce S100A4 with IPTG (Fig. 3*b*). The interaction *in vitro* of purified recombinant GST-S100A1 with S100A4 (purified or nonpurified) was detected in the presence of calcium ions and could be reversed in the presence of 1.0 mM EGTA (Fig. 3*b*).

To investigate in more detail the influence of calcium ions on the interaction between S100A4 and S100A1, the GST-S100A1

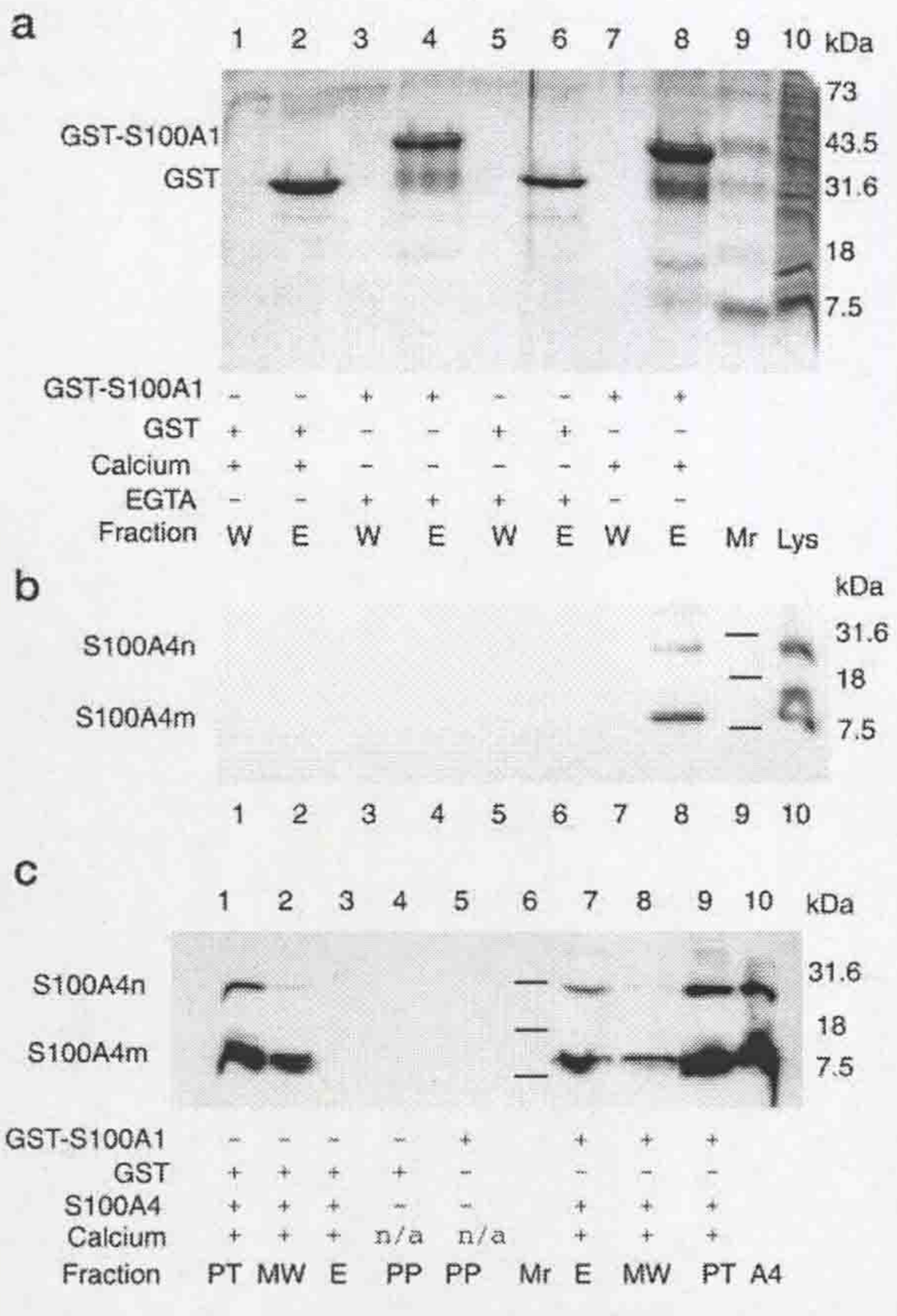

FIG. 3. **Interaction between S100A4 and S100A1 *in vitro*.** Recombinant GST (*panels a and b*, *lanes 1*, *2*, *5*, and *6*; *panel c*, *lanes 1–4*) or GST-S100A1 recombinant fusion protein (*panels a and b*, *lanes 3*, *4*, *7*, and *8*; *panel c*, *lanes 5*, *7*, *8*, and *9*) were purified and immobilized on glutathione-Sepharose columns. Either a bacterial extract containing recombinant S100A4 (*panels a* and *b*; shown in *lane 10*) or purified S100A4 (*panel c*; shown in *lane 10*) was passed through the columns using a Tris buffer (*panels a* and *b*) or a phosphate-buffered solution (*panel c*), as described under "Experimental Procedures." In *panels a* and *b*, the buffer contained either calcium (*lanes 1*, *2*, *7*, and *8*) or EGTA (*lanes 3–6*). The proteins that passed through the columns (designated *PT*) were collected (*panel c*, *lanes 1* and *9*). The columns were washed until no more protein was eluted, and the washes were either pooled (*panel c*, *lanes 2* and *8*, designated *MW* for mixed wash), or a final wash fraction was passed through (*panels a* and *b*, *lanes 1*, *3*, *5*, and *7*, designated *W*). Proteins remaining bound to the columns were eluted, designated by *E* (*panels a* and *b*, *lanes 2*, *4*, *6*, and *8*; *panel c*, *lanes 3* and *7*), as described under "Experimental Procedures." Samples of the fractions were subjected to SDS-PAGE as described under "Experimental Procedures," and a gel was stained (*panel a*) or the proteins were transferred onto membranes (*panels b* and *c*). S100A4 was detected by a rabbit anti-S100A4, which did not cross-react with S100A1 (*panels b* and *c*). The molecular masses of marker proteins (*panel a*, *lane 9*, designated M_r) are indicated in kDa alongside *panel a*. On *panel c* the markers on the original stained gel (*lane 6*, designated M_r) are not visible on the autoradiograph but have been drawn in to indicate their position. On *panel c*, samples of pure proteins (*PP*) of the recombinant glutathione *S*-transferase (*lane 4*), the GST-S100A1 recombinant fusion protein (*lane 5*), and recombinant S100A4 (*lane 10*, designated *A4*) were also subjected to electrophoresis and Western blotting. *m*, monomeric; *n*, multimeric; *n/a*, not applicable. The multiple weak bands in *panel a*, *lanes 4* and *8*, arise from degradation of the GST-S100A1 fusion protein, and the apparent doublet for S100A4m in *panel b* is an overloading artifact.

columns above were utilized, with buffers containing between 0 and 1.0 mM calcium ions or 0.5 or 1.0 mM EGTA. Interaction between S100A1 and S100A4 could be detected using the buffer with no added calcium; however, the amount of S100A4 retained on the GST-S100A1 column increased as the concentration of calcium in the buffer was increased (Fig. 4). 0.5 mM EGTA reduced the amount of S100A4 retained, and no detectable S100A4 was retained with 1.0 mM EGTA. These results suggest that the interaction of S100A4 with S100A1 is not markedly calcium ion-dependent over the normal range of calcium concentrations. However, removing all of the calcium with a high concentration of EGTA created conditions that reduced the retained S100A4 to an undetectable level.

FIG. 4. **Effect of calcium ions on the interaction *in vitro* between S100A4 and S100A1.** GST-S100A1 fusion recombinant protein was purified and immobilized on glutathione-Sepharose beads. The beads were incubated at 4 °C overnight with rS100A4 protein in Tris buffer containing no added $CaCl_2$ (*lanes 1–3*) or added $CaCl_2$ to 0.1 mM (*lanes 4*, *5*, and *7*), 0.5 mM (*lanes 8–10*), 1.0 mM (*lanes 11–13*) or EGTA added to 0.5 mM (*lanes 14–16*) or 1.0 mM (*lanes 17–19*). The mixtures were then applied to spun columns. After extensive washing, the GST-S100A1 was eluted from the beads with glutathione. The fractions, *P* (pass-through), *W* (last wash), and *E* (elute) were subjected to SDS-PAGE and Western blotting. The S100A4 that had been retained on the column was detected with anti-S100A4. The smear in the pass-through fractions arises from aggregation of the excess recombinant S100A4 protein. Molecular mass markers (M_r) of standard proteins on the stained gel are shown in *lanes 6* and *20*.

The interaction between S100A1 and S100A4 was also demonstrated using a gel overlay technique with purified rS100A1 and rS100A4 proteins (Fig. 5). Recombinant S100A4 protein binding to both His-S100A1 and GST-S100A1, but not to GST protein, was detected by the antibody to S100A4.

S100A1 and S100A4 Are Present in the Same Cells—To find out whether S100A1 and S100A4 coexist in the same cells naturally, the presence of S100A1 mRNA was sought in clonal breast tumor cell lines of known S100A4 status using a PCR-based assay. A correctly sized ethidium bromide-stained band of DNA on agarose gels was obtained following RT-PCR using human S100A1-specific primers on RNA from human mammary cell lines, MCF-7, MDA-MB-231, and SK-Br-3. The latter two cell lines have been shown previously to contain high levels of S100A4 mRNA (4) (Fig. 6). Sequencing of the PCR products confirmed that they corresponded to the human S100A1 mRNA. No bands were obtained with any of the RNAs when RT-PCRs were carried out in the absence of the Superscript reverse transcriptase. Thus, the mRNAs for both S100A1 and S100A4 were present in these clonal cell lines. The presence of both S100A1 and S100A4 protein in the same cells has been shown by Western blotting (Fig. 7) and by dual labeling immunofluorescence on MDA-MB-231 cells (Fig. 8). In the immu-

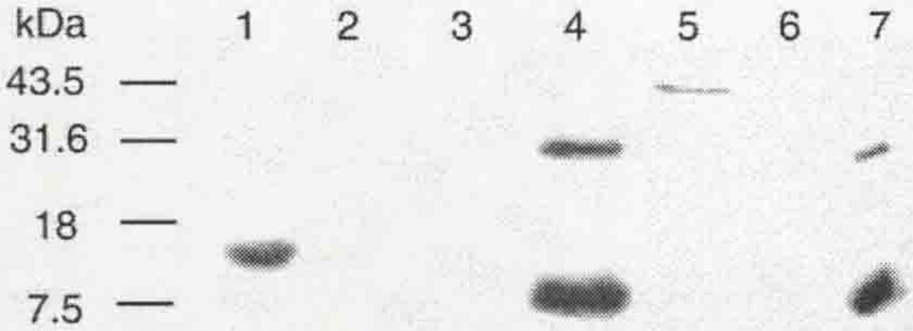

FIG. 5. **Interaction *in vitro* between S100A1 and S100A4 using gel overlay.** Purified recombinant proteins, His-S100A1 (*lane 1*), GST (*lane 3*), rat S100A4 (*lane 4*), GST-S100A1 (*lane 5*), GST (*lane 6*), and human S100A4 (*lane 7*) were separated by SDS-PAGE (15% (w/v)) and blotted onto PVDF membranes. The membranes were incubated with S100A4, and any binding of rS100A4 was detected by anti-S100A4 (see "Experimental Procedures"). The banding pattern of molecular weight markers is shown on the *left side* of the image with molecular masses in kDa indicated. *Lane 2* contained no protein.

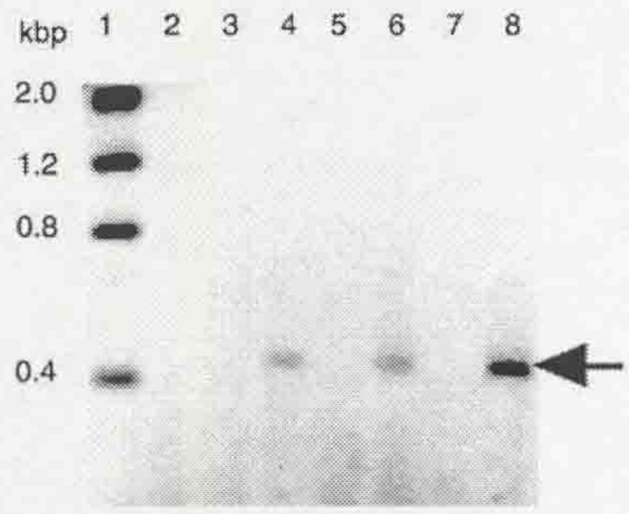

FIG. 6. **Detection of mRNA for S100A1 in breast tumor cell lines.** RNA from the malignant human breast cancer cloned cell lines, MCF-7 (*lanes 3* and *4*), SK-Br-3 (*lanes 5* and *6*), and MDA-MB-231 cells (*lanes 7* and *8*) was subjected to RT-PCR (*lanes 4*, *6*, and *8*) or control amplification in which the reverse transcriptase was omitted (*lanes 3*, *5*, and *7*), using primers specific for human S100A1, as described under "Experimental Procedures." A PCR without template was also carried out (*lane 2*). The resulting PCR products were subjected to agarose gel electrophoresis along with molecular size markers (*lane 1*), and the gel was stained with ethidium bromide. The image has been reversed. The band of S100A1 amplification product is indicated by the *arrow*.

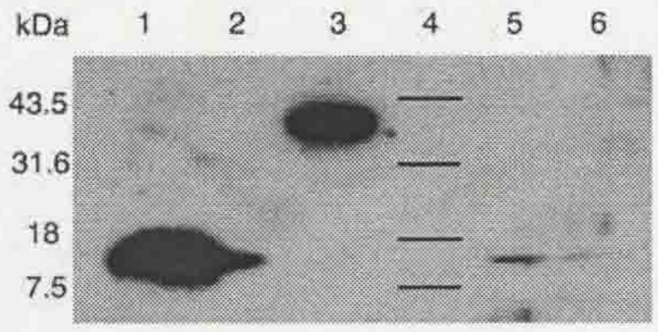

FIG. 7. **Western blot of S100A1 and S100A4 proteins in cell lines.** Recombinant proteins His-S100A1 (*lane 1*, 15 μg and *lane 2*, 2 μg), GST-S100A1 (*lane 3*, 5 μg), and lysates from cell lines SK-Br-3 (*lane 5*, 40 μg) and MDA-MB-231 (*lane 6*, 40 μg) were separated by SDS-PAGE (15% (w/v)) and blotted onto PVDF membranes. The S100A1 was detected by polyclonal anti-S100A1. Molecular weight markers are shown (*lane 4*), with their molecular masses indicated in kDa on the *left side*.

nofluorescent experiments, both S100A1 and S100A4 were localized to the perinuclear region and to the cytoskeleton, and the fluorescence of each could be removed by preincubating each antibody separately with its cognate, but not the other recombinant protein (Fig. 8). Superimposition of the staining shows their partial colocalization on stress fibers and in the perinuclear region.

DISCUSSION

S100A4 is shown to interact with S100A1 in *Saccharomyces cerevisiae* cells and also *in vitro*. Although it has been reported previously that S100A4 forms homodimeric forms (23, 35), this

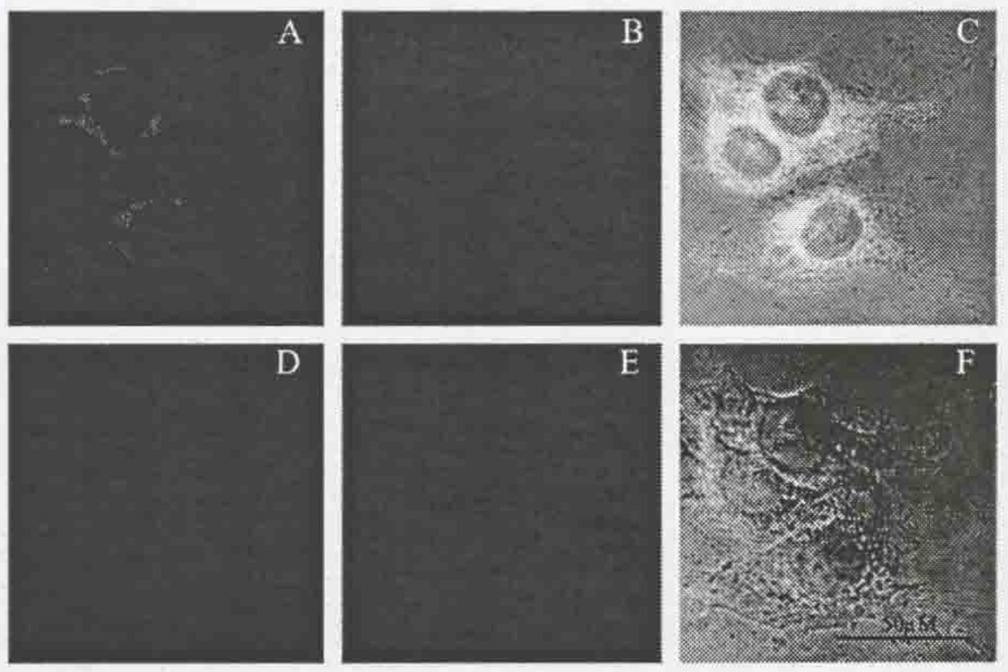

FIG. 8. **Immunofluorescent localization of S100A1 and S100A4 in human mammary cells in culture.** MDA-MB-231 cells were grown in chambered slides, fixed, and incubated with a mouse monoclonal anti-S100A1 and fluorescein isothiocyanate-conjugated anti-mouse IgG (*panel A*) or with a rabbit polyclonal anti-S100A4 and tetramethylrhodamine β-isothiocyanate-conjugated anti-rabbit IgG (*panel B*). Superimposition of the images in *A* and *B* indicates partial colocalization of the two S100A proteins around the nucleus and on stress fibers. Preincubation of the anti-S100A1 IgG with rS100A1 abolished the immunofluorescence caused by S100A1 (*panel D*) but not that caused by S100A4 (not shown), and preincubation of the anti-S100A4 with rS100A4 abolished the immunofluorescence resulting from S100A4 (*panel E*) but not that resulting from S100A1 (not shown). *Panels A–C* and the phase-contrast image (*panel F*) are of the same field. Magnification × 280; *bar* = 50 μm.

is the first report of S100A4 interacting with another member of the S100A family of EF-hand-containing proteins. Based upon the time taken for the blue dye arising from β-galactosidase activity to become visible, the interaction between S100A4 and S100A1 *in vivo* was more effective at stimulating reporter gene activity than the homodimeric interaction of S100A4 in the same system. S100A4 molecules that had been specifically mutated in conserved amino acid residues, reported previously to be associated with the dimer interface of S100A6 (calcyclin) (34), and which prevented S100A4 homodimerization in the yeast two-hybrid system, also failed to interact with S100A1, strongly suggesting that this latter interaction resembles the natural association of other S100 proteins into homo- (34) and hetero- (36) dimeric forms.

Homodimer and heterodimer formation of S100 proteins has been predicted from the three-dimensional structures of some S100 proteins and homology analysis (34). Natural homodimeric and heterodimeric association of S100A family members is well documented. Thus, S100A1 (37), S100B (22), S100A4 (23), and S100A6 (34) have been shown to form homodimers. Heterodimerization of S100A8 with S100A9 in neutrophils (21, 36) and of S100A1 with S100B (38) in neural tissue has been described, and the formation of heterodimers between S100B and S100A6 (39) in human melanoma has been reported recently.

The heterodimerization of S100A1 and S100A4 reported here might be expected to have biological significance if these S100 proteins occur in the same cells. These proteins have been shown to coexist in the same cultured human breast cancer cells and in rat mammary cells, Rama 29 (not shown) (30), and coexpression of S100A1 and S100A4 has been reported previously in primary cultures and cell lines of human vascular smooth muscle cells (14). In the present experiments, S100A1 and S100A4 are both located in the perinuclear region and on the stress fibers of the cytoskeleton. Localization of S100A4 (5, 12, 14) and of S100A1 to the cytoskeleton (14) and of S100A4 to the sarcoplasmic reticulum (14) has been reported previously.

These observations suggest that S100A1 and S100A4 might also be interacting inside the cell at these same locations.

Because S100A1 and S100A4 are capable of dimerizing, it is possible that they have a common intracellular target. Both S100A1 and S100A4 individually have been shown to interact with a range of non-S100 protein targets. S100A1 has been shown to interact with brain-specific C and muscle-specific A isoforms of aldolase (40), MyoD (41), and a dodecylpeptide of the actin-capping, Cap Z (42), F-actin (14), the calcium-release channel of skeletal muscles (43), and twitchin kinase of *Caenorhabditis elegans* (44). S100A4, in contrast, has been reported to interact *in vitro* with a more limited range of intracellular target proteins, in particular cytoskeletal actin (15), tropomyosin (16), and non-muscle myosin heavy chains (17–20). However, the interaction with actin might arise from a tendency of S100A4 to aggregate (14). The interaction of S100A4 with myosin occurs at a site on the non-muscle myosin heavy chains which has been reported to be phosphorylated by protein kinase C *in vivo* and *in vitro* (20). All of these interactions have been determined with single purified S100A4 protein, and it will be important to find out whether these interactions *in vitro* can be modulated by the presence of S100A1. It is possible that the interactions of S100A4 with myosin, which might be associated with the protein's metastasis-inducing capabilities, could be modulated by interaction with cytoskeleton-associated S100A1 (14). In this regard it might be interesting to note that S100A1 and S100A4 are colocalized in the high S100A4-expressing cultured Rama 29 cells (30), which do not express a metastatic phenotype.

The distribution of S100A1 and S100A4 proteins in normal cells is much more diverse. Although S100A1 was originally found in brain, where it interacts with S100B, it is also found in heart, slow twitch skeletal muscle, smooth muscle, and kidney (45). In contrast, S100A4 is not found in significant quantities in brain, but it is distributed widely and specifically elsewhere in the body, including kidneys, lungs, thymus, and muscle tissues, at least in the rat (28). The observation that S100A1 interacts with S100A4 as well as with S100B, but that S100B (46), but not S100A4 (28), is found widely in brain tissue, raises the possibility that S100A1 has different S100 partners depending upon the S100 proteins that are expressed in the particular cells concerned.

Acknowledgments—We thank Dr. Dave Spiller for advice and assistance with microscopy and Carl Zeiss for collaborative support.

REFERENCES

1. Hilt, D., and Kligman, D. (1991) in *Novel Calcium-binding Proteins: Fundamentals and Clinical Implications* (Heizmann, C. W., ed) pp. 65–103, Springer-Verlag, Berlin
2. Dunnington, D. J. (1984) *The Development and Study of Single Cell-cloned Metastasizing Mammary Tumour Cell Systems in the Rat.* Ph.D. thesis, University of London
3. Ebralidze, A., Tulchinsky, E., Grigorian, M., Afanayeva, A., Senin, V., Revazova, E., and Lukanidin, E. (1989) *Genes Dev.* **3,** 1086–1093
4. Nikitenko, L., Lloyd, B., Rudland, P., Fear, S., and Barraclough, R. (2000) *Int. J. Cancer* **86,** in press
5. Davies, B., Davies, M., Gibbs, F., Barraclough, R., and Rudland, P. (1993) *Oncogene* **8,** 999–1008
6. Lloyd, B., Platt-Higgins, A., Rudland, P., and Barraclough, R. (1998) *Oncogene* **17,** 465–473
7. Davies, M., Rudland, P., Robertson, L., Parry, E., Jolicoeur, P., and Barraclough, R. (1996) *Oncogene* **13,** 1631–1637
8. Ambartsumian, N., Grigorian, M., Larsen, F., Karlstrom, O., Sidenius, N., Rygaard, J., Georgiev, G., and Lukanidin, E. (1996) *Oncogene* **13,** 1621–1630
9. Takenaga, K., Nakanishi, H., Wada, K., Suzuki, M., Matsuzaki, O., Matsuura, A., and Endo, H. (1997) *Clin. Cancer Res.* **3,** 2309–2316
10. Takenaga, K., Nakamura, Y., and Sakiyama, S. (1994) *Biochem. Biophys. Res. Commun.* **202,** 94–101
11. Tulchinsky, E., Grigorian, M., Tkatch, T., Georgiev, G., and Lukanidin, E. (1995) *Biochim. Biophys. Acta* **1261,** 243–248
12. Gibbs, F. E. M., Wilkinson, M. C., Rudland, P. S., and Barraclough, R. (1994) *J. Biol. Chem.* **269,** 18992–18999
13. Takenaga, K., Nakamura, Y., and Sakiyama, S. (1994) *Cell Struct. Funct.* **19,** 133–141
14. Mandinova, A., Atar, D., Schäfer, B., Speiss, M., Aebi, U., and Heizmann, C. (1998) *J. Cell Sci.* **111,** 2043–2054
15. Watanabe, Y., Usada, N., Minami, H., Morita, T., Tsugane, S.-i., Ishikawa, R., Kohama, K., Tomida, Y., and Hidaka, H. (1993) *FEBS Lett.* **324,** 51–55
16. Takenaga, K., Nakamura, Y., Sakiyama, S., Hasegawa, Y., Sato, K., and Endo, H. (1994) *J. Cell Biol.* **124,** 757–768
17. Ford, H., and Zain, S. (1995) *Oncogene* **10,** 1597–1605
18. Ford, H., Silver, D., Cachar, B., Sellers, J., and Zain, S. (1997) *Biochemistry* **36,** 16321–16327
19. Kriajevska, M. V., Cardenas, M. N., Grigorian, M. S., Ambartsumian, N. S., Georgiev, G. P., and Lukanidin, E. M. (1994) *J. Biol. Chem.* **269,** 19679–19682
20. Kriajevska, M., Tarabykina, S., Bronstein, I., Maitland, N., Lomonosov, M., Hansen, K., Georgiev, G., and Lukanidin, E. (1998) *J. Biol. Chem.* **273,** 9852–9856
21. Bhardwaj, R. S., Zotz, C., Zwadloklarwasser, G., Roth, J., Goebeler, M., Mahnke, K., Falk, M., Meinardus-Hager, G., and Sorg, C. (1992) *Eur. J. Immunol.* **22,** 1891–1897
22. Kilby, P. M., Van Eldik, L. J., and Roberts, G. C. K. (1996) *Structure* **4,** 1041–1052
23. Pedrocchi, M., Schäfer, B., Durussel, I., Cox, J., and Heizmann, C. (1994) *Biochemistry* **33,** 6732–6738
24. Becker, D., and Fikes, J. (1993) in *Gene Transcription: A Practical Approach* (Hames, B., and Higgins, S., eds) pp. 295–319, IRL Press, Oxford
25. Engelkamp, D., Schäfer, B. W., Erne, P., and Heizmann, C. W. (1992) *Biochemistry* **31,** 10258–10264
26. Ho, S. N., Hunt, H. D., Horton, R. M., Pullen, J. K., and Pease, L. R. (1989) *Gene (Amst.)* **77,** 51–59
27. Laemmli, U. K. (1970) *Nature* **227,** 680–685
28. Gibbs, F., Barraclough, R., Platt-Higgins, A., Rudland, P., Wilkinson, M., and Parry, E. (1995) *J. Histochem. Cytochem.* **43,** 169–180
29. Engel, L. W., and Young, N. A. (1978) *Cancer Res.* **38,** 4327–4339
30. Bennett, D. C., Peachy, L. A., Durbin, H., and Rudland, P. S. (1978) *Cell* **15,** 283–298
31. Barraclough, R., Kimbell, R., and Rudland, P. S. (1987) *J. Cell. Physiol.* **131,** 393–401
32. Chirgwin, J. M., Przybyla, A. E., Macdonald, R. J., and Rutter, W. J. (1979) *Biochemistry* **18,** 5294–5299
33. Han, J. H., Stratowa, C., and Rutter, W. J. (1987) *Biochemistry* **26,** 1617–1625
34. Potts, B., Smith, J., Akke, M., Macke, T., Okazaki, K., Hidaka, H., Case, D., and Chazin, W. (1995) *Nat. Struct. Biol.* **2,** 790–796
35. Ilg, E., Schäfer, B., and Heizmann, C. (1996) *Int. J. Cancer* **68,** 325–332
36. Teigelkamp, S., Bhardwaj, R. S., Roth, J., Meinardus-Hager, G., Karas, M., and Sorg, C. (1991) *J. Biol. Chem.* **266,** 13462–13467
37. Isobe, T., Ishioka, N., Masuda, T., Takahashi, Y., Ganno, S., and Okuyama, T. (1983) *Biochem. Int.* **6,** 419–426
38. Kato, K., and Kimura, S. (1985) *Biochim. Biophys. Acta* **842,** 146–150
39. Yang, Q., Ohanlon, D., Heizmann, C. W., and Marks, A. (1999) *Exp. Cell Res.* **246,** 501–509
40. Zimmer, D. B., and Van Eldik, L. J. (1986) *J. Biol. Chem.* **261,** 11424–11428
41. Baudier, J., Bergeret, E., Bertacchi, N., Weintraub, H., Gagnon, J., and Garin, J. (1995) *Biochemistry* **34,** 7834–7846
42. Ivanenkov, V. V., Dimlich, R. V. W., and Jamieson, G. A. (1996) *Biochem. Biophys. Res. Commun.* **221,** 46–50
43. Treves, S., Scutari, E., Robert, M., Groh, S., Ottolia, M., Prestipino, G., Ronjat, M., and Zorzato, F. (1997) *Biochemistry* **36,** 11496–11503
44. Heierhorst, J., Kobe, B., Feil, S., Parker, M., Benian, G., Weiss, K., and Kemp, B. (1996) *Nature* **380,** 636–639
45. Zimmer, D. B., Cornwall, E. H., Landar, A., and Song, W. (1995) *Brain Res. Bull.* **37,** 417–429
46. Moore, B., and McGregor, D. (1965) *J. Biol. Chem.* **240,** 1647–1653